Understanding the role of ADP-ribose chain length on PARP1/2 dynamics at sites of DNA damage and on the PARP inhibitor response

Kira Schützenhofer

Lincoln College

Sir William Dunn School of Pathology

University of Oxford

A thesis submitted for the degree of

Doctor of Philosophy

Michaelmas Term 2024

Acknowledgment

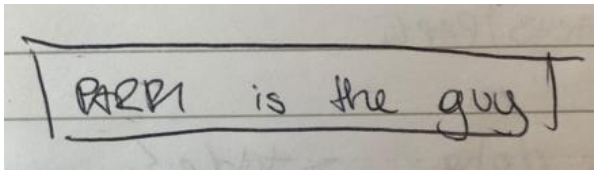

Unofficial Figure 1: A note I wrote in my lab book
after a two-hour meeting with Prof Ivan Ahel,
regarding the future of my project.

I would first like to thank Professor Ivan Ahel, for being such as steady and patient source of support and inspiration. You have given me the time and space to develop as a scientist, and have always been there when I needed guidance. As we know, I like to worry, and whenever I would despair, you would remind me of the fact that PARP1, is in fact, the guy, and that I could do it. Thank you.

The next person I would like to thank is Rebecca Smith. Not only have you become the mentor I needed, you have become a dear friend. Whenever I think of the dark, cold, lonely nights at the microscope (exactly as dramatic as it sounds) I also think of how you would come running down the second I told you the microscope was not working again (because I forgot to flip one switch or pressed one button too many). You manage to turn a frustrating mistake (forgetting to load the ladder for my Western Blot gel, again) into a laugh by giving me a goose sticker, and I have cherished every single rant we shared in your office (i.e. the cold room). You even make cleaning the lab enjoyable. We like to say we share one brain cell, but you have so much of my heart as well. You have been unfailing in your support and faith in me and I will never be able to express fully how much that means to me, and how much you have done for me. If I had the space, I would wax poetically about your greatness and my appreciation for you, but alas, there must be some pages left for science, so I can only say: You have been the wind beneath my wings, dude.

Joséphine Groslambert and Nina Đukić I want to thank for making this DPhil such a fun, wholesome experience. I could not have asked for better lab-mates and friends these past four years. Every lunch with you, every girls' night, every chat in TC has meant so much, and you have made this experience so much more enjoyable.

I would further like to thank all the members of the Ivan Ahel lab; in particular, Domagoj Baretic and Chatrin, who have been very generous with their time. I will always remember the lab fondly, and this is to a great part due to the brilliant, wonderful scientists in the lab who have helped me along the way, in so many ways.

To Sinan Shi: your presence and friendship mean so much to me, and you have made my time in Oxford so much less lonely. It would not have been the same without you. Your wisdom and insight will forever inspire me. You are also the person who introduced me to Zhang Ji, and I will always be grateful for that.

I also want to say thank you to Christopher Gallacher, because you have been a steady force of good, and silliness, and because you will watch terrible movies with me just to make me happy.

To Archie Morfoot, the housemate I never knew I wanted, the man whose pizza makes angels sing, the friend who managed to lure me out of my room when all I wanted was to be a hermit. You do not know how much your presence has cheered me up over the years.

To Dorian, Richard, Kenneth and Crudgington. Thank you for being there for me, for making me laugh when I don't want to, for listening to me yap, and for holding my hands through the sun and the rain on our little bench. Every time I walked into the lab and saw your back, it made my day a little better.

Thank you to Delal Bektas, my fiercest supporter and hype woman, and always an inspiration.

Thank you to Kaising Hii, because who knows who I would be if I had not befriended you on the first day of our undergrad?

Thank you to Kathrin Jarosik, you are just *glunga*, and always my comfort blanket.

To countless other friends, who have been there for me over the years, and who make my life so much richer, through a phone call, a pub trip, a visit, by sending me a meme, or by knowing that they exist. Thank you.

Finally, I would like to thank my parents. who have always supported and loved me without ever questioning that I could do whatever I set my mind to, especially when I have doubted myself. They have always given me everything they could give me, and provided me with the space to be myself. They have been so constant and unwavering in their presence and love for me that it is almost difficult to express how grateful I am. Because it would be so easy to take it for granted, it must be said: without you, I could not have done it. All I can aspire to do is to make you proud and give you back a sliver of what you have given me.

Declaration

I declare that the work presented in this thesis is entirely my own, except where stated otherwise.

No part of this thesis has been submitted elsewhere for any purpose, except for the findings presented in Figure 3.1, which were adapted from the following published paper:

Prokhorova E*****, Zobel F*, Smith R, Zentout S, Gibbs-Seymour I, Schützenhofer K, Peters A, Groslambert J, Zorzini V, Agnew T, Brognard J, Nielsen ML, Ahel D, Huet S, Suskiewicz MJ[#], Ahel I[#]. Serine-linked PARP1 auto-modification controls PARP inhibitor response. Nat Commun. 2021; 12(1):4055.

Figures that were taken from journals were either used with permission, as stated in the corresponding figure legends, or did not require permission for reuse. All figures are cited to their original publication.

Abstract

Upon sensing DNA damage, PARP1/2 are recruited to lesions where they ADP-ribosylate themselves and other proteins at sites of damage, including histones, thus promoting, and directing DNA repair. Loss of catalytic activity of PARP1 causes its prolonged retention, or ‘trapping', at sites of DNA breaks, which can exacerbate existing damage. This is exploited therapeutically in cancers with deficiencies in DNA repair pathways, in which catalytic inhibition of PARP1 causes synthetic lethality. Recent years have seen an increase in studies investigating the mechanism of action of these drugs, PARP inhibitors, with sometimes contradicting findings.

HPF1, an essential PARP1/2 co-factor, discovered more than 50 years after PARP1, forms a complex with PARP1/2 at sites of DNA damage and switches ADP-ribosylation to target serine residues on histones and many other DNA damage associated proteins. While this function of HPF1 has been studied and shown to be important for DNA repair and to reduce PARP inhibitor sensitivity, HPF1 also restricts ADP-ribose chain elongation. This function has not been as extensively studied, and its role in regulating PARP1 release and DNA repair is yet not well understood. Therefore, I created cell lines that allow inducible expression of wild-type or catalytically impaired versions of both HPF1 and PARP1, to allow better study of the structure/function relationships of these proteins, including the investigation of the roles of mono- vs poly-ADP-ribosylation in the DNA damage response and cellular survival. Using these mutants, I demonstrate that mono-ADP-ribosylation, and not only poly-ADP-ribosylation, is important for the release of PARP1 from sites of DNA damage.

In this work, I also demonstrate that the release of catalytic PARP1 mutants is promoted by a novel PARP1-selective inhibitor, which adds to a growing field of research into how these drugs work. Finally, by using a catalytic PARP1 mutant, and this novel, PARP1-selective

inhibitor, I am able to provide new insights into the relationship between PARP1 and PARP2 at sites of DNA damage.

Contents

Acknowledgment 2
Declaration 5
Abstract 6
List of Figures 11
List of Tables 12
List of Abbreviations 13
1. Introduction 15
1.1 ADP-ribosylation 15
1.1.1 Structure and Significance 15
1.1.2 Writers of ADP-ribosylation 17
1.1.3 Readers of ADP-ribosylation 20
1.1.4 Erasers of ADP-ribosylation 24
1.2 ADP-ribosylation in the DNA damage response 27
1.2.1 PARP1 structure and activation 27
1.2.2 PARP1 in DNA repair 32
1.2.3 PARP2 and PARP3 in DNA repair 38
1.3 The ADP-ribosylation code in the DNA damage response 40
1.3.1 HPF1 and serine ADPr – discovery of a crucial PARP1/2 co-factor 40
1.3.2 Importance of ADP-ribose chain length in the DDR 45
1.4 PARP inhibitors and therapeutic targeting of ADP-ribosylation 46
1.4.1 Clinical use of PARP inhibitors 46
1.4.2 Molecular mechanism of PARP inhibition 54
1.5 Aims 71
2. Materials and Methods 73
2.1 Cell Biology 73
2.1.1. Cell lines 73
2.1.2. DNA damage and cell lysis 73
2.1.4 Transfections 74
2.1.5 Recombination in U2OS Flp-In cells 75
2.1.6 Clonogenic assays 76
2.1.7 Microirradiation assays 76
2.1.8. Western Blotting 78
2.1.9 Immunostaining and microscopy 78

2.2 Cloning 79
2.2.1 Gateway Cloning 79
2.2.2. Site-directed mutagenesis PCR 80
2.2.3. Plasmid propagation 80
2.2.4. Sequencing 81
2.2.5 Statistical Analysis 81
2.3. Materials 82
2.3.1. Antibodies 82
2.3.2 Chemicals 83
2.3.3. Buffer solutions and media 83
2.3.4 Expression Vectors 86
3. Results 89
3.1 HPF1 controls PARP1-mediated ADP-ribose chain length and the PARP inhibitor response 89
3.1.1 Over-expression of HPF1 provides resistance to PARP inhibition 89
3.1.2 HPF1 catalytic activity is required for PARP inhibitor resistance 93
3.2 PARP1 release from sites of DNA damage depends on ADP-ribose chain length 99
3.2.1 Different PARP1 catalytic mutants differ in the ADP-ribose chains they produce 101
3.2.2 ADP-ribose chain length corresponds to PARP1 trapping at sites of DNA damage 104
3.2.3 Testing U2OS Flp-In T-REx PARP1 KO cells stably expressing YFP-PARP1 mutants 108
3.2.4 Expression of a mono-ADP-ribosylation PARP1 mutant is toxic to cells 111
3.3 Some PARP1 mutants are resistant to a novel PARP1-selective PARP inhibitor 113
3.3.1 The toxicity of PARP1 E988Q is rescued by treatment with saruparib 113
3.3.2 The toxicity of PARP1 E988Q is due to increased replication stress and DNA damage, and can be rescued with saruparib 116
3.3.3 Saruparib promotes the release of some catalytic PARP1 mutants from sites of DNA damage 118
3.3.4 Other PARP inhibitors do not have the same “pro-release” effect on PARP1 E988Q 121
3.3.5 Identification of additional PARP1 mutants that are released from sites of DNA damage by saruparib 126
3.3.6 Catalytic impairment of PARP1 reveals the pro-release allosteric effect of saruparib 131
3.3.7 The pro-release response of certain PARP1 mutants to saruparib is not based on a lack of catalytic inhibition 135

3.3.8 The PARP1 helical domain is crucial for regulating the PARP inhibitor response 139
3.3.9 The effect of endogenous PARP1 on the pro-release effect of saruparib on PARP1 E988Q 142
3.4. Investigating the behaviour and relationship of PARP1 and PARP2 at sites of DNA damage 148
3.4.1 The effect of PARP2 on PARP1 recruitment and release from sites of DNA damage 149
3.4.2 The effect of PARP1 on PARP2 recruitment and release from DNA damage site 152
4. Discussion and Future Plans 158
4.1 The “right” amount of ADP-ribosylation 158
4.2 The pro-release effect of saruparib on PARP1 catalytic mutants 164
4.3 The interplay between PARP1 and PARP2 169
4.4 Conclusion 171
Bibliography 173
Appendix 216

List of Figures

Figure 1.1: Molecular structure of ADP-ribosylation……...17

Figure 1.2: Overview of the clade classification of the human PARP superfamily and their domain architecture……...……19

Figure 1.3: Overview of common ADP-ribose reader domain binding preferences……21

Figure 1.4: Schematic overview of the preferences and function of different ADP-ribose erasers……...26

Figure 1.5: Schematic representation of PARP1 activation……..30

Figure 1.6: HPF1 and the PARP1/2 catalytic domain (CAT) form a composite active site.....43

Figure 1.7: Analysis of binding modes of different PARP inhibitors……...52

Figure 1.8: Clinical PARP inhibitors, and veliparib, ranked by their trapping potency of PARP1 in cells……..54

Figure 2.1: Vector maps……....86

Figure 3.1: HPF1 is responsible and required for maintaining PARP1 auto-modification despite PARP inhibitor treatment…….91

Figure 3.2: Loss of HPF1 catalytic activity reduces PARP1 auto-modification with PAR chains……....94

Figure 3.3: Catalytically inactive HPF1 sensitises cells more to PARP inhibitor than loss of HPF1…….97

Figure 3.4: Comparison of catalytic activity of different PARP1 mutants…….102

Figure 3.5: Recruitment and release of different PARP1 mutants is linked to their catalytic activity…….106

Figure 3.6: Treatment of U2OS Flp-In PARP1 KO cells with Doxycycline induces expression of complemented YFP EV, YFP-PARP1 WT, YFP-PARP1 E988Q and YFP-PARP1 E988Q…….109

Figure 3.7: Impairment and loss of catalytic activity leads to reduced cellular survival…...111

Figure 3.8: Saruparib rescues the toxicity induced by expression of PARP1 E988Q……....114

Figure 3.9: Increased replication stress and DNA damage upon expression of PARP1 E988Q can be rescued by treatment with the PARP1-specific inhibitor, saruparib……...116

Figure 3.10: Saruparib increases the release of PARP1 E988Q from DNA sites of DNA damage……....119

Figure 3.11: Other PARP inhibitors do not have the same pro-release effect on PARP1 E988Q…….123

Figure 3.12: Identification of additional PARP1 mutants that are released from DNA damage sites by saruparib……....127

Figure 3.13: Loss of catalytic activity reveals the pro-release effect of saruparib…….133

Figure 3.14: Saruparib effectively reduces catalytic activity of PARP1 WT and catalytic mutants……....136

Figure 3.15: The pro-release effect of saruparib on PARP1 E988Q is not dependent on a specific concentration…….....137

Figure 3.16: The PARP1 HD is involved in the regulation of the PARP inhibitor response……..140

Figure 3.17: Presence of endogenous PARP1 abrogates the pro-release of saruparib on PARP1 E988Q……....144

Figure 3.18: Recruitment and release dynamics of PARP1 WT and E988Q are differently affected by the presence of PARP2……150

Figure 3.19: Total recruitment of YFP-PARP2 is affected by the presence or absence of PARP1 WT or PARP1 E988Q……...153

Figure 3.20: Recruitment and release dynamics of PARP2 are affected by the presence or absence of PARP1 WT or E988Q……..156

Figure A.1: Radioactive ADPr experiment showing the catalytic activity of PARP1 WT and other mutants……..215

Figure A.2: Recruitment and release dynamics of YFP PARP1 WT and YFP PARP1 E988Q in response to olaparib, veliparib and saruparib…….....216

Figure A.3: Recruitment and release dynamics of different PARP1 catalytic mutants in response to olaparib or saruparib……...217

Figure A.4: Comparison of the ADP-ribosylation activity in cells lacking PARP1, PARP2, or both…….....218

Figure A.5: Total amount of mCherry-PARP1 WT and E988Q recruited to DNA damage sites in the presence or absence of YFP-PARP2……...219

List of Tables

Table 1.1 Relevant PARP inhibitors, their selectivity, FDA approval status and disease indications…….……48

Table 2.1 List of commercial antibodies used in this work..... 83

Table 2.2: List of commercial drugs and reagents used in this work. 83

Table 3.1 Summary of PARP1 catalytic domain residues, their role and the effect of their mutation on catalytic activity……99

List of Abbreviations

ADPr	ADP-ribosylation
ARH3	ADP-ribosylhydrolase
ART	ADP-ribosyltransferase
BER	Base excision repair
BRCA1	Breast Cancer gene 1
BRCA2	Breast Cancer gene 2
BRCT	BRCA1 C-terminus
DDR	DNA damage response
DSB	Double-strand break
GFP	Green fluorescent protein
H_2O_2	Hydrogen peroxide
HD	Helical Domain
HPF1	Histone PARylation factor 1
HR	Homologous recombination
kDA	kilodalton
KO	Knockout
MAR	Mono(ADP-ribose)
MARylation	Mono(ADP)ribosylation
MMS	Methyl methanesulfonate
NAD	Nicotine adenine dinucleotide
NER	Nucleotide excision repair
PAR	Poly(ADP-ribose)
PARylation	Poly(ADP)ribosylation
PARG	Poly(ADP-Ribose) glycohydrolase
PARP	Poly(ADP-ribose) polymerase
PARPi(s)	PARP1/2 inhibitor(s)
PBM	PAR-binding motif

PBZ	PAR-binding zinc finger
PTM	Posttranslational modification
SSB	Single-strand break
TNKS	Tankyrase
WGR	Tryptophan-glycine-arginine-rich
WT	Wild-type
YFP	Yellow fluorescent protein
Zn	Zinc finger

1. Introduction

Post-translational modification (PTMs), the attachment of covalent modifications to proteins, greatly enhances the functional output and complexity of the cellular proteome, influencing gene transcription, protein conformation, localisation, activity, stability, and function. The majority of PTMs are reversible, and their addition and removal are regulated by various enzymes. PTMs include modifications through small chemical groups such as acetylation, phosphorylation, or methylation, as well as redox modifications, whereby the chemical properties of an amino acid are altered, as well as the covalent linkage of another protein to a target, such as during ubiquitination or SUMOylation. Dysregulation of PTMs is a cause and consequence of a multitude of pathologies, including aging, cancer, neurodegenerative diseases, immune diseases and metabolic disorders (Zhong et al., 2023). Thus, gaining a deeper understanding of how PTMs influence healthy physiology and disease has been a crucial research focus since their discovery.

1.1 ADP-ribosylation

ADP-ribosylation was first discovered as a PTM in the 1960s, as a polymer made up of adenosine diphosphate ribose, derived from nicotinamide adenine dinucleotide (NAD^+) (Chambon et al., 1963, Chambon et al., 1966). Today, it is known that ADP-ribosylation is widespread in all kingdoms of life, including prokaryotes and all six major eukaryotic supergroups, likely due to the ubiquitous and reactive nature of the donor molecule NAD^+ (Suskiewicz et al., 2023).

1.1.1 Structure and Significance

During ADP-ribosylation, “writers” transfer a single, or multiple units of ADP-ribose from nicotinamide adenine dinucleotide (NAD^+) onto specific amino acid residues of substrate proteins or nucleic acids, releasing nicotinamide as a by-product.

The adenosine-distal ribose of ADP-ribose units are attached to the acceptor amino acid of a target protein (Asp, Glu, Ser, Tyr, Arg, His, Thr or Cys) through an O-, N- and S-glycosidic bond, to the 2'-hydroxyl of the adenosine-proximal ribose of the preceding ADP-ribose unit during elongation, or to the distal ribose of another ADP-ribose unit during branching through formation of a glycosidic bond (Figure 1.1). *In vitro*, these ADP-ribose chains may include up to 200 ADPr units, encompassing diverse morphologies and branching points (Alvarez-Gonzalez & Jacobson, 1987). 5'- or 3' terminal phosphates of a single- or double-stranded break of DNA or RNA can also serve as targets for the attachment of ADP-ribose (Groslambert et al., 2021; Munnur et al., 2019).

ADP-ribosylation influences cellular function in many ways, including signal transduction by providing a scaffold for the recruitment and binding of ADP-ribose binding proteins ("readers") and modification of the biochemical properties of a target protein by affecting its catalytic activity or its charge profile. In prokaryotes, ADP-ribosylation was first discovered as a method of warfare, with cholera and diphteria toxins killing host cells by ADP-ribosylating essential cellular proteins (Honjo et al., 1968). ADP-ribosylation has since been shown to be involved in the cellular stress response, microbial metabolism, transcription, cellular proliferation and differentiation, apoptosis, inflammation, viral infection and the maintenance of genome integrity (Cohen & Chang, 2018; Crawford et al., 2021; Mikolčević et al., 2021; Palazzo et al., 2019; Perina et al., 2014; H. Wei & Yu, 2016). As such, homeostasis of ADP-ribosylation is tightly regulated by "writers", the enzymes catalysing ADP-ribosylation, "readers", proteins containing ADP-ribose binding domains important for signal transduction, and "erasers", which modify or remove ADP-ribosylation. The dysregulation of this PTM is associated with several diseases, including neurodegeneration and cancer, and as such, it has increasingly become a therapeutic target, particularly for cancer.

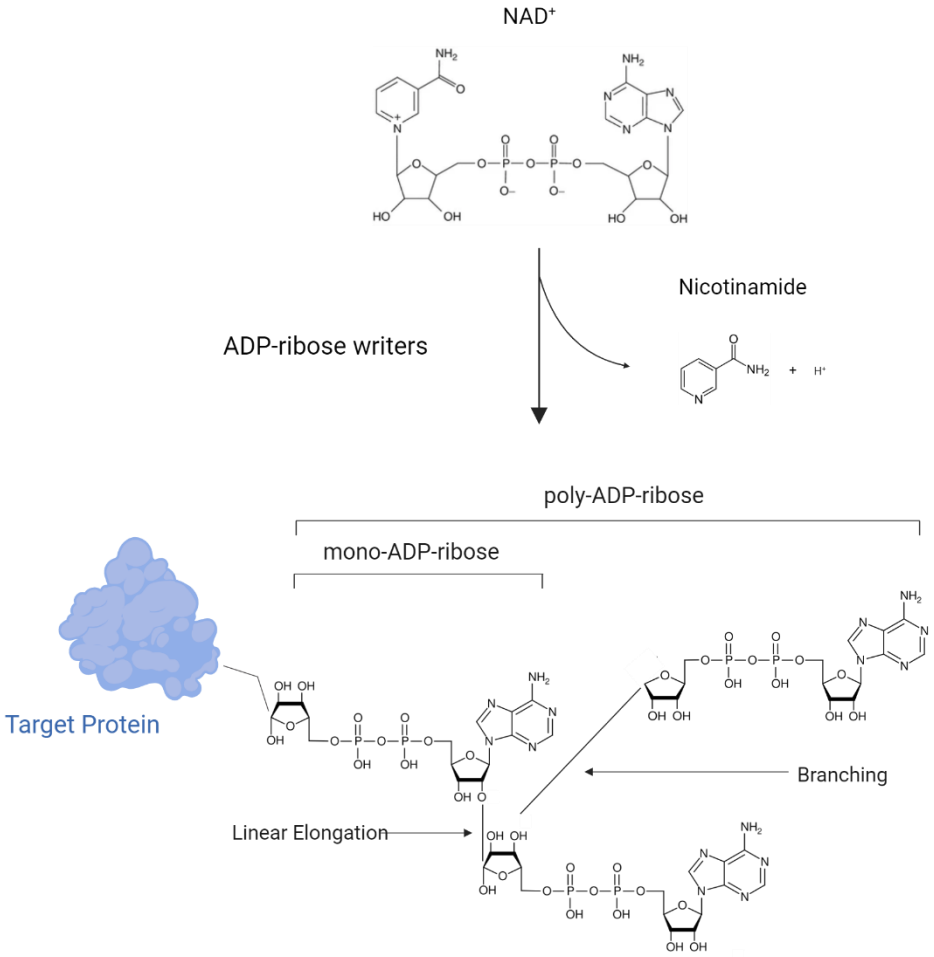

Figure 1.1: Molecular structure of ADP-ribosylation. NAD^+ serves as a substrate for ADP-ribose writers to attach single or multiple units of ADP-ribose onto a target protein (or nucleic acid). ADP-ribose chain extension can occur in a linear or branched fashion.

1.1.2 Writers of ADP-ribosylation

The majority of writers of ADP-ribosylation, and the best studied, are part of the ADP-ribosyltransferase (ART) superfamily, which are further divided into three clades based on the amino acid composition of their active sites (clade I: H-Y-[EDQ], clade II: R-[ST]-E, clade III: H-H-h) (Lüscher et al., 2021). The majority of clade I eukaryotic ART enzymes are referred to as ARTDs (diphteria-like) and are intracellular, while eukaryotic clade II ART

enzymes that are secreted are designated ARTCs (cholera-like) (Lüscher et al., 2021). The intracellular ARTD branch of the family comprises 17 members in humans, consisting of PARPs (poly(ADP-ribose)-polymerases), and tankyrase 1 and 2 (TNKS1/2, or PARP5a/b). Despite their name, only the founding member PARP1, and its close homologue PARP2, as well as TNKS1/2, are capable of producing poly-ADP-ribose (PAR) chains, with all others only capable of catalysing mono-ADP-ribose (MAR), or are catalytically inactive (Lüscher et al., 2021; Vyas et al., 2014). Due to this inconsistency, it was recently suggested that "PARPs" be used as a name in its own right, rather than as an abbreviation (Lüscher et al., 2021). All ARTs share a common core "split β sheet", comprising two three-stranded antiparallel β sheets and two α-helical regions, with the NAD^+ binding pocket located between the two β sheets (Suskiewicz et al., 2023). All 17 PARP family members share a C-terminal (with the exception of PARP4) PARP-typical ART domain, with otherwise variable domain composition (Figure 1.2).

Eukaryotic ARTD, or PARP, family members are classified into 6 clades. Clade 1, or the PARP1 clade, in humans contains PARP1, PARP2 and PARP3, and is defined by the presence of a WGR domain and their involvement in DNA repair (Perina et al., 2014). Clade 2 consists of plant PARPs and Clade 3 is heterogeneous and in humans consists of PARP7 and PARP9-15. Clade 4 is made up of tankyrases (TNKS1/2, or PARP5a/b), which contain ankyrin repeats, Clade 5 contains PARP4 and homologues that share characteristics of vault proteins (vault PARPs), and Clade 6 is made up of human PARP6, PARP8 and PARP16, all of which have MARylation activity (Perina et al., 2014). The structure and activation of PARP1 and PARP2, which will be the main focus of this study, will be discussed in the following sections. Other proposed writers of ADP-ribosylation include sirtuins, originally discovered in yeast, which primarily function as NAD^+-dependent deacetylases and epigenetic silencers. Some bacterial and fungal sirtuins act as pathogens, with ADP-ribosylation as their

primary function, with evidence for some secondary ADP-ribosylating activity in some human sirtuins (SIRT4, SIRT6 and SIRT7) (Suskiewicz et al., 2023).

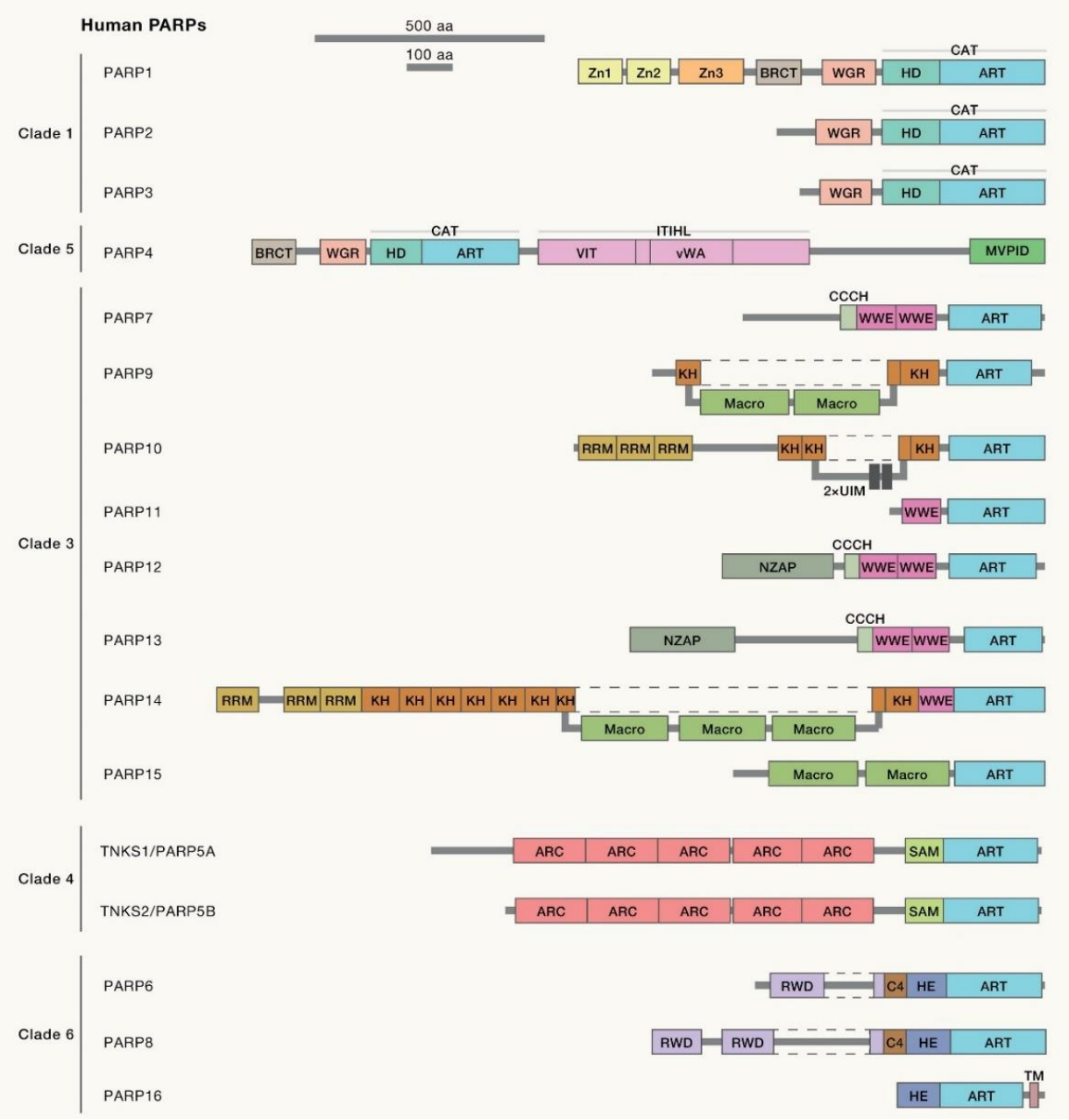

Figure 1.2: Overview of the clade classification of the human PARP superfamily and their domain architecture. Clade 1 PARPs contain a WGR domain, and an autoinhibitory helical domain (HD) as part of their catalytic domain. Clade 3 contains PARP7 and PARP9-15, a heterogeneous group. Clade 4 is made up of tankyrases, which carry multiple ankyrin repeats that serve as scaffolds for protein-protein interactions. Clade 5 consists of PARP4, which contains VIT and vWA domains characteristic for vault proteins. Clade 6 consists of PARP6/8/16, and is thought to have MARylation activity. Adapted from Suskiewicz et al., (2023).

1.1.3 Readers of ADP-ribosylation

One of the ways by which the ADP-ribosylation signal is transduced is through proteins which can recognise and non-covalently bind ADP-ribose through specific ADP-ribose binding domains, in turn changing their localisation or interaction with other proteins. Many proteins contain ADP-ribose binding motifs, and several classes have been identified to date, Specific ADP-ribose domains can determine the preference of a protein for a certain type of ADP-ribose (Figure 1.3), and these domains can in turn be exploited to study the types of ADP-ribose modifications generated by different ADP-ribose writers under different circumstances. Some of the most common and best studied ADP-ribose binding domain classes are described below.

PAR-binding motifs (PBMs)

First discovered as DNA checkpoint proteins, PBMs contain conserved sequences of interspersed hydrophobic and basic amino acid residues preceded by a cluster of positively charged residues such as lysine or arginine, interacting with ADP-ribose through electrostatic affinity (Pleschke et al., 2000). Proteins containing PBM motifs include p53, p21, DNA Ligase III, XRCC1, DNA-PKCs, Ku70, NF-kappaB, and telomerase (Pleschke et al., 2000). PBMs are predicted to be found in over 800 proteins (P. Li et al., 2022), many of which are contained within other domains involved in DNA binding, protein-protein interactions and nuclear localisation. Mutation of the PBM motif within the PCNA binding region of p21 was shown to abolish its interaction with PCNA, causing its degradation (Pleschke et al., 2000). PBMs prefer to bind long and branched PAR chains (Krietsch et al., 2013).

PAR-binding zinc fingers (PBZs)

PBZ domains are roughly 30 amino acids in length, with the consensus sequence [K/R]-X-X-C-X-[F/Y]-G-X-X-C-X-[K/R]- [K/R]-X-X-X-X-H-X-X-X-[F/Y]-X-H, containing two zinc-ion coordinating cysteines and histidines each (I. Ahel et al., 2008). PBZs specifically interact with ADP-ribose at the junctions between two ADP-ribose units through hydrogen bonds, thus specifically recognising PAR chains (Li et al., 2022). PBZs were first identified in APLF, an endonuclease and histone chaperone important in non-homologous end-joining (NHEJ), which contains tandem repeats of PBZs and has a correspondingly high affinity for ADP-ribose (I. Ahel et al., 2008; P. Li et al., 2022). PBZs are not found as widely as other ADP-

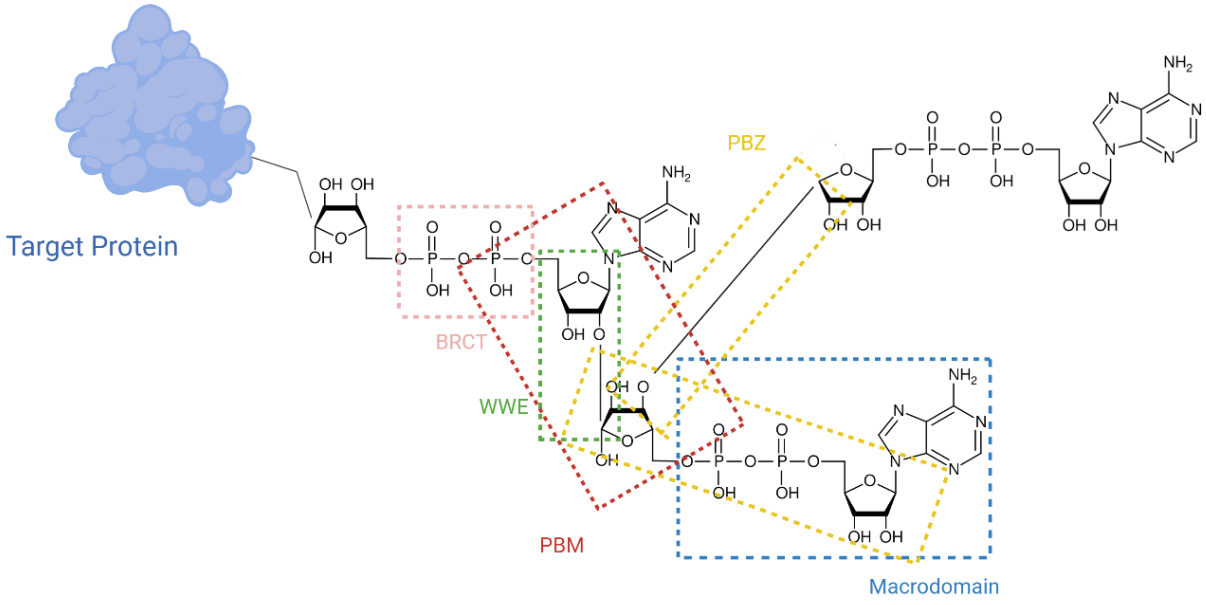

Figure 1.3: Overview of common ADP-ribose reader domain binding preferences. PBMs prefer long and sometimes branched PAR chains. PBZs recognise PAR chains by interacting with the junctions between ADPr units. Macrodomains vary in their ADP-ribose binding properties, and are classified into different types based on their preference. Most WWE domains bind PAR chains by recognising the iso-ADP-ribose link between ADP-ribose units. BRCT domains recognise the phosphate group of an ADPr unit through electrostatic interactions.

ribose binding domains, but one functional PBZ was identified in CHFR, an E3 ubiquitin ligase which binds and ubiquitinates auto-modified PARP1, initiating the first wave of ubiquitination following DNA damage and promoting the eviction of PARP1 from DNA damage (C. Liu et al., 2013). A PBZ variant is also found in CHK1, a key checkpoint kinase of the DNA damage response, mutation of which impairs CHK1-mediated S-phase checkpoint activation and its retention at stalled replication forks (Min et al., 2013).

Macrodomains

Having likely co-evolved with PARP proteins and sirtuins, macrodomains are widespread, found in prokaryotes, archaea, eukaryotes, and even some viruses, ranging from 130 to 190 amino acids in length (Rack et al., 2016). They share a conserved structure consisting of a three-layered globular α/β/α sandwich made of a central six-stranded β-sheet surrounded by five α-helices, but low sequence homology (Li et al., 2022). Owing to this low sequence conservation, different macrodomains range widely in their ADP-ribose binding, and even hydrolysing, ability, and can in humans be classified into the following classes with differing preferences: MacroH2A-like, MacroD-type, PARG-like and ALC1-like (Rack et al., 2016). Twelve proteins in humans contain macrodomains, some of which are different variants of histone H2A (Li et al., 2022), providing a mechanism for ADP-ribosylation to directly impact chromatin. MacroH2A1.1 specifically recognises MAR and the terminal ADP-ribose unit of PAR chains, and by recognising auto-modified PARP1 it promotes a transient increase in chromatin density, γH2AX levels and inhibits recruitment of NHEJ protein Ku70 to sites of damage. (Timinszky et al., 2009). Meanwhile, the splice variant macroH2A1.2, or histone MacroH2A2 do not bind ADP-ribose, and do not transduce PARP1-mediated chromatin rearrangement (Timinszky et al., 2009).

ALC1 (Amplified in Liver Cancer 1/CHD1L), a SNF2-family type chromatin remodeller and oncogene amplified in many solid tumours, also contains a macrodomain (Karras et al., 2005).

The macrodomain of ALC1 was shown to interact with PAR oligomers of between at least 3 and 20 units of ADP-ribose and above, but not MAR, causing ALC1 to be recruited to sites of DNA damage by the activity of PARP1, which in turn relieves its autoinhibition and triggers its own catalytic activity, inducing nucleosome remodelling and chromatin relaxation (D. Ahel et al., 2009; Singh et al., 2017). Multiple macrodomains are also found in PARP9, PARP14 and PARP15; PAP14 contains three macrodomains, two of which (macrodomain 2 and 3) are readers of mono-ADPr, while one of them (macrodomain 1) has hydrolytic activity (Dukić et al., 2023). The MacroD-type and PARG like macrodomains will be discussed below as hydrolytic macrodomains.

WWE domains

WWE domains, named after their conserved tryptophane and glutamate residues, are roughly 80 amino acids in length, globular, and have been identified in three different groups of proteins. The first group only contains one protein, DDHD2, the WWE domain of which does not bind PAR *in vitro* (Li et al., 2022). The next group are ADP-ribosylating proteins, such as PARP7, PARP11, PARP12, PARP13 and PARP14, none of which are capable of catalysing PARylation (Li et al., 2022). The third group of proteins containing WWE domains are ubiquitin ligases, such as RNF146, Deltex1-4 and TRIP12. Binding to PAR by the WWE domain of RNF146 causes a conformational change in the protein, stimulating its catalytic activity (DaRosa et al., 2015), and TRIP12 binds auto-modified PARP1, targeting it for proteasomal degradation (Gatti et al., 2020). WWE domains vary in their ADP-ribose recognising properties. While RNF146 and TRIP12 recognise the iso-ADP-ribose link between ADP-ribose units of PARylated proteins, the WWE domain of PARP11 interacts with the terminal ADP-ribose moiety (He et al., 2012).

BRCT domains

Originally understood to be readers of phosphorylation and regulators of protein-protein interactions, some BRCT domains have been shown to also bind ADPr, likely recognising the phosphate groups in the ADP-ribose through electrostatic interactions (M. Li & Yu, 2013a; Rudolph, Muthurajan, et al., 2021). Despite low sequence homology, typical BRCT domains are globular structures of between 90 and 100 amino acids arranged in a four-pronged β sheet interspersed by α-helices (β α β β α β α) (Wu et al., 2015). Twenty three genes in humans have been identified as having at least one BRCT domain, many of which are involved in the DNA damage response (DDR), such as XRCC1 (X-ray repair cross-complementing protein 1), DNA Ligase III, DNA Ligase IV, and BARD1 (BRCA1-associated RING domain protein 1) (Teloni & Altmeyer, 2016). In XRCC1, the first BRCT domain is responsible for interaction with PAR and DNA and likely allows for the recruitment of XRCC1 to the damage site by PAR followed by retention at the damage site through interaction with DNA, where it acts as a scaffold for DNA repair factors (Polo et al., 2019).

1.1.4 Erasers of ADP-ribosylation

As a dynamic PTM that affects a multitude of cellular processes, ADP-ribosylation must be spatially and temporally regulated, making its removal an integral part of ADP-ribosylation signalling and cellular homeostasis. Owing to the different linkages that connect ADP-ribose units to their target (the *N*, *O*, or *S*-glycosidic bond between the terminal ADP-ribose and an amino acid or nucleic acid, the ribose-ribose bond between ADP-ribose units of a linear PAR chain, and the ribose-ribose bond at a PAR branching point), different enzymes are employed to digest the variety of these linkages. Erasers can be classified into three distinct families: the macrodomain-containing enzymes, the ADP-ribosyl-acceptor hydrolases, and phosphodiesterases, the latter of which were the most recently identified, and will not be discussed in this work.

Macrodomain-containing hydrolases

Like their ADP-ribose binding ability, macrodomains also differ in which substrates they prefer for their hydrolytic activity. Members of the PARG-like class of macrodomains are generally associated with hydrolysis of PAR chains and members of the MacroD and ALC1-like classes with MAR hydrolysis (Rack et al., 2016).

Mammalian PARG (poly-ADP-ribose glycohydrolase), the macrodomain of which is the founder of the PARG-like class of macrodomains, is encoded by a single gene, alternative splicing of which provides diversity in sub-cellular location of the protein (Rack et al., 2016). PARG is recruited to DNA damage sites by PARP1/2 generated PAR, where its hydrolase activity is important for efficient DNA repair (Mortusewicz et al., 2011). PARG, as the only hydrolytic macrodomain to do so, hydrolyses the glycosidic bond between two ADP-ribose units by positioning the *O*-glycosidic ribose-ribose bond close to its catalytic glutamates (Rack et al., 2016). It shows preference for the end of ADP-ribose chains, acting predominantly as an exo-glycohydrolase *in vivo*, preferring PAR chains longer than four ADPr units, and is capable of hydrolysing PAR branch points (Barkauskaite et al., 2013; Rack et al., 2016, 2021) (Figure 1.4). PARG, however, is unable to remove the terminal ADP-ribose unit from a target protein or nucleic acid. For this removal of the terminal ADP-ribose moiety, other hydrolases are required.

MacroD1 and MacroD2 (mono-ADP-hydrolase 1 and 2) both hydrolyse mono-ADP-ribosylated substrates *in vitro*, removing the terminal ADPr moiety preferentially from acidic amino acids, and share a common macrodomain fold, but are associated with different subcellular localisations and distinct functions, although they are poorly understood (Crawford et al., 2021; Jankevicius et al., 2013; Rosenthal et al., 2013).

MacroD1 is predominantly found in mitochondria, and is highly expressed in skeletal muscle, and was implicated as an essential co-factor in NF-κB activation and for estrogen and androgen receptor signalling (Han et al., 2007; J. Yang et al., 2009). MacroD2 is highly expressed in the brain and largely found in the nucleus and cytoplasm and has been linked to a variety of neurological and psychiatric conditions, including autism, ADHD and schizophrenia (Crawford et al., 2021). In agreement with skeletal muscle expression and estrogen/androgen receptor association, *MacroD1* knockout (KO) mice show female-specific motor-coordination defects, while *MacroD2* KO mice exhibit hyperactivity and gait disturbances consistent with the reported neurological phenotype (Crawford et al., 2021). Dysregulation of both has also been implicated in cancer, although the validity of these findings has been put into question (Feijs et al., 2020). TARG1, part of the ALC1-class of macrodomain hydrolases, is primarily located in the nucleus and like MacroD1 and MacroD2, specifically removes MAR from acidic residues, such as glutamate and aspartate (Sharifi et al., 2013) (Figure 1.4).

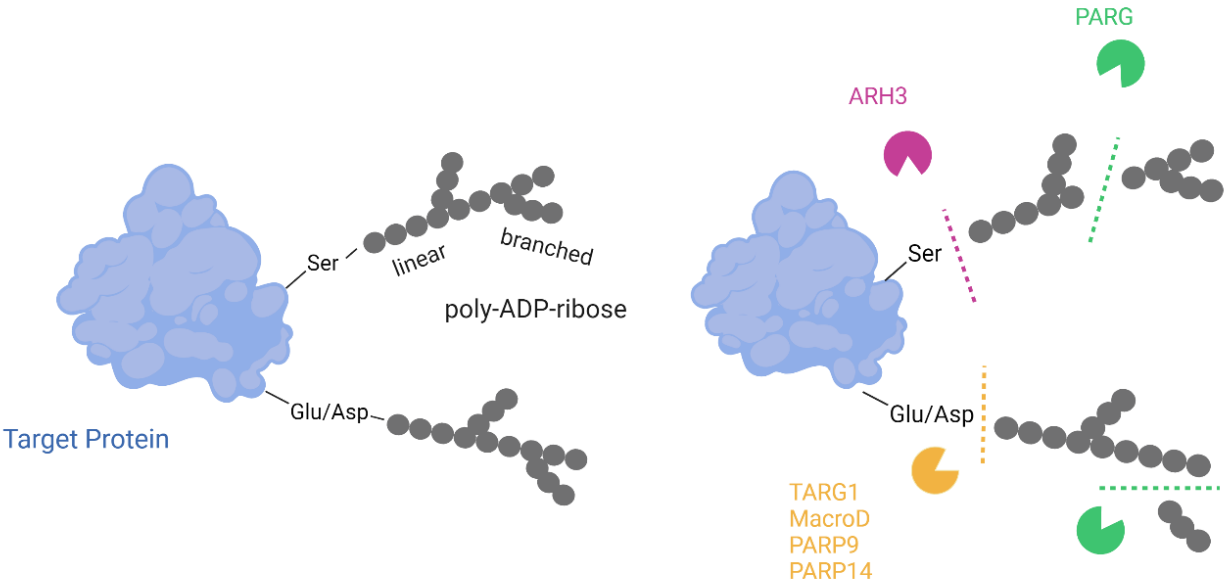

Figure 1.4: Schematic overview of the preferences and function of different ADP-ribose erasers. ARH3 removes the terminal MAR from serine residues, while TARG1, MacroD, PARP9 and PARP14 can hydrolyse the bond between the terminal ADP-ribose and Glu/Asp. PARG is able to digest linear and branched PAR chains, but cannot remove the terminal ADP-ribose unit.

ADP-ribosyl-acceptor hydrolases (ARHs)

The ADP-ribosyl-acceptor hydrolase (ARH) family of ADPr erasers consist of three members, ARH1-3. ARH1 specifically removes the *N*-glycosidic bond between the terminal ADPr and arginine residues, while ARH3 is the only human enzyme capable of hydrolysing the *O*-glycosidic bond between ADPr and serine residues, and at least *in vitro* is capable of hydrolysing linear, but not branched, PAR chains, albeit with much lower activity than PARG (Fontana et al., 2017a; Oka et al., 2006) (Figure 1.4). ARH3 was further shown to hydrolyse the *O*-glycosidic bond between ADPr and nucleic acids (Li et al., 2022). ARH3 is localised to the nucleus, cytoplasm and mitochondria (Schützenhofer et al., 2021). In its inactive state, ARH3 is autoinhibited by interaction of one catalytic glutamate with Mg^{2+} and sequestering of the other, which is relieved by substrate binding (Schützenhofer et al., 2021). ARH2 was not shown to have any enzymatic activity (Li et al., 2022).

1.2 ADP-ribosylation in the DNA damage response

With DNA under constant threat of both endogenous and exogenous damage, maintenance of genome integrity is crucial for cellular and organismal health. Because of this, cells have evolved highly conserved signalling pathways to detect and repair damaged DNA, known as the DNA damage response (DDR). Failure to do so underlies a plethora of pathologies, including ageing, neurodegenerative disease, and cancer. PARP1-3, are directly involved in DNA repair, and recruitment of PARP1, the founding member of the PARP family of proteins, to the site of damage is one of the earliest events of the DDR. In the following sections, I will discuss the structure and activation of PARP1-3, and their role in DNA repair.

1.2.1 PARP1 structure and activation

PARP1 is a multidomain protein consisting of 1014 amino acids and a molecular weight of roughly 113 kDa. In eukaryotes, it is, after histones, the most abundant nuclear protein, and produces up to 90% of the ADP-ribosylation induced in response to DNA damage (D'amours

et al., 1999; C. Thomas et al., 2019). At its N-terminus, PARP1 contains three DNA-binding zinc fingers (Zn1-3), followed by a BRCT and WGR domain, both of which are also involved in DNA binding (Figure 1.5, a). At its C-terminus, the catalytic domain is divided into the HD and ART subdomains (Figure 1.5, a). Before binding of PARP1 to DNA, in its inactivate state, the HD is folded over the catalytic residues in the ART domain to avoid undue access of NAD^+, providing an autoinhibitory mechanism. Biochemical modelling and structural analyses have shown that upon binding to DNA through its Zn1, Zn3 and WGR domains, an intramolecular signal wave travels through PARP1, resulting in allosteric changes that allow NAD^+ access to the ART and catalytic activation.

Unlike other zinc fingers, Zn1-3 recognise DNA structures, rather than specific sequences; Zn1 and Zn2 form hydrophobic contacts with the phosphate backbone of DNA via positively charged grooves on their surface, and hydrogen bonds with exposed bases at the break (Ali et al., 2012; M. F. Langelier et al., 2011). While Zn1 is crucial for DNA-dependent activation of PARP1, Zn2, despite having much greater DNA binding affinity than Zn1, is dispensable but might be important for rapid PARP1 recruitment to DNA and/or its retention at the break site (Haince et al., 2008; M. F. Langelier et al., 2011). Zn2 of PARP1 was also shown to be primarily responsible for binding of PARP1 to single-stranded breaks (SSBs) (Eustermann et al., 2011). Zn3 mediates interdomain communication, and is structurally and functionally distinct from Zn1 and Zn2, binding the minor groove of the DNA phosphate backbone adjacent to Zn1 (Langelier et al., 2012). The crystal structure of PARP1 bound to a double-stranded break (DSB) revealed that Zn1 and Zn3 reside next to each other on DNA, facing one side of the WGR domain, which binds to the 5' terminus of one strand and which in turn is facing the HD (M.-F. Langelier et al., 2012) (Figure 1.5, a). DNA binding positions Zn1 D45 to form a salt bridge with R591 of the WGR domain, which on its other side contacts

hydrophobic residues in the HD (M.-F. Langelier et al., 2012). Similarly, W318 in Zn3 forms an interface with WGR K633 and R735 of the HD (Langelier et al., 2012).

As a result of the Zn1-WGR-HD and Zn3-WGR-HD contacts, the HD interface with the ART is affected. Contact of the HD with WGR displaces conserved leucine residues (L698 and L701) that form part of a hydrophobic HD core (Langelier et al., 2012). A later study showed that the allosteric changes going through the HD, especially α helices B and F were extensive, demonstrating how this "leucine switch"-mediated HD distortion opens up the catalytic cleft for NAD^+ to access the ART (Dawicki-McKenna et al., 2015). Mutations of any of these zinc finger or WGR interface contacts abolishes DNA-dependent activation of PARP1, and mutation of core hydrophobic residues of the HD was shown to lead to constitutive activation of the protein (Langelier et al., 2012; Dawicki-McKenna et al., 2015).

The BRCT domain sits between Zn3 and the WGR domains and is dispensable for PARP1 DNA-dependent activation, and while initially thought to mainly serve protein-protein interactions, it was recently shown to be another DNA binding module (Rudolph, Muthurajan, et al., 2021). Unlike the other PARP1-DNA binding domains, the BRCT binds intact DNA; this was suggested to provide PARP1 with a rapid way of searching for DNA lesions through a "monkey bar" mechanism, allowing it to rapidly dissociate from DNA breaks by binding intact DNA and moving through undamaged chromatin without activation of its catalytic activity (Rudolph et al., 2021).

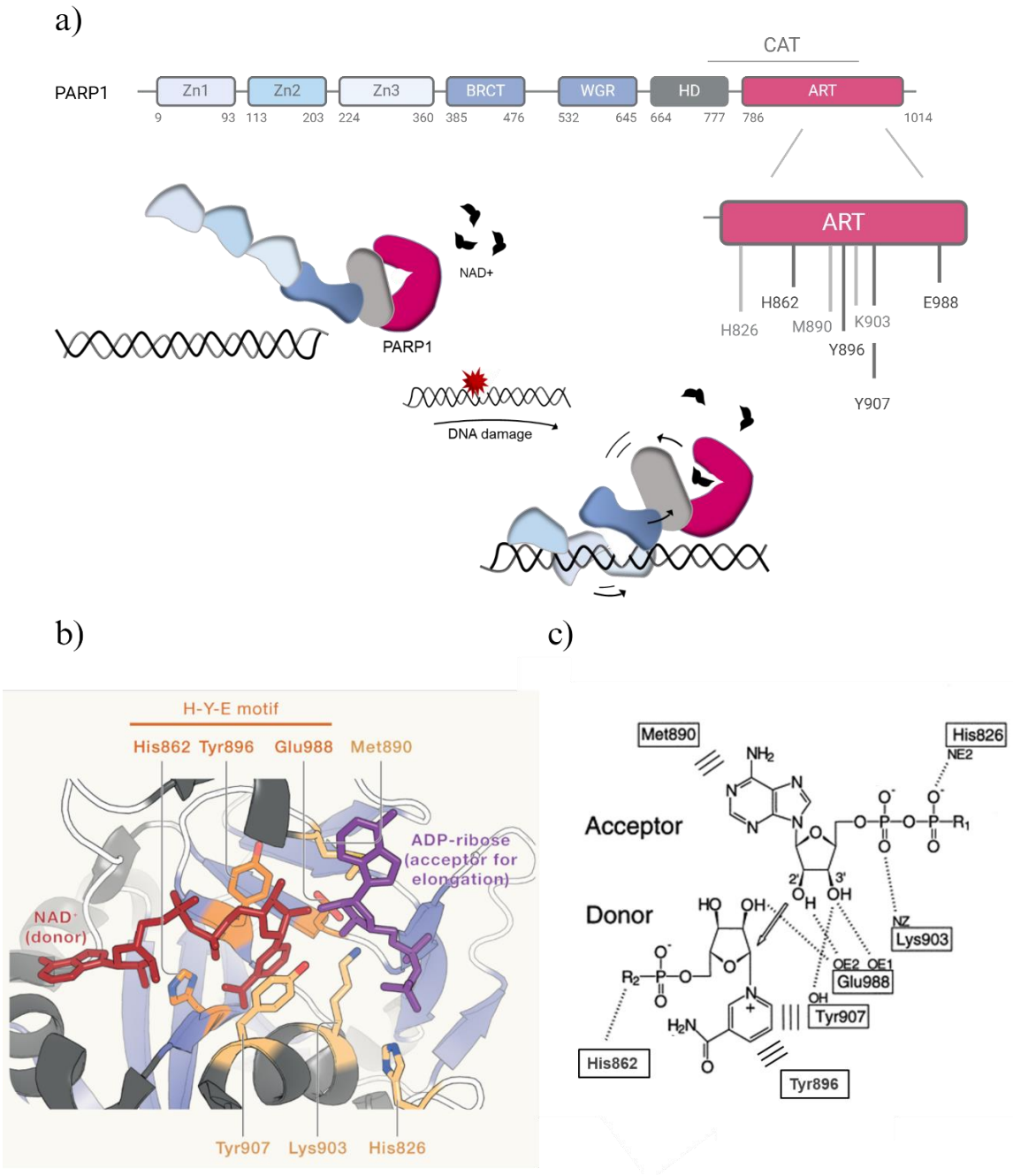

Figure 1.5: Schematic representation of PARP1 activation and the catalytic reaction. a) In its inactive state, PARP1 is thought to assume an unstructured conformation, with the HD domain blocking the catalytic cleft. Upon binding of a DNA break, the allosteric changes travel through the Zn1-WGR-HD and Zn3-WGR-HD interface, allowing access of the substrate NAD^+ to the active site. **b)** Structural model of the PARP1 active site during PAR chain elongation. Taken from Suskiewicz et al., 2023. **c)** Schematic drawing showing the role of key PARP1 residues in the PAR chain elongation reaction. Hydrogen bonds are shown in dotted lines, nonpolar stacking interactions are shown by parallel bars, and the nucleophilic attack is denoted by the arrow. Donor and acceptor NAD+ molecules are incomplete. Adapted from Ruf et al., 1998, reused by permission from Elsevier and Copyright Clearance Center on behalf of the Journal of Molecular Biology (License Number 5983110134910).

The ART domain of PARP1 is composed of a NAD^+ binding site, or donor site, which positions ADP-ribose for the transferase reaction, and an acceptor site which binds either the protein target during initiation or the distal ADPr unit of a growing PAR chain (Barkauskaite et al., 2015). The donor site of PARP1 contains the conserved His-Tyr-Glu triad, with His862, Tyr896 and Glu988 (Barkauskaite et al., 2015) (Figure 1.5, b). During the enzymatic process, the nucleophile of a side-chain of the acceptor amino acid, or the 2'-OH of a preceding PAR chain, is positioned for a nucleophilic attack on the $C1'_N$ atom of the donor NAD^+, resulting in the formation of a glycosidic bond, and the release of nicotinamide as a byproduct (Suskiewicz et al., 2023; Figure 1.5, c). In the donor site, E988 forms hydrogen bonds to the 2'-OH and the 3'-OH of the donor nicotinamide ribose, positioning it for nucleophilic attack (Figure 1.5, c). While E988 was shown to be dispensable for initiation, with intrinsic nucleophiles of target amino acids not requiring activation by E988, it also hydrogen bonds to the 2'-OH of the acceptor ribose of a terminal PAR unit, and its function as a base is essential for nucleophilic attack and elongation (Marsischky et al., 1995; Alemasova & Lavrik, 2019). Y896 binds the donor NAD^+ by stacking with the nicotinamide ring (Figure 1.5, c), and H862 binds to the 2'-OH of the donor adenine ribose (Figure 1.5, c). Y907 also hydrogen bonds to the 3'-OH of the donor nicotinamide moiety, orienting it for nucleophilic attack.

The acceptor site binds and poises the acceptor amino acid or terminal ADPr unit of a PAR chain: during elongation, H826 engages the β-phosphate of the acceptor ADP (Figure 1.5, c), and K903 forms hydrogen bonds with the α-phosphate of the acceptor ADP, and its role in elongation was demonstrated by replacement of this residue in other mono-ADPr PARPs, and the fact that its mutation restricts catalytic output of PARP1 to MARylation (Alemasova & Lavrik, 2019; Carter-O'Connell et al., 2014; Ruf et al., 1998) (Figure 1.5, c). M890 of the acceptor site stacks against the acceptor adenine moiety (Figure 1.5, c), and random mutation

of this residue to valine also causes a loss of PARylation activity due to clashing with the side chain of Y896 or ADP (Alemasova & Lavrik, 2019; Rolli et al., 1997).

In summary, the structure and function of PARP1 are intricately tied to its ability to recognize DNA damage and mediate cellular responses through ADP-ribosylation. The cooperative interactions among its zinc fingers, WGR domain, the HD and catalytic domains ensure the efficient activation of the protein in response to DNA breaks.

1.2.2 PARP1 in DNA repair

PARP1 and chromatin remodelling

One of the major targets of PARP1 are histones (Gibbs-Seymour et al., 2016), and PARP1 itself (Satoh & Lindahl, 1992). The modification with ADP-ribose adds negative charge onto the target, which is thought to lead to electrostatic repulsion between the ADP-ribose polymer and DNA (Satoh & Lindahl, 1992). The modification of histones with ADP-ribose is responsible for the rapid decondensation of chromatin observed at sites of DNA damage (Messner & Hottiger, 2011; Strickfaden et al., 2016), allowing access of DNA repair factors to stalled replication forks or DNA breaks. PARP1 itself being a major target, is extensively auto-modified upon DNA-dependent activation; as observed *in vitro*, this auto-modification is required for PARP1 to efficiently dissociate from DNA (Satoh & Lindahl, 1992). This is thought to underlie the rapid recruitment and dissipation of PARP1 from sites of DNA damage; loss of PARP1 catalytic activity leads to prolonged retention of PARP1 at the site of damage, which is associated with unfavourable repair outcomes. PARP "trapping" at damage sites and PARP inhibitors will be discussed in further detail in section 1.4.

ALC1 (Amplified in Liver Cancer 1), is a SNF2-family chromatin remodeller that is rapidly recruited to DNA-damage associated PAR via its C-terminal macrodomain, and its ATPase activity is strongly stimulated by interaction with PAR (D. Ahel et al., 2009). It is

overexpressed in many solid tumours and is associated with tumour progression and poor patient outcomes (Ma et al., 2008). Recruitment of ALC1 to DNA lesions depends on PARP1 catalytic activity, and its resulting ATPase activity is a key mediator of PAR-induced chromatin relaxation (Sellou et al., 2016). It appears that chromatin relaxation is the main factor promoting recruitment of a host of DDR factors following ADP-ribosylation; one study found that it is this PAR-dependent chromatin relaxation, rather than direct interaction of proteins with PAR chains, that was responsible for recruitment of a host of DNA-binding DDR factors (Smith et al., 2019). PARP1 activity therefore creates a permissive chromatin microenvironment around the DNA damage site.

ADPr-dependent chromatin relaxation was also shown to depend on a site-specific ADP-ribosylation code, allowing the choice of one cellular pathway over another. For instance, ADP-ribosylation of histone H3S10 was found to be mutually exclusive with acetylation of H3K9 and phosphorylation of H3S10, modifications associated with active gene transcription and mitosis, respectively. This provides a mechanism for ADP-ribosylation to block unwelcome transcription and DNA replication after DNA damage and direct cells towards DNA repair (Bartlett et al., 2018). Meanwhile, methylation of H3K9 and H3K27, which are associated with transcriptional repression, was shown to coexist with ADP-ribosylation at proximal residues, as this agrees with cellular pathway choice (Bartlett et al., 2018).

PARP1 in single-stranded break repair

PARP1 was shown to play an important role in base-excision-repair (BER). BER is responsible for the repair of alkylated, oxidated or deaminated bases, abasic sites and SSBs, which, if left uncorrected, stall DNA replication and transcription, and can ultimately lead to the generation of DSBs (Spiegel et al., 2021). BER involves removal of an altered base by a family of enzymes called DNA glycosylases, leaving an abasic site, which is then excised by another endonuclease, leaving nicked DNA with a one-base gap (Spiegel et al., 2021). This

single-stranded DNA nick is then recognised by PARP1, and PARP1-mediated ADP-ribosylation is required for recruitment of XRCC1, a scaffold protein that coordinates various other DNA repair factors. For instance, XRCC1 mediates DNA end-processing by recruiting enzymes such as APE1, PKNP and TDP1, and nick-sealing, through its recruitment of DNA polymerase β, DNA ligases I and III, ultimately leading to ligation and repair of the gap in the DNA (Caldecott, 2019; Polo et al., 2019; Reber et al., 2023).

XRCC1, which binds ADP-ribose via its BRCT domain, was shown to have a clear preference for PAR chains, as its recruitment to damage sites was significantly impaired when PARP1 mutants were used that only produced MAR and short ADPr chains (Aberle et al., 2020).

Certain genotoxic stressors, such as metabolic by-products and chemotherapeutic agents, as well as UV-irradiation, can induce bulky DNA lesions which can distort the DNA helix. These consist of DNA-protein crosslinks (DPCs), interstrand crosslinks (ICLs), 6-4-photoproducts, UV-induced thymine dimers and other cyclobutene pyrimidine dimers (Naumenkoa et al., 2022). These lesions are repaired by the nucleotide excision repair (NER) pathways, which can be split into transcription-coupled (TC-)NER, which removes lesions from actively transcribed genes, and the global genomic (GG-)NER, which involves the removal of a 24-32 nucleotide stretch of single-stranded DNA containing the bulky lesion, followed by filling of the gaps and ligation of the nicks (Cleaver et al., 2009). PARP1 activity was shown to be activated by UV-induced damage early on (Vodenicharov et al., 2005). GG-NER is initiated upon recognition of the lesion by DDB2 (XPE), which as part of the UV-DDB-E3 ligase complex ubiquitinates and recruits XPC (Xeroderma Pigmentosum C), to the site of damage (Fei et al., 2011; Sugasawa et al., 2005). XPC, in tandem with RAD23B, recognises unpaired bases and mediates unwinding of DNA, paving the way for subsequent strand incision, gap filling and DNA ligation (Kusakabe et al., 2019). Upon binding to the

break site, catalytic activity of PARP1 was shown to promote its interaction with and ADP-ribosylation of the UV-DDB ligase complex, which in turn promotes recruitment of XPC and efficient repair of UV-induced DNA lesions (Robu et al., 2013). It was further shown to form a stable complex with XPC independently of the UV-DDB ligase complex, rapidly escorting it to sites of UV-lesions (Robu et al., 2017). Consequently, loss or inhibition of PARP1 catalytic activity impairs recruitment of XPC, and repair of UV-lesions (Robu et al., 2017).

PARP1 in double-stranded break repair

The predominant form of double-stranded break (DSB) repair during S/G2 phases is homologous repair (HR). It allows for the non-erroneous, faithful correction of the break by using the homologous strand as a template. It is accomplished through a series of steps, which can be divided into initiation, strand invasion, branch migration, resolution, and DNA synthesis (Prakash et al., 2015). The first step involves recruitment of the MRN (MRE11-RAD50-NBS1) complex and CtIP, which resects the DNA strand, exposing a single-stranded (ss)DNA overhang on either side of the break, which is subsequently bound and protected by RPA (Replication Protein A). The MRN complex also activates the checkpoint kinase ATM, which phosphorylates a variety of proteins, including H2AX (γH2AX), to signal the damage. Following generation of ssDNA overhangs by DNA end resection, which is promoted by BRCA1, BRCA1 recruits the PALB2 (Partner and Localiser of BRCA2)-BRCA2-RAD51 complex to DSB sites, where RAD51 replaces RPA and scans the surrounding chromatin for the sister chromatid. Once found, the RAD51-nucleoprotein filament invades the homologous strand, forming a displacement loop (D-loop) that can move along the strand. Following strand invasion, several different sub-pathways can be engaged, with the two major ones being Holliday junctions and synthesis-dependent strand annealing (SDSA). PARP1 was shown to bind DSBs (Ali et al., 2012; M.-F. Langelier et al., 2012), and its presence and catalytic activity in response to break detection were found to promote recruitment of both the

MRN complex and BRCA1 to DSBs (M. Li & Yu, 2013; Ray Chaudhuri & Nussenzweig, 2017). The exact role of PARP1 in HR is not fully understood, with loss of PARP1 causing an increase in RAD51 loading and sister chromatid exchange and recombination (Ray Chaudhuri & Nussenzweig, 2017); one study found that PARP1-mediated ADP-ribosylation of BRCA1 prevents excessive HR and hyper-recombination, indicating PARP1 is involved in fine-tuning the HR process (M. Li & Yu, 2013). Loss-of-function of either BRCA1 or BRCA2, and resulting deficiency in HR, is associated with an increased risk of certain cancers, particularly breast and ovarian cancers (Prakash et al., 2015). The exploitation of this deficiency with PARP inhibitors will be discussed in section 1.4.

Devoid of a sister chromatid that can serve as a template outside of G2/S phases, cells utilise an error-prone pathway termed NHEJ (Non-Homologous End Joining) as the primary repair pathway for DSBs (Stinson & Loparo, 2021). Ku70 and Ku80 are loaded onto a variety of DSB structures, where they serve as a scaffold for downstream repair factors, including DNA-dependent protein kinase (DNA-PK), which signals the presence of the DSB and recruits the XRCC4-Ligase IV-XLF complex that mediates ligation of the break, as well as DNA synthesis factors such as Artemis and polymerases μ and λ, if necessary. PARP1 activity was shown to form a complex with DNA-PK and stimulate its kinase activity (Ray Chaudhuri & Nussenzweig, 2017). PARP1 activity also promotes the recruitment of CHD2, a SWI2/SNF2 ATPase chromatin remodeller, which in turn triggers deposition of histone H3.3 at sites of damage, creating an accessible chromatin environment for NHEJ factors (Luijsterburg et al., 2016). Other studies found PARP1 to be in direct competition with binding of Ku to damage sites (Wang et al., 2006), and implicate PARP1 as a main mediator of a Ku-independent, error-prone alternative (a-)NHEJ, which was shown to be completely dependent on functional PARP1 (Mansour et al., 2010). Some evidence also suggests a role for PARP1 in promoting

the cellular choice for HR over NHEJ, protecting the HR pathway from interference by Ku70 through competition at the damage site (Hochegger et al., 2006).

PARP1 at replication forks

During replication, upon encountering an obstacle, such as secondary DNA structures, repetitive sequences, misincorporated ribonucleotides, dormant replication origins or DNA lesions, replication forks are stalled (Mazouzi et al., 2014).

Prolonged replication stress, if left unresolved, may lead to fork collapse, ultimately resulting in genotoxic DSBs (Liao et al., 2018). To avoid collapse, cells have evolved mechanisms to stabilise and restart stalled replication forks; this involves protection of ssDNA, fork reversal, in which newly generated daughter strands anneal, and a 3-way reverse DNA junction is formed, and controlled DNA resection (Liao et al., 2018). The role of PARP1 in this has been implicated by many studies; PARP1 activity is increased in response to replication stress, and PARP1 is located to progressing and stalled forks (Ray Chaudhuri & Nussenzweig, 2017). PARP1 activity is also associated with recruitment of Mre11, part of the MRN complex, and thereby promotes resection at stalled forks and efficient fork restart, and PARP1-deficient cells are hypersensitive to hydroxyurea, a replication fork-stalling agent (Bryant et al., 2009; Y. G. Yang et al., 2004). Loss of PARP1, or catalytic inhibition, leads to increased replication fork stalling and inefficient re-start, and it is through this mechanism that PARP inhibitors have been proposed to kill HR-deficient cells, by promoting replication fork collapse and resulting generation of DSBs (Helleday, 2011). There has been some controversy about whether this collapse of replication forks is caused simply by the loss of catalytic activity, or the encountering of trapped PARP1 on DNA by replication forks, similar to trapping of topoisomerase on DNA through inhibitors (Pommier et al., 2022); this will be discussed in section 1.4.

1.2.3 PARP2 and PARP3 in DNA repair

PARP2 was discovered as a close homologue of PARP1 upon investigation of the remaining ADP-ribosylation in PARP1 knock-out (KO) mouse embryonic fibroblasts, which was shown to be DNA-damage dependent (Amé et al., 1999). While PARP1 KO mice are viable, loss of both PARP1 and PARP2 is embryonically lethal (Ménissier de Murcia et al., 2003a). PARP2 has a disordered N-terminal region, lacking the specialised DNA-binding zinc fingers and BRCT domain of PARP1, which is followed by a WGR domain and a catalytic domain, which consists of the HD and ART subdomains (Obaji et al., 2016) (Figure 1.2). The disordered N-terminus is not required for DNA binding or DNA-dependent activation, but increases the affinity of PARP2 for SSB structures (Riccio et al., 2016a). DNA-dependent allosteric activation of PARP2 is mediated by the WGR domain, which contacts DNA and the HD (M. F. Langelier et al., 2014). PARP2 binds SSBs as a monomer and DSBs as homodimer or heterodimer with PARP1 (Obaji et al., 2016). Unlike PARP1, PARP2 is preferentially activated by binding to DNA breaks with an exposed 5' phosphate, suggesting a preference for DNA break intermediates before the final step of DNA ligation (M. F. Langelier et al., 2014). PARP2 also has a preference for flap-containing DNA, and lower affinity for earlier BER DNA intermediate structures (Kutuzov et al., 2013; Sukhanova et al., 2019). PARP2 resides longer at sites of DNA damage than PARP1, and its recruitment to sites of damage occurs later than PARP1 (roughly 30 seconds post-irradiation), and was reported to be at least partially dependent on the catalytic activity of PARP1 (Mortusewicz et al., 2007). In fact, one study found that PARP2 catalytic activity could be activated by PAR *in vitro*, and loss of PARP1 catalytic activity impaired the recruitment of PARP2 to damage sites (Chen et al., 2018). The same study also found that PARP2 was largely responsible for the generation of branched PAR chains, which are recognised by fewer of the ADP-ribose readers. APLF, a histone chaperone and nuclease associated with the DDR, was shown to specifically bind these branched PAR chains with its tandem PBZ domains. Its recruitment to, and subsequent

eviction of histone H3 from the damage site, is dependent on PARP2 (Chen et al., 2018). Combined, this suggests that PARP2 is involved in the later stages of DNA repair, that its recruitment and activity rely on PARP1, and that it generates a distinct ADP-ribose code which is interpreted by a specific set of DDR factors. In general, this suggests that due to the reliance of PARP2 on PARP1 activity, the recruitment of some DDR factors could be misconstrued as being directly dependent on PARP1, hiding the role of PARP2 in the process.

To a large degree, the functions of PARP2 in the DNA damage response are redundant with those of PARP1; loss of PARP2 increases sensitivity to ionising radiation, alkylating agents and X-ray radiation, indicating a role for PARP2 in SSB and DSB repair, as well as restarting of replication forks (Szántó et al., 2024). Evidence for the involvement of PARP2 in BER comes from slowed BER in PARP2 KO cells, and the interaction of PARP2 with BER proteins such as XRCC1, DNA polymerase β and DNA ligase III (Szántó et al., 2024).

Some of the specific functions of PARP2 are distinct from PARP1, while serving the same goal within a pathway. PARP1 stimulates DNA end resection at DSBs through PAR-dependent recruitment of the MRN complex (Haince et al., 2008; Wang et al., 2006) and PARP2, independently of its catalytic activity, was shown to restrict the accumulation of 53BP1 (Fouquin et al., 2017), an antagonist of resection and pro-NHEJ factor, thereby promoting PARP1-mediated loading of MRN to the break site and HR pathway choice.

PARP2, rather than PARP1, is particularly implicated in the maintenance of genomic stability in frequently proliferating cell types, such as erythropoiesis, and lymphocyte and B cell development (Farreś et al., 2013; Farrés et al., 2015; Galindo-Campos et al., 2022). A recent study also found a role for PARP2, but not PARP1, in the response to replication stress at telomeres and the prevention of associated telomere loss (Muoio et al., 2024).

PARP3 strongly resembles PARP2 in its domain architecture, and shares its affinity for 5' phosphorylated nicks (M. F. Langelier et al., 2014). PARP3 has been indicated in HR and NHEJ pathway choice: it was shown to PARylate Ku70/Ku80 and recruit the complex to DNA lesions, thereby limiting DNA end resection and promoting c-NHEJ (Beck et al., 2014). One study reported that PARP3 modifies the 5'-phosphate of gapped DNA *in vitro* with MAR, which could be effectively extended by PARP1 and PARP2, and allowed for ligation of the gap by different DNA ligases (Belousova et al., 2018).

This would agree with its reported role in the recruitment of APLF, a PAR-binding histone chaperone, which in turn promotes XRCC4/DNA ligase IV-mediated break ligation (Rodriguez-Vargas et al., 2019). Expression of PARP3 was also positively correlated to increased tumour aggressiveness, making it an attractive target for future therapeutic targeting (Rodriguez-Vargas et al., 2019).

1.3 The ADP-ribosylation code in the DNA damage response

As discussed in previous sections, ADP-ribosylation differs in its length and branching, depending on the writer, which in turn is interpreted by different ADP-ribose readers, resulting in different functional outcomes depending on the ADPr "code". PARP1/2-mediated ADPr in the DDR has widespread consequences for the chromatin environment, and recent developments have updated current understanding of the DDR-specific ADPr code.

1.3.1 HPF1 and serine ADPr – discovery of a crucial PARP1/2 co-factor

Traditionally, glutamates and aspartates were thought to be the predominant acceptors of PARP1/2-mediated ADP-ribosylation (Daniels et al., 2015; Gibson et al., 2016). However, more recent studies using more sensitive mass spectrometry technology revealed serine to be a more robust target for ADPr in the DDR (Bonfiglio et al., 2017; Larsen et al., 2018; Leidecker et al., 2016; Palazzo et al., 2018). This finding coincided with the discovery of HPF1 (Histone Parylation Factor 1). HPF1 (previously known as protein C4orf27) was

initially linked to DNA repair PARPs due to the presence of a PBZ domain (I. Ahel et al., 2008). Later, it was shown that HPF1 interacts specifically with PARP1 and PARP2, and promotes their efficient modification of histones (Bonfiglio et al., 2017; Gibbs-Seymour et al., 2016). This interaction of HPF1 with PARP1 and PARP2 is independent of PARP1 catalytic activity and generation of ADP-ribosylation. Consequently, the recruitment of HPF1 to DNA damage sites depends on direct physical interaction with PARP1 and does not require the prior presence of an ADP-ribosylation signal (Gibbs-Seymour et al., 2016; Prokhorova, Zobel, et al., 2021; Suskiewicz et al., 2020). Loss of HPF1 greatly increases cellular sensitivity to treatment with DNA alkylating agent MMS (methyl methanesulfonate) and sensitises cells to PARP inhibition (Gibbs-Seymour et al., 2016). HPF1 was further shown to limit PARP1 hyper-automodification *in vivo* and *in vitro*, instead redirecting its catalytic activity towards histones and other substrates (Gibbs-Seymour et al., 2016). HPF1 not only boosts the ADPr activity on histones and other targets, it is also the determining factor in swapping PARP1 specificity from Glu/Asp residues to the generation of specific serine-linked ADPr (Bonfiglio et al., 2017). Proteomic and cell based analyses confirmed that HPF1 is essential for ADPr of serine residues in histones, PARP1, PARP2 and hundreds of other proteins (Juan José Bonfiglio et al., 2017; Hendriks et al., 2021). Interaction of HPF1 with PARP1 *in vitro* depends on the presence of DNA and NAD^+, and binding is only activated upon HD unfolding of PARP1/2, thus providing a mechanism to regulate binding of the much less abundant HPF1 with PARP1 and restrict it to DNA damage detection (Suskiewicz et al., 2020).

Solving of the crystal co-structure and CryoEM structures of HPF1 with PARP2 revealed a first insight into the structural basis for the HPF1-mediated serine switch (Bilokapic et al., 2020; Suskiewicz et al., 2020). These data were confirmed by NMR and crystallography for PARP1 (Sun et al., 2021; Suskiewicz et al., 2020). Two highly conserved aspartate residues in

the C-terminal region of HPF1 were found to be critical for interaction with PARP1 and PARP2 and consequently for PARP1/2 serine-ADP ribosylation activity (Suskiewicz et al., 2020). These residues contact His826 in PARP1 (His381 in PARP2). Additionally, the extreme C-terminal residues of PARP1/2 (L1013/W1014) latch onto HPF1 from the back and are critical for stable interaction and activity of the complex (Suskiewicz et al., 2020).

Structural analysis of the HPF1-PARP2 complex also revealed that the HPF1-mediated amino acid preference switch of PARP1/2 can be explained by the provision of a second catalytic glutamate residue by HPF1 (Suskiewicz et al., 2020). PARP1 and PARP2 by themselves only contain a single catalytic glutamate residue (E988 and E545, respectively), allowing for efficient targeting of aspartate or glutamate residues, but not for serine deprotonation. The interaction of HPF1 and PARP1/2 places E284 of HPF1 near the catalytic glutamate of PARP1/2 and the NAD^+ molecule, allowing the formation of a composite active site that is capable of catalysing efficient serine ADPr (Suskiewicz et al., 2020) (Figure 1.6). Mutational analysis further showed that it is E284 of HPF1, as opposed to E988Q of PARP1, that is necessary and sufficient for serine-ADPr (Suskiewicz et al., 2020). The same study also found that the HPF1-PARP1/2 complex forms a putative peptide-binding cleft with a strong negative charge provided by HPF1, which was suggested to explain the abundance of serine-ADPr within Lys-Ser (KS) consensus motifs (Bonfiglio et al., 2017; Leidecker et al., 2016). Not only does HPF1 switch the amino acid residue preference of PARP1/2, but it also restricts the length of ADP-ribose chains produced, both on PARP1/2 and on histones (Gibbs-Seymour et al., 2016; Suskiewicz et al., 2020). The basis for this is that D283 of HPF1 was shown to occupy H826 of PARP1 (H381 of PARP2), which would otherwise contact the second phosphate of the ADP fragment of an incoming NAD^+, thereby preventing the extension of ADPr chains (Suskiewicz et al., 2020). Despite being about 20-fold less abundant in cells than PARP1 (Bonfiglio et al., 2017), HPF1 manages to influence PARP1

catalytic activity efficiently towards initiation on serine residues and histone trans-modification, rather than elongation, by rapidly cycling between PARP1 molecules (Langelier et al., 2021).

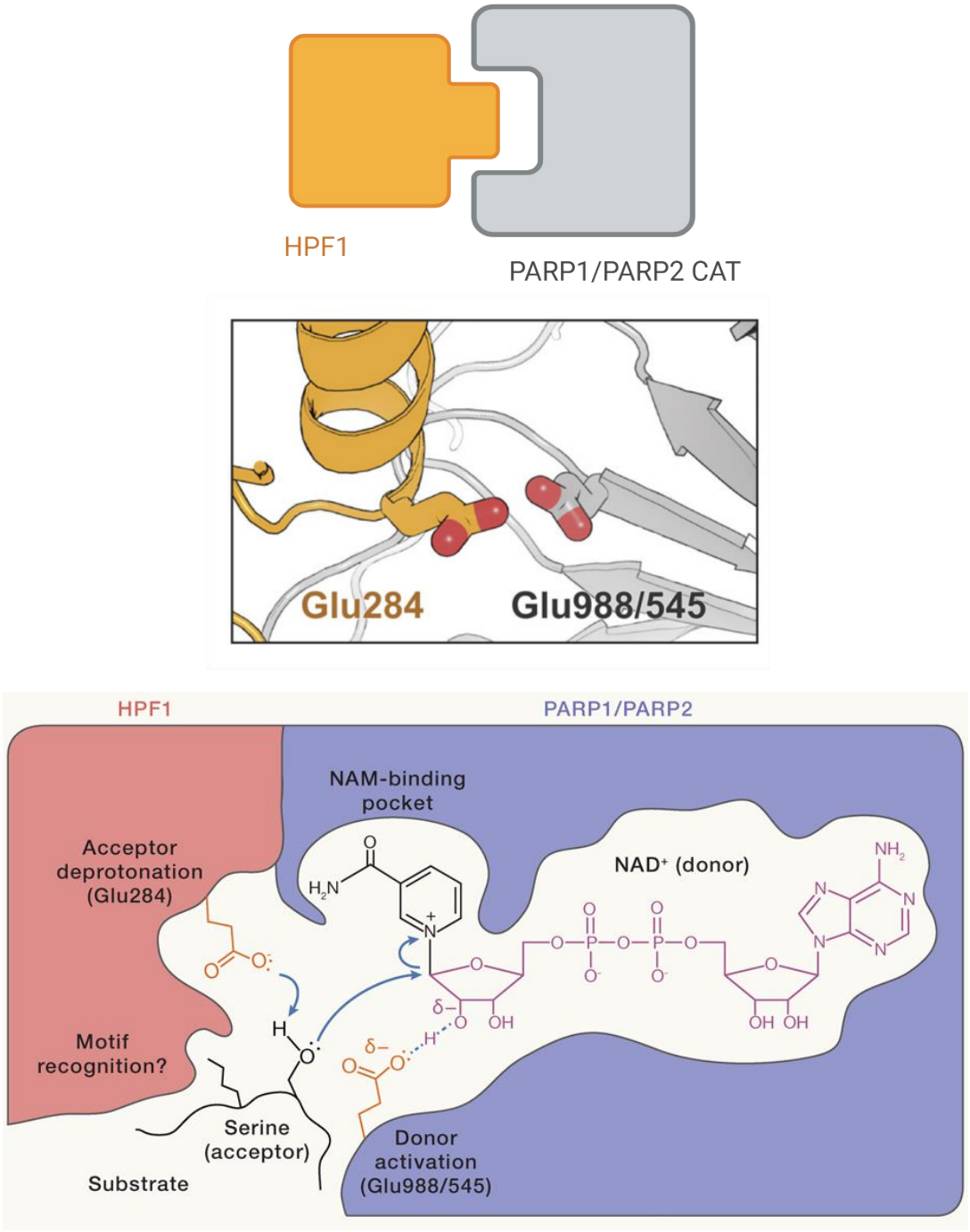

Figure 1.6: HPF1 and the PARP1/2 catalytic domain (CAT) form a composite active site. HPF1 places Glu284 next to the catalytic glutamate of PARP1 (Glu988) and PARP2 (Glu545). The middle panel was made by Marcin Suskiewicz. The bottom panel was taken from Suskiewicz et al., 2023.

More recent studies have investigated this ADPr-directing function of HPF1 in cells, supporting a model in which HPF1 produces a distinct, second wave of serine-linked ADP-ribosylation on histones preferably consisting of MAR and shorter chains, following a rapid burst of HPF1-independent PARylation, leading to a slightly delayed but longer-lived chromatin signal that promotes recruitment of MAR-binding chromatin remodellers and repair factors (Longarini et al., 2023; Prokhorova, Agnew, Wondisford, Tellier, et al., 2021; Smith et al., 2023).

This distinct, HPF1-dependent, serine-linked ADPr code is specifically removed by ARH3, the only known human enzyme to cleave the *O*-glycosidic bond between the serine and the ADPr unit (Fontana et al., 2017). While loss of HPF1 sensitises cells to PARP inhibition, loss of ARH3 causes resistance (Prokhorova, Agnew, Wondisford, Tellier, et al., 2021), identifying HPF1 and ARH3 as two opposing regulators of this pathway. Loss of ARH3 alone leads to a well-tolerated, persistent serine-MAR signal on chromatin throughout the cell cycle, but concomitant inhibition of PARG leads to persistence of long, serine-linked PARylation, which causes cell death (Prokhorova, Agnew, et al., 2021). This also points towards a role of PARG, which is recruited to sites of DNA damage rapidly in a PAR-dependent manner (Mortusewicz et al., 2011), in trimming PAR chains from histones, contributing together with HPF1 towards the generation of a more persistent MAR signal on chromatin.

1.3.2 Importance of ADP-ribose chain length in the DDR

The coordinated efforts of PARP1/2, HPF1, ARH3 and PARG illustrate the tight, temporal, and spatial regulation of ADP-ribosylation by specific enzymes in response to DNA damage, and how targeting any of the members of this pathway could be therapeutically exploited. The discovery of HPF1 has also hugely impacted the current understanding of the type and diversity of ADP-ribose chains produced in response to DNA damage.

It has also helped evolve our understanding of the requirements for PARP1 automodification. PARP1 automodification is required for its rapid dissociation from DNA lesions; loss of catalytic activity, either through mutation of ART domain residues, or the use of inhibitors, will lead to prolonged retention ("trapping") of PARP1 on chromatin. While HPF1 directs PARP1/2 catalytic activity towards histones, its loss also reduces PARP1 automodification, as does mutation of critical serine residues (Ser499, Ser507, Ser519) near the PARP1 BRCT domain, both of which lead to trapping of PARP1 at the DNA lesion (Gibbs-Seymour et al., 2016; Prokhorova, Zobel, et al., 2021). HPF1-dependent histone ADPr itself was shown to be important for PARP1 release from chromatin, independent of PARP1 automodification (Zentout et al., 2024).

The fact that HPF1 restricts ADPr chain length adds another layer of complexity, posing the question of "how much" ADP-ribosylation is required for PARP1 dissociation from chromatin, chromatin relaxation in general, and cellular survival in response to DNA damage.

This is particularly relevant in addressing ADP-ribosylation in therapy: PARP inhibitors are clinically used against certain cancers, but most of the therapeutic potential of targeting DDR-linked ADP-ribosylation remains untapped. A better understanding of the cellular requirements for ADP-ribose chain length, and its consequences for PARP1/2 trapping, can help identify specific pathways, and could allow a more fine-tuned modulation of this PTM in therapy.

1.4 PARP inhibitors and therapeutic targeting of ADP-ribosylation

1.4.1 Clinical use of PARP inhibitors

The realisation that PARP1 plays a role in the cellular response to genotoxic stress inspired the development of small-molecule PARP inhibitors early on. The very first compound to be identified as an effective PARP inhibitor was benzamide (Shall, 1975), a close analogue to nicotinamide, both of which compete with NAD^+ as a PARP1 substrate. However, due to its

hydrophobic nature and resulting low aqueous solubility, its use for studying the cellular role of PARP1 was limited. This inspired the specific development of such an inhibitor, laying the foundation for the first generation of benzamide-derived PARP inhibitors (Purnell & Whish, 1980). Shortly thereafter, the potential of this first PARP inhibitor, 3-aminobenzamide, as an onco-therapeutic agent was demonstrated when it was shown that it could block DNA repair processes and caused hypersensitivity to DNA methylating agents in murine leukaemia cells (Durkacz et al., 1980).

More evidence of PARP inhibitors as promising potentiators of other chemotherapeutic agents and ionising radiation accumulated over the years (Griffin et al., 1995), but poor solubility, low potency and selectivity stalled better understanding of their effect on PARP1, and their potential role in chemotherapy for a long time. This led to the development of second-generation PARP inhibitors in the 1990s and 2000s with improved potency, their design still primarily based on interaction with and inhibition at the NAD^+ binding site, which entered clinical trials primarily as radio- and chemosensitisers, ultimately still failing due to poor solubility or side effects such as increased myelotoxicity (Ferraris, 2010; Mateo et al., 2019).

Two seminal studies in 2005 laid the groundwork for the current clinical use of PARP inhibitors. BRCA1 and BRCA2 are key tumour suppressors involved in HR, and loss-of-function of either of them is responsible for the majority of hereditary breast and ovarian cancer (HBOC), with women carrying a mutation in either experiencing a 50-80% lifetime risk of developing breast cancer, and a 30-50% risk of developing ovarian cancer (Roy et al., 2011). The studies showed that tumour cells with defects in BRCA1 or BRCA2 are hypersensitive to treatment with PARP inhibitors, theorised to be due to the development of unrepaired SSBs into DSBs, which could not be repaired in BRCA1/2 deficient cells (Bryant et al., 2005a; Farmer et al., 2005). Importantly, cells with intact BRCA1/2 were shown to be able to repair the lesions, thus providing a way to specifically kill cancer cells with defects in

HR. This was coined synthetic lethality, referring to the fact that either PARP1 inhibition or BRCA1/2 loss is tolerated by the cell, but simultaneous loss of functions will lead to cell death. This proved for the first time that the DNA damage defect causing the cancer could be exploited by targeting a non-essential protein, and it indicated the potential of PARP inhibitors as monotherapy for a specific patient population. The latter especially served as a good incentive for the development of novel PARP inhibitors and a new research direction for their clinical use.

Olaparib (Lynparza, KuDOS Pharmaceuticals/AstraZeneca), its predecessor having been used by Farmer et al. in their 2005 study, was the first PARP inhibitor to be approved by the FDA and the EMA in 2014 as monotherapy against advanced ovarian cancer with germline mutations in BRCA who had undergone multiple lines of chemotherapy (Kim & Nam, 2022). Olaparib has since received FDA approval for multiple other indications, notably amongst them in 2018 for treatment of germline BRCA-mutated metastatic breast cancer, in 2019 for use as a first-line maintenance treatment against BRCA-mutated metastatic pancreatic adenocarcinoma and in 2020 for men with BRCA- mutated advanced metastatic prostate cancer (Kim & Nam, 2022) (Table 1.1).

Inhibitor	Selectivity	FDA Approval	Indications	References
Olaparib (AstraZeneca)	PARP1 and PARP2	Yes, first 2014	Advanced gBRCA **ovarian** cancer; gBRCA metastatic **breast** cancer; (g)BRCA-mutated metastatic **pancreatic** and **prostate** cancer; maintenance therapy against recurrent **epithelial ovarian**, **fallopian, peritoneal** cancer	Kim & Nam, 2022
Rucaparib (Clovis)	PARP1 and PARP2	Yes, first 2016	g/sBRCA/HR-deficient advanced **ovarian** cancer; BRCA-mutated metastatic **prostate** cancer	Kim & Nam, 2022
Niraparib (GSK)	PARP1 and PARP2	Yes, first 2017	**Epithelial ovarian, fallopian** and **peritoneal** carcinoma, maintenance treatment against **platinum-sensitive ovarian** cancer independent of BRCA or HR status	Kim & Nam, 2022
Talazoparib (Pfizer)	PARP1 and PARP2	Yes, first 2018	BRCA-mutated HER2-negative **breast** cancer; in combination with enzalutamide (testosterone blocker) against metastatic castration-resistant **prostate** cancer with HR gene mutations	Kim & Nam, 2022; Ettl et al., 2019; Heiss et al., 2024; Shen et al., 2013
Veliparib (Abbvie)	PARP1 and PARP2	Phase III	Phase III: in combination with temozolomide against **glioblastoma**; mono- or combination therapy with carboplatin/paclitaxel against BRCA-mutated advanced **breast** cancer and **ovarian cancer**; monotherapy and in combination with carboplatin/etoposide against **small cell lung cancer**	Kim & Nam, 2022; Sarkaria et al., 2024; Boussios et al., 2020; Coleman et al., 2019; Daei Sorkhabi et al., 2023; Swisher et al., 2022
Saruparib (AstraZeneca)	PARP**1**	Phase III	Phase III: hormonal combination therapy against metastatic castration-resistant **prostate** cancer; in combination with camizestrant against advanced HR-defective **breast** cancer	Clinical Trial IDs: NCT06120491, NCT06380751

Table 1.1: Relevant PARP inhibitors, their selectivity, FDA approval status and disease indications. gBRCA = germline BRCA mutations, sBRCA = somatic BRCA mutations, HR = homologous recombination.

Other PARP inhibitors have followed, with rucaparib (Rubraca, Agouron Pharmaceuticals/Clovis Oncology), its forerunner used by Bryant et al. in 2005, FDA-approved for BRCA-mutated ovarian cancer and BRCA-mutated metastatic advanced prostate cancer (Kim & Nam, 2022). Niraparib (Zejula, Merck/Tesaro) is clinically used against advanced epithelial ovarian, fallopian and peritoneal carcinoma, and as maintenance treatment against platinum-sensitive recurrent ovarian cancer (Kim & Nam, 2022). Importantly, for the latter, use of niraparib is not limited to ovarian cancers with germline BRCA mutations, since treatment of non-BRCA-mutated patients benefitted from its use (Mirza et al., 2016) (Table 1.1), proving that a wider patient population could benefit from PARP inhibitor treatment. Further FDA approvals for multiple indications, including breast cancer and castration-resistant prostate cancer, followed for talazoparib (Talzenna, Pfizer), the to date most potent PARP inhibitor (Ettl et al., 2019; Heiss et al., 2024; Murai et al., 2014; Shen et al., 2013) (Table 1.1). Pamiparib (Patruvix), was approved in 2021 in China for treatment of germline-BRCA mutated recurrent ovarian, fallopian and peritoneal cancer (Markham, 2021). Other PARP inhibitors are currently undergoing clinical trials, with veliparib (Abbott/Abbvie) the most advanced among them, with several ongoing phase III clinical trials for treatment against ovarian, breast and non-small lung cancer (Boussios et al., 2020; Coleman et al., 2019; Daei Sorkhabi et al., 2023; Swisher et al., 2022) (Table 1.1).

All clinically used PARP inhibitors, as well as veliparib, target the NAD^+ binding site of both PARP1 and PARP2, effectively leading to inhibition of both enzymes (Johannes et al., 2021). Unsurprisingly, despite overall being well tolerated, their use is associated with several adverse effects. They include myelosuppression and haematological toxicities, chiefly amongst them anaemia, neutropenia, and thrombocytopenia, as well as gastrointestinal toxicities such as nausea, constipation and diarrhoea, and general fatigue (Hatch et al., 2021; LaFargue et al., 2019). It was previously shown that PARP2, but not PARP1, plays an

essential role in hematopoietic homeostasis and response to irradiation, and that its loss disrupts erythropoiesis, leading to chronic anaemia in mice (Farreś et al., 2013; Farrés et al., 2015), providing an explanation for the haematological toxicities observed as a side effect of PARP inhibitors.

Further, the fact that the synthetic lethality of PARP inhibitors with BRCA defects is mediated through PARP1, rather than PARP2 (Bryant et al., 2005; Murai et al., 2012), inspired the recent development of a selective PARP1 inhibitor, aiming to prevent the haematological toxicity associated with PARP2 inhibition while maintaining the cytotoxic effect on HR defective tumours. This would be particularly useful for the potential use of PARP inhibitors in combination with other therapies, such as antiangiogenic agents, which was previously shown to increase the risk of adverse events (Wei et al., 2024).

Saruparib (AZD5305, AstraZeneca) has a 500-fold greater selectivity for PARP1 over PARP2, while retaining its function as a PARP1 trapper and synthetic lethality with BRCA1/2 (Illuzzi et al., 2022; Johannes et al., 2021). Apart from good clinical activity, saruparib has also been shown to have a favourable safety profile and a lower incidence of adverse events, particularly haematological and gastrointestinal toxicities, compared to approved PARP inhibitors in an ongoing phase I/II study (NCT04644068) (Yap et al., 2022). Saruparib has also entered phase III clinical trials for use in prostate and breast cancer (NCT06120491, NCT06380751) (Table 1.1).

The selectivity of saruparib for PARP1 over PARP2 is achieved by a more extensive network of intra-ART domain and HD contacts: The structure of saruparib bound to PARP1 is not currently publicly available on PDB; it was, however, recently modelled by one study as part of synthesis of derivatives with further improved selectivity and trapping ability (Ren et al., 2022). Key residues contacted by the saruparib nicotinamide mimetic core via hydrogen bonds include S904 and G863, stacking against Y907 of the donor site, as well as a water

bridge with a water molecule and H862 of the catalytic triad (Figure 1.7, a). This water bridge with H862 was previously suggested to confer a large part of the selectivity of saruparib for PARP1 over PARP2, and while olaparib and niraparib share the contacts with S904 and G863, the H862 contact is not (Figure 1.7, c) (Johannes et al., 2021; Ren et al., 2022). Further, saruparib hydrogen bonds with I879, which improves selectivity (Ren et al., 2022) and contacts D766 (Figure 1.7, a), contacts not shared by niraparib and olaparib. A comparison model (Figure 1.7, c) of binding contacts for olaparib, niraparib and the saruparib analogue shown in Figure 1.7, b shows that saruparib forms a greater network of contacts, and that it extends further towards residues in the HD (Figure 1.5). The catalytic cleft between the ART domain and the HD domain was previously shown to differ between PARP1 and PARP2, with greater space in the PARP1 molecule for PARP inhibitors (Langelier et al., 2023); key contacts with the PARP1 HD by saruparib likely affect its selectivity for PARP1 over PARP2 as well.

Following clinical approval and success of PARP inhibitors, much focus was put on improving the current understanding of the molecular mechanism of these compounds. The past few years especially have seen a surge in new and sometimes contradictory theories, which will be reviewed in the next section.

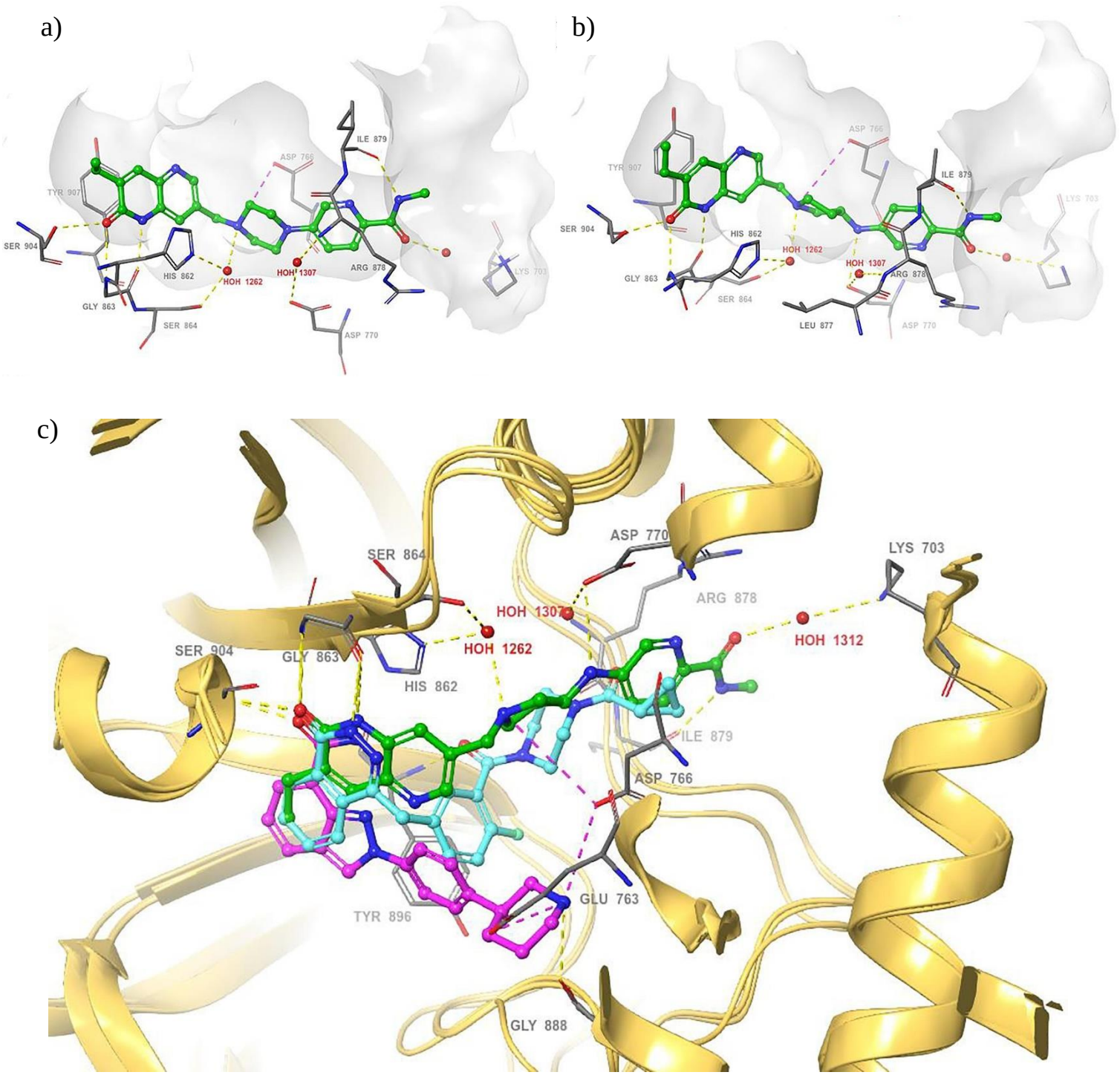

Figure 1.7: Analysis of binding modes of different PARP inhibitors. Binding mode of **a)** saruparib and **b)** a saruparib derivative. **c)** Comparison of binding modes of olaparib (blue), niraparib (purple) and the saruparib analogue (green) shown in **b)** in the PARP1 catalytic domain. Taken from Ren et al., 2022. Reused by permission from Elsevier and Copyright Clearance Center on behalf of the Journal of Molecular Biology (License Number 5983110772086).

1.4.2 Molecular mechanism of PARP inhibition

Discrepancies between the effect of PARP inhibition and its genetic disruption were observed early on. PARP1 KO mice are viable, and several studies found cells to be more sensitive to PARP inhibitor than to loss of PARP1, in a BRCA-mutated synthetic lethality context and in combination with DNA-damaging drugs (Bryant et al., 2005; Heacock et al., 2010; Horton et al., 2005), adding confusion to the long-held theory that it was the loss of ADP-ribosylation, and the resulting impaired repair of DNA damage, underlying the cytotoxic effects of PARP inhibitors. To explain this difference, the theory of PARP "trapping" appeared (Helleday, 2011), suggesting that PARP inhibitor-induced loss of ADP-ribosylation would lead to physical stalling of PARP1 at the site of damage, in accordance with PARP1 auto-modification being required for its release from chromatin (Satoh & Lindahl, 1992). Observations of increased association of PARP1 with DNA following PARP inhibitor treatment, leading to SSB intermediate structures, seemed to confirm this theory (Kedar et al., 2012; Ström et al., 2011).

A seminal study managed to demonstrate several things: Loss of PARP1 was shown to render cells resistant to PARP inhibitor treatment, indicating that their cytotoxic effect is mediated through PARP1, rather than PARP2 or other targets (Murai et al., 2012). Further, they showed that PARP inhibitor treatment led to stalling of PARP1 and PARP2 at sites of damaged chromatin (Murai et al., 2012). This study was also the first to show that despite complete catalytic inhibition of PARP1 at the inhibitor concentration used, different inhibitors varied in their trapping potency. Niraparib was proven to be the strongest trapper, followed by olaparib, and veliparib as the weakest trapper, with corresponding cellular toxicities. Based on these results, this study for the first time implicated that trapping potency, independent of catalytic inhibition, was the main factor underlying PARP inhibitor cytotoxicity.

A follow-up study, using the same methodology and cell lines as the previous one, tested talazoparib in comparison to rucaparib and olaparib, leading to a ranking of PARP inhibitors by trapping potency as follows: talazoparib >> niraparib ≈ olaparib ≈ rucaparib > veliparib with the PARP1-selective inhibitor saruparib ranking near veliparib according to a recent study (Figure 1.8) (Murai et al., 2014; A. Thomas et al., 2018; Kanev et al., 2024).

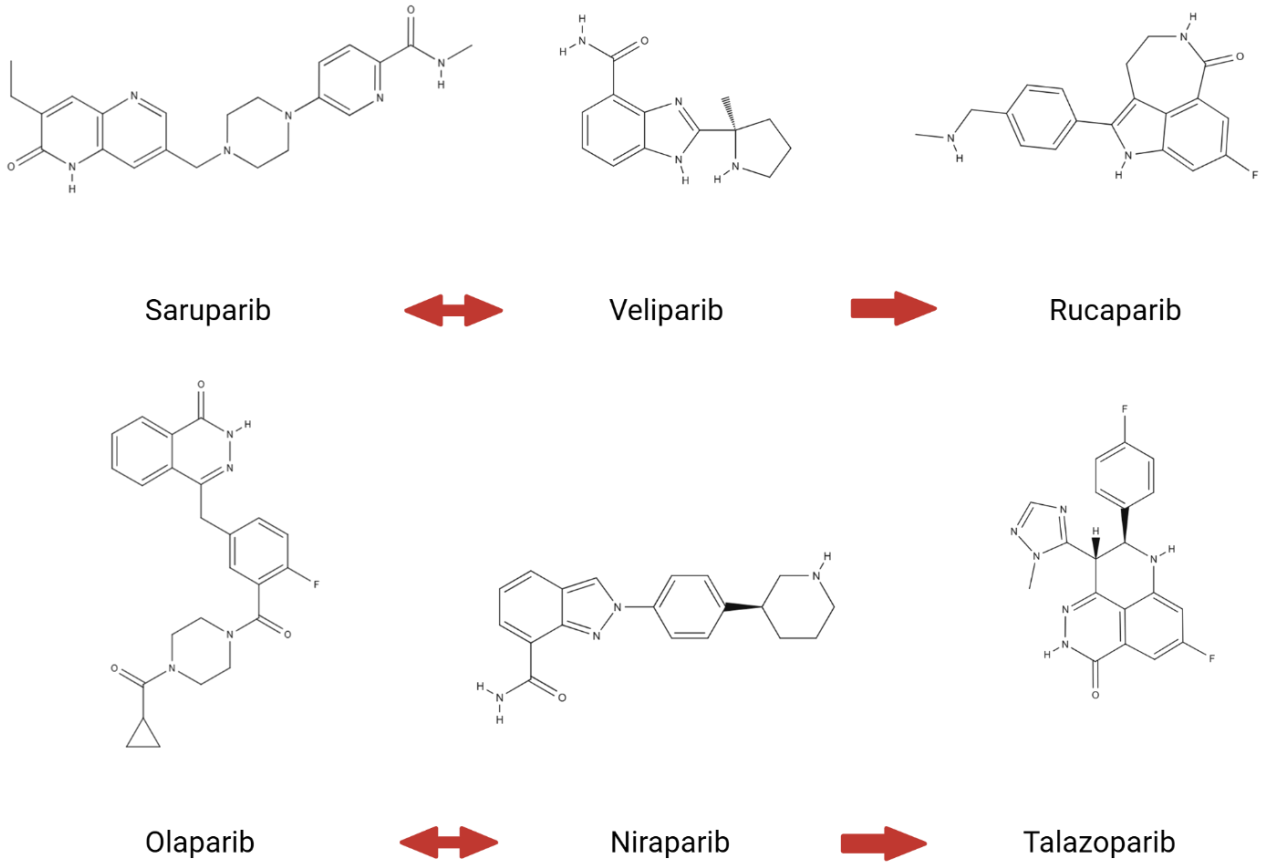

Figure 1.8: Clinical PARP inhibitors, veliparib, and saruparib, ranked by their trapping potency of PARP1 in cells. Saruparib and veliparib are the weakest trappers, followed by rucaparib, olaparib and niraparib, with talazoparib being the strongest trapper.

While the PARP inhibitor-induced loss of ADP-ribosylation was one theory offered as an explanation for the stalling of PARP1/2 at damage sites, another was the potential for PARP inhibitors to induce allosteric changes in PARP1 through their binding, thereby affecting its DNA binding affinity (Murai et al., 2012). The latter could explain the non-linear relationship between trapping potency and enzymatic inhibition. This was particularly supported by talazoparib, being the bulkiest compound, and veliparib, being the smallest (Figure 1.8), being the most and least potent trappers, respectively.

Improving our understanding of how PARP inhibitors affect PARP1, and thereby improve our understanding of how to best employ them clinically, has become an important area of research. Investigations into their effect on PARP1 allostery, the resulting trapping potency and cytotoxicity, PARP1-inhibitor binding affinity, the role of HPF1, and the molecular nature of "trapping", have revealed the astounding complexity of this class of drugs and their mechanism of action. In the following sub-sections I will consider each of these aspects, aiming to provide an overview of the current field, key studies, their methodology, and the questions that remain open.

Allosteric Changes

The first study addressing whether allosteric changes are responsible for the differential trapping potential and cytotoxicity of PARP inhibitors did not confirm this theory (Hopkins et al., 2015). The authors used competitive time resolved-FRET (TR-FRET), comprising a complex formed by a fluorescently labelled, digested DNA duplex and PARP1-bound, labelled antibody, onto which a much higher concentration of an unlabelled, but identical DNA competitor probe is added, in the presence or absence of inhibitor (Hopkins et al., 2015). Upon binding of PARP1 to the competitor, the FRET signal diminishes, allowing a read-out of the dissociation rate.

These experiments were conducted without the addition of NAD^+, which would confuse interpretation of the relative contributions of catalytic inhibition and allosteric influence of PARP inhibitors on PARP1-DNA-binding affinity. Addition of inhibitors (olaparib, niraparib, talazoparib and veliparib) was not found to stabilise the PARP1-DNA complex, however, nor did it affect PARP1-DNA-binding affinity (Hopkins et al., 2015). To further corroborate that trapping relies on the loss of PARP1 catalytic activity, rather than changes in affinity for DNA, the authors used a selective NAMPT inhibitor to deplete cellular NAD^+, showing that after treatment with MMS, PARP1 was trapped on chromatin to a similar extent as with PARP inhibitors in a chromatin fractionation assay (Hopkins et al., 2015).

However, another seminal study using slightly different methodology and a wider range of inhibitors found the opposite. Hydrogen/deuterium exchange-mass spectrometry (HXMS) measures the exchange of protons between exposed protein backbone amides and a deuterated solvent, the rate of exchange thereby providing information on protein allostery, folding dynamics and stability of an interaction (Masson et al., 2019). Analysis of a nicked DNA duplex-PARP1 complex incubated with PARP inhibitors showed their differing effects on PARP1 folding (Zandarashvili et al., 2020). EB-47, a non-clinical NAD^+ mimic, greatly destabilised the HD domain and stabilised interdomain contacts around the HD and WGR domains. Olaparib and talazoparib had no or minor effects on PARP1 allostery, respectively, while niraparib, rucaparib and veliparib showed allosteric effects on HD conformation opposite to those induced by EB-47 (Zandarashvili et al., 2020). Further, the authors used fluorescence polarisation assays and surface plasmon resonance to study the effect of PARP inhibitors on PARP1 DNA-binding affinity and dissociation rates without NAD^+. Confirming the HXMS results, EB-47 increased PARP1 DNA-binding affinity, talazoparib and olaparib had no significant effect, and rucaparib, niraparib and veliparib decreased the DNA-binding affinity (Zandarashvili et al., 2020). Based on these findings, the authors proposed a

classification of PARP inhibitors into three categories: Type I (pro-retention) inhibitors, such as EB-47 and BAD (M. F. Langelier et al., 2018), lead to destabilisation of the HD and increase interdomain contacts, resulting in stronger DNA binding. Type II (no/mild retention) inhibitors, such as olaparib and talazoparib, cause a mild increase in DNA-binding affinity, while Type III (pro-release) inhibitors, such as niraparib, rucaparib and veliparib, destabilise the HD in a way opposite to Type I inhibitors, favouring release of PARP1 from DNA. The authors identified key residues in the HD, WGR and ZnF1 and ZnF3 domains as part of an allosteric network, mutation of which disrupted the pro-retention effect of Type I PARPi, supporting the theory of an inhibitor-driven reverse allosteric effect driving the increase in DNA-binding affinity. Further, development of a bulkier version of Veliparib, the smallest of the inhibitors, converted it into a Type I inhibitor by inducing contacts with the HD (Zandarashvili et al., 2020). According to this study, some inhibitors are able to activate a "reverse" allosteric network, and in a similar, but opposing manner to DNA-dependent activation of PARP1, causing its dissociation from DNA.

The differences in results between the Hopkins et al (2015) and Zandarashvili et al. (2020) studies could lie in a multitude of reasons, including the sensitivities of employed methodologies and the DNA duplex used. Interestingly, in a follow-up study, the authors investigated the effect of the same inhibitors on PARP2, with surprising results. While the pro-retention phenotype of EB-47 is retained, only veliparib has a pro-release effect on PARP2 (M. F. Langelier et al., 2023b). Niraparib, rucaparib, olaparib and talazoparib all had a pro-retention effect on PARP2 instead. Alignments of PARP1/2 crystal structures with PARP inhibitors showed that inhibitors had more space in the cleft between the HD and ART domains in PARP1, whereas in PARP2 most inhibitors contact the N-terminal part of helix F of the HD domain, which in turn communicates with the WGR domain, causing this reverse allosteric pro-retention effect (M. F. Langelier et al., 2023b). The same was found for EB-47

with PARP1, and mutations in key residues in the HD and WGR domains of both PARP1 and PARP2 could ablate this effect and confer resistance to inhibitors (M. F. Langelier et al., 2023; Zandarashvili et al., 2020).

However, while these studies provide important insights into the allosteric component of PARP trapping, they do not offer any information about the contributions of catalytic inhibition versus allosteric modulation, as is relevant for a more physiological context. Despite their classification as "pro-release" inhibitors, niraparib, rucaparib and veliparib still lead to prolonged association of PARP1 with damaged chromatin in a cellular context, as do all PARP inhibitors to differing degrees, which can likely be ascribed to the presence of NAD^+, and the major effect of inhibitor-induced loss of PARP1 automodification in this scenario. Another study sought to answer this by using single-molecule co-localisation assays, allowing for high-resolution capture of kinetics of labelled PARP1 molecules binding and unbinding to immobilised gap ssDNA, in combination with inhibitors and NAD^+ (Xue et al., 2022). First, in the absence of NAD^+, the previously established classifications of inhibitors were confirmed (Zandarashvili et al., 2020). The pro- or anti-retention effect of all inhibitors except rucaparib was also abolished by an HD mutant, D766/770A (Xue et al., 2022), further supporting the notion of steric clashes between inhibitors and the HD driving allosteric modulation. Addition of NAD^+ demonstrated that PARP1-DNA retention depended on competitive inhibition, with higher concentrations of inhibitor leading to greater retention, with talazoparib and olaparib causing the highest retention, followed by EB-47 and then veliparib and rucaparib, with no discernible change for niraparib (Xue et al., 2022). This agrees with other reports of PARP inhibitor dissociation constants (Rudolph et al., 2022), and the allosteric-change resistant D766/770A mutant showed no difference in retention in responses to EB-47, olaparib and talazoparib in the presence of NAD^+ (Xue et al., 2022). This indicates that in a physiological setting, despite the allosteric changes induced by PARP

inhibitors, PARP trapping by inhibitors relies more on efficient competition of PARP inhibitors with NAD^+.

PARP-PARPi binding and inhibitor potency

Studying the potency of small molecule inhibitors involves the determination of the binding constant (K_D), inhibition constant (K_I), and the manner of inhibition (competitive vs noncompetitive vs uncompetitive). Since PARP1/2 are their own prime substrates, measuring their activity and effect of inhibitors on it comes with difficulties, as it does not allow for enzyme versus substrate titrations to determine enzyme activity and inhibitor potency, and every ADP-ribosylation event leads to a changed enzyme (Rudolph et al., 2022). A recent study by the Luger group pointed out that the high concentration of PARP1/2 required in most assays, and the tight binding of inhibitors to PARP1, leads to quenching of inhibitor, and the measured binding constant will reflect the concentration of leftover active enzyme (Jarmoskaite et al., 2020; Rudolph et al., 2022). Due to this, previous enzymatic activity assays, surface plasmon resonance and fluorescence polarisation assays have often reported PARP inhibitors as being nearly equipotent (Hopkins et al., 2015; Murai et al., 2012; Shen et al., 2013; Thorsell et al., 2017). A more recent study measured PARP inhibitor binding affinity using fluorescence polarisation involving a complex of PARP1, PARP inhibitor and DNA, followed by subsequent addition of NAD^+. By measuring the rate of DNA release, the authors could calculate the competition between PARP inhibitor and NAD^+, with a stronger binding affinity of PARP inhibitor leading to slower release. This found talazoparib to be the most potent by far, followed by rucaparib and olaparib (Rudolph, Roberts, & Luger, 2021a). Talazoparib as the bulkiest compound was shown to have the most extensive interaction network within PARP1, potentially explaining its increased affinity and potency (Rudolph et al., 2022).

Crucially, all current PARP inhibitors were developed and tested before the discovery of HPF1. While HPF1 was naturally present i*n vivo,* these tests were performed *in vitro,* in the absence of this physiological co-factor. Its tight interaction with the PARP1 catalytic site affects amino acid specificity and ADP-ribose chain length; it is likely to affect the binding of some inhibitors. The same study that measured PARP inhibitor binding affinity using fluorescence polarisation (Rudolph, Roberts, & Luger, 2021a) repeated this in the presence of HPF1. HPF1 significantly increased the binding of olaparib and niraparib to PARP1 in this experimental setting, but not for PARP2, and due to the already tight binding of talazoparib and rucaparib to PARP1, it was not possible to discern any difference in the presence of HPF1. In a follow-up study, the authors measured the rate of association of different PARPi to PARP1/PARP1-HPF1 using the same experimental set-up, with varied time points at which NAD^+ was added. Measured association rates and binding constants were used to calculate the dissociation rates for different PARP inhibitors. Comparison of the calculated PARPi dissociation rates from PARP1/PARP1-HPF1 with the previously published IC_{50} values of different PARPi in a survival assay measuring their efficacy in a BRCA2-mutant cell line (Johannes et al., 2021), showed the highest correlation for the PARP inhibitor dissociation rate from the HPF1-PARP1 complex. Tight binding to the PARP1-HPF1 complex by talazoparib and saruparib, the PARP1-specific inhibitor, were shown to be driven by extremely slow dissociation rates (Stojanovic et al., 2023), and had the lowest IC_{50} values (Johannes et al., 2021).

These studies indicate that PARP inhibitor binding to PARP1 is influenced by HPF1, and thus PARP inhibitor potency. According to these findings, talazoparib is the most potent inhibitor due to its increased binding affinity, which could in turn explain increased association with chromatin through tighter binding of PARP1, and less opportunity for PARP1 to associate

with NAD^+. They therefore support a catalytic-inhibition based model of PARP1 trapping, in which inhibitor binding potency determines NAD^+ competition.

A potential caveat of these studies and their methodology, however, is their use of the release of the PARP-HPF1 complex from DNA release as a read-out for PARP inhibitor binding. The same method was used by other studies to study the effect of inhibitors on PARP1 binding to DNA, showing that in the absence of NAD^+, inhibitors affect PARP1 DNA-binding affinity (M. F. Langelier et al., 2023; Zandarashvili et al., 2020). This potentially complicates the interpretation of this data; if PARP inhibitors can affect PARP1 binding to DNA, it might make it more difficult to reliably calculate PARP inhibitor binding to PARP1 by using its release from DNA as a proxy. The authors do not mention these other papers in their study, or that any changes in the fluorescence polarisation upon addition of PARP inhibitors were observed.

Understanding "trapping" *in vivo*

While a lot of focus was directed towards investigating the underlying mechanisms of PARP1/2 trapping, other studies raised the question of what exactly "trapping" is. Trapping was traditionally understood as the physical retention of PARP1 on damaged DNA, as observed *in vitro* in the absence of NAD^+ or in response to PARP inhibition, the lack of automodification and/or allosteric modulation hindering dissociation. This was thought to translate into a cellular context: inhibition and stalling of PARP1 on a DNA break would lead to replication fork collapse, and exacerbation of existing damage. However, *in vitro* studies cannot fully recapitulate physiological conditions and do not necessarily reflect cellular processes.

Many studies used chromatin fractionation assays to detect changes in chromatin association of PARP1 in response to inhibitors (Hopkins et al., 2015; Murai et al., 2012, 2014), and laser

microirradiation assays with improved temporal resolution followed (Prokhorova, Zobel, et al., 2021; Zentout et al., 2024), but neither offer any information on whether the continued association of PARP1 with chromatin is through physical trapping on DNA or a recurrent cycle of binding and unbinding. To address this, Shao et al. (2020) induced DNA damage in PARP1 KO cells expressing GFP-tagged PARP1 using a 405nm laser in a single spot, followed by subsequent photobleaching of the same spot. Fluorescence recovery after photobleaching (FRAP) was used as a readout for GFP-PARP1 re-association at the bleached spot; if the PARP1 molecules previously bound to the bleached site were physically trapped in the presence of PARP inhibitors, fluorescence recovery through unbinding of the old and replacement by new fluorescent PARP1 should not occur, or be much slower. Despite prolonged retention with the damaged spot after treatment with PARP inhibitor, fluorescence recovery was not abrogated, although the exchange kinetic was slowed, to similar degrees in response to niraparib and talazoparib (Shao et al., 2020a). Loss of XRCC1 also caused prolonged chromatin retention of PARP1, and slowed the exchange kinetics of PARP1. The authors therefore suggested that it is the resulting impaired repair of damage that leads to continuous recruitment of PARP1 in response to PARP inhibitor treatment and loss of ADP-ribosylation. Interestingly, PARP1 H862D, a catalytic mutant, did show significant slowing of exchange kinetics, indicating physical stalling. Moreover, treatment of PARP1 H862A/D with niraparib, but not talazoparib, accelerated its release from chromatin. The authors did not show how treatment of PARP1 H862A/D with niraparib or talazoparib affected catalytic activity, which would have revealed if the catalytic inhibition of niraparib was lost. Similar experiments done *in vitro* by Zandarashvili et al (2020) showed that mutation of key contacts could render PARP1 resistant to the effect of inhibitors, but the results from this study indicate that they can result in the opposite effect, speeding up release, potentially through a reverse allosteric mechanism.

While this study showed that *in vivo*, trapping does not consist of physical stalling on DNA, but rather continuous re-binding and exchange of PARP1 molecules at the site of damage, it only tested two inhibitors and did not provide a way to differentiate between the effect of catalytic inhibition and any potential allosteric effects.

The to date most comprehensive cellular study aiming to establish the nature of PARP1 trapping, and its underlying basis, used UV laser microirradation, FRAP and mathematical modelling to unravel this. To be able to distinguish between the contributions of catalytic inhibition and allosteric modulation to PARP1 chromatin retention, the authors measured three separate behaviours: PARP1 retention, or gross PARP1 behaviour, was measured by delayed release of PARP1 from DNA damage. PARP1 trapping was measured by a decrease in the exchange rate of PARP1 at damage sites due to prolonged DNA-binding, and PARP1 inhibition was measured by reduced recruitment of ARH3 to the damage site (Kanev et al., 2024). All PARP inhibitors were shown to increase PARP1 retention at damage sites in a concentration-dependent manner, with veliparib only leading to a moderate delay in resolution of PARP1 foci, followed by olaparib and rucaparib, and niraparib and talazoparib leading to the longest retention, agreeing with previous cellular findings (Murai et al, 2012; Murai et al., 2014; Pommier et al., 2016). The authors were further able to confirm that PARP inhibition does not abolish PARP1 turnover at sites of damage, as shown previously (Shao et al., 2020), even at very high concentrations. However, they did show that some inhibitors affect the rate of fluorescence recovery, and that this rate of delay was strongly correlated with overall PARP1 retention at the damage site; veliparib did not exhibit any trapping activity, olaparib and rucaparib had intermediate trapping potency, and niraparib and talazoparib had the strongest trapping effect (Kanev et al., 2024). This agrees with previously published trapping potentials (Murai et al., 2012; Murai et al., 2014; Pommier et al., 2016). A previous study using FRAP also found that a catalytically dead PARP1mutant, PARP1

E988K, still retained dynamic exchange at DNA lesions (Juhász et al., 2020), indicating that loss of catalytic activity alone does not lead to physical trapping, but rather that it depends on certain allosteric changes induced by some inhibitors.

Assuming catalytic inhibition has the same contribution to the overall PARP1 retention for all inhibitors, at an appropriate concentration, it is therefore differential PARP1 trapping, i.e. the increased binding of PARP1 to DNA in the presence of some inhibitors, that underlies the differences in overall PARP1 retention at damage sites. Prolonged PARP1 retention is therefore reliably induced through catalytic suppression by all inhibitors, but catalytic suppression alone does not trap PARP1, as is the case for veliparib. The authors reason that "trapping", or increased unproductive binding-unbinding cycles of PARP1 to damaged DNA are a result of allosteric changes induced by some inhibitors. To test this model, using measurement of either PARP1 retention, or PARP1 trapping (as measured by FRAP), and mathematical modelling, the authors aimed to predict one or the other for previously untested inhibitors. PARP1 trapping induced by A-966492, a novel PARP inhibitor, could be used successfully to predict its effect on PARP1 retention. Interestingly, retention of PARP1 by saruparib, the novel PARP1-specific inhibitor, was the lowest of all inhibitors tested, and predicted to speed up PARP1 turnover. This was indeed the case when testing it, indicating that saruparib has a true "pro-release" effect on PARP1 *in vivo*, reducing its DNA binding affinity.

1.4.3 Future Directions for Therapeutic Targeting of ADP-ribosylation

As outlined in the previous section, many studies have been conducted on the molecular mechanisms governing PARP inhibitors, their results varied and often contradictory. When looking at the consensus of many studies, there does appear to be an underlying allosteric effect of some inhibitors that drives increased association of PARP1 with DNA.

The contribution of allostery and PARPi-PARP binding affinity are also difficult to disentangle: Despite extremely tight binding of saruparib to PARP1, it had “anti”-trapping potential *in vivo,* indicating that allosteric effects might be more influential on cellular physiology than inhibitor binding potency. However, talazoparib binding to PARP1 is also very strong, and correlates to its extremely high trapping potential. Comparison of these studies shows that the exact mechanism by which different PARPi affect PARP1/2, is still not fully understood. Further, the fact that HPF1 was shown to affect binding of some PARPi to PARP1 will likely inform future drug design to consider HPF1.

The increased interest in understanding the differences in PARP inhibitor efficacies coincides with the rising issue of resistance against PARP inhibitors and the discovery of the distinct HPF1-dependent ADPr code. Dysregulation of ADP-ribosylation is both a cause and consequence of a variety of diseases, and this opens the field to investigations about new indications for PARP inhibitor use, novel biomarkers and new targets for therapeutic intervention.

Overcoming PARP inhibitor resistance

Only roughly half of all patients with BRCA-deficient tumours respond to treatment, and despite initial response to treatment with PARP inhibitors, many patients develop resistance to these agents after a few months (X. Li & Zou, 2024; Mohyuddin et al., 2020). Restoration of HR capacity in BRCA-deficient tumours is one of the major ways for PARPi resistance to arise, allowing cells to repair DSBs and thereby no longer suffer from the synthetic lethality induced by PARPi (Rose et al., 2020). This is often caused by the acquisition of BRCA reversion mutations in tumours, either intragenic or epigenetic, or by copy number gain of BRCA or upregulation of the functional allele, after long-term treatment with PARPi and the resulting restoration of BRCA1/2 function (Norquist et al., 2011; Edwards et al., 2008; Pettitt et al., 2020; Mweempwa & Wilson, 2019). HR-restoring mutations in PARPi-resistant

tumours were also identified in other proteins involved in HR and pathway choice: for instance, loss of 53BP1, a determining factor of NHEJ pathway choice, promotes resection of DSBs and promotes recruitment of RAD51 in BRCA1-deficient cells (Bouwman et al., 2010; Dias et al., 2021). Similarly, secondary mutations were also identified in PALB2 and RAD51 paralogs in PARP inhibitor resistant tumours (Domchek, 2017; Kondrashova et al., 2017). The high genomic instability in HR-deficient cells might be an underlying driver for the occurrence of these reversion mutations (Dias et al., 2021).

With BRCA1/2, as well as PARP1, also involved in protection of stalled replication forks and replication-associated ssDNA gaps (Hanzlikova et al., 2018; Hashimoto et al., 2010; Panzarino et al., 2021; Schlacher et al., 2011, 2012), common pathways of PARP inhibitor resistance constitute improved function of these pathways. Use of PARP inhibitors is known to cause an accumulation of gaps, nicks, and SSBs (Lord & Ashworth, 2012), and PARP1 was recently implicated to play an important role in Okazaki fragment processing during lagging-strand synthesis; accumulation of gaps was shown to be suppressed in a PARP inhibitor resistant BRCA-deficient cancer cell line (Cong et al., 2021), and loss of DNA Ligase III, which is involved in filling the gaps of the lagging strand, was shown to re-sensitise resistant tumour cells to PARP inhibitor treatment (Dias et al., 2021). In the absence of BRCA1/2, MRE11 resects reversed forks and ssDNA gaps (Lemaçon et al., 2017; Schlacher et al., 2011, 2012): loss of PTIP was shown to underlie resistance of BRCA2-deficient cells to PARP inhibitor by inhibiting recruitment of the MRE11 nuclease to stalled replication forks, preventing excessive degradation of nascent DNA strands (Chaudhuri et al., 2016). This suggests that degradation of reversed forks, and subsequent generation of gaps in BRCA-deficient cells are a key factor underlying PARP inhibitor sensitivity, and presents an opportunity for use of combination therapies targeting replication forks, to further sensitise cells to PARP inhibitors.

Another mechanism of PARP inhibitor resistance is upregulation of drug efflux pumps; increased expression of members of certain transporter families, such as the ABCB1, is a well-established source of resistance against several chemotherapeutic agents (Dias et al., 2021). In these cases, resistance might be circumvented by using PARPi that are poor targets for ABCB1, such as veliparib and niraparib, or concurrent use with ABCB1 inhibitors, such as tariquidar (Dias et al., 2021).

Loss of PARG, the enzyme responsible for cleaving the majority of ADP-ribose chains in response to PARP1 activation, was also found to be the driver of PARPi resistance in some cancers, by boosting the number of ADPr chains present despite inhibitor treatment (Gogola et al., 2018). Use of small-molecule inhibitors against PARG concomitantly with PARPi in these cases could provide a mechanism against resistant tumours, and fast-track designation for a PARG inhibitor, IDE161, was granted by the FDA in 2023, and it is currently in a phase I clinical trial (NCT05787587, Abed et al., 2023).

Similarly, one study identified reduced expression of PARP1 as a potential driver of resistance against PARP inhibitors in ovarian cancer cell lines and presented a PARP1 radiotracer as a potential option to survey PARP1 expression in patient tumour tissues (Makvandi et al., 2018). In one olaparib-resistant ovarian cancer patient, a mutation was identified in PARP1 itself, R591C (Pettitt et al., 2018). As discussed in section 1.2.1, R591 is part of the Zn1-WGR-HD interdomain network that leads to allosteric activation of PARP1 upon DNA binding; this mutant, while recruited effectively to sites of DNA damage, dissociates rapidly from damage sites, and was shown to be resistant to trapping by talazoparib (Pettitt et al., 2018). Other PARP1 mutations shown to cause resistance to PARPi in a CRISPR screen were situated in DNA-binding regions, such as M43del, and F44I, in Zn1, N329Q in Zn3, as well as in the catalytic domain with HD742F located in the HD, and Y848del (Pettitt et al., 2018).

Findings of resistance-causing PARP1 mutations give further incentive to screen patients for potential alterations in PARP1, and for an improved understanding of the contacts different PARP inhibitors rely on for their function, both catalytic and allosteric, for the potential to better fine-tune which inhibitor should be chosen for treatment.

Dysregulation of ADP-ribosylation in disease

Given the importance of PARP1/-2-mediated ADP-ribosylation as a signalling factor for a variety of mechanisms, it is unsurprising that its dysregulation is involved in the pathogenesis of several diseases. This can be distinguished into the physiological role of PARP1 in pathogenesis as part of its role in the DDR, as well as the dysregulation of the ADPr pathway as the causation of disease, both of which potentially serve as therapeutic targets.

PARP1 was shown to be activated in brains of patients who died of ischaemic stroke or brain trauma (Love et al., 1999). Over-activation of PARP1, as is the case following production of reactive oxygen species (ROS) and resulting DNA damage, leads to excessive ADP-ribosylation, which can deplete cellular NAD^+. PARP1 knockout mice were shown to be resistant to different types of ischaemia-reperfusion injury (Eliasson et al., 1997), suggesting that PARP1 inhibition could serve as a therapeutic target in such conditions. Recently, a blood-brain-barrier permeable PARP inhibitor, AZD9574, was developed, which could in the future be re-purposed for these indications (Staniszewska et al., 2024).

Recently, a biallelic mutation in PARP1 was for the first time linked to a neurodegenerative disease, in a patient suffering from childhood-onset neurodegeneration with progressive cerebellar ataxia and oculomotor apraxia. The nonsense mutation resulted in a truncation of PARP1, leaving only the first 127 amino acids encoding the first DNA-binding zinc finger, and part of the second (Hailstone et al., 2023). Patient-derived cells showed a significant loss

of ADPr, consistent with loss of PARP1, and an increased sensitivity to SSB-inducing genotoxins and reduced SSB repair (Hailstone et al., 2023).

Loss of both ARH3 and PARG has been shown to cause increased sensitivity to DNA damage (Cortes et al., 2004; Mashimo et al., 2013; Shirai et al., 2013). Loss-of-function of PARG in *Drosophila*, which is functionally equivalent to both human ARH3 and PARG (Fontana et al., 2023), leads to developmental lethality in flies, while the surviving fraction grown at a permissive temperature suffers from progressive neurodegeneration in adulthood, exemplified by neuronal accumulation of PAR, reduced locomotion and a shortened lifespan (Hanai et al., 2004). Similarly, knock-out of PARG in mice leads to early embryonic lethality, and the toxicity caused by PARG deletion in mouse trophoblast-derived stem cells could be rescued by growing the cells in media containing PARP inhibitors, thereby counteracting the excessive accumulation of PAR (Koh et al., 2004).

Recently, loss of cellular activity of ARH3 was found in patients with a progressive autosomal recessive neurodegenerative disease termed CONDSIAS, occurring in several families. CONDSIAS is characterised by paediatric-onset of infection/stress-induced neurodegeneration leading to impaired or declining cognitive development, muscle atrophy, seizures, gait ataxia and childhood death in severe cases (Beijer et al., 2021; Danhauser et al., 2018; Ghosh et al., 2018). Toxicity and hydrogen peroxide sensitivity in ARH3-deficient patient-derived fibroblasts could be rescued by transfection with functional ARH3, or by treating cells with PARP inhibitor (Danhauser et al., 2018). Having identified two different disease-associated ARH3 mutations, one of which causes loss of nuclear localisation, it seems that it is the stress-induced accumulation of nuclear PAR that causes the neurodegenerative phenotype (Beijer et al., 2021). Similarly, a truncation in the TARG1 gene was found to be responsible for severe and progressive neurodegeneration inherited recessively in a family (Sharifi et al., 2013). Excessive ADP-ribosylation on both serines and glutamates/aspartates

was shown to be cytotoxic, confirming these findings (Groslambert et al., 2023; Prokhorova, Agnew, Wondisford, Tellier, et al., 2021).

1.5 Aims

PARP1/2-mediated ADP-ribosylation is a major therapeutic target, not only in cancer, but potentially also for many other diseases. In recent years, huge strides have been made in improving our understanding of the DDR-specific ADP-ribosylation code, as well as our understanding of PARP1 trapping. HPF1, counteracted by ARH3 and PARG, directs PARP1 activity towards a DDR-specific, serine-linked, shorter ADPr code, the specific results of which are yet to be determined. This opens the possibility of targeting other members of this pathway in different diseases.

Interestingly, PAR chains were long thought to be required for PARP1 dissociation from chromatin, and for chromatin relaxation overall, but the newly discovered HPF1-dependent ADPr code challenges this paradigm; frequent initiation on serine residues, but not elongation, appears to be favourable for PARP1 release from lesions and downstream repair (Juan José Bonfiglio et al., 2017; M. F. Langelier et al., 2021; Prokhorova, Zobel, et al., 2021; Rudolph, Roberts, Muthurajan, et al., 2021; Smith et al., 2023). Loss of HPF1 leads to prolonged retention of PARP1 on damaged chromatin, while allowing for ADPr chain extension (M. F. Langelier et al., 2021; Prokhorova, Zobel, et al., 2021; Suskiewicz et al., 2020). This poses the question of "how much" ADP-ribosylation is required for efficient release of PARP1 from DNA damage, and how this is dynamically regulated by ARH3 and PARG.

It is well established that PARP1 trapping is a major driver of cytotoxicity, whether through inhibition or mutation of catalytic residues. A recent study showed that mice that heterozygously express a catalytic inactive mutant of PARP1, E988A, suffered from early embryonic lethality and genomic instability, highlighting the difference between loss of PARP1 and loss of ADP-ribosylation (Shao et al., 2023). This indicates that less than physiological levels of ADP-ribosylation, as well as trapped PARP1, are not tolerated well by cells. Similarly, excessive levels of ADP-ribosylation are also toxic for cells (Prokhorova, Agnew, Wondisford, Tellier, et al., 2021; Yu et al., 2006).

The better understand this DDR-specific ADPr code, and the determinants of PARP inhibitor sensitivity, the following work can be broken down into three major aims:

1: Discern the roles of mono vs poly-ADP-ribosylation for PARP1 behaviour and trapping at DNA damage sites, DNA repair, and cellular survival.

2. Investigate the sensitivity of PARP1 mutants to different PARP inhibitors.

3: Investigate the relationship and dynamic between PARP1 and PARP2 at the DNA damage site using various PARP mutants and PARP inhibitors.

2. Materials and Methods

2.1 Cell Biology

2.1.1. Cell lines

Cellular experiments were undertaken in human embryonic kidney (HEK293T), osteosarcoma (U2OS), and modified U2OS Flp-In T-REx cells (U2OS Flp-In). HEK293T (CRL-3216, ATCC) and U2OS (HTB-96, ATCC), were acquired from ATCC, while U2OS Flp-In cells were a generous gift from Fumiko Esashi at the University of Oxford.

U2OS and HEK293T cells were grown in DMEM (31966-021, Gibco or D6429, Sigma Aldrich) and supplemented with 10% FBS (F9665, Sigma-Aldrich), and Penicillin/Streptomycin (100U/mL, Gibco) at 37 °C with 5% CO_2. U2OS Flp-In cells, before integration of the desired plasmid into the genome, were grown in DMEM (31966-021, Gibco or D6429, Sigma Aldrich) supplemented with 10% FBS, 4 µg/mL Blasticidin (ant-bl-1, Invivogen) and 50 µg/mL Zeocin (R25001, Thermo Fisher). Following recombination of the target gene into the U2OS Flp-In genome, Zeocin was replaced by 200 µg/mL Hygromycin (ant-hg-2, Invivogen). Cells were split on average twice a week, at roughly 1:10, and were not kept past 20 passages. Media was aspirated, followed by a wash with 1x room temperature PBS and TrypLE Express (12604013, Gibco) was added. Following 5-10 minutes of incubation at 37 °C, cells were resuspended in appropriate media, and spun down at 145 x g for 5 minutes (U2OS) or at 100 x g for 3 minutes (HEK293T) to dispose of remaining trypsin, and resuspended in fresh media.

2.1.2. DNA damage and cell lysis

When treated with hydrogen peroxide (H_2O_2), media in 6 cm dishes was aspirated and cells washed with 1X DPBS containing calcium and magnesium (14040133, Gibco), followed by incubation with 2 mM H_2O_2 in 3 mL DPBS for 10 minutes at 37 °C. Following incubation,

cells were washed once more with 1X DPBS, placed on ice and lysis buffer was added to the dishes.

Cells were lysed in lysis buffer (100mM NaCl, 50mM Tris-HCl pH 8.0, 1 % TritonX-100), which was supplemented with 1X protease inhibitor (P2714-1BTL, Sigma Aldrich), 1X phosphatase inhibitor (4906837001, Sigma Aldrich), 250 units/mL benzonase (E1014-25KU, Sigma Aldrich), PARP inhibitor olaparib (HY-10162, MedChemExpress), PARG inhibitor PDD00017273 (SML1781, Sigma Aldrich) immediately before lysis. For U2OS cells, 1 mM of each inhibitor was used, while for HEK293T cells 2 mM were used. This was done to maintain physiological levels of ADP-ribosylation during the lysis process. If cells were treated with another PARP inhibitor prior to lysis, 1 mM of the corresponding inhibitor was added into the lysis buffer as well.

The cell suspension was collected in Eppendorf tubes, which were left at 4 °C to rotate for 30 minutes at 20 rounds per minute in a table-top rotator. The lysate was subsequently separated into soluble and insoluble fractions by centrifugation for 15 minutes at 21,130 x g and 4 °C. Spectroscopy using the Bradford assay was used to measure the protein concentration of the soluble fraction, and whole cell lysates were mixed with 4X LDS (NP0008, NuPAGE) buffer with TCEP (646547, Sigma) at a 3:1 ratio, the concentration normalised to the sample with the lowest protein concentration. Samples were then heated for 5 minutes at 95 °C and spun down for 1 minute at 21,130 x g. The residual whole cell lysates were then stored at -20 °C for potential future use.

2.1.4 Transfections

Cells were transfected using Mirus TransIT-LT1 (MIR 2305, Cambridge Bioscience). Cells were seeded aiming for confluency of around 60-80% on the day of transfection, with varying transfection reagent volumes depending on the cell culture dishes used according to the manufacturers' instructions.

For 6 cm dishes, 2.5 µg DNA was mixed with 500 µL Opti-MEM (31985070, Gibco), and 7.5 µL transfection reagent was added. While the mixture was incubated at room temperature for 15-30 minutes, the media in the dish was replaced with 4 mL of fresh media. Finally, the transfection mixture was added to the cells with a pipette in a dropwise fashion, the dish gently rocked, and the cells incubated for another 24 - 48 hours.

2.1.5 Recombination in U2OS Flp-In cells

Following the generation of a U2OS Flp-In PARP1 knock-out clone using CRISPR-Cas9 by Florian Zobel, the strain was complemented with wild-type and mutant PARP1 in a Flp-In compatible vector, pDEST-YFP. For each wild-type and mutant PARP1 variant, as well as the empty pDEST-YFP vector, 24 hours prior to transfection, 80,000 U2OS Flp-In cells were seeded in a well of a 6-well plate, cultured in DMEM with 10% FBS, 4 µg/mL Blasticidin and 50 µg/mL Zeocin. 900 ng of pDEST-YFP carrying the desired PARP1 variant was mixed with 900 ng of pOG44, the vector encoding Flp-In recombinase required for genomic integration of the gene of interest and combined with 100 µL Opti-MEM. After adding 3 µL Mirus TransIT-LT1 to the mixture, it was incubated at room temperature for 15-30 minutes, during which the media in the wells was replaced with 2 mL fresh media. Subsequently, the transfection mixture was added to the wells in a dropwise fashion. In addition to the empty-vector control, one well was also left un-transfected to control for the efficacy of the antibiotics. Following 24 hours incubation of the cells with the transfection mixture, cells were trypsinised and transferred to a 15 cm dish, re-suspended in DMEM with 10% FBS without antibiotics, to allow for formation of separate colonies. Another 24 hours later, the media was replaced with DMEM containing 10% FBS, 4 µg/mL Blasticidin and 200 µg/mL Hygromycin, the latter selecting for successfully integrated PARP1 variant or empty pDEST YFP. Media was refreshed every 2-3 days for the next two weeks, and as expected, un-transfected cells started to die 3 – 4 days after treatment with Hygromycin.

2.1.6 Clonogenic assays

For each condition, U2OS or U2OS Flp-In cells were seeded in three technical repeats in either 6 well or 12 well plates, with 2000 or 1000 cells per well, respectively. Increasing concentrations of drugs, as indicated in the *Results* section, were dissolved in DMSO and added to the media in a ratio of 1:1,000, and DMSO in the same volume was added to the control wells. To induce expression of the desired gene, U2OS Flp-In cells were treated with Doxycycline at the concentration indicated in the *Results* section. After 10 days, the media in the wells was removed and the wells were washed once with 1X DPBS and subsequently submerged in a 0.5% crystal violet (115940, Sigma Aldrich) in 25% methanol solution and left at room temperature for 30 minutes. Afterwards, the crystal violet solution was aspirated to be re-used, and plates were washed to remove excess solution. The plates were left to be dried overnight. The plates were then scanned with the wells against a white background to better visualise the stained colonies and the images analysed in ImageJ/Fiji with the ColonyArea plugin (Guzmán et al., 2014). Survival was calculated in percent after normalisation, comparing the total well area occupied by colonies for each condition against the DMSO-treated control of the respective cell line. Each experiment was performed in triplicates.

2.1.7 Microirradiation assays

Cells were seeded and imaged in 8-well glass bottom dishes, with 10mm growth area per well (80807, ibidi). To sensitise cells prior to imaging, the media was replaced with fresh media containing 0.15 µg/mL Hoechst 33342 (H3570, Life Technologies) for 1 hour at 37 °C. Following sensitisation with Hoechst, media in the wells was replaced with 250 µL of CO_2-independent, phenol-red free Leibovitz's L-15 media (Life Technologies) supplemented with 10% FBS, 100 U/mL Pen/Strep solution (15140122, Gibco), containing the either DMSO or a drug at the indicated concentration. Live-imaging was done on the Olympos IX-83 inverted

microscope equipped with a Yokogawa SoRa spinning disk, with a 60x/1.5 numerical aperture oil-immersion objective, and a Prime 95B scientific complementary metal-oxide semiconductor camera. The chamber surrounding the objective was pre-warmed to 37 °C prior to adding the dish, but due to the media used, no CO_2 was added to the chamber. The fluorescence of YFP and mCherry tags were excited with lasers at 488 nm and 561 nm, respectively, and fluorescence was detected with band-pass filters adapted to the fluorophore emission spectra. Laser microirradiation and resulting DNA damage induction was carried out with a 405nm laser, along a 15-µm line through the nucleus for 250 milliseconds using a single-point scanning head (Olympus cellFRAP) coupled to the epifluorescence backboard of the microscope. To ensure consistency between experiments, laser power was measured at 405 nm prior to imaging and set to 110 µW at the sample level. For the 12-minute time course, images were captured every 5 seconds, and for the 30 minute time course, images were captured every 30 seconds. Protein recruitment was quantified manually using Fiji/ImageJ, measuring the mean intensity within the damaged region (Id), the mean nuclear fluorescence (In), and the mean background signal outside of the cell (Ibg). Protein accumulation at sites of damage (Ad) was calculated as:

$$A_d = \frac{I_d - I_{\mathrm{bg}}}{I_n - I_{\mathrm{bg}}}$$

The above equation results in the mean intensity recruitment, or total recruitment, at a given time point. To better represent recruitment and release dynamics, the fluorescence intensity within the micro-irradiated area was subsequently subtracted from the intensity prior to damage induction and then normalised to the maximum intensity (normalised recruitment). The dissipation time used to quantify PARP1 release speed was measured as the time required to dissipate half of the maximum recruitment intensity reached, and calculated using R (Zentout et al., 2024).

2.1.8. Western Blotting

After boiling, samples in 1x NuPage LDS buffer (Invitrogen) with TCEP were resolved on NuPage Novex 4-12% Bis-Tris gels (Invitrogen) and transferred onto nitrocellulose membranes (Bio-Rad) using the Trans-Blot Turbo Transfer System (Bio-Rad). The membranes were blocked in PBS buffer with 0.1% Tween 20 (PBS-T) and 5% non-fat dried milk for 1 hour at room temperature and incubated overnight with primary antibodies (antibodies and respective concentrations are specified in *2.3.1 Antibodies*) at 4 °C overnight. The following day, after washing the membranes thrice for 10 minutes in PBS-T, membranes were incubated with peroxidase-conjugated secondary anti-mouse (Agilent, P0447, 1:2000) or anti-rabbit (Agilent, P0399, 1:2000) antibody for 1 hour at room temperature. After another 30 minutes wash step, membranes were developed using ECL (Pierce, 32106, Thermo Fisher Scientific), and analysed by exposing them to films.

2.1.9 Immunostaining and microscopy

U2OS Flp-In PARP1 KO cells complemented with YFP PARP1 WT or YFP PARP1 E988Q were seeded on a 24-well glass bottom plate and treated with 0.1 µg/mL Doxycycline and either 1 µM olaparib or 5 nM saruparib (HY-132167, MedChemExpress) for 4 days. Doxycycline-induced YFP fluorescence was detected at the microscope without requiring immunostaining. Cells were washed with PBS, and fixed with 20 mM Pipes-KOH, pH 6.8, 0.2% Triton X-100, 1 mM $MgCl_2$, and 4% paraformaldehyde (PFA, Sigma) supplemented with 1 µM olaparib and 1 µM PARGi for 20 minutes, washed with PBS, followed by permeabilization with 0.5% Triton X-100 in PBS supplemented with olaparib and PARGi for 5 minutes and blocked with 5% BSA in PBS-T for 30 minutes. Incubation with primary antibodies (antibodies and respective concentrations are specified in *2.3.1 Antibodies*) was done for 1 hour at room temperature, followed by a PBS wash step, and a 1-hour incubation with Alexa Fluor 488-conjugated goat anti-rabbit secondary antibody (Thermo Fisher

Scientific, A11034, 1:500). This was followed by another PBS wash step, before cells were stained with 1 µg/mL Hoechst 33342 for 30 minutes. For imaging, the EVOS M7000 fluorescent microscope was used, with the 20X/0.75 N.A UPlanSApo objectives under non-saturating conditions. Image quantification was performed using CellProfiler (McQuin et al., 2018). Nuclei identification was done using two-class Otsu thresholding and identified nuclei objects were then used as a mask across all image channels. RPA32 pS4/8 and γH2AX were identified using three-class Otsu thresholding and nuclei containing more than 10 foci of each antibody were counted for each image.

2.2 Cloning

2.2.1 Gateway Cloning

To allow expression in mammalian cells, the gene of interest was cloned into a Flp-In compatible pDEST-YFP-tagged vector. Gateway cloning from the donor to the destination vector was performed using the Gateway LR Clonase II Enzyme mix (11791-020, Invitrogen). Gateway cloning from the destination vector to the donor vector was achieved using the BP Clonase II Enzyme mix (11789-020, Invitrogen). Reactions were left at room temperature between 1 – 18 hours, and the reaction was stopped by incubation with 1 µL of Proteinase K at 37 °C. This was followed by transformation of 5 µL of the reaction mixture with 50 µL of DH5α *E.coli,* incubation on ice for 30 minutes, a 45 second heat shock at 42°C, and another incubation on ice for 2 minutes. The bacteria were mixed with 150 µL of S.O.C media (15544034, Life Technologies) and incubated at 37 °C and 1000 rounds per minute in a table-top shaker. The cell suspension was then plated either on an Ampicillin plate (containing 100 µg/mL Ampicillin) or a Kanamycin plate (containing 30 µg-mL Kanamycin), and the plate left over-night in a 37 °C incubator.

2.2.2. Site-directed mutagenesis PCR

Site-directed mutagenesis was carried out using the NEB Q5® High-Fidelity 2X Master Mix, or the Q5® High-Fidelity DNA Polymerase and the accompanying kit (M0492S and M0491S, New England Biolabs).

The NEBaseChanger® tool (https://nebasechanger.neb.com) was used for primer design, and the resulting suggested annealing temperatures were adhered to. The suggested protocol for a 25 µL reaction was followed, as well as the suggested PCR conditions with adjusted annealing temperatures and extension times. Transformation of the PCR protocol then follows the same protocol as described in section 2.2.1, with 5 µL of the PCR reaction and 50 µL of DH5α *E.coli*.

2.2.3. Plasmid propagation

Depending on whether a MiniPrep or a MaxiPrep was made, the following steps apply. For MiniPreps, between one and three colonies were picked from the plate and grown in 5 mL LB media containing either 100 µg/mL Ampicillin or 30 µg/mL Kanamycin and incubated for 15-18 hours at 37 °C at 200 rounds per minute in an incubator shaker. Afterwards, 3-4 mL of the suspension was spun down for 3 minutes at 4,500 x g at room temperature, and the supernatant discarded. The QIAprep Spin Miniprep Kit (27104, Qiagen) was used to extract the plasmid DNA, and its protocol followed.

For MaxiPreps, the 1 mL of a starter culture was added to 200 mL LB media containing 100 µg/mL Ampicillin or 30 µg/mL Kanamycin and incubated for 15-18 hours at 37 °C at 200 rounds per minute in an incubator shaker. The cell suspension was spun down for 10 minutes at 37 °C at 4,500 x g and the supernatant discarded. The PureLink HiPure Plasmid Maxiprep Kit (K210006, Invitrogen) was used to prepare a maxiprep from the cell pellet.

2.2.4. Sequencing

All sequencing was performed by Sanger Sequencing, by submitting samples and primers at the desired volume and concentrations to Source Bioscience.

2.2.5 Statistical Analysis

GraphPad Prism 10 was used for statistical analysis and data visualisation.

For survival assays, the bars represent the mean and the error bars represent the standard deviation. Cell survival was normalised to the untreated condition of each cell line (where survival of the untreated cell line = 100%). Each experiment was performed in triplicates. Statistical analysis was performed using an unpaired, two-tailed Student's t-test, assuming unequal variance.

For micro-irradiation experiments, the time-lapse curves represent the mean ± standard error of the mean of n amount of cells per condition, whereby n is stated as a range from minimum to maximum amount of cells in the figure legend. Statistical analysis of multiple conditions was performed using one-way ANOVA, which allows testing how a response is affected by a single factor (drug treatment), and allows comparison of the means of multiple groups. The box limits of the box plots correspond to the 25th and 75th percentiles and the bold line indicates the median value; the whiskers extend to minimum and maximum values.

Statistical significance is denoted by * $p < 0.05$, ** $p < 0.01$, *** $p < 0.001$, **** $p < 0.0001$.

2.3. Materials

2.3.1. Antibodies

Below (Table 2.1) is shown a list of primary antibodies used. Secondary antibodies against rabbit and mouse (P0399 and P0447, Agilent) primary antibodies were used at a dilution of 1: 2,000 in 5% milk in PBS-T, and prepared fresh each time.

Target	ID	Manufacturer	Dilution	Species
ARH3	HPA027104	Sigma Aldrich	1: 1,000	Rabbit
FLAG	A8592	Sigma Aldrich	1: 5,000	Mouse
GFP	ab290	Abcam	1: 5,000	Rabbit
Histone H3	07-690	Merck Millipore	1: 50,000	Rabbit
HPF1	NBP1-93973	Novus Biologicals	1: 1,000	Rabbit
Mono-ADPr	647	Ivan Matic	1: 1,5000	Rabbit
Mono/poly-ADPr	83732S	Cell Signalling	1: 1,000	Rabbit
Pan-ADPr	MABE1016	Sigma Aldrich	1: 1,500	Rabbit
PARP1	ab32138	Abcam	1: 5,000	Rabbit
PARP2	ALX-804-639-L001	Enzo Life Sciences	1: 500	Mouse
Poly-ADPr	MABE1031	Merck Millipore	1: 1,000	Rabbit
pRPA pS4/8	A300-245A	Bethyl	1:1000	Rabbit
γH2AX	ab2893	Abcam	1:1000	Rabbit
Polyclonal anti-rabbit, Alexa Fluor 488-conjugated	A-11034	Thermo Fisher Scientific	1:1000	Goat
Polyclonal anti-mouse, HRP-conjugated	P0447	Agilent	1:2000	Goat

Polyclonal anti-rabbit, HRP-conjugated	P0399	Agilent	1:2000	Swine

Table 2.1 List of antibodies used in this work.

2.3.2 Chemicals

Reagent Name	**Manufacturer**	**ID**
Saruparib (AZD5305)	MedChemExpress	HY-132167
Olaparib	MedChemExpress	HY-10162
Niraparib	MedChemExpress	HY-10619
Rucaparib	MedChemExpress	HY-10617A
Veliparib	Enzo Life Sciences	ALX-270-444M005
Talazoparib	MedChemExpress	HY-16106
Doxycycline	Sigma Aldrich	D9891-1G
PDD00017273	Sigma Aldrich	SML1781
Hydrogen peroxide (H_2O_2)	Sigma Aldrich	H1009

Table 2.2: List of commercial drugs and reagents used in this work.

2.3.3. Buffer solutions and media

The compositions of buffer solutions and different growth media are outlined below.

1X PBS-T (10L)

- 1 L 10X PBS (D1408-500ML, Sigma Aldrich)
- TWEEN 20 viscous liquid (P1379, Sigma Aldrich), 10 mL (0.1%)
- 9 L milliQ water

Triton X-100 lysis buffer (1 L)

- NaCl (S9888-25KG, Honeywell), 100 mM (5,844 mg)
- 1M Tris-HCl pH 8.0 (51238, Lonza), 50 mM (50 mL)
- Triton X-100 (X100-500ML, Sigma Aldrich), 1% (10mL)
- 940 mL milliQ water

HEK293T cell lysis buffer (5 mL)

- Triton X-100 lysis buffer (4.3 mL)
- 10X phosphatase inhibitor (4906837001, Sigma Aldrich) in Triton X-100 lysis buffer solution, 1X (0.5 mL)
- 25X protease inhibitor (P2714-1BTL, Sigma Aldrich) in Triton X-100 lysis buffer solution, 1X (0.2 mL)
- 250,000 units/mL benzonase (E1014-25KU, Sigma Aldrich), 250 units/mL (5 µL)
- 10 mM Olaparib (HY-10619, MedChemExpress), 2 µg/mL (0.5 µL)
- 10 mM PARG inhibitor PD00017273 (SML1781, Sigma Aldrich), 2 µg/mL (0.5 µL)

U2OS cell lysis buffer (5 mL)

- Triton X-100 lysis buffer (4.3 mL)
- 10X phosphatase inhibitor (4906837001, Sigma Aldrich) in Triton X-100 lysis buffer solution, 1X (0.5 mL)
- 25X protease inhibitor (P2714-1BTL, Sigma Aldrich) in Triton X-100 lysis buffer solution, 1X (0.2 mL)
- 250,000 units/mL benzonase (E1014-25KU, Sigma Aldrich), 250 units/mL (5 µL)
- 10 mM Olaparib (04402, LKT Labs), 1 µg/mL (0.5 µL)
- 10 mM PARG inhibitor (PD00017273, Selleck Chemicals), 1 µg/mL (0.5 µL)

1X MOPS Buffer (10 L)

- 20X NuPAGE MOPS SDS Running Buffer (B000102, Invitrogen), 1X (500 mL)
- MilliQ water, 9.5 mL

HEK293T and U2OS growth media (550 mL)

- DMEM (D6429, Sigma Aldrich or 31966-021, Gibco), 1X (500 mL)
- FBS (F9665-500ML, Merck Millipore), 10% (50 mL)
- 10,000 Units/mL Penicillin-Streptomycin (15140122, Gibco), 1% (5mL)

U2OS Flp-In growth media (550 mL):

- DMEM (D6429, Sigma Aldrich or 31966-021, Gibco), 1X (500 mL)
- FBS (F9665-500ML, Merck Millipore), 10% (50 mL)
- Zeocin (R25001, Thermo Fisher), 50 µg/mL (275 µL)
- Blasticidin (ant-bl-1, Invivogen), 4 µg/mL (220 µL)

Complemented U2OS Flp-In growth media (550 mL):

- DMEM (D6429, Sigma Aldrich or 31966-021, Gibco), 1X (500 mL)
- FBS (F9665-500ML, Merck Millipore), 10% (50 mL)
- Hygromycin (ant-hg-2, Invivogen), 200 µg/mL (1,100 µL)
- Blasticidin (ant-bl-1, Invivogen), 4 µg/mL (220 µL)

Imaging media for U2OS and U2OS Flp-In (50 mL)

- Phenol red-free Leibovitz's L-15 medium (21083027, Gibco), 1X (45 mL)
- FBS (F9665-500ML, Merck Millipore), 10% (4.5 mL)
- 10,000 Units/mL Penicillin-Streptomycin (15140122, Gibco), 1% (0.45 mL

2.3.4 Expression Vectors

pDONR221 (12536017, Thermo Fisher) was used for the generation of mutants and the transfer of gene inserts between compatible mammalian expression vectors through BP and LR clonase reactions. The vector maps of pDEST-YFP, pDEST-FLAG CMV, and pmCherry C1, which we kindly received from Dr Sébastien Huet's lab along with pmCherry PARP1 (Smith et al., 2023), are shown in Figure 2.1. PARP1 and HPF1, both having only one isoform, were cloned into the pDEST-YFP or pDEST-FLAG vectors, which were used to transiently over-express the construct, or were integrated into U2OS Flp-In T-REx cells to allow Doxycycline-inducible expression. The PARP1 cDNA used contains a natural variation, V762A. For integration into the FRT site, Flp-In recombinase encoded in the pOG44 plasmid (V6005-20, Thermo Fisher) was used.

a)

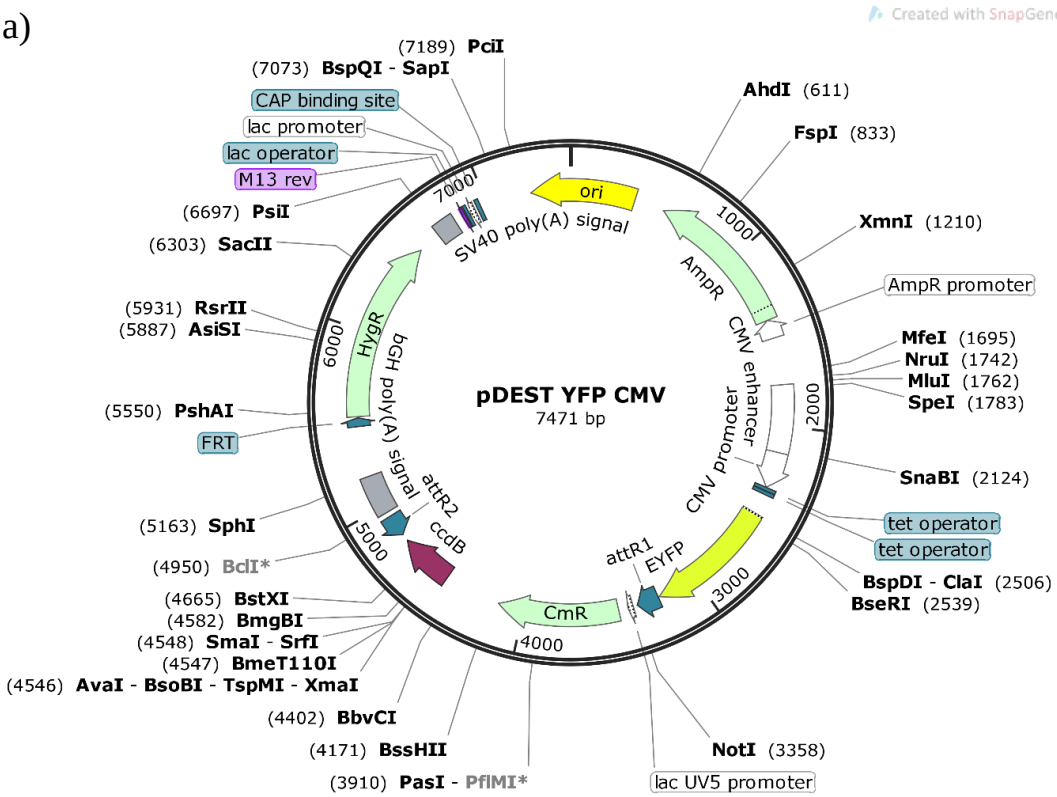
Created with SnapGene®
pDEST YFP CMV
7471 bp
ori
SV40 poly(A) signal
AmpR
CMV enhancer
CMV promoter
attR2
ccdB
attR1
EYFP
CmR
HygR
bGH poly(A) signal
FRT
1000
2000
3000
4000
5000
6000
7000
(7189) PciI
(7073) BspQI - SapI
CAP binding site
lac promoter
lac operator
M13 rev
(6697) PsiI
(6303) SacII
(5931) RsrII
(5887) AsiSI
(5550) PshAI
(5163) SphI
(4950) BclI*
(4665) BstXI
(4582) BmgBI
(4548) SmaI - SrfI
(4547) BmeT110I
(4546) AvaI - BsoBI - TspMI - XmaI
(4402) BbvCI
(4171) BssHII
(3910) PasI - PflMI*
AhdI (611)
FspI (833)
XmnI (1210)
AmpR promoter
MfeI (1695)
NruI (1742)
MluI (1762)
SpeI (1783)
SnaBI (2124)
tet operator
tet operator
BspDI - ClaI (2506)
BseRI (2539)
NotI (3358)
lac UV5 promoter

b)

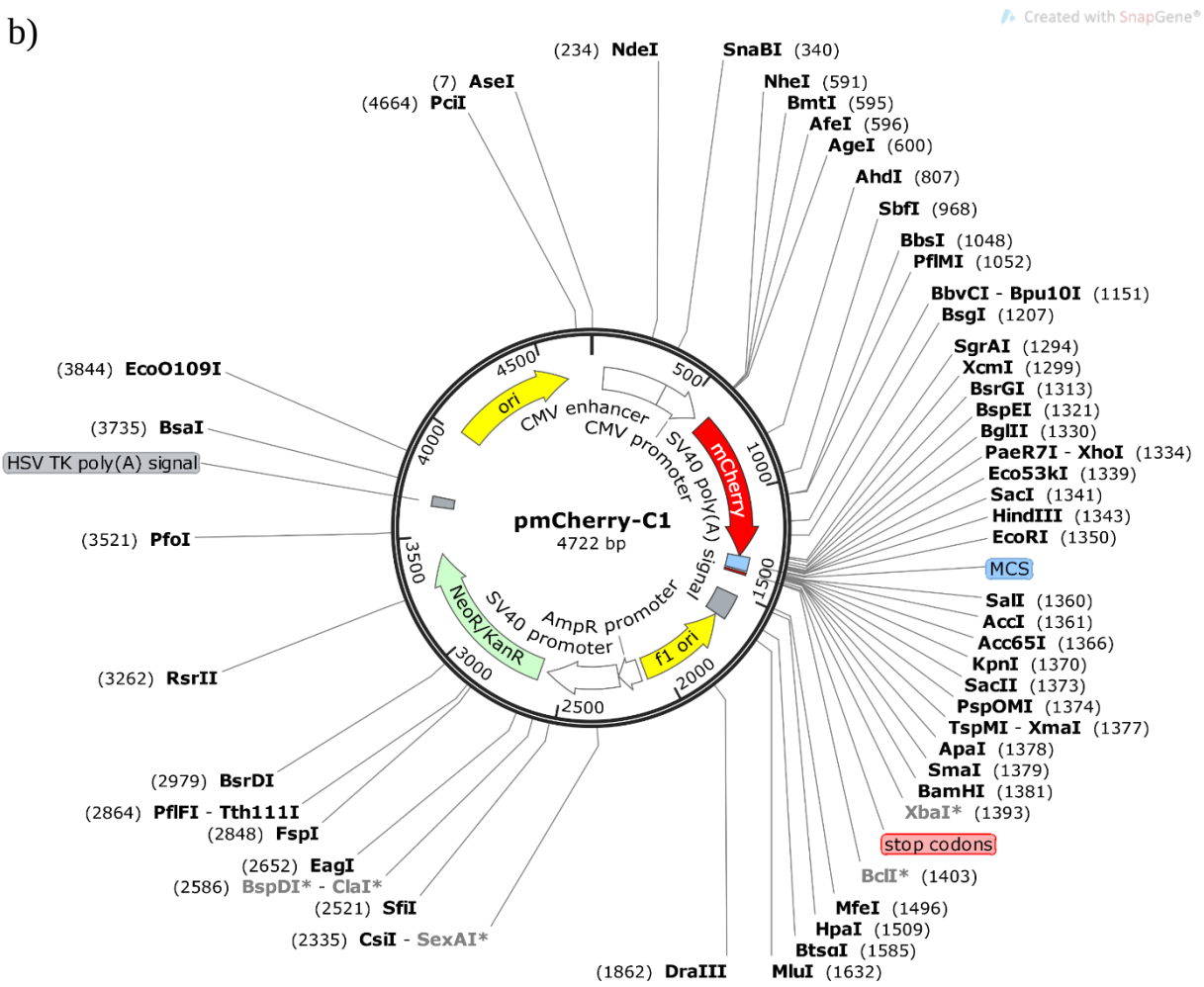
Created with SnapGene®
pmCherry-C1
4722 bp
ori
CMV enhancer
CMV promoter
SV40 poly(A) signal
mCherry
AmpR promoter
SV40 promoter
NeoR/KanR
f1 ori
500
1000
1500
2000
2500
3000
3500
4000
4500
(234) NdeI
(7) AseI
(4664) PciI
SnaBI (340)
NheI (591)
BmtI (595)
AfeI (596)
AgeI (600)
AhdI (807)
SbfI (968)
BbsI (1048)
PflMI (1052)
BbvCI - Bpu10I (1151)
BsgI (1207)
SgrAI (1294)
XcmI (1299)
BsrGI (1313)
BspEI (1321)
BglII (1330)
PaeR7I - XhoI (1334)
Eco53kI (1339)
SacI (1341)
HindIII (1343)
EcoRI (1350)
MCS
SalI (1360)
AccI (1361)
Acc65I (1366)
KpnI (1370)
SacII (1373)
PspOMI (1374)
TspMI - XmaI (1377)
ApaI (1378)
SmaI (1379)
BamHI (1381)
XbaI* (1393)
stop codons
BclI* (1403)
MfeI (1496)
HpaI (1509)
BtsαI (1585)
MluI (1632)
(1862) DraIII
(2335) CsiI - SexAI*
(2521) SfiI
(2586) BspDI* - ClaI*
(2652) EagI
(2848) FspI
(2864) PflFI - Tth111I
(2979) BsrDI
(3262) RsrII
(3521) PfoI
HSV TK poly(A) signal
(3735) BsaI
(3844) EcoO109I

c)

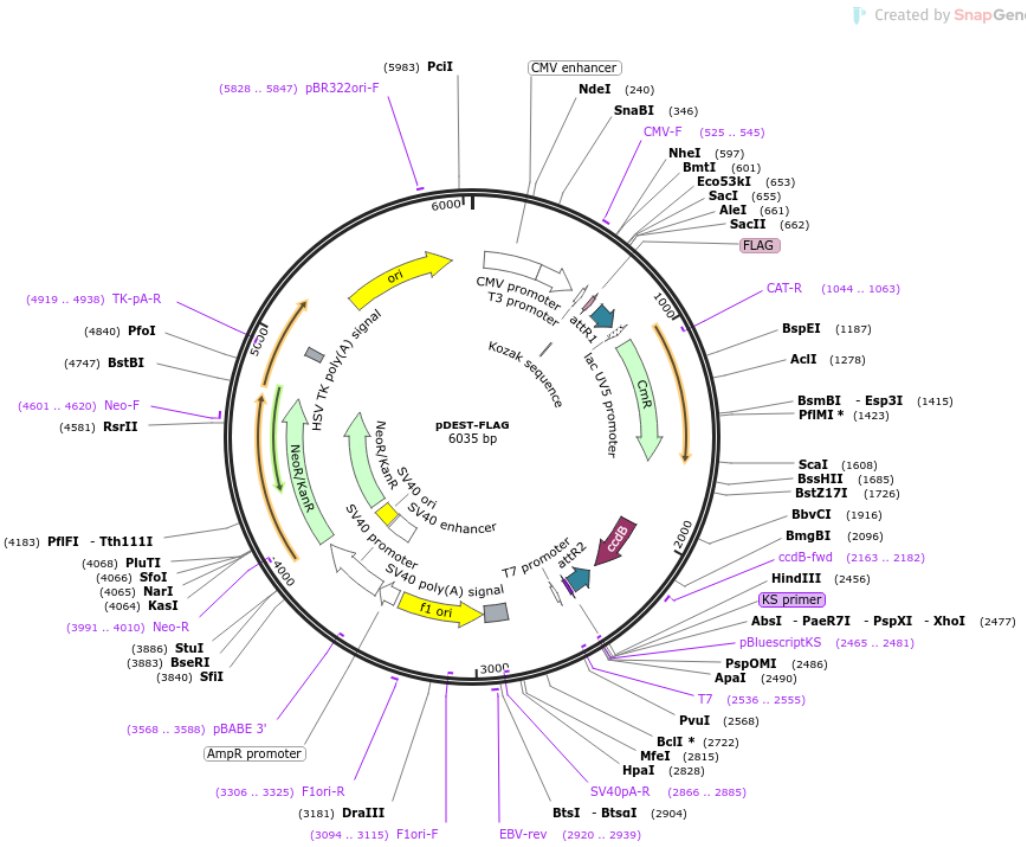

Figure 2.1: Vector maps. a) pDEST YFP, **b)** pmCherry-C1, and **c)** pDEST FLAG. .

3. Results

3.1 HPF1 controls PARP1-mediated ADP-ribose chain length and the PARP inhibitor response

HPF1 was previously shown to be important for the cellular response to PARP inhibitors. Loss of HPF1 not only alters the target residues from serines to glutamates and aspartates and alters the type of ADP-ribose chains produced, but sensitises cells to treatment with PARP inhibitors (Gibbs-Seymour et al., 2016; M. F. Langelier et al., 2021; Palazzo et al., 2018; Prokhorova, Zobel, et al., 2021; Rudolph, Roberts, Muthurajan, et al., 2021; Smith et al., 2023). PARP inhibitors were developed before the discovery of HPF1, and as such, the understanding of how HPF1-dependent ADP-ribosylation regulates the PARP inhibitor response is in its infancy. Having emerged as a potential novel biomarker over the past few years, a better understanding of how HPF1 affects PARP1/2-mediated ADP-ribosylation, and affects the PARP inhibitor response, is crucial.

3.1.1 Over-expression of HPF1 provides resistance to PARP inhibition

To better understand how HPF1 levels correspond to ADP-ribosylation and PARP inhibitor sensitivity, I performed a talazoparib titration in HEK 293TWT and HPF1 KO cells to assess the corresponding ADP-ribosylation levels in the absence of external DNA damage as part of the Prokhorova et al. (2021) study (Figure 3.1, a). A subset of HEK293T HPF1 KO cells were additionally transfected with FLAG HPF1, raising the amount of HPF1 to supra-physiological levels. PARP1 and histones are the major targets of DNA-damage dependent PARP1 activity (D'Amours et al., 1999; Langelier et al., 2012; Leidecker et al., 2016; Smith et al., 2023); The ADPr signal around 97 kDa is lost in 293T WT cells in response to treatment with increasing concentrations of talazoparib (Figure 3.1, a, lanes 1-6), and it is well established that the ADP-ribosylation signal between 97 kDa and 191 kDa reflects PARP1 (113 kDa) automodification (Prokhorova, Zobel et al., 2021), and loss of PARP1 abolishes this signal, as

shown in Figure 3.1, b, Figure 3.4, Figure 3.6, b, and Appendix Figure A.4. When looking at HPF1 KO cells, it is clear that even before the addition of talazoparib, PARP1 automodification is substantially reduced, and that histone ADP-ribosylation is lacking entirely. Core histones have a molecular weight of between 10-15 kDa, and the ADP-ribosylation signal around these molecular weight bands is lost upon loss of HPF1 (Figure 3.1, a, lanes 7-12) (Prokhorova, Zobel et al., 2021; Leidecker et al., 2016; Smith et al., 2023). Both antibodies used, pan-ADPr (MABE1016, Sigma-Aldrich) and mono/poly-ADPr (83732, Cell Signalling Technology) recognise mono and poly-ADPr.

The pan-ADPr antibody specifically consists of a macrodomain with preference for mono-ADPr as well as chains, and as can be seen by how the ADPr signal in the same condition varies between the antibodies, the pan antibody appears to have stronger recognition of mono-ADPr. This loss of ADP-ribosylation in HPF1 KO cells (Figure 3.1, a, lanes 7-12) observed with both antibodies is rescued efficiently by over-expression of HPF1, which not only restores the original ADP-ribosylation levels of HEK293T WT cells, but also causes an increase in the modification of histones (Figure 3.1, a, lanes 13 – 18). It also tends to increase more specifically modification with mono-ADP-ribose (MAR), as reflected by the increase in crisp lines on histones; meanwhile despite over-expression of HPF1, the smears representing long chains of poly-ADP-ribose (PAR) found in lysates from HEK 293T WT cells are lacking. This agrees with the notion that the presence of HPF1 at supra-physiological levels would further impede ADP-ribose chain extension, more so than the presence of endogenous HPF1, which is roughly 20 times less abundant than PARP1, and is more likely to restrict chain extension only at the initial step (Langelier et al., 2021; Suskiewicz et al., 2020). Despite the lower relative levels of PARylation in HPF1-over-expressing cells, cellular resistance to talazoparib is increased: PARP1/2 automodification and histone ADP-ribosylation persist at higher levels of talazoparib than HEK293T WT cells. This suggests

that, by directing a switch from longer PAR chains to shorter chains and single ADPr units, and increased modification of histones, HPF1 can promote PARP inhibitor resistance. The same was observed in an identical experiment for olaparib (Prokhorova et al., 2021). Without DNA damage, however, the affinity of inactive PARP1/2 for HPF1 is relatively low (Suskiewicz et al., 2020).

To understand how the presence of HPF1 affects the PARP inhibitor response under DNA-damage conditions, I simultaneously treated 293T WT and HEK293T PARP1 KO cells with 2 mM hydrogen peroxide (H_2O_2), and 1 µM olaparib (Figure 3.1, b). Treatment of HEK293T WT cells with 1 µM olaparib is sufficient to abolish the H_2O_2-independent and dependent increase in PARP1 automodification. Any DNA-damage dependent ADP-ribosylation is lost in HEK293T PARP1 KO cells, and this is not rescued by over-expression of PARP1 WT alone (lane 7, Figure 3.1, b). Meanwhile, simultaneous over-expression of HPF1 and PARP1 WT rescues PARP1 automodification, and over-expression of HPF1 and PARP1 ΔHD, a constitutively active PARP1 mutant (Dawicki-McKenna et al., 2015), effectively restores histone ADP-ribosylation as well. Importantly, loss of the HD was previously shown to not significantly impact olaparib binding to the ART (Dawicki-McKenna et al., 2015). Together, these results show that HPF1 promotes PARP inhibitor resistance, and that it does so despite it suppressing the production of long PAR chains by PARP1/2. This indicates that rather than PARylation alone being important for PARP1 release from sites of DNA damage, and for modification of target proteins, short chains and MARylation seem to play a significant, if not essential role.

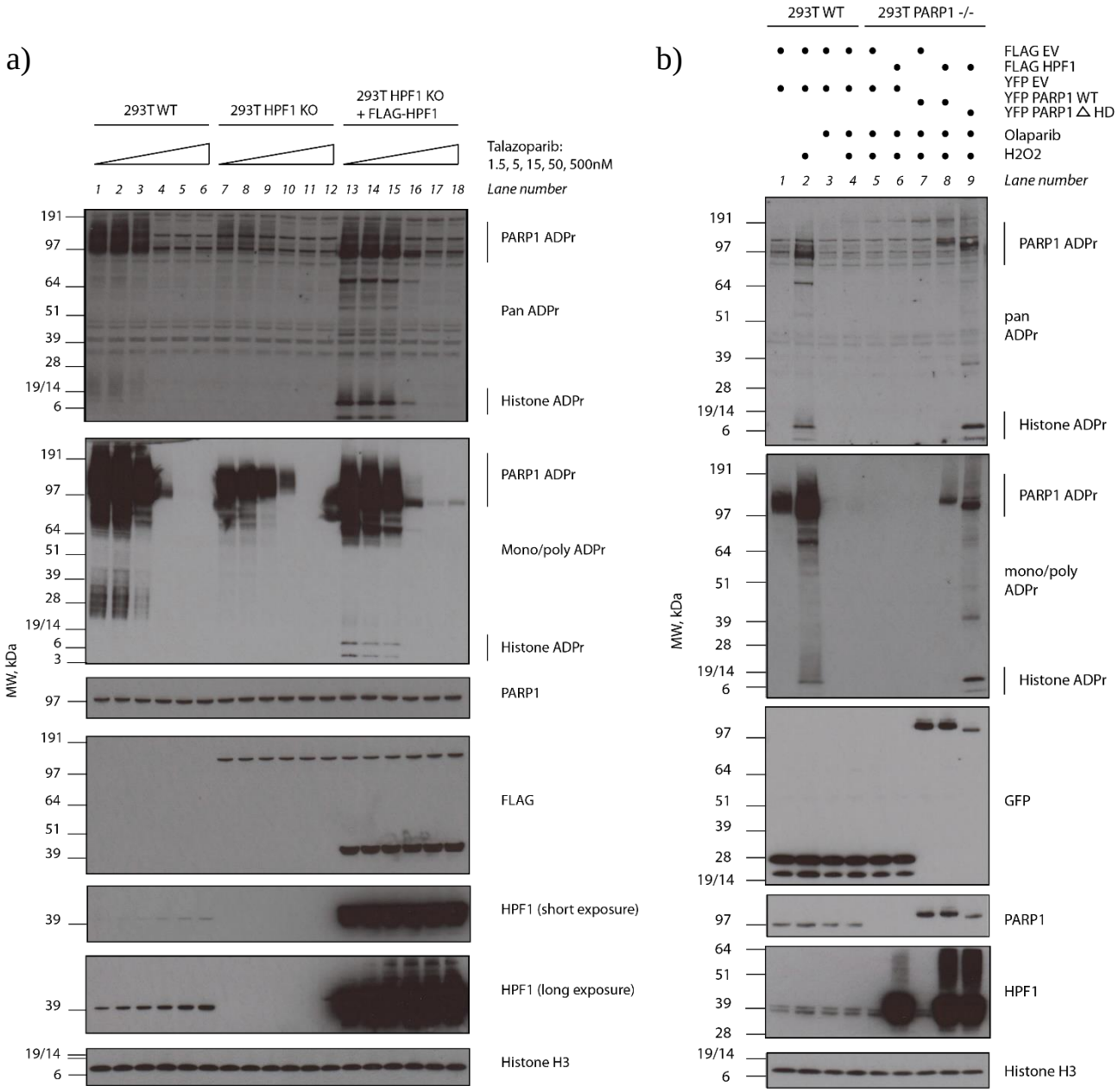

Figure 3.1: HPF1 is responsible and required for maintaining PARP1 auto-modification despite PARP inhibitor treatment. a) Loss of ADP-ribosylation in HEK293T WT and HPF1 KO cells induced by increasing concentrations of the PARP inhibitor talazoparib for 12 hours is rescued by over-expression of FLAG-HPF1 WT. **b)** Simultaneous over-expression of FLAG-HPF1 with either YFP-PARP1 WT or PARP1 ΔHD rescues ADP-ribosylation despite the presence of 1 µM olaparib in hydrogen peroxide-treated cells. Figures adapted from Prokhorova, Zobel et al., 2021.

3.1.2 HPF1 catalytic activity is required for PARP inhibitor resistance

HPF1 is able to direct the ADP-ribosylation activity of PARP1 and PARP2 towards serine residues by providing an additional catalytic glutamate residue, E284 (Suskiewicz et al., 2020). At the same time, by forming the composite active site, HPF1 restricts the length of ADP-ribose chains generated by PARP1/2 (Suskiewicz et al., 2020). With the use of the HPF1 E284A mutant it is possible to distinguish between the importance of ADP-ribose chain length, and the targeting of serine residues. HPF1 E284A binds PARP1 with high affinity, but lacks the catalytic glutamate residue required for ADP-ribosylation of serine residues (Langelier et al., 2021).

To better study the cellular effect of this mutation, and with its potential toxicity in mind, the U2OS Flp-In^{TM} T-REx^{TM}-background was chosen for generation of stable cell lines to allow better control over expression, both temporally and in terms of the desired expression level of the protein of interest. The genomic FRT site allows for integration of a gene of interest using Flp recombinase from an appropriate vector, and the integrated tetracycline response element ensures expression of the integrated gene only occurs upon treatment with Tetracycline/Doxycycline (Yao et al., 1998; Thermo Fisher Scientific/Flp-In System). HPF1 was previously knocked out by Florian Zobel in the U2OS-Flp-In cell line, to ensure the presence of endogenous HPF1 would not interfere, and integration of the desired constructs was achieved as outlined in Section *2.1.5* of *Materials and Methods*. The U2OS Flp-In HPF1 KO cells were complemented with YFP empty vector, YFP HPF1 WT, YFP HPF1 E284A and YFP HPF1 D286A, which has weakened interaction with PARP1/2 (Suskiewicz et al., 2020). Based on previous reports, wild-type HPF1 stimulates the ADP-ribosylation activity of PARP1/2, while simultaneously restricting the length of ADP-ribose chains produced, leading to more frequent initiation of ADP-ribosylation, but less elongation of ADPr chains (Langelier et al., 2021; Prokhorova et al., 2021). Meanwhile, loss of catalytic activity of HPF1

E284A should retain its restriction of ADPr chain elongation, while no longer stimulating initiation of ADP-ribosylation on serines, either on PARP1 or other targets (Rudolph, Roberts, Muthurajan, et al., 2021). Cells expressing HPF1 D286A, a mutant that has weaker interaction with PARP1/2 (Sun et al., 2021; Suskiewicz et al., 2020), should behave similarly to HPF1 KO cells, with PARylation mostly targeted to glutamates and aspartates. The behaviour of these cells is schematically represented in Figure 3.2, a. In Figure 3.2, b, the ADP-ribosylation pattern of these cells expressing different HPF1 variants in response to two different concentrations of doxycycline, but without induction of DNA damage, are shown. Loss of HPF1 leads to a complete loss of the ADP-ribosylation signal on PARP1, which is rescued by expression of YFP HPF1 WT (Figure 3.2, b). As shown in the GFP and HPF1 blots, expression is only induced following treatment with doxycycline, with 0.5 µg/mL sufficient for induction of expression. Meanwhile, in cells expressing YFP HPF1 E284A, despite being equal to expression levels of YFP HPF1 WT, the PARP1 automodification signal resembles that of HPF1 KO cells. Expression of HPF1 D286A leads to PARP1 automodification levels between those cells expressing HPF1 WT and those expressing HPF1 E284A, consistent with an HPF1 mutant which has lowered interaction with PARP1/2, but retains catalytic activity (Sun et al., 2021; Suskiewicz et al., 2020).

This blot shows that the cell lines work as intended, but it does not show how these cells behave in response to DNA damage. Therefore, I treated a subset of these cells with 0.5 µg/mL doxycycline to induce expression, followed by H_2O_2 treatment to induce DNA damage. In U2OS Flp-In WT cells, treatment with H_2O_2 leads to a strong increase in automodification of PARP1/2 and ADP-ribosylation of histones and other targets (Figure 3.2, c). This is successfully reduced by treatment with two different PARP inhibitors, olaparib and saruparib. Loss of HPF1 reduces the automodification pre-damage, and there is no discernible increase in ADP-ribosylation in response to DNA damage. PARP1 automodification is

rescued by YFP-HPF1 WT expression, both pre- and post-damage. No MARylation of histones can be observed in this condition, but this might be due to lower expression levels of HPF1 compared to U2OS Flp-In WT cells (Figure 3.2, c, HPF1 blot). Meanwhile, expression of HPF1 E284A leads to similar levels of PARP1 automodification as in cells expressing HPF1 WT pre-DNA damage, but this is reduced upon H_2O_2 treatment compared to HPF1 WT-expressing cells. Similarly, ADP-ribosylation of other targets is largely lost, which agrees with simultaneous chain restriction and reduced initiation of ADP-ribosylation of this HPF1 mutant.

a)

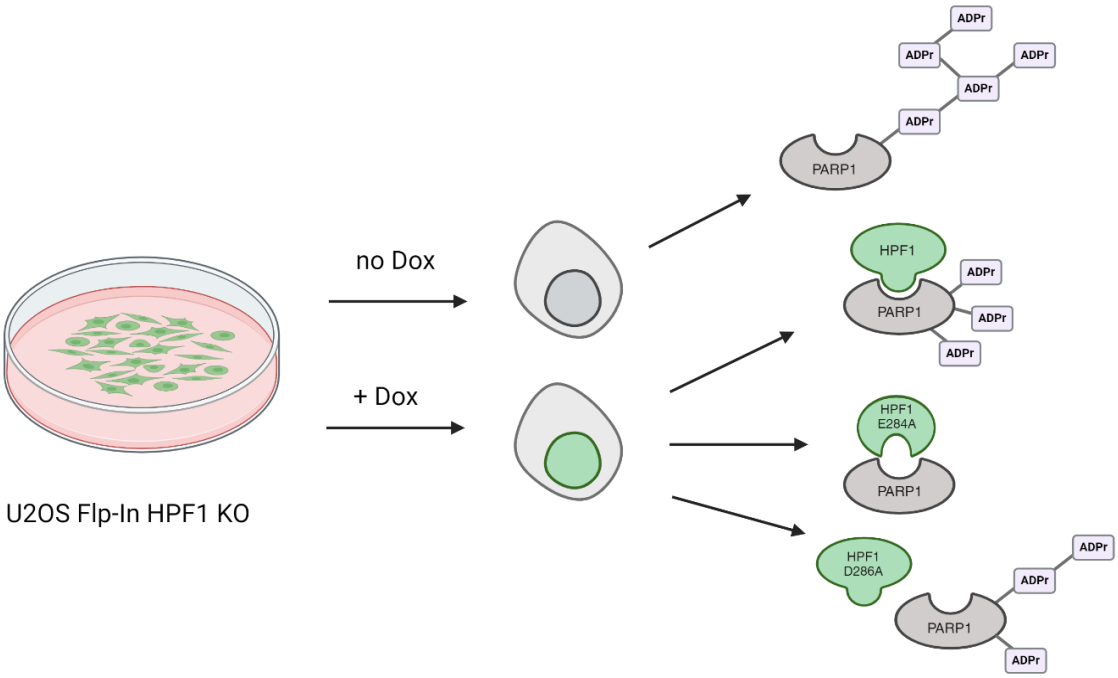

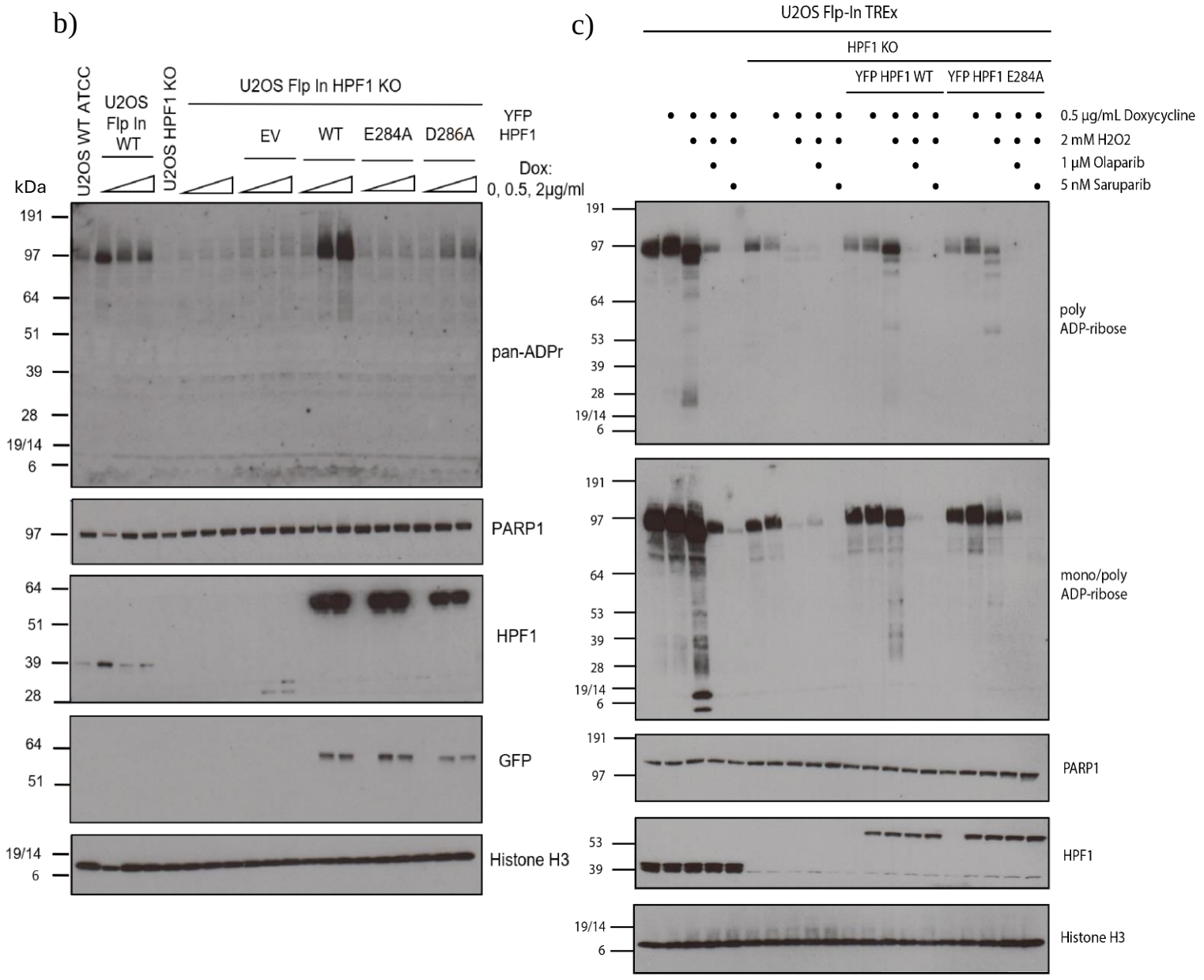

Figure 3.2: Loss of HPF1 catalytic activity reduces PARP1 auto-modification with PAR chains. **a)** Schematic representation of U2OS Flp-In HPF1 KO cells. **b)** U2OS Flp-In HPF1 KO cells substituted with the indicated HPF1 variants are treated with varying concentrations of doxycycline to induce expression. **c)** U2OS Flp-In HPF1 KO cells were treated with doxycycline to induce expression of either YFP HPF1 WT or YFP HPF1 E284A and a subset were treated with hydrogen peroxide to induce damage, and treated with either 1 µM olaparib or 5 nM saruparib.

Having confirmed that these cell lines work as intended, I next wanted to test their sensitivity to PARP inhibitor treatment. I therefore treated these cells with 0.5 µg/mL Doxycycline to induce expression, and performed an olaparib titration for 10 days. The olaparib concentrations ranged from 0.005 to 0.5 µM. These concentrations are relatively low, as 1 µM olaparib was not sufficient to entirely abolish the H_2O_2-induced ADP-ribosylation signal in these cells (Figure 3.2, b). U2OS Flp-In WT, and U2OS Flp-In HPF1 KO cells expressing YFP HPF1 WT behave similarly and are not sensitive to treatment with these concentrations of olaparib (Figure 3.3, a, b). U2OS Flp-In HPF1 KO cells, and U2OS Flp-In HPF1 KO cells expressing either YFP-EV or YFP HPF1 D286A all behave similarly as well, showing a slight, but not significant trend towards reduced survival in response to 0.5 µM olaparib. Meanwhile, at the same concentration of olaparib, survival of cells expressing YFP HPF1 E284A is significantly reduced. This clearly illustrates that expression of this mutant, which restricts chain elongation without simultaneously stimulating initiation of ADP-ribosylation of serine residues like wild-type HPF1, is more far more toxic to cells in the context of PARP inhibition than loss of HPF1 altogether. This mutant does not only have clear consequences for PARP1 automodification, but also for the modification of other targets, such as histones (Figure 3.2, a, b), and could affect PARP1/2 release from sites of DNA damage, as well as the recruitment of chromatin remodellers and DNA repair factors that depend on the HPF1-mediated DNA damage signal.

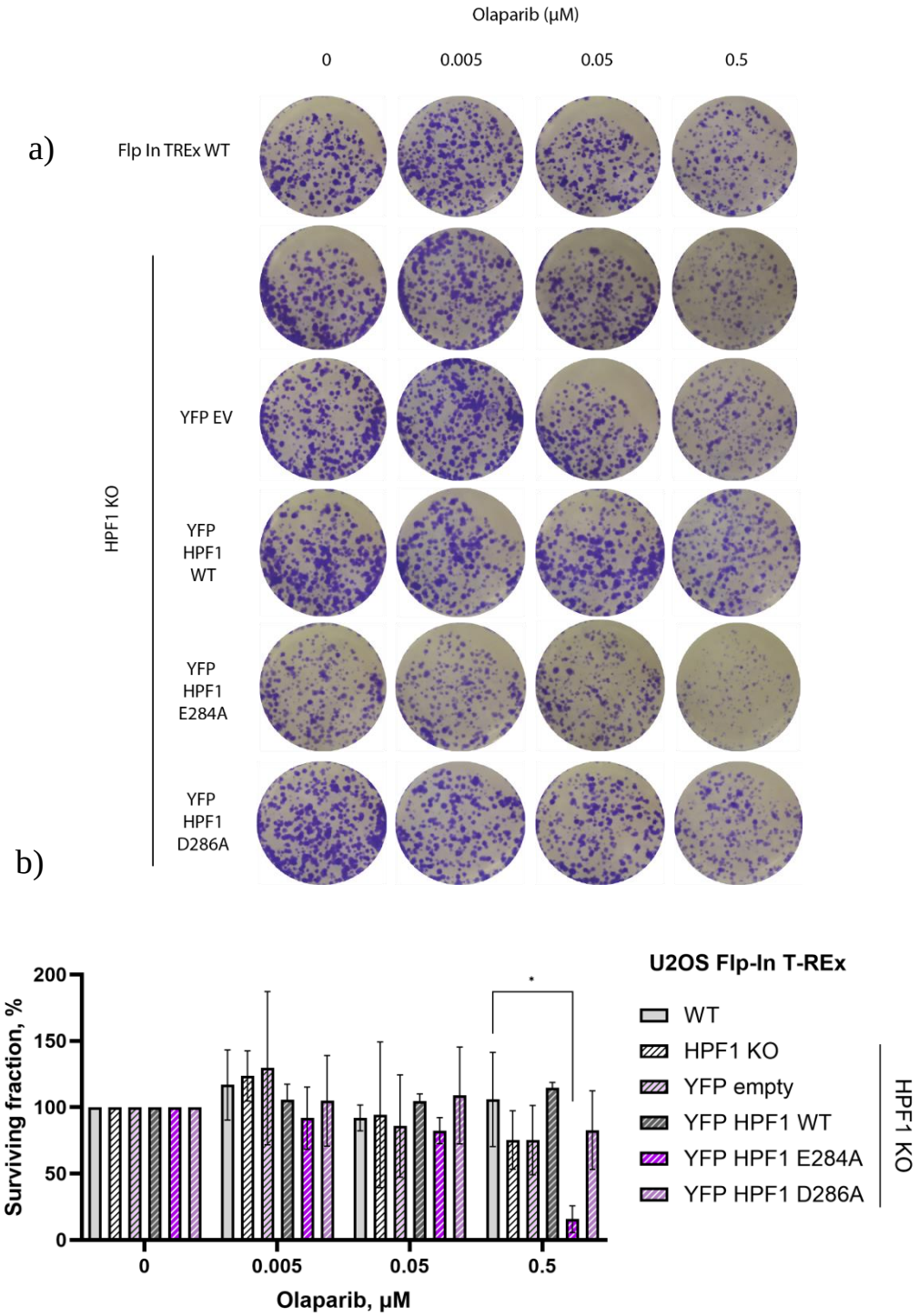

Figure 3.3: Catalytically inactive HPF1 sensitises cells more to PARP inhibitor than loss of HPF1. **a)** Expression of complemented YFP EV, YFP HPF1 WT, E284A and D286A mutants in U2OS Flp-In HPF1 KO cells was induced with 0.5 μg/mL doxycycline, and cells were treated with an increasing range of olaparib as indicated. **b)** Quantification of the experiment performed in a). * indicates a p value of < 0.05. (unpaired, two-tailed Student's *t*-test, assuming unequal variance). Bars represent the mean, and error bars represent the standard deviation. Experiment was performed in triplicates. Cell survival was normalised to the untreated condition of each cell line.

3.2 PARP1 release from sites of DNA damage depends on ADP-ribose chain length

As discussed in the previous sections, the discovery of HPF1 has changed our understanding of the type of ADP-ribose chains produced by PARP1/2, and required for the DNA damage response (DDR). As the only PARPs in the family, except for Tankyrases 1 and 2, capable of poly-ADP-ribosylation (PARylation), PARylation by PARP1/2 was assumed to be critical for the pathway. However, the requirement for HPF1 during the DDR, which restricts chain extension during initiation of ADP-ribosylation, has raised the question of the type of ADP-ribosylation required for efficient PARP1 removal from sites of DNA damage. This is particularly relevant for the question of how different ADP-ribose lengths of PARP1 automodification affect its behaviour at sites of DNA damage; the potential to trap PARP1 at DNA lesions is the major determinant of the toxicity of different PARP inhibitors (Murai et al., 2012, 2014; A. Thomas et al., 2018). To better understand how different ADP-ribose chain lengths determine PARP1 trapping, I mutated different residues in the ART domain of PARP1 required for NAD^+ binding or elongation (Table 3.1) and tested their behaviour, both in terms of their catalytic activity and at sites of DNA damage.

Residue/domain	Role in PARP1	Mutation	Mutation Output	References
E998	Member of the **catalytic triad** Forms a hydrogen bond with the 2'-OH of the adenosine ribose or nicotinamide ribose of terminal PAR unit Primes incoming 2'-OH for nucleophilic attack, important for elongation	E988Q/A	E988Q mutation reduces catalytic activity resulting in only mono-ADPr. E988A mutation is (nearly) catalytically inactive	Marsischky et al., 1995; Shao et al., 2023; Alemasova & Lavrik, 2019
H862	Member of the **catalytic triad** Forms a hydrogen bond with the 2'-OH of adenine-ribose of the donor NAD^+	H862A	H862A reduces MARylation (initiation) activity E988Q/H862A completely abolishes catalytic activity	Shao et al., 2020; Shao et al., 2023
M890	Part of the acceptor site Adenine base of acceptor ADP rests against M890 Corresponding residue in MAR-only PARP3 replaced by arginine	M890R/A	M890R mutant has strong mono-ADPr activity but no poly-ADPr activity. M890A mutant behaves very similarly to WT PARP1	Steffen et al., 2013; Rolli et al., 1997; Frigon & Pascal, 2023
HD	Helical domain, auto-inhibitory. Required for DNA-binding dependent allosteric activation of PARP1 through Zn-WGR-HD network. Required for reverse allosteric effect of some PARP inhibitors on DNA binding affinity.	ΔHD	Removal of HD leads to a constitutively active protein Removal of HD abolishes reverse allosteric effect of some PARP inhibitors	Dawicki-McKenna et al., 2015; Zandarashvili et al., 2020
K903	Part of the acceptor site Conserved in poly-ARTD sub-class Interacts with the α-phosphate of the acceptor ADP	K903A	K903A mutation reduces catalytic activity resulting in only mono-ADPr.	Carter-O'Connell et al., 2015; Ruf et al., 1998

Table 3.1: **Summary of PARP1 catalytic domain residues, their role and the effect of their mutation on catalytic activity.** Different residues in the PARP1 ART domain involved in ADPr initiation or elongation were targeted, with the role of the residues and the effect of the mutation outlined.

3.2.1 Different PARP1 catalytic mutants differ in the ADP-ribose chains they produce

The catalytic residues chosen for mutation, as well as the effect of the mutation, are summarised in Table 3.1. Following mutagenesis and validation of the plasmids by sequencing, U2OS PARP1 KO cells were transfected with YFP-PARP1 WT and various YFP-PARP1 mutants, and their catalytic output with and without DNA damage was analysed using antibodies that recognise different forms of ADP-ribosylation. While WT PARP1 is auto-modified slightly before induction of DNA damage, treatment with hydrogen peroxide (H_2O_2) potently stimulates both PARP1 automodification as well as modification of histones (Figure 3.4). PARP1 E988 is part of the catalytic H-Y-E triad (i.e. the donor site), where it hydrogen bonds to the 2'-OH of the donor adenosine ribose and the nicotinamide ribose of the terminal ADP ribose of a PAR chain (i.e. the acceptor). While this residue is not strictly required for initiation, as amino acids can initiate the nucleophilic attack without a base, it is essential for the elongation reaction (Alemasova & Lavrik, 2019). As a result, the E988Q mutation renders PARP1 unable to produce PAR chains, but retains its ability to initiate ADPr and MARylate itself and other targets in response to DNA damage (Marsischky et al., 1995) (Table 3.1, Figure 3.4). The PARP1 E988A mutant was previously shown to have severely reduced initiation in addition to its reduced elongation, effectively acting as a nearly catalytically dead protein (Marsischky et al., 1995). This was confirmed in this assay (Figure 3.4). H862, which is also part of the catalytic triad of PARP1, binds the 2' hydroxyl of the NAD^+ adenine ribose, and substitution of this residue with alanine (H862A) was previously shown significantly reduce catalytic activity under physiological NAD^+ conditions *in vitro* (Shao et al., 2020). H862 is part of the donor site, but is not involved in acceptor binding (Table 3.1). Unsurprisingly, in this assay and other repeats, PARP1 H862A accordingly shows reduced MARylation activity, but retains strong PARylation activity. Moreover, its catalytic activity does not appear tied to the induction of DNA damage by H_2O_2, as is the case with PARP1 WT. Simultaneous introduction of E988Q and H862A mutations (EQHA),

renders PARP1 completely catalytically inactive, both under basal conditions and in response to DNA damage (Figure 3.4). This is likely due to impaired binding of the donor molecule, severely restricting initiation of ADPr (Table 3.1). Seeking to use different mono-ADPr mutants, I decided to use the PARP1 M890A/R mutants, which is part of the catalytic acceptor site, and rests against the adenine base of the terminal ADPr unit (Alemasova & Lavrik, 2019). The M890V mutation was previously shown to reduce catalytic output due cause clashing between the valine and either the Y896 side chain or the N1-atom of ADP, thereby likely disrupting elongation (Rolli et al., 1997; Alemasova & Lavrik, 2019) (Table 3.1). PARP1 M890A/R had previously been indicated in an *in vitro* assay by our lab to be mutants capable of producing MAR (Appendix Figure A.1). However, as can be seen in Figure 3.4, only the M890R mutant solely produces mono-ADPr, while M890A retains some PARylation activity. This could be because arginine causes clashing similar to valine, while the smaller alanine does not. M890R further appears to be highly active, with MARylation levels comparable to that of YFP-PARP1 WT, and much greater than that of the canonical MARylation mutant PARP1 E988Q. PARP1 M890R can thus serve as a separation-of-function mutant that allows distinction between the importance of the frequency of initiation compared to elongation of ADP-ribosylation. Interestingly, PARP1 M890A appears to lose some PARylation activity following H_2O_2 treatment, while its MARylation activity is increased. K903, like M890, is part of the acceptor site of PARP1, where it interacts with the α-phosphate of the acceptor ADP ribose and is thereby involved in the elongation reaction (Table 3.1). Substitution with an alanine was previously shown to transform PARP1 into a MARylation mutant in another study (Ruf et al., 1998; Carter-O'Connell et al., 2014) (Table 3.1) and in our lab's previous *in vitro* assay (Appendix Figure A.1). This was confirmed in this assay, with PARP1 K903A only showing MARylation activity in response to DNA damage (Figure 3.4).

Expression levels of both YFP-PARP1 E988Q and PARP1 K903A are low in this particular assay; increased film exposure does show that low levels of ADP-ribosylation remain, and other iterations of this experiment show that low levels of ADP-ribosylation are not a result of low expression, but rather the mutation, as can be seen in Figure 3.14.

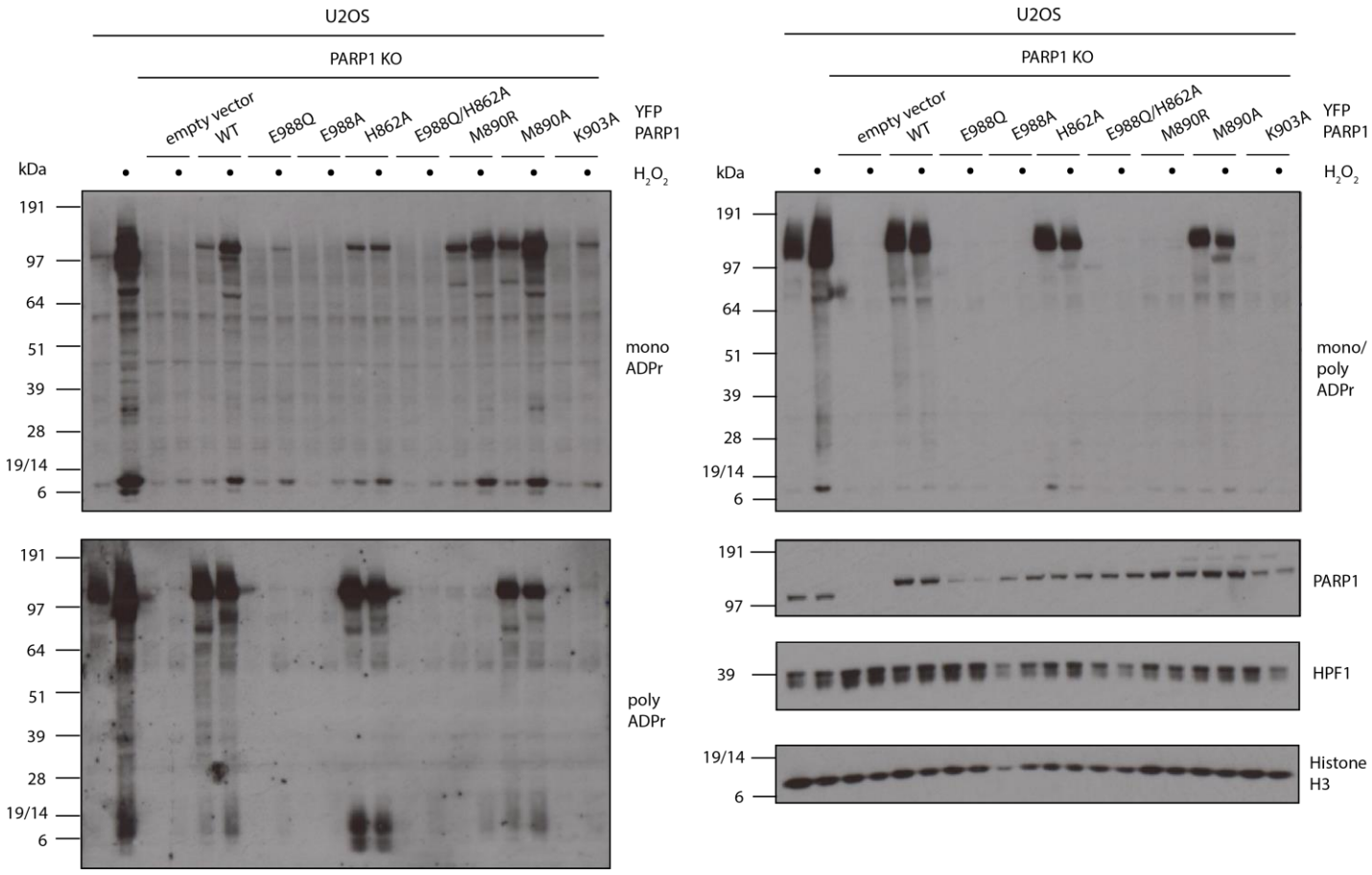

Figure 3.4: Comparison of catalytic activity of different PARP1 mutants. ADP-ribosylation activity of different transiently expressed catalytic PARP1 mutants was tested by western blot with and without DNA damage in U2OS PARP1 KO cells with the indicated antibodies. Catalytic activity of each mutant was tested in at least two different experiments. Histone H3 was used as a loading control. Hydrogen peroxide was used at 2 mM.

3.2.2 ADP-ribose chain length corresponds to PARP1 trapping at sites of DNA damage

Following initial testing of catalytic activity of these PARP1 mutants by western blot, I decided to test their recruitment and release behaviour at sites of DNA damage. I transfected U2OS PARP1 KO cells with the same set of YFP-PARP1 mutants, and induced damage with a 405 nm laser following sensitisation with 0.15 µg/mL Hoechst for 1 hour. YFP-PARP1 WT, as expected, arrives promptly at the damage site, peaking around 15 seconds following DNA damage induction, and leaves the damage site soon after, with on average only 25% of the fluorescence intensity signal remaining 160 seconds post DNA damage induction. The release behaviour of all the different PARP1 mutants tested, at the 160s post-irradiation point, differs significantly from PARP1 WT (Figure 3.5, c). YFP-PARP1 E988Q, only capable of MARylation, peaks 60 seconds after DNA damage induction, with 87% of the total fluorescence intensity remaining at the micro-irradiated site 160 seconds post damage induction. Interestingly, YFP-PARP1 E988A behaves similarly to PARP1 E988Q, despite the complete lack of catalytic activity. Again, the MARylation mutant YFP-PARP1 K903A behaves very similarly to both PARP1 E988Q and PARP1 E988A. Meanwhile, YFP-PARP1 E988Q/H862A, lacking any catalytic activity, peaks the latest at the damage site, after nearly two minutes, and with more than 93% still present at the site of damage site after 160 seconds, is the most trapped of the mutants tested. YFP-PARP1 H862A, which presented as quite catalytically active in the western blot assay with and without stimulation by DNA damage, and was capable of both MARylation and PARylation (Figure 3.4), peaks 30 seconds after irradiation, with 57% of the peak fluorescence intensity left at the damage site after 160 seconds. Interestingly, despite PARylation levels comparable to PARP1 WT (Figure 3.4), its release is considerably slower than that of PARP1 WT. Its MARylation activity appears much lower than that of WT PARP1, indicating that MARylation activity and the resulting automodification with mono-ADPr, could be a factor underlying this difference in release speed.

The behaviour of PARP1 M890A supports this; despite having considerably lower PARylation activity than PARP1 WT, while differing significantly (Figure 3.5, c), is closest to PARP1 in its behaviour at DNA lesions, peaking after 25 seconds at the damage site, and roughly 43% left of the original fluorescence intensity after 160 seconds. YFP-PARP1 M890A showed even greater MARylation activity following H_2O_2 treatment than YFP-PARP1 WT (Figure 3.4). YFP-PARP1 M890R, which is solely capable of MARylation, but highly active, demonstrates greater MAR-automodification than YFP-PARP1 WT (Figure 3.4), and exhibits remarkably similar behaviour to YFP-PARP1 H862A, which shows much weaker MARylation activity, yet greater PARylation activity. The behaviour of these mutants supports the notion that a high level of initiation of ADP-ribosylation is sufficient for the swift release of PARP1 from damage sites; either because a high frequency of MARylation is sufficient, or because PARP1-generated MARylation could be further extended by either PARP2 or TNKS1/2.

a)

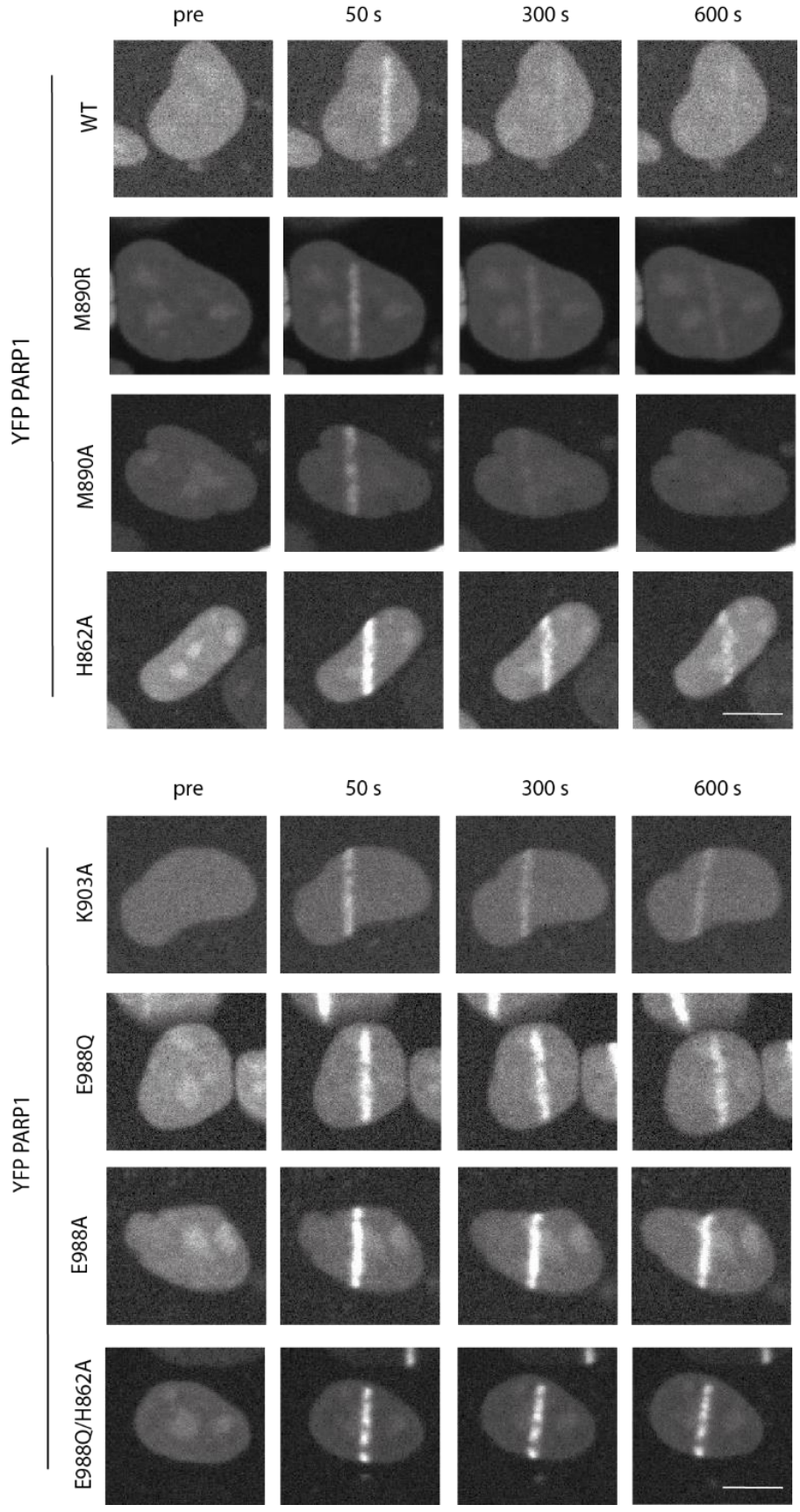
pre
50 s
300 s
600 s
YFP PARP1
WT
M890R
M890A
H862A
pre
50 s
300 s
600 s
YFP PARP1
K903A
E988Q
E988A
E988Q/H862A

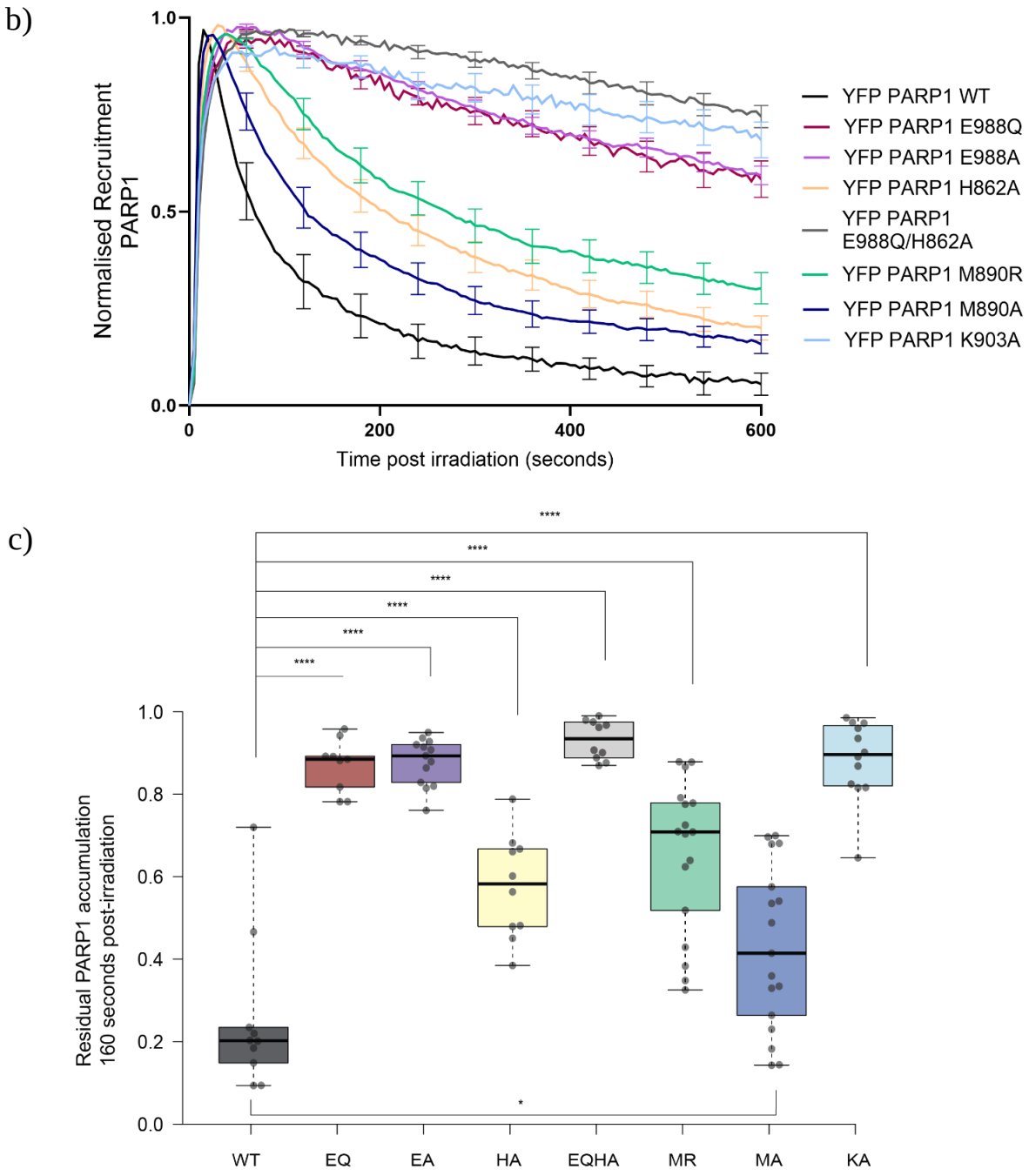

Figure 3.5: Recruitment and release of different PARP1 mutants is linked to their catalytic activity. a) Representative confocal images of U2OS PARP1 KO cells transiently expressing the indicated YFP PARP1 variants. **b)** Quantification of fluorescence intensity, representing YFP-PARP1, at the site of laser-microirradiation, normalised to the maximum fluorescence reached per condition. Data are shown as mean ± standard error of the mean. The scale bar represents 10 µM. c) Residual PARP1 accumulation at the site of laser micro-irradiation, taken from the normalised recruitment data 160 seconds post damage induction. The box limits correspond to the 25th and 75th percentiles and the bold line indicates the median value; the whiskers extend to minimum and maximum values. *$p < 0.05$; **$p < 0.01$; ***$p < 0.001$ (one-way ANOVA). Data were collected from 10–17 cells per condition.

3.2.3 Testing U2OS Flp-In T-REx PARP1 KO cells stably expressing YFP-PARP1 mutants

It is well established that loss of PARP1 catalytic activity leads to poor cellular outcomes, especially in the context of homologous repair defects (Bryant et al., 2005b; Farmer et al., 2005; Shao et al., 2023). However, the discovery of HPF1, and the resulting modification of ADP-ribose chains in the DDR, has led to questions regarding the type of chains required for a healthy DDR response. Similar to the HPF1 E284A mutant, I had the potential toxicity of long-term expression PARP1 catalytic mutants in mind, and therefore chose again to integrate them into the U2OS Flp-In™ T-REx™ background, which allows inducible expression (Figure 3.6, a). PARP1 was previously knocked out by Florian Zobel in these cell lines, to ensure the presence of endogenous, catalytically active PARP1 would not distort any results derived from PARP1 mutant-expressing cells. Integration of the desired constructs was achieved as outlined in Section *2.1.5* of *Materials and Methods*. Two catalytic mutants, PARP1 E988Q, and PARP1 E988Q/H862A, were chosen to investigate the effect of ADP-ribose chain length on cellular survival. To ensure the cell lines work as intended, U2OS Flp-In PARP1 KO cells complemented either with pDEST-YFP empty vector, YFP-PARP1 WT, YFP-PARP1 E988Q or YFP-PARP1 E988Q/H862A were left untreated, or treated with 0.1 µg/mL Doxycycline for two days to induce expression of the integrated PARP1 variants. A subset of Doxycycline-treated cells were further exposed to 2 mM H_2O_2 for 10 minutes before harvesting. Unmodified U2OS Flp-In WT cells were used as a control. Treatment of complemented cells with the indicated concentration of Doxycycline is sufficient to induce expression of all YFP-PARP1 variants at a comparable level to WT cells, and YFP in the empty-vector control cell line (Figure 3.6, b). Treatment of U2OS Flp-In PARP1 KO cells expressing YFP- PARP1 WT with both Doxycycline and H_2O_2 causes an increase in automodification and histone ADP-ribosylation comparable to that of U2OS Flp-In WT cells.

It must be noted that the cells complemented with YFP-PARP1 WT demonstrate low levels of expression even without the addition of Doxycycline; since my focus in this project was to understand the toxicity of PARP1 catalytic mutants, and low-grade expression of wild-type PARP1 did not interfere with this, I continued using this cell line. Expression of YFP-PARP1 E988Q is induced upon treatment with Doxycycline, and further treatment with H_2O_2 shows a modest increase in both PARP1 automodification and histone ADP-ribosylation in agreement with its MARylation activity. YFP-PARP1 E988Q/H862A is induced at similar levels to the other YFP-PARP1 variants, but completely lacks catalytic activity, even after DNA damage induction. Interestingly, the ADPr-band around the 64 kDa mark appears greatly diminished in the YFP-PARP1 E988Q expressing cells, and completely abolished in the YFP-PARP1 E988Q/H862A expressing cell line, while it appears robustly in response to treatment with H_2O_2 in U2OS Flp-In PARP1 KO and YFP-EV complemented cell lines. The molecular weight of this modification could correspond to PARP2 automodification. As can be seen in Appendix Figure A.4, there remains an ADPr signal slightly below 64 kDa in two different U2OS PARP1 KO clones, which is completely lost, upon simultaneous loss of PARP2 in U2OS PARP1/PARP2 KO cells.

This experiment demonstrates that these cell lines behave as expected, and can be used to reliably induce expression of the desired PARP1 variants.

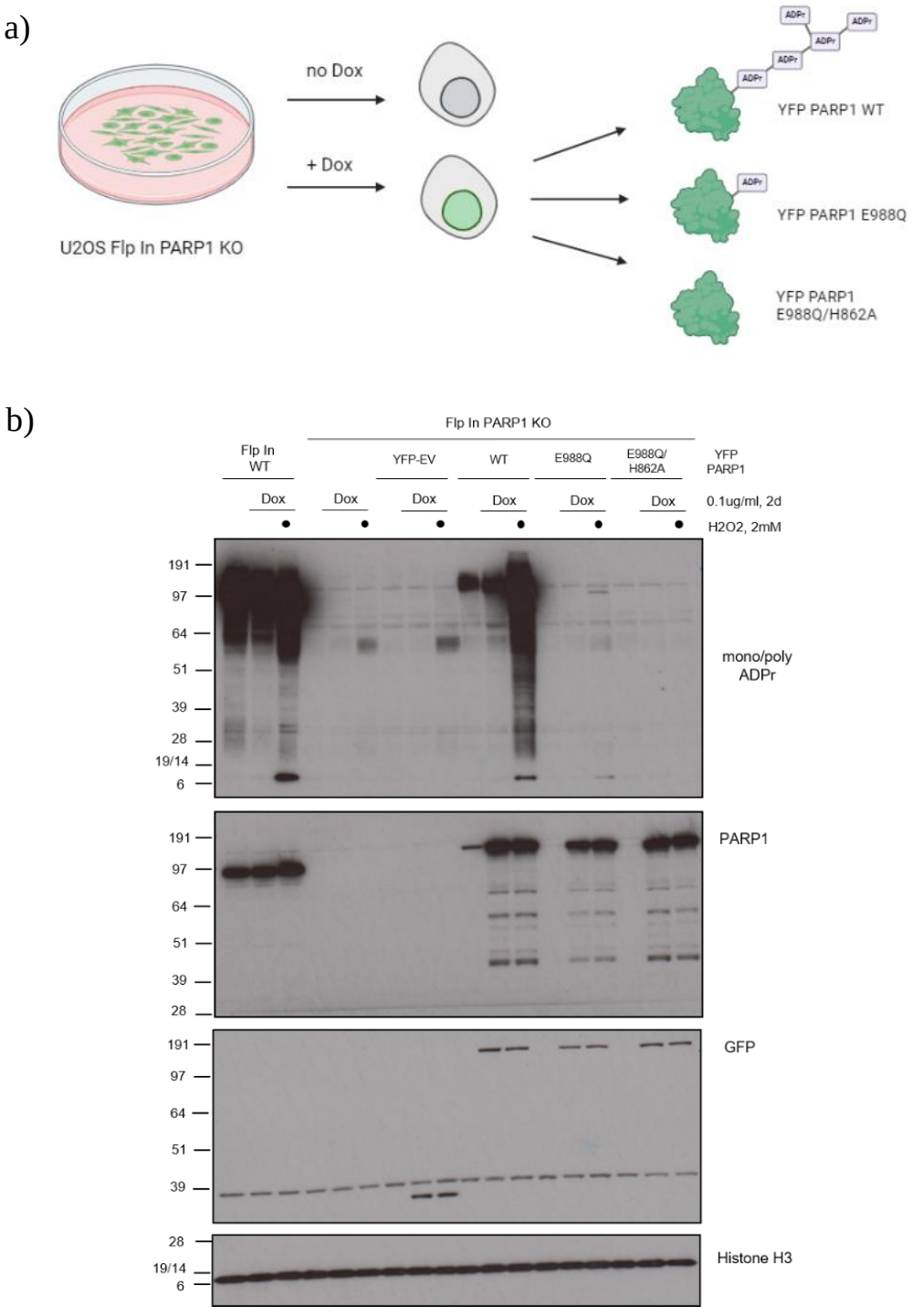

Figure 3.6: Treatment of U2OS Flp-In PARP1 KO cells with Doxycycline induces expression of complemented YFP EV, YFP-PARP1 WT, YFP-PARP1 E988Q and YFP-PARP1 E988Q. **a)** Schematic representation of the cell lines. **b)** Western blot showing that the catalytic output of the cell lines is as expected in response to doxycycline and hydrogen peroxide treatment. Cell extracts were examined with the indicated antibodies. Histone H3 serves as a loading control.

3.2.4 Expression of a mono-ADP-ribosylation PARP1 mutant is toxic to cells

Having established that the complemented U2OS Flp-In PARP1 KO cell lines behave as intended, I sought to test the impact these catalytic mutations have on cellular survival. Recently, mice expressing PARP1 E988A heterozygously were shown to suffer from genomic instability and embryonic lethality (Shao et al., 2023); indicating that even in otherwise healthy tissue devoid of DNA repair defects, inactive PARP1 is toxic. Cells were seeded in triplicates for every condition, and left either untreated or supplemented with 0.1 µg/mL Doxycycline for 10 days. Untreated, all cell lines behave as PARP1 KOs, displaying robust growth. Upon addition of Doxycycline, expression of the desired PARP1 variant, or YFP empty vector is induced. As can be seen in Figure 3.7, there is no significant change in survival after re-introduction of YFP-PARP1 WT, while expression of YFP-PARP1 E988Q drastically reduces survival to roughly 17% of its untreated population. Expression of YFP-PARP1 E988Q/H862A completely abolishes survival, leaving virtually no surviving colonies.

These experiments show that use of these endogenous PARP1 KO cell lines complemented with PARP1 catalytic mutants is advantageous over experiments using PARP inhibition to study the effect of catalytic loss, since it is all-encompassing.

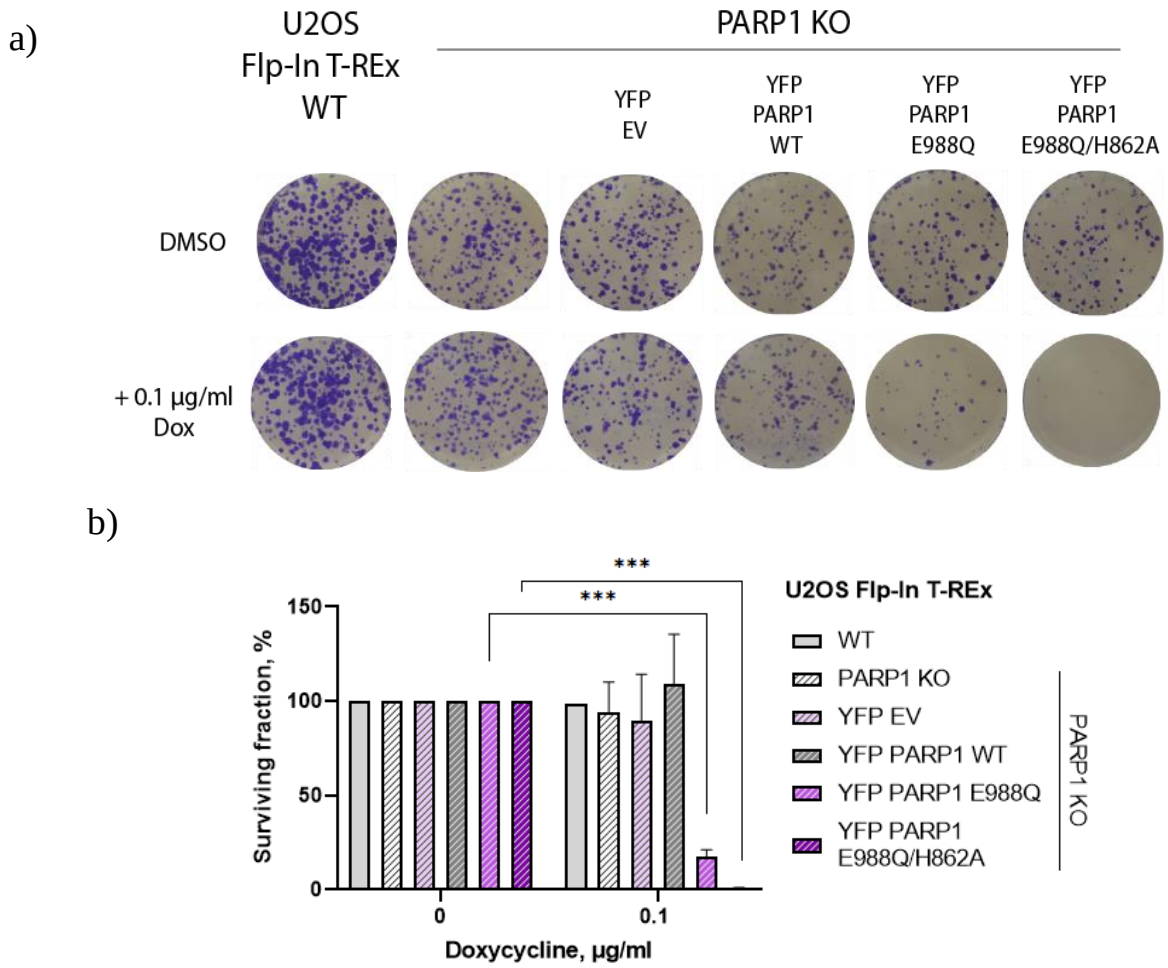

Figure 3.7: Impairment and loss of catalytic activity leads to reduced cellular survival. a) Survival of U2OS Flp-In PARP1 KO cells expressing PARP1 E988Q or PARP1 E988Q/H862A is much lower than that of YFP PARP1 WT-expressing cells or cells lacking PARP1. Cells were cultured for 10 days in media containing either DMSO or 0.1 µg/mL Doxycycline. **b)** Quantification of the experiment performed in a). Cell survival was normalised to the untreated condition of each cell line. * indicates a p value of < 0.05, ** a p value of <0.01, and *** a p value of < 0.001 (unpaired, two-tailed Student's *t*-test, assuming unequal variance). Bars represent the mean, and error bars represent the standard deviation. Experiment was performed in triplicates.

3.3 Some PARP1 mutants are resistant to a novel PARP1-selective PARP inhibitor

The first aim of this project was to study how the catalytic activity of various PARP1 mutants would affect its behaviour at sites of DNA damage, and specifically how ADP-ribose chain length would influence cellular survival. Secondly, I was interested to see how different PARP inhibitors would affect the trapping of these PARP1 mutants. This revealed that certain catalytic PARP1 mutations not only render PARP1 resistant to some PARP inhibitors, but induce a reversing effect of the inhibitor on the behaviour of the protein, which will be outlined in detail in the following sections.

3.3.1 The toxicity of PARP1 E988Q is rescued by treatment with saruparib

After having observed that expression of both PARP1 E988Q and PARP1 E988Q/H862A is toxic to cells, I wanted to confirm that the lower toxicity of PARP1 E988Q compared to PARP1 E988Q/H862A could be attributed to the fact that it is capable of MARylation. To do so, I repeated the survival assay discussed in section *3.2.4*, but in addition to the 10-day treatment with Doxycycline, I treated a subset of cells with two different concentrations of both olaparib, and saruparib, reasoning that treatment with a PARP inhibitor would abolish any residual catalytic activity, and make PARP1 E988Q expression resemble PARP1 E988Q/H862A more closely in its effect on cellular survival. I chose to use the novel PARP1-selective saruparib (AZD5305) as a control to ensure that any observed effect could be attributed to the loss of catalytic activity of PARP1, rather than the added loss of catalytic activity of PARP2, as would be the case with olaparib treatment. As previously observed (Figure 3.7), rescuing PARP1 expression in U2OS Flp-In PARP1 KO cells with YFP-PARP1 WT has no significant effect on survival, while treatment of YFP-PARP1 WT expressing cells with olaparib has a detrimental effect on survival (Figure 3.8). Again, Doxycycline-dependent induction of expression in both U2OS Flp-In PARP1 KO YFP-PARP1 E988Q and YFP-

PARP1 E988Q/H862A cells leads to a drastic reduction in cellular survival, more so upon expression of the catalytically dead E988Q/H862A mutant. Treatment of both cell lines with olaparib did not have an additive effect on survival. However, treatment of PARP1 E988Q expressing cells with either 0.5 nM or 5 nM saruparib significantly increased survival. There was a slight trend towards increased survival with E988Q/H862A expressing cells upon saruparib treatment as well, but a negative trend was observed for YFP-PARP1 WT expressing cells (Figure 3.8, b). The experiment was repeated thrice, and the surprising pro-survival effect of saruparib on PARP1-E988Q expressing cells was observed each time.

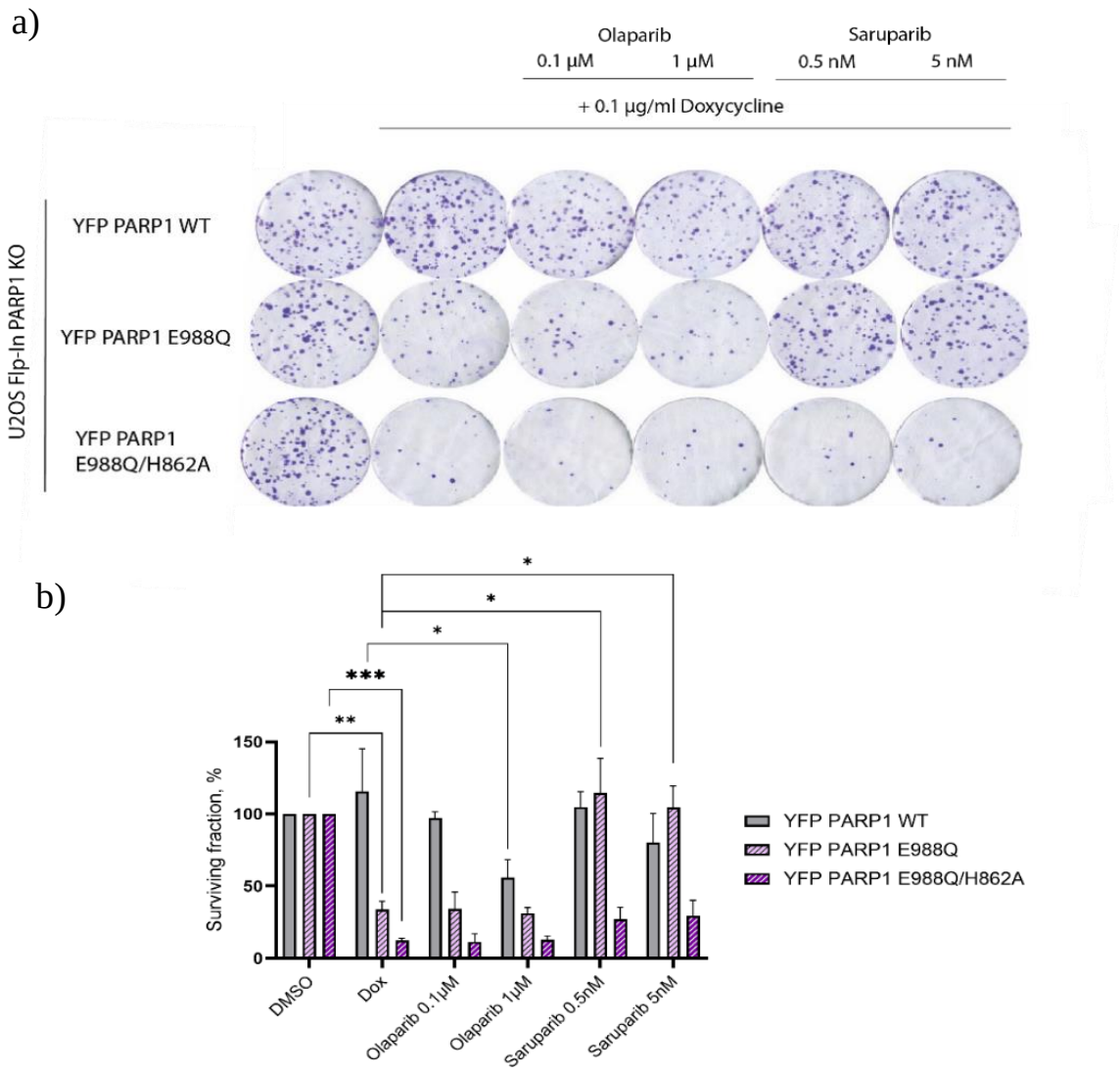

Figure 3.8: Saruparib rescues the toxicity induced by expression of PARP1 E988Q. a) Survival of U2OS Flp-In PARP1 KO cells expressing YFP PARP1 E988Q is significantly improved by treatment with saruparib. Cells were treated with 0.1 µg/mL Doxycycline to induce expression of PARP1 variants, followed by treatment with olaparib or saruparib at the indicated concentrations for 10 days. **b)** Quantification of the experiment performed in **a)**. Cell survival was normalised to the untreated condition of each cell line. * indicates a p value of < 0.05, ** a p value of <0.01, and *** a p value of < 0.001 (unpaired, two-tailed Student's *t*-test, assuming unequal variance). Bars represent the mean, and error bars represent the standard deviation. Experiment was performed in triplicates. This experiment was repeated at least three times.

3.3.2 The toxicity of PARP1 E988Q is due to increased replication stress and DNA damage, and can be rescued with saruparib

Next, I wanted to test why expression of catalytically impaired PARP1 mutants was toxic for cells. Trapped PARP1 is known to cause an increase in replication stress, and can ultimately lead to the generation of DSBs (see *Introduction*, *section 1.2* and *1.4*). Previously, heterozygous expression of PARP1 E988A was shown to cause embryonic lethality in mice, increased trapping at the site of DNA damage and impaired single-stranded break repair (Shao et al., 2023). I treated U2OS Flp-In PARP1 KO YFP-PARP1 WT and YFP-PARP1 E988Q expressing cells with 0.1 µg/mL Doxycycline, and added either 1 µM olaparib or 5 nM saruparib to the media. As expected, treatment with Doxycycline induces expression of YFP-PARP1 WT and YFP-PARP1 E988Q (Figure 3.9). Simultaneously, expression of YFP-PARP1 E988Q, but not that of YFP-PARP1 WT, leads to a significant increase in the levels of both phosphorylated RPA, and γH2AX. The antibody used recognises RPA32 modified at serines 4/8, which is induced upon replication stress by DNA PKcs and ATM, and regulates replication arrest, origin firing, recombination and mitotic catastrophe (Ashley et al., 2014; S. Liu et al., 2012). γH2AX is an established marker of DSBs (Valdiglesias et al., 2013). This agrees with the role of catalytically active PARP1 at replication forks and the prevention of DSBs. Treatment with olaparib of both YFP-PARP1 WT and the E988Q mutant tended to slightly, but not significantly, increase γH2AX and pRPA signals. Meanwhile, treatment of YFP-PARP1 E988Q with saruparib (AZD5305) significantly decreased the amount of both stress signals (Figure 3.9). This was not the case in the YFP-PARP1 WT condition, where treatment with saruparib had little effect, but trended towards increased expression of γH2AX and pRPA. This finding suggests that the cellular toxicity observed upon expression of catalytically impaired PARP1 can be linked to replication stress, which, if unresolved, results in increased levels of DNA damage. It also shows that treatment of PARP1 E988Q, but not PARP1 WT, with PARP1-selective saruparib, decreases both stress signals significantly.

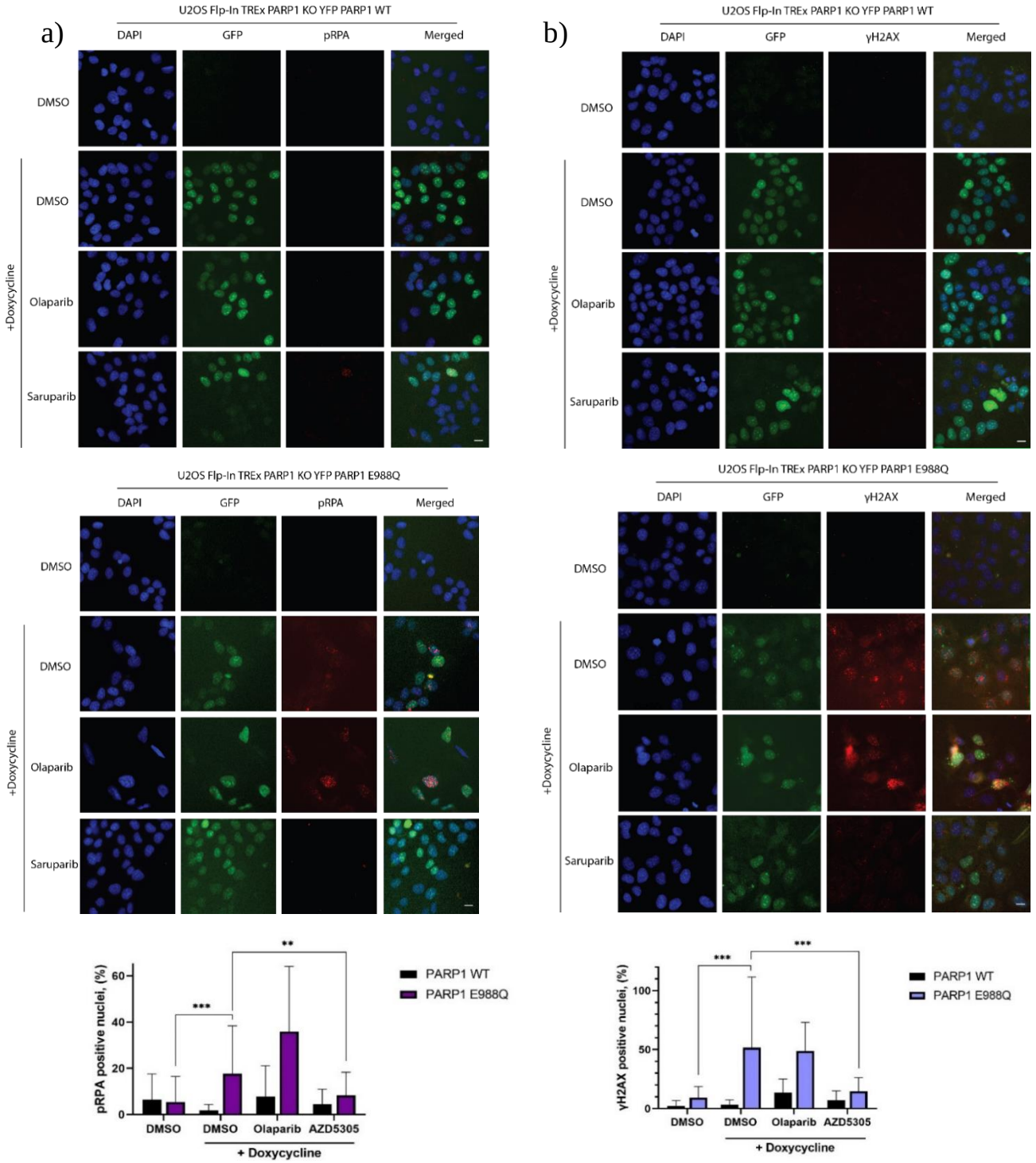

Figure 3.9: Increased replication stress and DNA damage upon expression of PARP1 E988Q can be rescued by treatment with the PARP1-specific inhibitor, saruparib. Representative immunofluorescence images of cells treated with the indicated drugs. Expression of both YFP-PARP1 WT and E988Q was induced using 0.1 µg/mL Doxycycline, followed by treatment with 1 µM olaparib and 5 nM saruparib, and examined for the presence of a) pRPA, and b) γH2AX was tested and quantified. * indicates a p value of < 0.05, ** a p value of <0.01, and *** a p value of < 0.001 (unpaired, two-tailed Student's *t*-test, assuming unequal variance). The graphs below indicate the percentage of the total cells which show positive staining for pRPA or γH2AX and the error bars represent the standard deviation. The scale bars represent 10 µM.

3.3.3 Saruparib promotes the release of some catalytic PARP1 mutants from sites of DNA damage

Since increased replication stress is a marker of trapped PARP1, I next intended to investigate how treatment of PARP1 E988Q, as well as other PARP1 catalytic mutants, with saruparib affected their behaviour at sites of DNA damage. To this end, I first treated U2OS Flp-In PARP1 KO cells with 0.1 µg/mL Doxycycline 24 hours before imaging to induce expression of either YFP-PARP1 WT or YFP-PARP1 E988Q. One hour before imaging, cells were sensitised with 0.15 µg/mL Hoechst, and following this, treated with either DMSO, 1 µM olaparib or 5 nM saruparib. DNA damage was induced with a 405 nm laser and images were captured every 5 seconds, for a period of 10 minutes. This protocol was followed for all the experiments described in the following sections, except where stated differently.

As seen in Figure 3.10, a, treatment of YFP-PARP1 WT with olaparib, as expected, leads to prolonged retention at the damage site. In this experiment, near the end of capture, after 560 seconds, 25% of the maximum amount remains at the damage site in untreated cells (Figure 3.10, a). Treatment with olaparib raises this to 58%. Saruparib, which by all previous reports is not as potent a trapper as olaparib, (Kanev et al., 2024; Langelier et al., 2023; Stojanovic et al., 2023), also increases retention of PARP1 at sites of DNA damage, with 38% remaining after 560 seconds, not to the same extent as olaparib (Figure 3.10, a). Meanwhile, after 560 seconds, almost 61% of YFP-PARP1 E988Q remains at the site of damage in untreated conditions, compared to 25% of PARP1 WT (Figure 3.10, b), agreeing with data from transiently transfected PARP1 E988Q (Figure 3.5). Treatment with olaparib leads to further trapping of PARP1 E988Q, likely due to the loss of the remaining MARylation, with 80% of the maximum amount of protein left after 560 seconds. However, treatment with saruparib has the opposite effect; it significantly promoted the release of PARP1 E988Q, with only 40% remaining after 560 seconds, 21% less than in untreated cells (Figure 3.10, b). This suggests

that the reduced toxicity of PARP1 E988Q-expressing cells treated with saruparib (Figures 3.8, 3.9) is due to reduced trapping of this mutant at sites of DNA damage.

I therefore intended to better understand several things: First, I wanted to exclude that other PARP inhibitors, which are considered “pro-release” have the same effect on PARP1 E988Q. Secondly, and inversely, I wanted to ensure that it is not this mutant specifically that reacts differently to some PARP inhibitors. Thirdly, I also wanted to see whether the fact that this inhibitor only targets PARP1, but not PARP2, contributes to its effect on PARP1 E988Q.

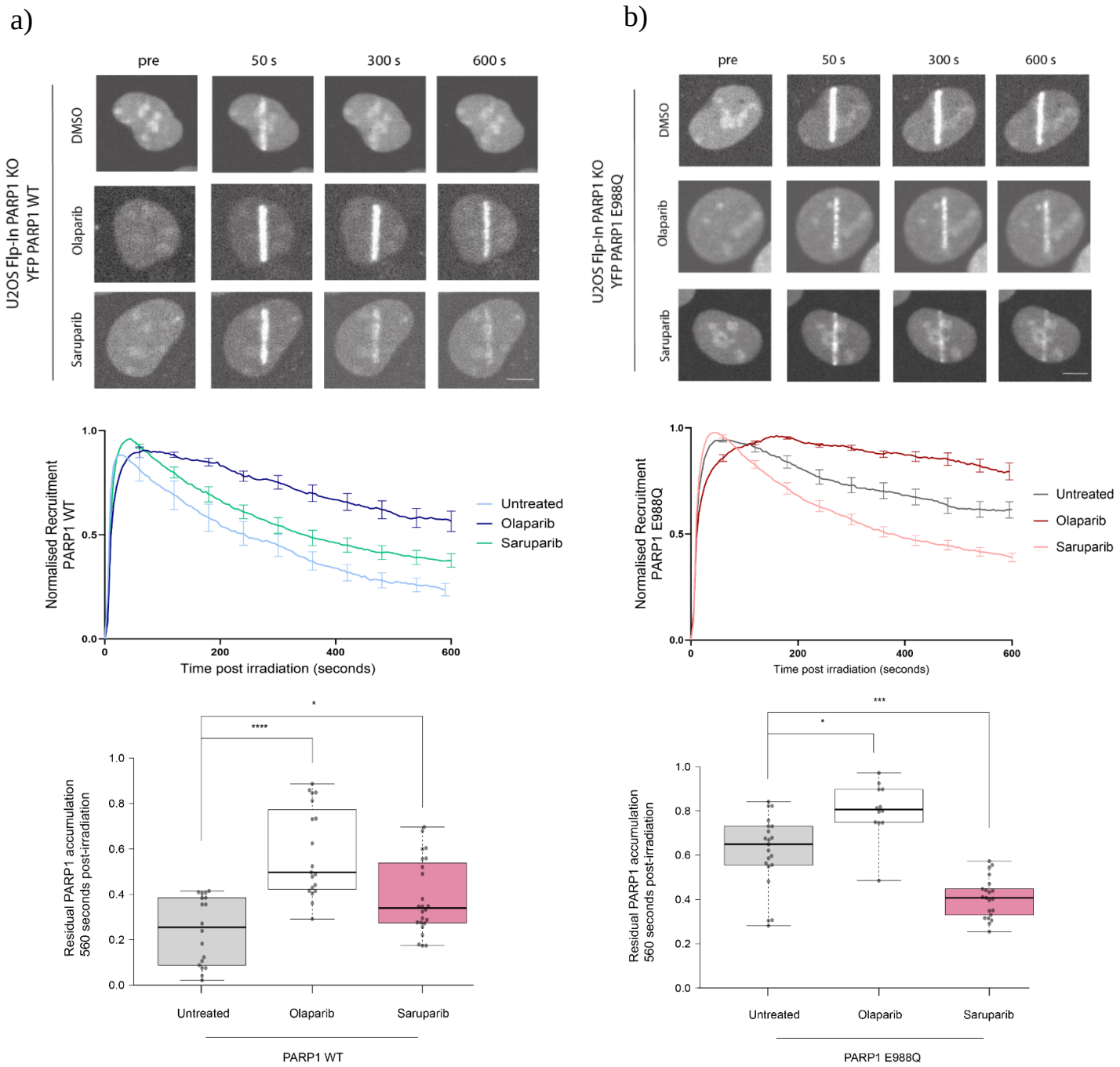

Figure 3.10: Saruparib increases the release of PARP1 E988Q from sites of DNA damage.

Representative confocal images of U2OS Flp-In PARP1 KO cells expressing **a)** YFP-PARP1 WT or **b)** YFP-PARP1 E988Q. The scale bars represent 10 µM. Quantification of fluorescence intensity representing YFP PARP1 WT or YFP PARP1 E988Q at the site of DNA damage are shown below the representative images of either, normalised to the maximum fluorescence reached per condition, with the data shown as mean ± standard error of the mean. Expression was induced with 0.1 µg/mL Doxycycline, and 1 µM olaparib or 5 nM saruparib were used. Data were collected from 12–21 cells per condition. Below is shown the residual PARP1 WT and E988Q accumulation at the site of laser micro-irradiation, taken from the normalised recruitment data 560 seconds post damage induction. The box limits correspond to the 25th and 75th percentiles and the bold line indicates the median value; the whiskers extend to minimum and maximum values. ns = not significant, *$p < 0.05$; **$p < 0.01$; ***$p < 0.001$ (one-way ANOVA). Data were collected from 10–17 cells per condition.

3.3.4 Other PARP inhibitors do not have the same "pro-release" effect on PARP1 E988Q

As extensively discussed in the Introduction in section *1.4*, PARP inhibitors have previously been shown to influence the DNA binding affinity of PARP1 in different ways, leading to their classification as "pro-retention" type I (EB-47, BAD), non-allosteric or mild pro-retention type II (talazoparib and olaparib) or "pro-release" type III (niraparib, rucaparib, veliparib) inhibitors (Zandarashvili et al., 2020). This classification was based on *in vitro* experiments, in the absence of NAD^+, and therefore do not represent the effect of PARP inhibitors in a physiological setting; despite their classification as "pro-release", veliparib, niraparib and rucaparib prolong retention of PARP1, or "trap" it, at the damage site. I therefore wanted to test the effect of other clinically used inhibitors on the PARP1 E988Q mutant.

Following the same steps as described previously, I used U2OS Flp-In PARP1 KO cells expressing YFP-PARP1 WT or YFP-PARP1 E988Q following treatment with 0.1 µg/mL Doxycycline. As shown in Figure 3.11, a, the trapping of PARP1 WT very closely aligns with the previously published *in vivo* trapping potentials of current PARP inhibitors (Introduction, section 1.4, Figure 1.7) (Kanev et al., 2024; Murai et al., 2012, 2014; A. Thomas et al., 2018). At the end of capture, 14% of the total amount of PARP1 WT is still present at the micro-irradiation site in untreated conditions, which is raised to merely 20% in response to treatment with veliparib. The second weakest trapper in this assay is saruparib, which traps 35% of the total PARP1 measured at the lesion. Reports on the trapping ability of saruparib vary, with some showing that it can be considered to have no allosteric effect (Langelier et al., 2023), and others indicating that it is strongly "pro-release" (Kanev et al., 2024). Next are olaparib and rucaparib, which in this assay trap PARP1 WT to an almost identical degree, as treatment with either leaves roughly 65% of PARP1 at the site of damage after 10 minutes. This agrees with previous reports of their trapping ability *in vivo* (Kanev et al., 2024; Murai et al., 2012,

2014; Pommier et al., 2016). The strongest trappers in this assay are niraparib and talazoparib, causing 77% and 85% of PARP1 to remain at the damage site after 10 minutes, respectively. This supports other cellular studies which found niraparib to be the second most potent trapper after talazoparib, despite its previous classification as a pro-release type III inhibitor *in vitro* (Kanev et al., 2024; Murai et al., 2012, 2014; Zandarashvili et al., 2020). Treatment with PARP inhibitors can also be seen to cause a general delay in recruitment to the damage site. The amount of PARP1 WT recruited to the micro-irradiated site peaks after roughly 20 seconds, and the delay induced by different PARP inhibitors is roughly proportional to their trapping ability (Figure 3.11, a).

Similarly, arrival of PARP1 E988Q at the damage site is slower than that of PARP1 WT, only peaking after a minute (Figure 3.11, b). As before, treatment with saruparib significantly speeds up the release of PARP1 E988Q from the damage site, with only 23% of the original amount remaining at the damage site after 10 minutes, compared to roughly 60% without inhibitor. Interestingly, in this experiment, treatment with both olaparib and veliparib appears to slightly promote release from sites of DNA damage as well. For olaparib, this is a surprising result, since in all other instances of PARP1 E988Q treatment with olaparib, it has a slight trapping effect. I therefore repeated the exact same experiment with only olaparib, veliparib and saruparib to validate these findings; the results are shown in Appendix Figure A.2. The trapping of PARP1 WT follows the previously observed pattern: it is most trapped by olaparib, followed by saruparib, and least trapped by veliparib (Appendix Figure A.2). YFP-PARP1 E988Q, as usual, is further trapped by olaparib, and its release promoted by saruparib (Appendix, Figure A.2). In this repeat, there also appears to be a slight pro-release trend by treatment with veliparib, but this is very minor (Appendix Figure A.2). It is therefore possible that veliparib, to a smaller degree than saruparib, has a mild pro-release effect on PARP1 E988Q. Returning to the original experiment (Figure 3.11, b), treatment with

rucaparib does not appear to affect PARP1 E988Q at sites of DNA damage. This could be a result of PARP1 E988Q being resistant to it, either through less efficient binding or catalytic inhibition, but further experiments, including assays for catalytic activity, would be required to confirm this. YFP-PARP1 E988Q is further trapped at the damage site by niraparib and talazoparib to a similar degree, raising its retention at the end of capture from roughly 60% to 75% and 70%, respectively.

To compare the extent to which catalytic inhibition was ensured at the given concentration of PARP inhibitor, a titration of all the inhibitors in U2OS WT cells was performed (Figure 3.11, c). When comparing ADP-ribosylation levels in the western blot with trapping in the micro-irradiation experiment (Figure 3.11, a, b), it is clear that catalytic inhibition does not correspond to trapping potency of a PARP inhibitor; catalytic inhibition of PARP1 at 5 nM talazoparib is not as efficient as 1 μM of olaparib, rucaparib or niraparib, and more closely resembles the catalytic activity of PARP1 in response to 1 μM veliparib. Veliparib and talazoparib are the furthest apart in their trapping ability, however, and despite very efficient catalytic inhibition at 5 nM, saruparib is the second weakest trapper.

This experiment found that apart from potentially veliparib, there are no other PARP inhibitor candidates that have this effect on PARP1 E988Q, suggesting that it is the inhibitor, saruparib, which has this specific pro-release effect on PARP1 E988Q, rather than an unusual response by the mutant to certain PARP inhibitors.

a)

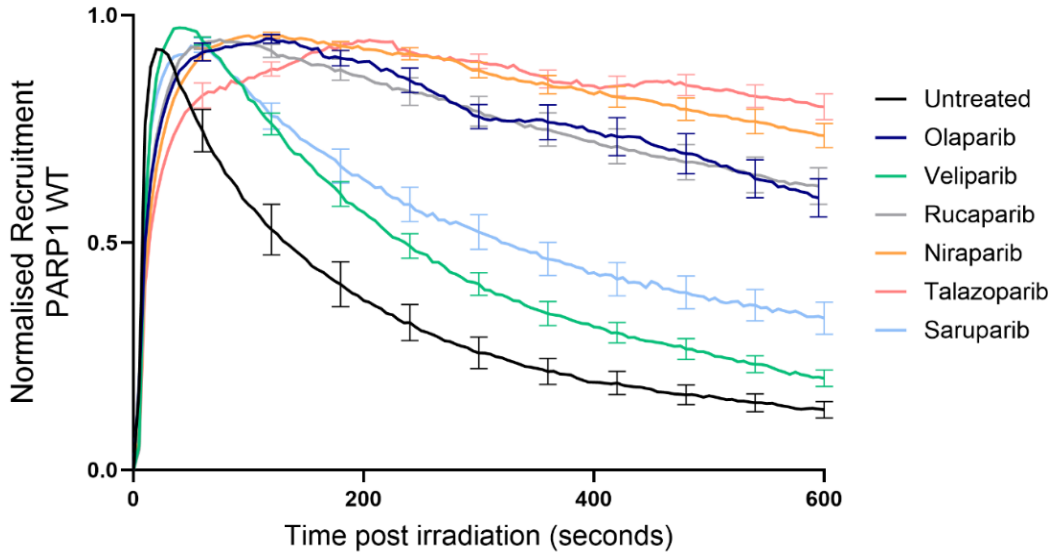
Normalised Recruitment
PARP1 WT
1.0
0.5
0.0
0
200
400
600
Time post irradiation (seconds)
Untreated
Olaparib
Veliparib
Rucaparib
Niraparib
Talazoparib
Saruparib

b)

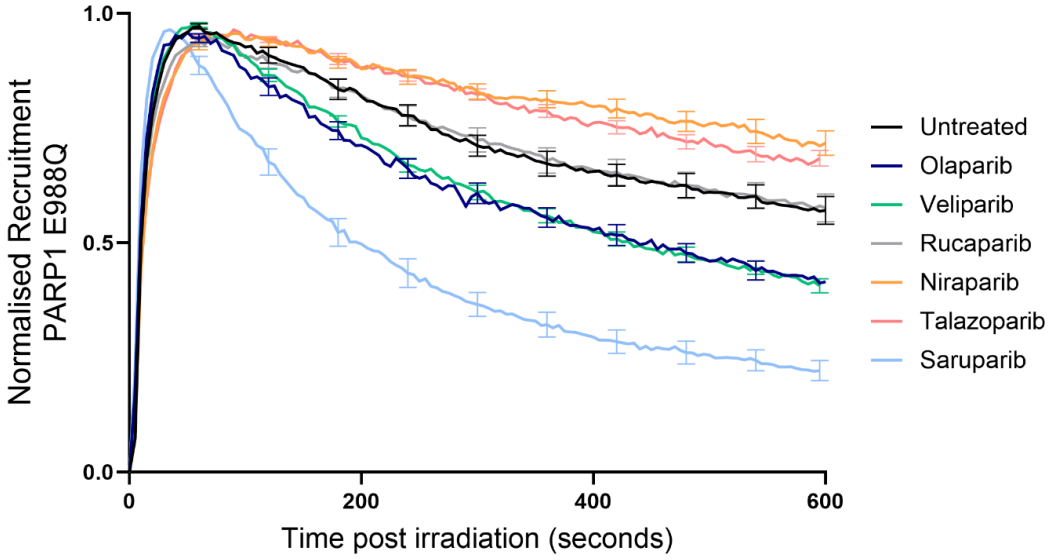
Normalised Recruitment
PARP1 E988Q
1.0
0.5
0.0
0
200
400
600
Time post irradiation (seconds)
Untreated
Olaparib
Veliparib
Rucaparib
Niraparib
Talazoparib
Saruparib

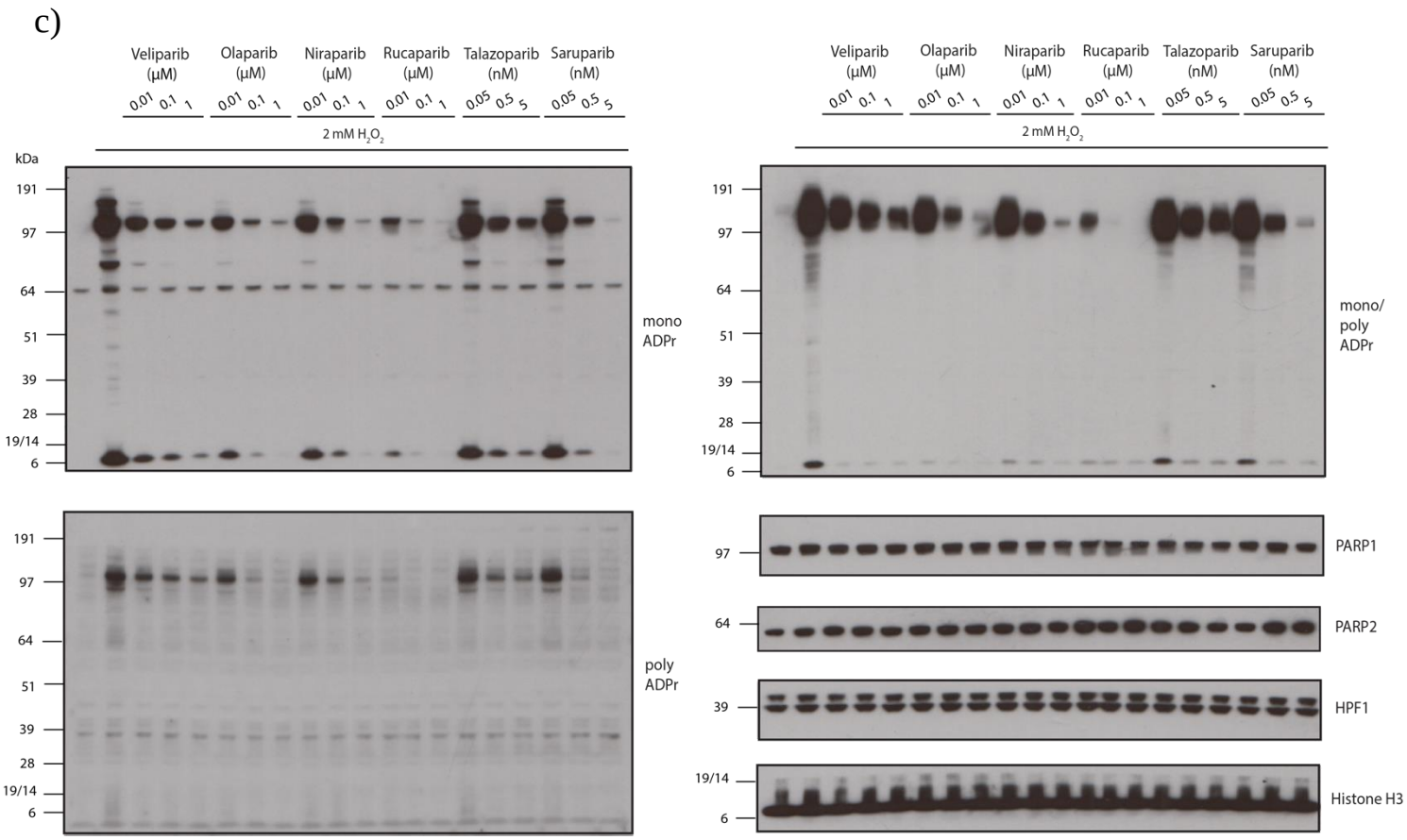

Figure 3.11: Other PARP inhibitors do not have the same pro-release effect on PARP1 E988Q. Normalised recruitment and release dynamics of **a)** YFP-PARP1 WT and **b)** YFP-PARP1 E988Q in response to the indicated inhibitors is shown. Expression was induced by treatment with 0.1 µg/mL Doxycycline 24 hours before imaging. U2OS Flp-In PARP1 KO cells were treated with 1 µM olaparib, 1 µM veliparib, 1 µM niraparib, 1 µM rucaparib, 5 nM talazoparib or 5 nM saruparib. Data are shown as mean ± standard error of the mean. Data were collected from 10–17 cells per condition. **c)** Western blot showing ADPr in WT cells treated with a **t**itration of the different PARP inhibitors used in a) and b) in U2OS WT cells shows the loss of catalytic activity at the indicated concentration. Blots were examined with the indicted antibodies. Histone H3 was used as a loading control. The western blot presented in Figure c) was performed by Michael Simmons.

3.3.5 Identification of additional PARP1 mutants that are released from sites of DNA damage by saruparib

Having found that saruparib, and to a lesser degree, veliparib, promotes the release of PARP1 E988Q, a MARylation mutant, I wanted to test whether other mutants respond similarly to treatment with this inhibitor. Having already tested different PARP1 mutants for their catalytic activity (Figure 3.4), I decided to expose this set of mutants to treatment with saruparib. I reasoned that this could tell me whether this pro-release response is dependent on the E988 residue, or, if treatment of other heavily catalytically impaired mutants with this inhibitor had a similar effect, this might be a shared response of catalytic PARP1 mutants to saruparib.

To do so, I treated U2OS PARP1 KO cells transiently expressing YFP-PARP1 wild-type and mutants with either olaparib or saruparib, or, saruparib alone, if the mutant had been tested previously with both (see Appendix Figure A.3). Importantly, the previously observed pro-release effect of saruparib persists in transiently expressed YFP PARP1 E988Q in a different cell line, confirming that this is not an artefact of the U2OS Flp-In PARP1 KO YFP-PARP1 E988Q-expressing cell line. PARP1 E988A, which has no catalytic activity at all (Figure 3.4), but behaves similarly to PARP1 E988Q in terms of its recruitment and release dynamics (Figure 3.5), is significantly de-trapped by treatment with saruparib, from 87% remaining at the damage site 160 seconds post-irradiation to 65% in response to saruparib (Figure 3.12, a, b). The release of PARP1 E988Q/H862A, another completely catalytically dead mutant which exhibits the most trapped phenotype of the catalytic mutants tested (Figure 3.5), shows a very slight increase in release upon treatment with saruparib, but the trend is not significant (Figure 3.12, a, b). PARP1 H862A, which has very low MARylation, but strong PARylation activity, which is independent of DNA damage (Figure 3.4), is slightly more trapped than PARP1 WT, and is not affected at all by treatment with saruparib, with roughly 60% fluorescence intensity

remaining after 10 minutes with and without inhibitor, compared to 25% of PARP1 WT without inhibitor, and 56% with saruparib after 160 seconds (Figure 3.12, a, b). Interestingly, it was previously reported that treatment of niraparib causes PARP1 H862A to display increased release from sites of DNA damage (Shao et al., 2020). I therefore also treated PARP1 H862A with niraparib, but found it to cause trapping rather than release (Figure 3.12, a). PARP1 M890R, which is a hyperactive MARylation mutant, is only slightly more trapped at sites of DNA damage than PARP1 H862A, and much less so than the other MARylation mutants PARP1 E988Q and PARP1 K903A (Figure 3.5). It responds to olaparib by being trapped, while saruparib seems to have a very modest, non-significant de-trapping effect (Figure 3.12). This might rather reflect lack of a response to saruparib, and the difference merely variation in the experimental condition. Future testing of this mutant, and all the others, via western blot in a catalytic activity assay, would clarify whether this mutant responds to treatment with saruparib. Retention at the damage site of PARP1 M890A is prolonged in response to treatment with both saruparib and olaparib, following the same pattern as PARP1 WT (Figure 3.12, a, b). Finally, PARP1 K903A, which behaves similarly to PARP1 E988Q and PARP1 E988A at sites of DNA damage (Figure 3.5), does not appear to respond to olaparib treatment at all, but its release is much faster in response to saruparib, with a significantly decreased fluorescence intensity at the damage site 160 seconds post irradiation from 88% to 58%.

Three of the tested mutants, PARP1 E988Q, PARP1 E988A and PARP1 K903A, were shown to be unambiguously de-trapped by saruparib. This indicates that it is not the site, E988, specifically which is important for the response to saruparib, but weak, or absent, catalytic activity, which reveals this pro-release effect of saruparib.

a)

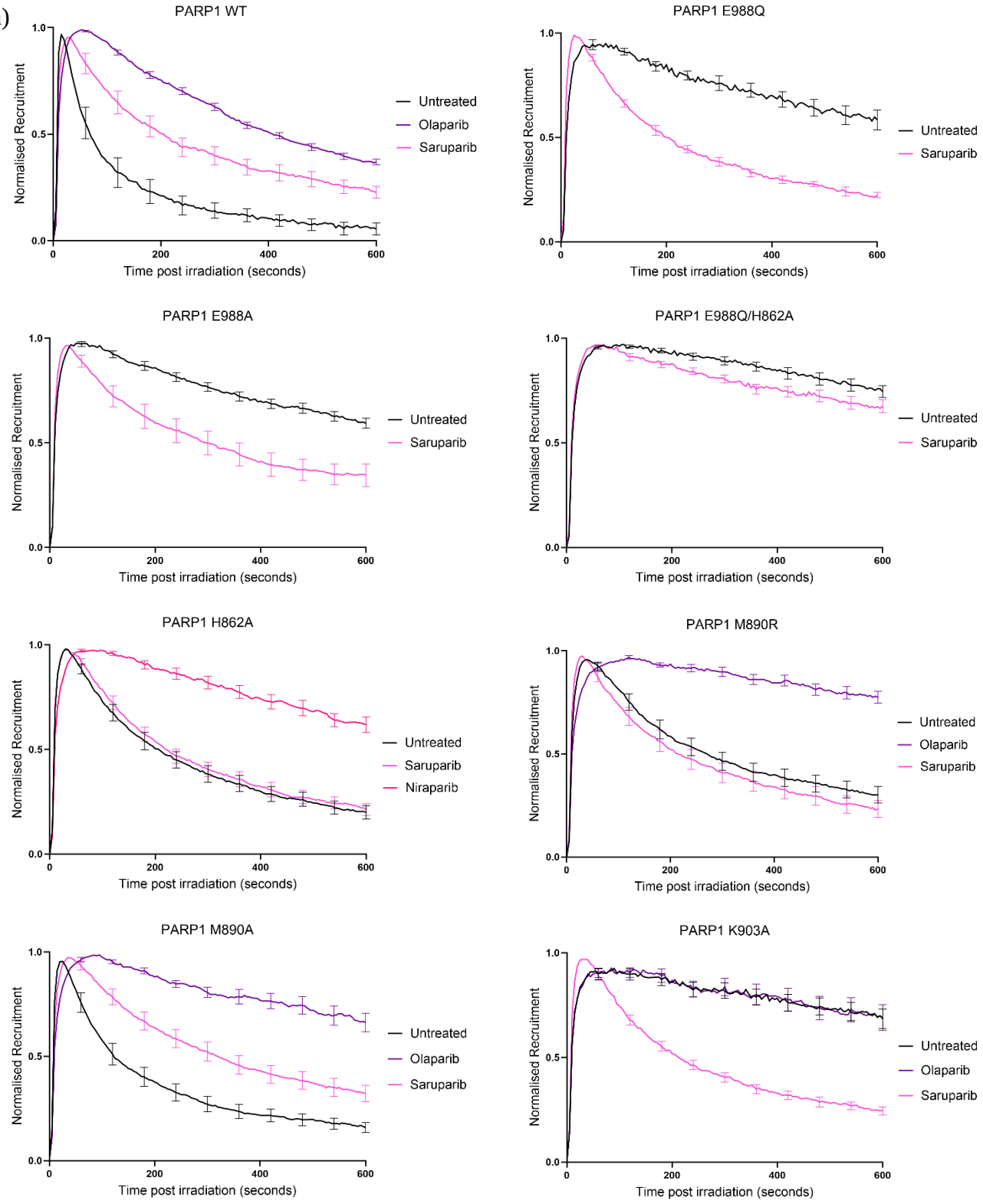
PARP1 WT
Normalised Recruitment
Time post irradiation (seconds)
Untreated
Olaparib
Saruparib
PARP1 E988Q
Untreated
Saruparib
PARP1 E988A
Untreated
Saruparib
PARP1 E988Q/H862A
Untreated
Saruparib
PARP1 H862A
Untreated
Saruparib
Niraparib
PARP1 M890R
Untreated
Olaparib
Saruparib
PARP1 M890A
Untreated
Olaparib
Saruparib
PARP1 K903A
Untreated
Olaparib
Saruparib

b)

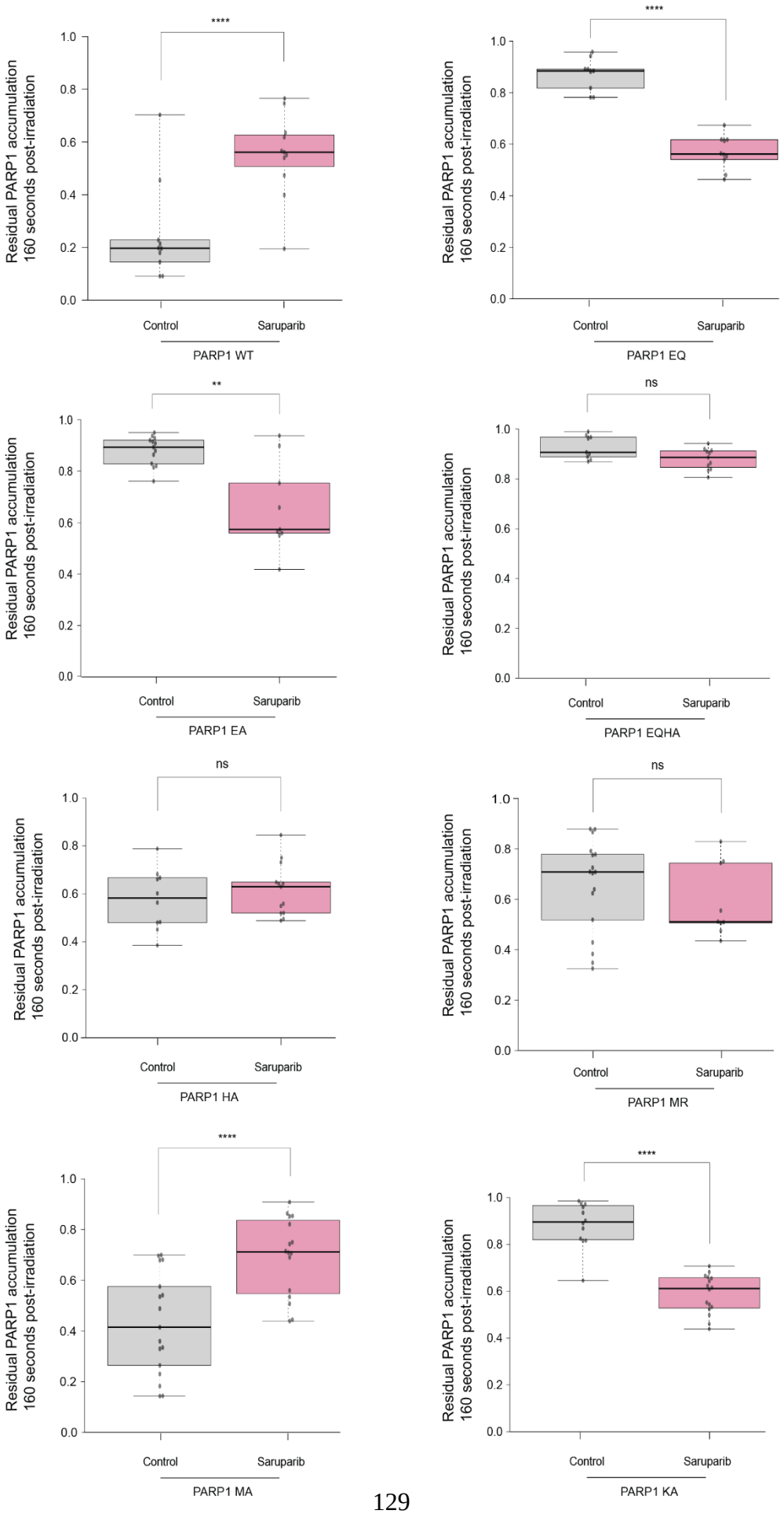
Residual PARP1 accumulation 160 seconds post-irradiation
1.0
0.8
0.6
0.4
0.2
0.0
****
Control
Saruparib
PARP1 WT
PARP1 EQ
**
ns
PARP1 EA
PARP1 EQHA
PARP1 HA
PARP1 MR
PARP1 MA
PARP1 KA

Figure 3.12: Identification of additional PARP1 mutants that are released from DNA damage sites by saruparib. PARP1 E988A and PARP1 K903A are also released by saruparib. Recruitment to sites of DNA damage of the indicated transiently expressed PARP1 variants is shown. U2OS PARP1 KO cells were treated with either 1 µM olaparib, 1 µM niraparib, or 5 nM saruparib. Expression was induced with 0.1 µg Doxycycline, and 1 µM olaparib or 5 nM saruparib were used. **a)** Recruitment was normalised to the maximum fluorescence reached per condition, with the data shown as mean ± standard error of the mean. **b)** Residual PARP1 WT and mutant accumulation at the site of laser micro-irradiation, taken from the normalised recruitment data 160 seconds post damage induction. The box limits correspond to the 25th and 75th percentiles and the bold line indicates the median value; the whiskers extend to minimum and maximum values. ns = not significant, *$p < 0.05$; **$p < 0.01$; ***$p < 0.001$ (one-way ANOVA). Data were collected from 8–17 cells per condition.

3.3.6 Catalytic impairment of PARP1 reveals the pro-release allosteric effect of saruparib

To better understand how the catalytic mutants behave at sites of micro-irradiation over a longer period of time, and to see whether a pro-release effect of saruparib on PARP1 E988Q/H862A would be revealed more clearly, I treated U2OS Flp-In PARP1 KO cells expressing YFP-PARP1 WT, YFP-PARP1 E988Q and YFP-PARP1 E988Q/H862A with olaparib and saruparib, and prolonged capture to 30 minutes, acquiring images every 30 seconds. As seen before, after 10 minutes, the usual endpoint of capture, 10% of YFP-PARP1 WT, roughly 60% of YFP-PARP1 E988Q, and 80% of YFP-PARP1 E988Q/H862A remains at the site of damage (Figure 3.13, a), similar to what was observed previously (Figure 3.5). After 30 minutes, 2% of YFP-PARP1 WT is present at the damage site, 31% of YFP-PARP1 E988Q, and 43% of PARP1 E988Q/H862A (Figure 3.13, a). While treatment of YFP-PARP1 WT with olaparib and saruparib leads to trapping, with 36% left and 20% left at the damage site after 10 minutes, at the end of capture this is reduced to 8% and 4%, respectively (Figure 3.13, b). This confirms olaparib as a stronger trapper than saruparib, but could also point towards the role of PARP2 in PARP1 release, since olaparib also inhibits PARP2. In olaparib-treated cells, the contribution of PARP1 vs PARP2 inhibition is more difficult to decipher, since inhibition is likely to be incomplete, and residual ADP-ribosylation by either can drive chromatin relaxation and DNA repair factor recruitment. However, even in YFP-PARP1 E988Q/H862A expressing cells, where there is no PARP1-mediated ADPr-ribosylation at all, the majority of PARP1 has left the damage site after 30 minutes (Figure 3.13, a). This removal from sites of DNA damage could possibly be attributed to the presence of PARP2, which is able to modify histones and surrounding proteins, promoting the recruitment of DNA repair proteins and chromatin remodellers, as well as the eventual repair of the break site even in the absence of (PARP1- or PARP2-mediated) ADP-ribosylation.

For YFP-PARP1 E988Q, its behaviour after 30 minutes closely resembles the pattern observed after 10 minutes; treatment with olaparib further prolongs retention, trapping roughly 50% at the damage site compared to 31% without olaparib (Figure 3.13, c). Treatment with saruparib continues to de-trap PARP1 E988Q, leaving approximately 10% at the site of damage, comparable to un-inhibited PARP1 WT (Figure 3.13, c), further explaining why treatment with saruparib rescues the toxicity of PARP1 E988Q so drastically. Next, I looked at the dissipation time of PARP1 WT and PARP1 E988Q, which is defined as the time required for half of the maximum recruitment intensity to dissipate ($t_{1/2}$) (Zentout et al., 2024). Measurement of $t_{1/2}$ for PARP1 E988Q/H862A was not possible, since its release is so slow that during the period of capture, more than half of its maximal recruitment intensity remained. Following measurement of $t_{1/2}$ from the normalised recruitment, it can be seen that PARP1 E988Q dissipates significantly faster in response to saruparib treatment, with a $t_{1/2}$ of 236 seconds, close to the $t_{1/2}$ of untreated PARP1 WT, compared to the $t_{1/2}$ (880 seconds) of untreated PARP1 E988Q (Figure 3.13, e). PARP1 E988Q/H862A could not be analysed for its half-life, because in no condition does it approach 50% in the timeframe of capture. When studying the response of PARP1 E988Q/H862A to inhibitor treatment, it appears that both olaparib and saruparib slightly promote release from sites of DNA damage (Figure 3.13, d). For saruparib, this is not surprising, as this trend was already observed after 10 minutes (Figure 3.12), while this was not previously observed for olaparib. The pro-release effect for saruparib is stronger than for olaparib, however, and seems to confirm that PARP1 E988Q/H862A too, is affected in this way by this inhibitor. This corroborates the idea that it is lack, or impairment of, catalytic activity that regulates the pro-release response to saruparib.

a)

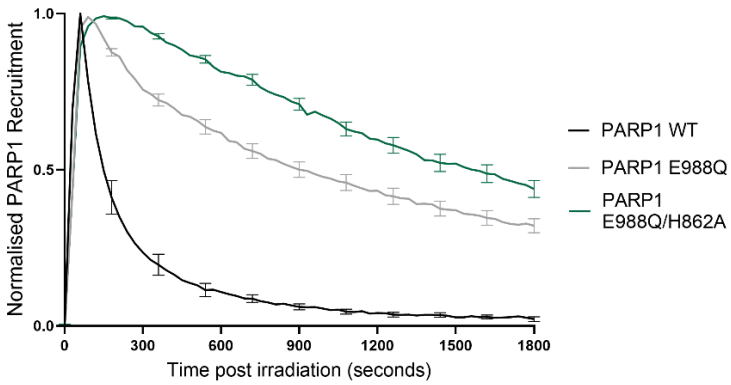
Normalised PARP1 Recruitment
1.0
0.5
0.0
0
300
600
900
1200
1500
1800
Time post irradiation (seconds)
PARP1 WT
PARP1 E988Q
PARP1 E988Q/H862A

b)

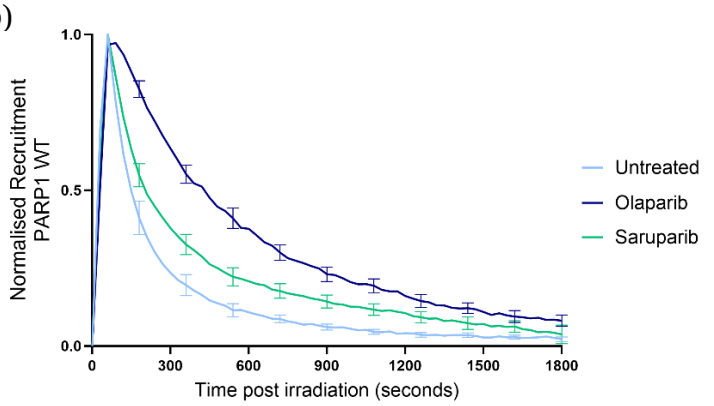
Normalised Recruitment PARP1 WT
1.0
0.5
0.0
0
300
600
900
1200
1500
1800
Time post irradiation (seconds)
Untreated
Olaparib
Saruparib

c)

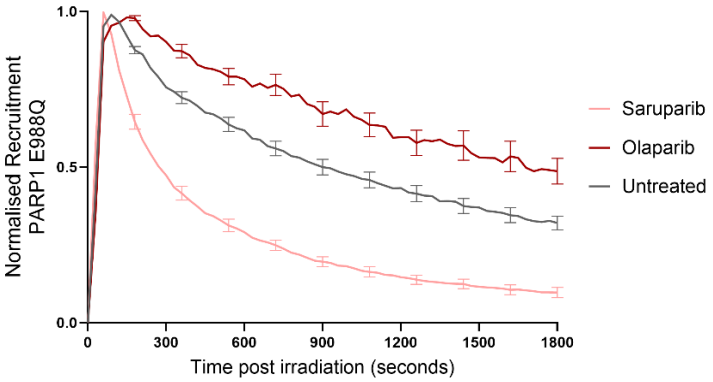
Normalised Recruitment PARP1 E988Q
1.0
0.5
0.0
0
300
600
900
1200
1500
1800
Time post irradiation (seconds)
Saruparib
Olaparib
Untreated

d)

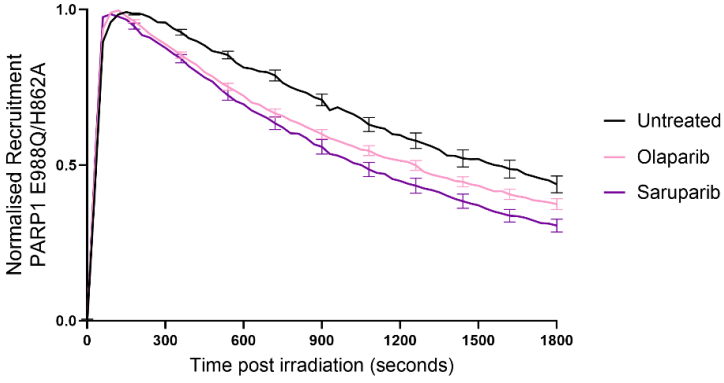
Normalised Recruitment PARP1 E988Q/H862A
1.0
0.5
0.0
0
300
600
900
1200
1500
1800
Time post irradiation (seconds)
Untreated
Olaparib
Saruparib

e)

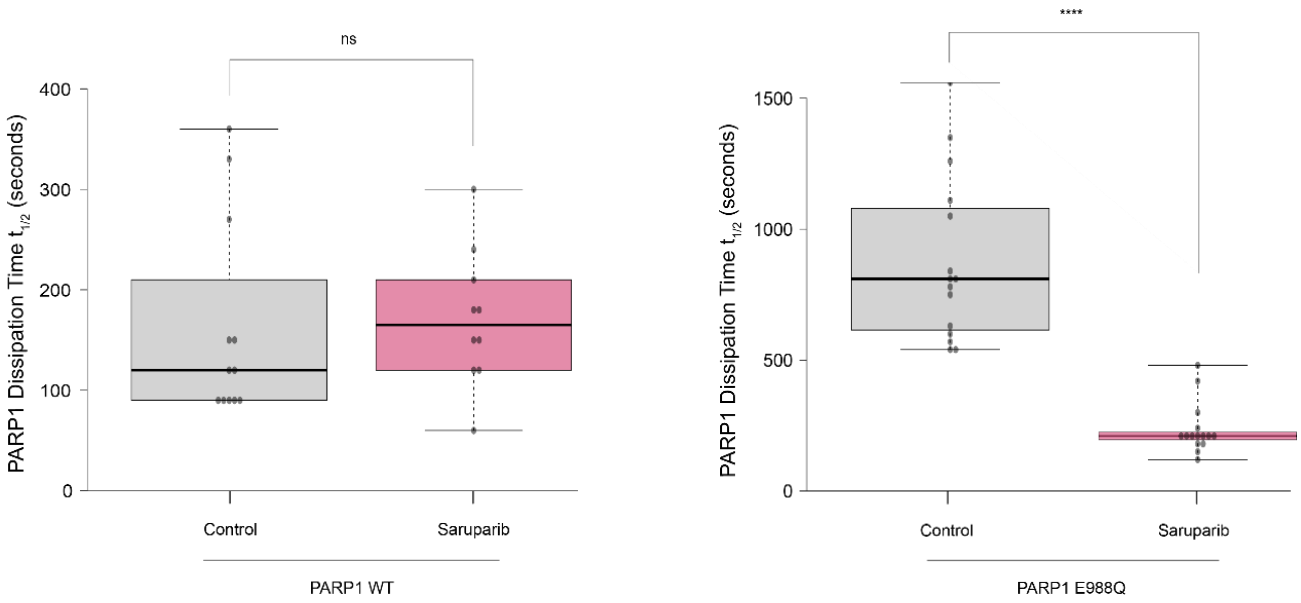
ns
PARP1 Dissipation Time t1/2 (seconds)
400
300
200
100
0
Control
Saruparib
PARP1 WT
****
PARP1 Dissipation Time t1/2 (seconds)
1500
1000
500
0
Control
Saruparib
PARP1 E988Q

Figure 3.13: Loss of catalytic activity reveals the pro-release effect of saruparib. Expression of the indicated PARP1 variants was induced with doxycycline in U2OS Flp-In PARP1 KO cells. **a)** Recruitment to sites of laser micro-irradiation of YFP-PARP1 WT, YFP-PARP1 E988Q and YFP-PARP1 E988Q/H862A without inhibitors is shown. Recruitment to laser micro-irradiation sites of YFP-PARP1 WT **(b)**, YFP-PARP1 E988Q **(c)** and YFP-PARP1 E988Q/H862A **(d)** with and without inhibitors (1 µM olaparib, 5 nM saruparib). Recruitment was normalised to the maximum fluorescence reached per condition with the data shown as mean ± standard error of the mean. Data were collected from 10–18 cells per condition. **e)** Dissipation time of PARP1 WT and PARP1 E988Q from the site of laser micro-irradiation, corresponding to the time required to dissipate 50% of the maximum PARP1 signal. The box limits correspond to the 25th and 75th percentiles and the bold line indicates the median value; the whiskers extend to minimum and maximum values. ns = not significant, *$p < 0.05$; **$p < 0.01$; ***$p < 0.001$ (unpaired, two-tailed Student's *t*-test).

3.3.7 The pro-release response of certain PARP1 mutants to saruparib is not based on a lack of catalytic inhibition

In the previous sections, the effect of saruparib on various mutants was mainly tested under the microscope, which informs about the live recruitment and release dynamics of PARP1, but not its effect on the catalytic activity per se. I therefore decided to compare the catalytic activity of PARP1 WT and the PARP1 mutants with the strongest pro-release response, PARP1 E988Q and PARP1 K903A (Figure 3.12), to saruparib both in un-treated and inhibitor-treated conditions.

I transfected U2OS PARP1 KO cells with YFP-PARP1 WT, YFP-PARP1 E988Q, or YFP-PARP1 K903A. To induce DNA damage, I treated cells with 2 mM H_2O_2 10 minutes prior to harvest, and treated a subset of the H_2O_2-treated cells with either 1 µM olaparib or 5 nM saruparib for an hour prior to and during the H_2O_2 treatment to ensure thorough inhibition. For the western blot, antibodies against both mono or poly-ADP-ribose were used to better compare the ADP-ribosylation activity of different mutants. Due to the sensitive nature of the experiment, and to ensure that any results were not artefacts or due to any potential mistakes, this experiment was repeated thrice, with the same results confirmed each time. As can be seen in Figure 3.14, H_2O_2 treatment greatly increases the mono-ADP-ribosylation activity of wild-type PARP1, both in terms of its automodification and its modification of histones. Poly-ADP-ribosylation activity of PARP1 WT also increases upon DNA damage induction. Olaparib treatment greatly reduces both MARylation and PARylation activity of PARP1 WT, to lower than pre-damage levels. Similarly, saruparib can be seen to effectively inhibit PARP1 catalytic activity, not quite as strongly as olaparib, but with less remaining automodification than in basal, un-damaged conditions. The MARylation activity of PARP1 E988Q increases after DNA damage induction, and both PARP1 and histones are modified with mono-ADP-ribose (Figure 3.14). This is completely abolished in response to olaparib treatment. While

PARP1 E988Q automodification is also completely abolished in response to saruparib, a small amount of histone ADP-ribosylation remains. The basal activity of YFP-PARP1 K903A is lower than that of PARP1 E988Q, but upon DNA damage, its automodification and histone ADP-ribosylation with MAR are stimulated effectively. PARP1 automodification is almost entirely lost upon treatment with olaparib, and completely lost in response to saruparib, while a small amount of histone MARylation remains in both conditions. This shows that both PARP1 E988Q and PARP1 K903A, despite the differing effects of olaparib and saruparib on their release dynamics at sites of DNA damage, are effectively catalytically inhibited by both inhibitors. The reverse effect of saruparib on the PARP1 E988Q and K903A mutants is therefore not due to a lack of catalytic inhibition by saruparib.

Nevertheless, in this experiment, it appears that at the chosen concentration of 5 nM, saruparib is slightly less effective at inhibiting the catalytic activity of PARP1 WT and PARP1 E988Q than olaparib at 1 µM. Meanwhile, in the experiment shown in Figure 3.11, c, neither 1 µM olaparib nor 5 nM saruparib are sufficient to completely abolish catalytic activity. Therefore, in order to ensure that differing levels of catalytic inhibition are not the underlying cause of the differences in trapping between olaparib and saruparib, I induced expression of YFP-PARP1 WT and YFP-PARP1 E988Q in U2OS Flp-In PARP1 KO cells using 0.1 µg/mL Doxycycline, and treated them with increasing concentrations of both olaparib or saruparib. For olaparib, I chose two concentration points below the usual 1 µM, at 0.01 µM and 0.1 µM, and one above, at 5 µM. Even 0.01 µM olaparib is sufficient to induce trapping of PARP1 WT (Figure 3.15, a), and increasing concentrations of olaparib lead to a general upwards trend of PARP1 retention at the site of DNA damage. PARP1 E988Q is trapped similarly by 0.01 µM and 0.1 µM of olaparib, and slightly more by both 1 µM and 5 µM olaparib. Even the lowest concentration of olaparib, 0.01 µM, which was previously

shown to have considerable catalytic activity of endogenous PARP1 remaining (Figure 3.11, c), does not promote release of PARP1 E988Q.

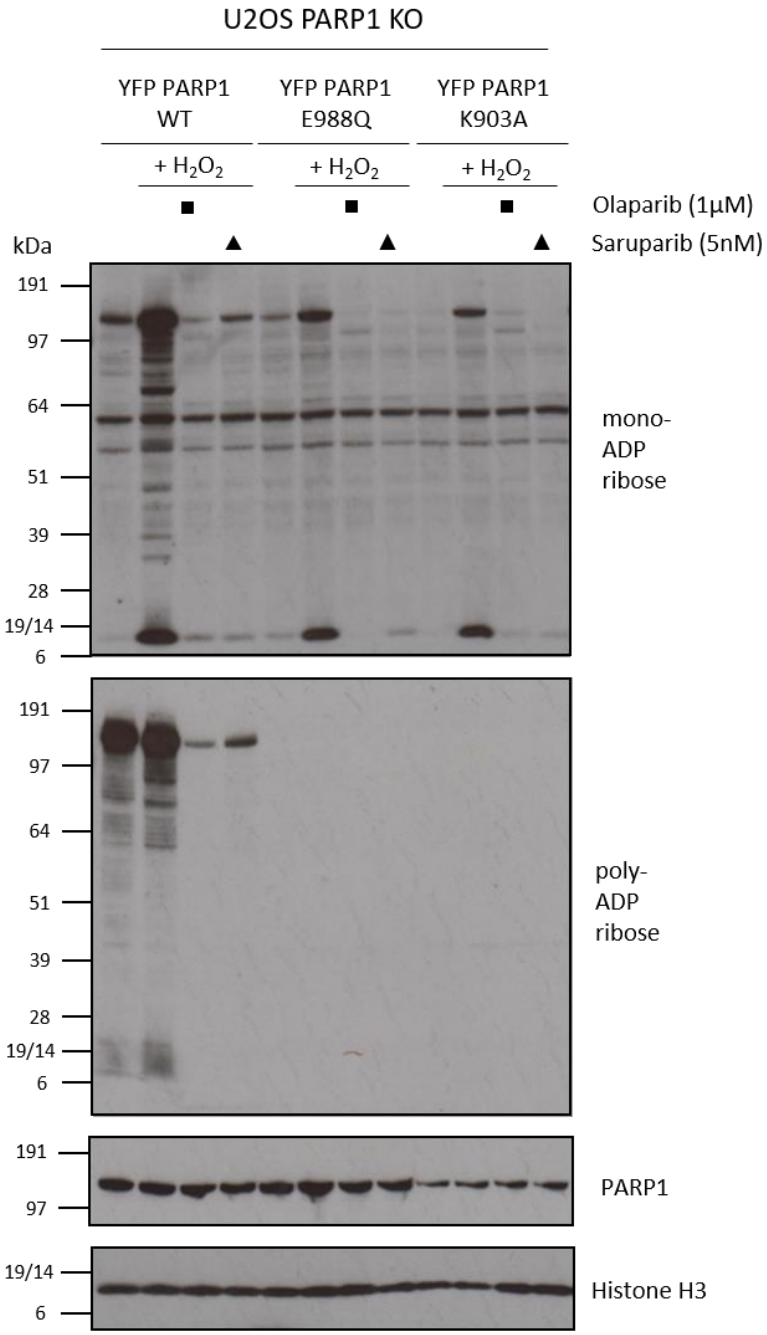

Figure 3.14: Saruparib effectively reduces catalytic activity of PARP1 WT and catalytic mutants. Western blot showing that the catalytic activity of transiently transfected YFP-PARP1 WT, YFP-PARP1 E988Q and YFP-PARP1 K903A in U2OS PARP1 KO cells in response to hydrogen peroxide treatment (2 mM), is reduced to a similar extent by treatment with 1 µM olaparib or 5 nM saruparib. Blots were examined with the indicted antibodies. Histone H3 was used as a loading control.

For saruparib, two concentration points higher than the usual 5 nM were included, 25 nM and 125 nM, concentrations that should be high enough to ensure complete catalytic suppression of PARP1. At 0.5 nM of saruparib, neither PARP1 WT nor PARP1 E988Q are affected, indicating that this concentration is too low to effectively influence PARP1 behaviour at the damage site (Figure 3.15, b). However, concentrations of 5 nM of saruparib or higher are barely distinguishable; all trap PARP1 WT equally, and all similarly promote the release of PARP1 E988Q. This provides further evidence that it is not incomplete catalytic inhibition of PARP1 by saruparib that causes the pro-release effect on PARP1 E988Q.

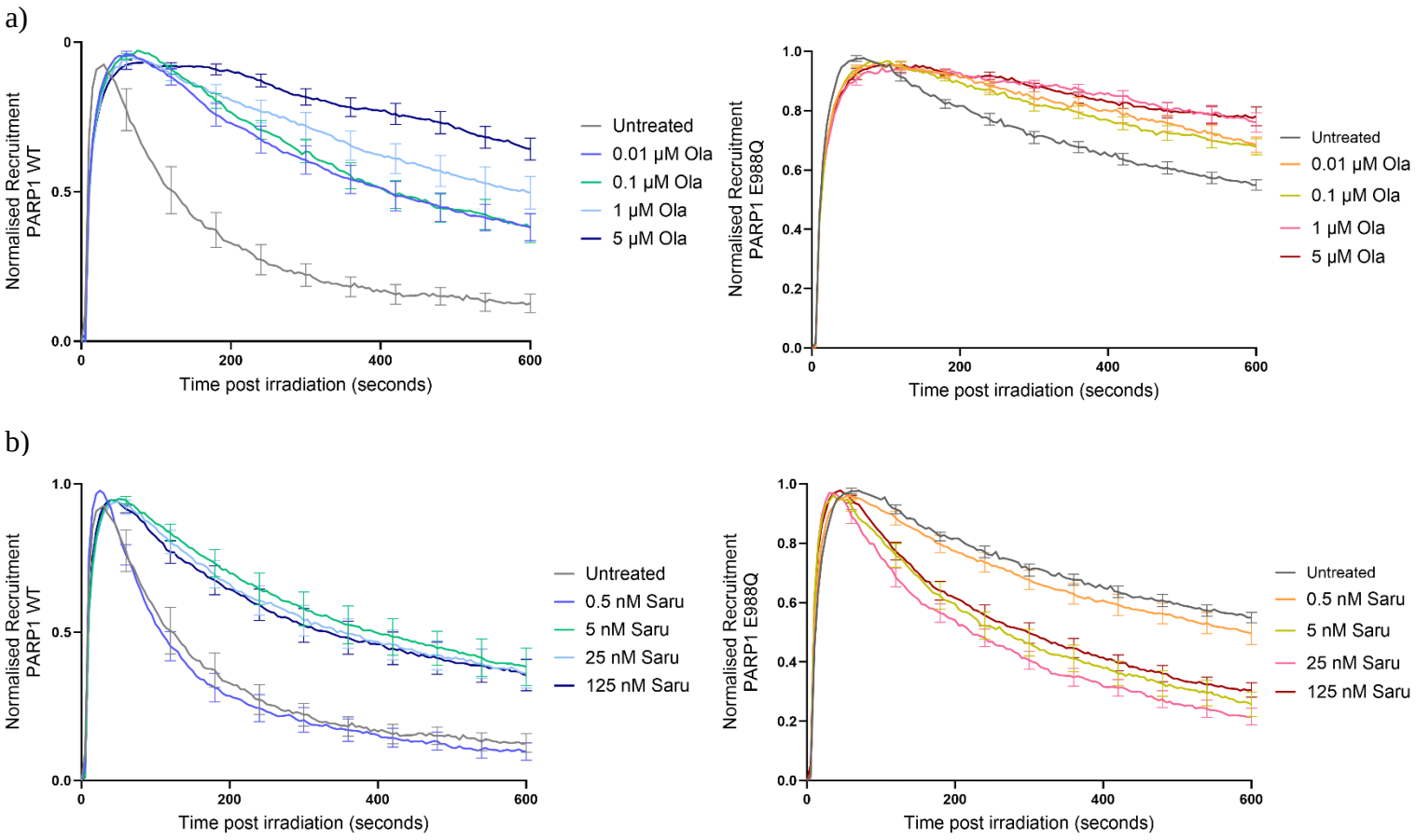

Figure 3.15: The pro-release effect of saruparib on PARP1 E988Q is not dependent on a specific concentration. Recruitment and release dynamics of PARP1 WT and PARP1 E988Q in response to varying concentrations of **a)** olaparib and **b)** saruparib are shown. U2OS Flp-In PARP1 KO cells were treated with 0.1 μg/mL Doxycycline to induce expression of YFP PARP1 WT or E988Q. Recruitment was normalised to the maximum fluorescence reached per condition. Data are shown as mean ± standard error of the mean. Data were collected from 10–18 cells per condition.

3.3.8 The PARP1 helical domain is crucial for regulating the PARP inhibitor response

The auto-inhibitory domain, or helical domain (HD), of PARP1 is known to play a crucial role in regulating PARP1 catalytic activity and the PARP1 inhibitor response. In its inactive state, the HD is folded over the catalytic site, preventing access of NAD^+ and thereby ADP-ribosylation. Upon binding to DNA by its N-terminal DNA binding domains, an allosteric pathway is activated that leads to local unfolding of the HD, allowing for catalytic activity. Loss of the HD (ΔHD) leads to a constitutively active protein that requires no activation through DNA binding (Dawicki-McKenna et al., 2015). Similarly, some PARP inhibitors have been shown to contact the HD in return, causing reverse allosteric effects that can negatively affect DNA binding affinity (Zandarashvili et al., 2020). Mutations in the HD have also been identified which render PARP1 resistant to PARP inhibitors; D766/770A in PARP1, situated in helix F of the HD, leads to resistance against EB-47 (Zandarashvili et al., 2020). However, it was also shown that PARP inhibitor binding to PARP1 was not affected by loss of the HD (Dawicki-McKenna et al., 2015; Zandarashvili et al., 2020); removal of the HD might therefore reveal any allosteric effects inhibitors exert on the HD-WGR-Zn pathway, while maintaining catalytic inhibition of the enzyme.

With this in mind, I wanted to test how loss of the HD would affect the response of PARP1 WT and E988Q to inhibitors. I transfected U2OS PARP1 KO cells with YFP-PARP1 WT, YFP-PARP1 WT ΔHD, YFP-PARP1 E988Q and YFP-PARP1 ΔHD E988Q, and tested their behaviour at sites of DNA damage in response to olaparib and saruparib. When comparing release dynamics of YFP-PARP1 WT and YFP-PARP1 ΔHD, there is little difference between the two, with YFP-PARP1 ΔHD releasing faster initially, but with roughly 20% of either remaining at the damage site after 10 minutes (Figure 3.16, a). However, loss of the HD in the PARP1 E988Q mutant significantly increases the speed of its release from the micro-irradiation site (Figure 3.16, b). This suggests that the hyperactivity of the ΔHD mutant does

not equate to faster release from sites of DNA damage. Instead, it indicates that excessive ADP-ribosylation could counteract PARP1 release from sites of DNA damage. Treatment of PARP1 WT ΔHD with olaparib and saruparib leads to a slightly longer retention at the damage site, with roughly 35% and 30% remaining at the damage site at the end of capture, respectively (Figure 3.16, a). While the trapping effect is not as strong as for PARP1 WT, this indicates that at least some of the catalytic inhibition is retained in the absence of the HD. YFP-PARP1 ΔHD E988Q is removed from sites of DNA damage much faster than YFP-PARP1 E988Q (Figure 3.16, b), which agrees with previous data from PARP1 M890R, a highly active MARylation mutant (Figure 3.4 and 3.5), and shows that large amounts of mono-ADP-ribosylation are sufficient for removal of PARP1 from sites of DNA damage. As with PARP1 WT, loss of the HD for PARP1 E988Q confers resistance to both olaparib and saruparib, abolishing the pro-release effect of saruparib (Figure 3.16, b). If anything, saruparib slightly traps this mutant, indicating that loss of the HD abolishes the pro-release effect of saruparib on this mutant. (Figure 3.16, b). This could have two potential reasons: one, that the increased catalytic activity of this mutant has rescued this phenotype, as only very catalytically impaired PARP1 mutants exhibit this pro-release response to saruparib, and two, that the pro-release effect of saruparib depends on contact with the HD, thereby influencing the HD-WGR-Zn axis, and in turn the DNA binding affinity of the protein.

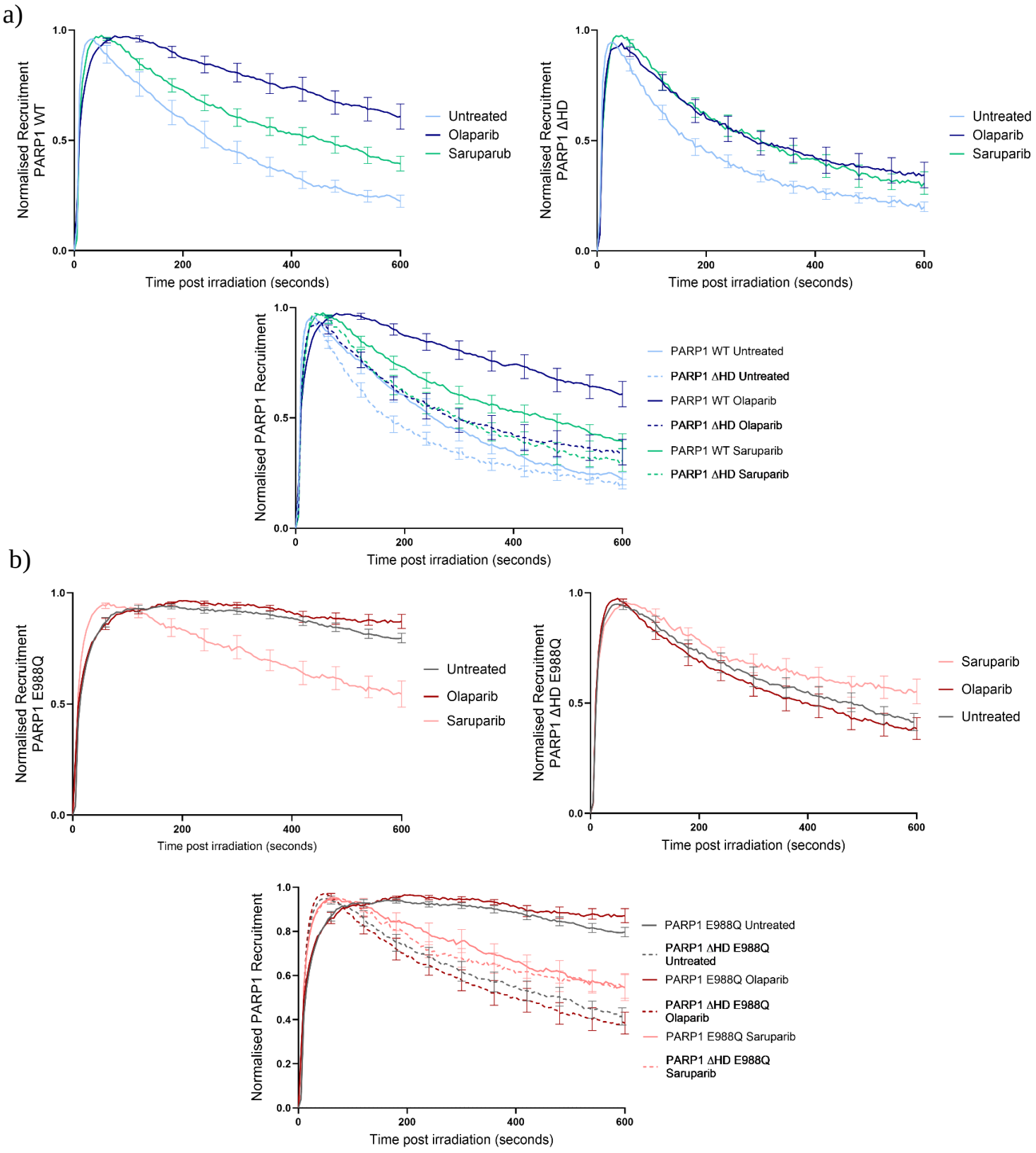

Figure 3.16: The PARP1 HD is involved in the regulation of the PARP inhibitor response.

Recruitment and release dynamics of transiently transfected **a)** YFP-PARP1 WT and PARP1 WT ΔHD and **b)** YFP-PARP1 E988Q and PARP1 ΔHD E988Q to sites of DNA damage in U2OS PARP1 KO cells. Cells were left un-treated, or treated with 1 μM olaparib or 5 nM saruparib. Recruitment was normalised to the maximum fluorescence reached per condition. Data are shown as mean ± standard error of the mean. Data were collected from 8–17 cells per condition.

3.3.9 The effect of endogenous PARP1 on the pro-release effect of saruparib on PARP1 E988Q

It was previously shown that the release of PARP1 from sites of DNA damage does not depend entirely on its automodification; modification of histones by PARP1 has a considerable influence on the mobilisation of PARP1 from DNA lesions (Zentout et al., 2024). Release of PARP1 E988K, which similarly to PARP1 E988A functions as a catalytically dead PARP1 mutant, is increased in the presence of co-transfected, or endogenous wild-type PARP1 (Zentout et al., 2024). This difference was shown not to be due to trans-modification of PARP1 E988K, which has been observed to occur *in vitro* (Eustermann et al., 2015), but rather due to ADP-ribosylation of histones, which also increased the cellular resistance to olaparib (Zentout et al., 2024). In accordance with findings that PARP1 undergoes unproductive cycles of association and disassociation at DNA lesions in the presence of PARP inhibitors (Kanev et al., 2024; Shao et al., 2020), ADP-ribosylated histones at the site of damage were therefore suggested to contribute to the timely release of PARP1 both through the recruitment of repair factors and by acting as a shield to prevent PARP1 re-association with the lesion through electrostatic repulsion (Zentout et at., 2024).

Therefore, I wanted to test how the presence of endogenous PARP1 would affect the behaviour of PARP1 E988Q at the damage site in the presence and absence of saruparib. To this end, I transfected both U2OS WT cells and U2OS PARP1 KO cells with either YFP-PARP1 WT or YFP-PARP1 E988Q, and tested their recruitment and release dynamics in the presence and absence of olaparib or saruparib. For YFP-PARP1 WT, the presence of endogenous PARP1 slows down its release in all conditions, while maintaining the trapping effects of olaparib and saruparib (Figure 3.17, a, d). Meanwhile, the presence of endogenous PARP1 speeds up the release of YFP-PARP1 E988Q from sites of DNA damage, in agreement with previous findings (Zentout et al., 2024) (Figure 3.17, b). The effect of

treatment with olaparib remains the same, trapping PARP1 E988Q further, to a greater degree in the WT background than in the PARP1 KO background. However, the pro-release effect of saruparib on PARP1 E988Q is not maintained in the WT background; while not as potent as olaparib, it leads to further trapping of the mutant at the site of the lesion (Figure 3.17, b, d). The presence of endogenous PARP1 could influence the observed release dynamics of over-expressed PARP1 in at least two main ways: Firstly, there is an overall greater amount of PARP1 in the nucleus; competition with endogenous PARP1 at DNA lesions could affect the recruitment and release dynamics of the over-expressed PARP1. This is corroborated by the fact that the total recruitment of both transfected YFP-PARP1 WT and E988Q to the damage site is lower in the presence of endogenous PARP1 (Figure 3.17, c). Secondly, endogenous PARP1 modifies surrounding histones and other proteins, changing the chromatin environment surrounding the break and signalling to repair proteins. Similar to the behaviour at sites of DNA damage of PARP1 WT ΔHD (Figure 3.16, a), the opposing effect that endogenous PARP1 has on YFP-PARP1 WT and YFP-PARP1 E988Q suggests that there might be a tightly regulated, "correct" amount of ADP-ribosylation that prevents PARP1 trapping. Interestingly, it was further noticeable that treatment of both YFP PARP1 WT and PARP1 E988Q with olaparib, but not with saruparib, in a WT background significantly delayed the recruitment of PARP1 to the micro-irradiated site, as measured by the time of peak recruitment (Figure 3.17, e). Over-representation of catalytically active wild-type PARP1 could prevent both access and removal from sites of DNA damage, through competition at lesions and an excessively ADP-ribosylated chromatin microenvironment. Once catalytic activity is inhibited through either olaparib or saruparib treatment, YFP-PARP1 WT trapping is even greater than in PARP1 KO cells, and could be due to greatly slowed exchange of PARP1 molecules at the damage site, both through loss of catalytic activity and the presence of additional PARP1. Meanwhile, release of PARP1 E988Q is increased in the presence of endogenous PARP1; this could be due to improved signalling at

the damage site through modified histones, which in turn can promote the recruitment of repair and remodelling factors, such as XRCC1 and ALC1, in turn abolishing the need for PARP1 re-association with repaired lesions (Juhász et al., 2020; Shao et al., 2020; Smith et al., 2023; Zentout et al., 2024). On the other hand, olaparib-trapped endogenous PARP1 at the could prevent access of YFP-tagged PARP1 WT and PARP1 E988Q to the site of damage, explaining the delayed recruitment in these conditions. Treatment with saruparib does not significantly delay recruitment of YFP-PARP1 WT or YFP-PARP1 E988Q in a WT background (Figure 3.17, e), indicative of its lesser trapping ability.

Meanwhile, treatment of YFP-PARP1 E988Q-expressing U2OS WT cells with saruparib could increase trapping, instead of promoting its release, by preventing its dissociation and exchange at lesions due to the over-representation of endogenous PARP1.

a)

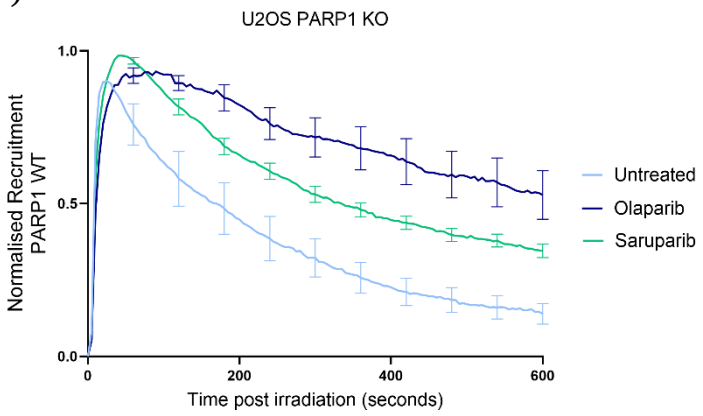
U2OS PARP1 KO
Normalised Recruitment PARP1 WT
1.0
0.5
0.0
0
200
400
600
Time post irradiation (seconds)
Untreated
Olaparib
Saruparib

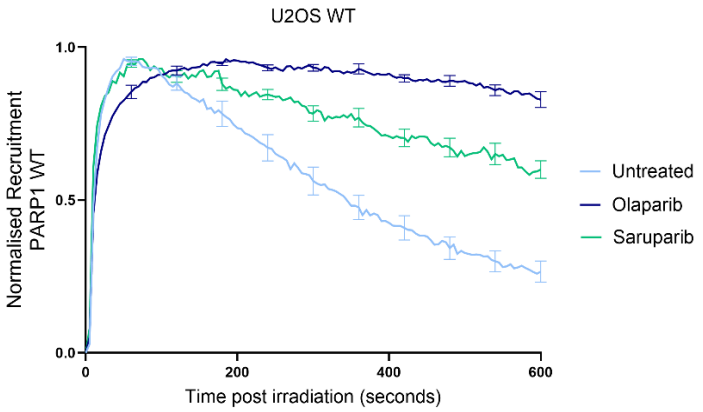
U2OS WT
Normalised Recruitment PARP1 WT
1.0
0.5
0.0
0
200
400
600
Time post irradiation (seconds)
Untreated
Olaparib
Saruparib

b)

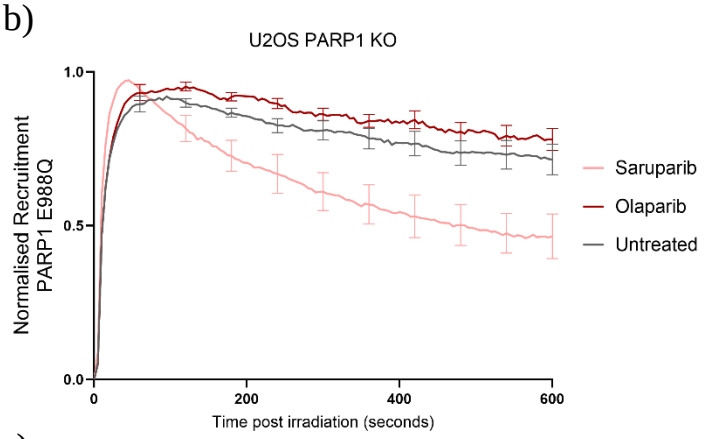
U2OS PARP1 KO
Normalised Recruitment PARP1 E988Q
1.0
0.5
0.0
0
200
400
600
Time post irradiation (seconds)
Saruparib
Olaparib
Untreated

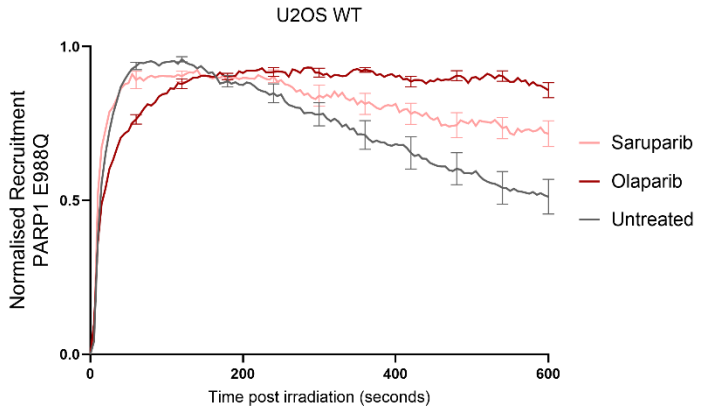
U2OS WT
Normalised Recruitment PARP1 E988Q
1.0
0.5
0.0
0
200
400
600
Time post irradiation (seconds)
Saruparib
Olaparib
Untreated

c)

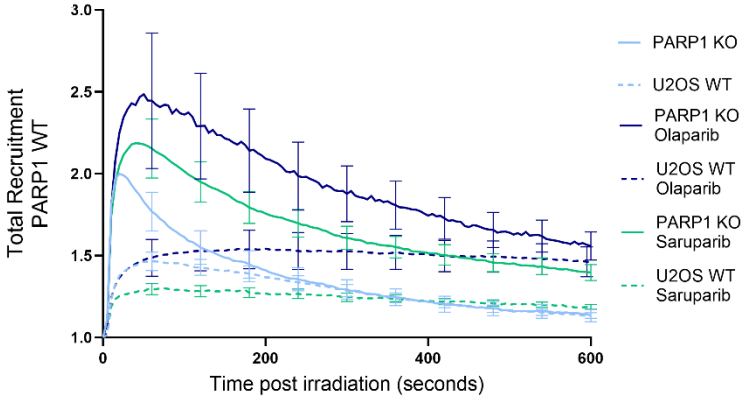
Total Recruitment PARP1 WT
3.0
2.5
2.0
1.5
1.0
0
200
400
600
Time post irradiation (seconds)
PARP1 KO
U2OS WT
PARP1 KO Olaparib
U2OS WT Olaparib
PARP1 KO Saruparib
U2OS WT Saruparib

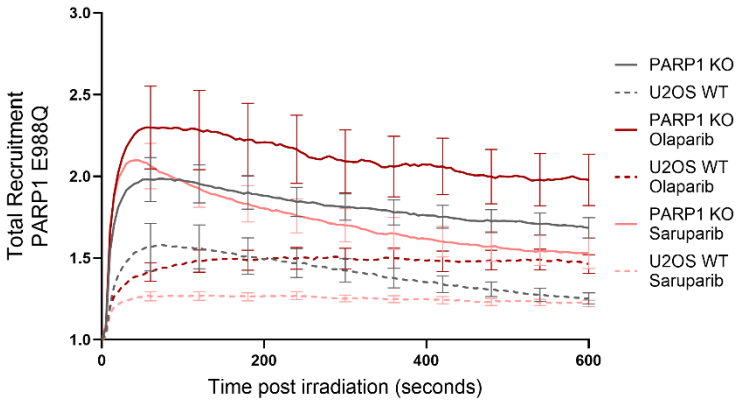
Total Recruitment PARP1 E988Q
3.0
2.5
2.0
1.5
1.0
0
200
400
600
Time post irradiation (seconds)
PARP1 KO
U2OS WT
PARP1 KO Olaparib
U2OS WT Olaparib
PARP1 KO Saruparib
U2OS WT Saruparib

d)

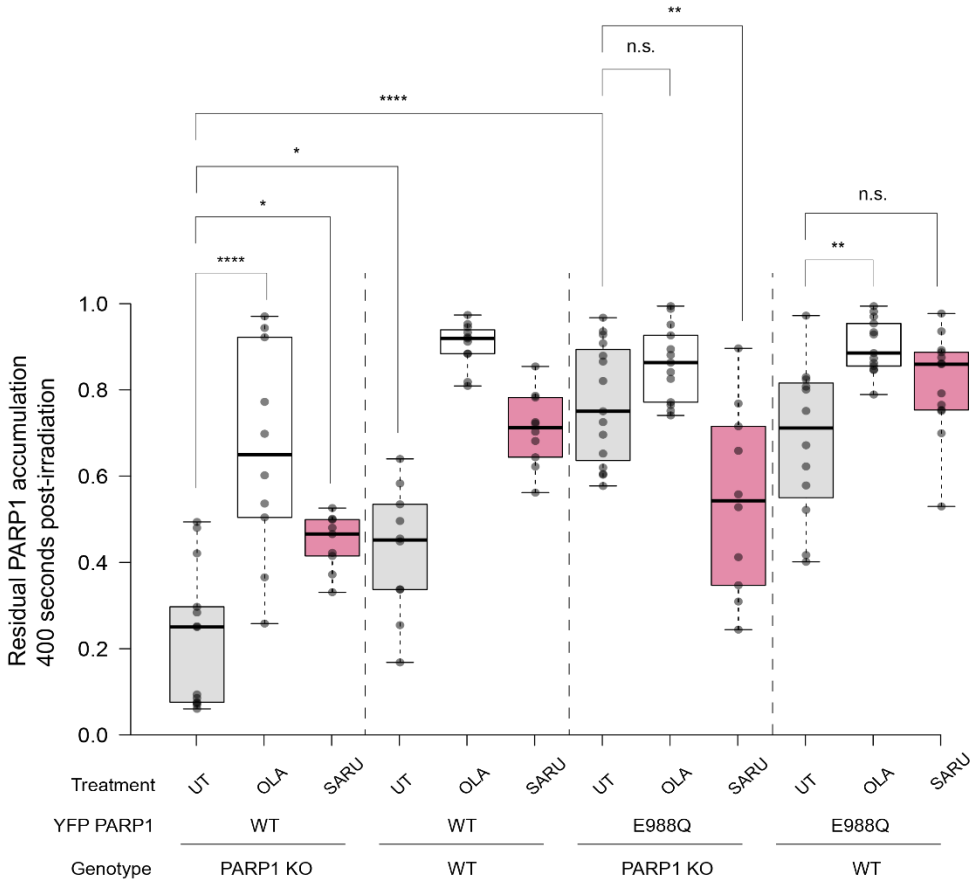
Residual PARP1 accumulation
400 seconds post-irradiation
1.0
0.8
0.6
0.4
0.2
0.0
****
*
*
****
n.s.
**
n.s.
**
Treatment
UT
OLA
SARU
YFP PARP1
WT
E988Q
Genotype
PARP1 KO
WT

e)

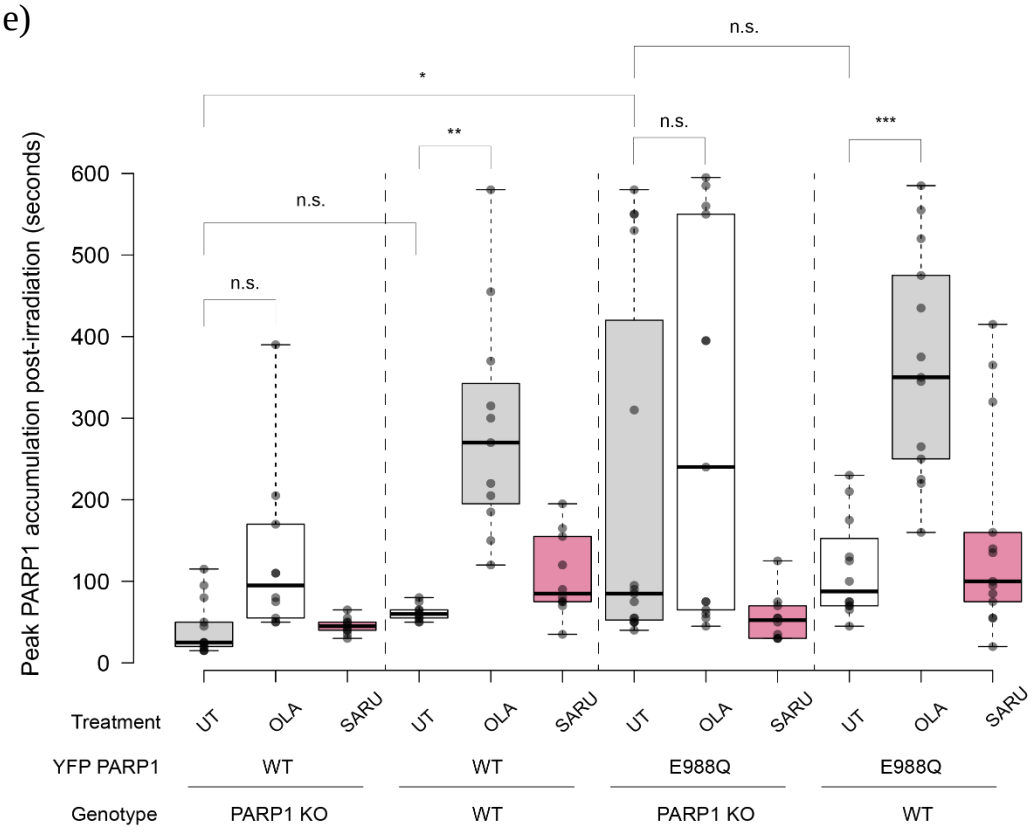
Peak PARP1 accumulation post-irradiation (seconds)
600
500
400
300
200
100
0
n.s.
n.s.
*
**
n.s.
***
Treatment
UT
OLA
SARU
YFP PARP1
WT
E988Q
Genotype
PARP1 KO
WT

Figure 3.17: Presence of endogenous PARP1 abrogates the pro-release of saruparib on PARP1 E988Q. Normalised recruitment of **a)** YFP-PARP1 WT and **b)** YFP-PARP1 E988Q to sites of laser micro-irradiation in U2OS PARP1 KO or U2OS WT cells. **c)** Total recruitment of YFP-PARP1 WT and YFP-PARP1 E988Q to sites of laser micro-irradiation. Cells were left un-treated, or treated with 1 μM olaparib or 5 nM saruparib. Recruitment was normalised to the maximum fluorescence reached per condition for a) and b) with the data shown as mean ± standard error of the mean. Data were collected from 9–15 cells per condition. d) Residual PARP1 WT and mutant accumulation at the site of laser micro-irradiation, taken from the normalised recruitment data 400 seconds post damage induction. e) Peak recruitment (t_{max}) of YFP PARP1 WT and YFP PARP1 E988Q to the site of laser microirradiation. The box limits correspond to the 25th and 75th percentiles and the bold line indicates the median value; the whiskers extend to minimum and maximum values. n.s. = not significant, *$p < 0.05$; **$p < 0.01$; ***$p < 0.001$ (one-way ANOVA).

3.4. Investigating the behaviour and relationship of PARP1 and PARP2 at sites of DNA damage

While loss of either PARP1 or PARP2 is tolerated by the cell, loss of both is embryonically lethal (Ménissier de Murcia et al., 2003b). PARP1 arrives first at the DNA damage site and PARP2, which lacks the many DNA binding domains of PARP1, is reported to arrive slightly after PARP2 (Mortusewicz et al., 2007). Further, there have been reports of PARP2 relying to some degree on the catalytic activity of PARP1 for its recruitment to sites of DNA damage; first, it was shown that the catalytic activity of PARP2 could not only be stimulated by DNA, but also by PAR *in vitro* (Chen et al., 2018), and loss of PARP1 or its catalytic activity, either through mutation or PARP inhibitor treatment, was shown to cause reduced recruitment of PARP2 to sites of DNA damage (Chen et al., 2018; Lin et al., 2022; Mortusewicz et al., 2007). The extent to which the loss of PARP1 catalytic activity affects PARP2 recruitment is unclear, however; the study published by Chen et al. (2018) found that expression of catalytically dead PARP1 E988A, or loss of PARP1, completely abrogated PARP2 recruitment to sites of DNA damage, while it was reported to merely be slightly impaired by other studies (Mortusewicz et al., 2007; Lin et al., 2022).

The availability of a PARP1-selective inhibitor provides an excellent opportunity to study how PARP2 recruitment is affected by the catalytic activity of PARP1; since all other PARP inhibitors also target PARP2, they cannot be used to study how loss of catalytic activity of PARP1 alone affects PARP2 without simultaneously inhibiting PARP2. Further, the MARylation mutant PARP1 E988Q can also provide information on the reliance of PARP2 on pre-existing PAR chains for its recruitment to DNA lesions. Moreover, the pro-release effect of saruparib on PARP1 E988Q, which was shown not to be linked to any inhibitor-induced increase in its catalytic activity (Figure 3.14), can be used to study how occupancy at the damage site alone can affect the turnover of PARP2.

In turn, the presence or absence of PARP2 can provide information on how PARP2 contributes to the release dynamics of PARP1. To investigate the relationship dynamics between PARP1 and PARP2, I used U2OS PARP1/PARP2 KO cells, which I transfected with either mCherry-PARP1 WT/E988Q or YFP-PARP2 WT alone, or together. I tested these cells by western blot to ensure they lacked both PARP1 and PARP2 (Figure A.4). When looking at either PARP1 or PARP2 alone, I co-transfected Histone H2B tagged with a photoactivatable fluorophore, to indicate the damage site and when the laser micro-irradiation occurs. This is particularly important to accurately determine the recruitment dynamics for PARP2, which arrives later than PARP1 at the damage site, and not as abundantly, which can make detection more difficult.

I split the results of this experiment into two sections: one, to assess the effect of presence or absence of PARP2 on PARP1, and two, how the presence and catalytic activity of PARP1 affects the total and relative recruitment and retention of PARP2.

3.4.1 The effect of PARP2 on PARP1 recruitment and release from sites of DNA damage

Forty-eight hours after transfection, I treated cells with 0.15 µg/mL Hoechst for an hour to sensitise them to DNA damage and added 1 µM olaparib or 5 nM saruparib to a subset of the cells. As shown in Figure 3.18, the general recruitment behaviours of PARP1 WT and PARP1 E988Q un-treated and in response to olaparib and saruparib are preserved with or without PARP2. At the end of capture, 13% of the total PARP1 recruited remains at the lesion in the absence of PARP2, with 10% left in the presence of YFP-PARP2 WT (Figure 3.18, a). This difference is negligible, but the presence of PARP2 does appear to promote the release of PARP1 earlier on; after 2 minutes, 64% of PARP1 WT remains at the site of damage without PARP2, while only 46% of PARP1 WT remains in the presence of YFP-PARP2 WT. This trend can also be observed in response to saruparib: it is decreased from 30% of PARP1 remaining at the damage site after 10 minutes to 22% in the presence of YFP-PARP2 WT.

The trend persists even with olaparib treatment, the presence of YFP-PARP2 reducing the remaining PARP1 WT from 60% to 38% at the end of capture. The presence of YFP-PARP2 also has a slight, but apparently weaker, de-trapping effect on mCherry-PARP1 E988Q in some conditions (Figure 3.18, b); 75% of the maximum amount of recruited PARP1 E988Q after 10 minutes is reduced to 65% in the presence of YFP-PARP2 WT, and saruparib-treated PARP1 E988Q is further decreased from 42% to 33% by YFP-PARP2. For olaparib-treated PARP1 E988Q this effect is not so apparent. This could generally stem from the strong trapping of olaparib-treated PARP1 E988Q, and the relatively strong trapping of PARP2 in this condition, as shown in Figure 3.20, d, and discussed in the following section. Importantly, the fact that saruparib de-traps mCherry-PARP1 E988Q validates that this effect is not an artefact of the YFP-PARP1 E988Q construct used in previous experiments, or the cell line, but rather an effect linked to the nature of the mutant.

This could be explained by PARP2 ADP-ribosylating the surrounding chromatin; as discussed in section *3.3.9*, the release of PARP1 from sites of DNA damage is not entirely reliant on its auto-modification, but also the modification of histones (Smith et al., 2023; Zentout et al., 2024). The presence of catalytically active PARP2 could therefore allow modification of histones, creating an "ADP-ribose shield" on chromatin that prevents PARP1 re-association with the damage site, and recruit chromatin remodellers and repair factors that would occupy the break site (Zentout et al., 2024), as explained in section *3.3.9*. However, the fact that the release of PARP1 WT is further sped up in the presence of YFP-PARP2 despite olaparib treatment would indicate that this effect does not depend on PARP2 catalytic activity, since it is also inhibited by olaparib. It could be that the presence of both mCherry-PARP1 WT and YFP-PARP2 leads to incomplete inhibition of either, which could be reflected by the lesser retention of PARP1 in this condition. To ensure that it is PARP2 catalytic activity that causes this pro-release effect on PARP1, it would be interesting to observe PARP1 dynamics in the

presence of wild-type and catalytically inactive PARP2, such as PARP2 E545A (Riccio et al., 2016b).

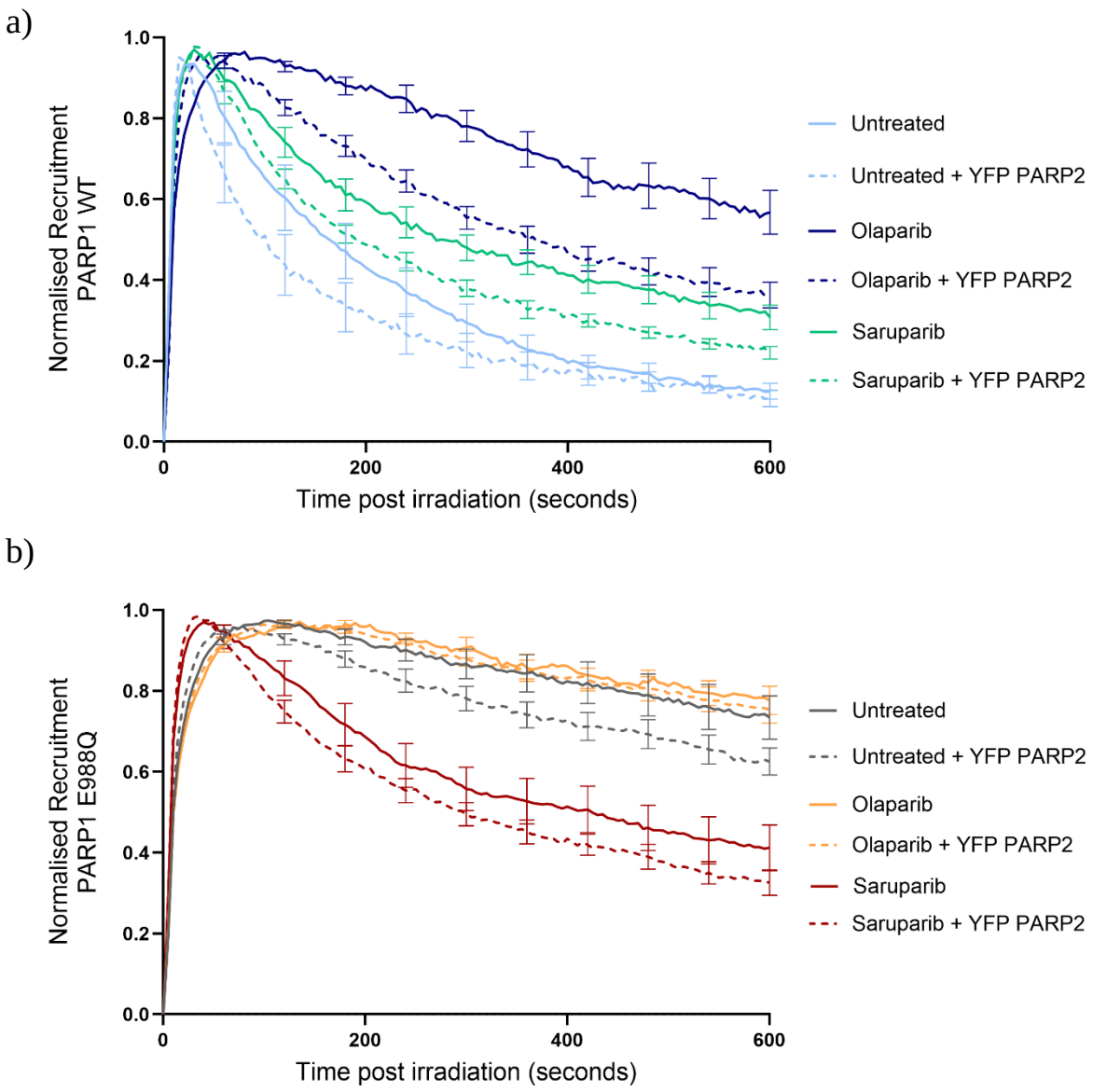

Figure 3.18: Recruitment and release dynamics of PARP1 WT and E988Q are differently affected by the presence of PARP2. Recruitment of mCherry-PARP1 WT or E988Q to sites of laser-microirradiation in U2OS PARP1/PARP2 KO cells, with or without co-transfected YFP-PARP2 WT. Olaparib was used at 1 µM, and saruparib at 5 nM. Recruitment was normalised to the maximum fluorescence reached per condition. Data are shown as mean ± standard error of the mean. Data were collected from 8–15 cells per condition.

3.4.2 The effect of PARP1 on PARP2 recruitment and release from DNA damage site

Following previous reports of PARP2 reliance on PARP1 for its recruitment to sites of DNA damage, I made sure to measure the total amount of PARP2 recruited in all conditions, in addition to the normalised recruitment, which better allows comparison of release dynamics between conditions. First, when comparing total recruitment of PARP2 to DNA lesions in the presence or absence of PARP1, it appears that there is no great difference between the PARP1/PARP2 KO condition, and when mCherry-PARP1 WT is co-transfected (Figure 3.19, a). However, recruitment appears to be much lower in the presence of PARP1 E988Q. Interestingly, this could indicate that PARP2 does not rely on PARP1 catalytic activity to be recruited to sites of DNA damage, but that the occupation of sites of DNA damage by trapped PARP1 E988Q could hinder its recruitment. This difference was not due to corresponding differences in the total amount of mCherry-PARP1 WT and PARP1 E988Q recruited to sites of damage (Appendix, Figure A.5). Comparing recruitment of PARP2 in PARP1/PARP2 KO cells lacking co-transfected PARP1 (Figure 3.19, b) shows that treatment with olaparib or saruparib does not have any effect on the amount arriving at the damage site, which makes sense in the absence of any PARP1 that can be inhibited or trapped. When looking at total PARP2 recruitment in the presence of wild-type PARP1 (Figure 3.19, c), it appears that treatment with saruparib has no effect on either the amount or the behaviour at the damage site, confirming on the one hand that it is not targeted by saruparib. On the other hand, it would suggest that mild trapping of PARP1 is not sufficient to affect PARP2 recruitment. Meanwhile, it seems that olaparib increases the total amount of PARP2 recruited to sites of DNA damage in all conditions (Figure 3.19, b, c, d). Particularly in the presence of mCherry-PARP1 E988Q, its recruitment seems very delayed, and increases with time (Figure 3.19, c, d).

This effect appears to be dependent on olaparib, rather than loss of catalytic activity of PARP1, as in the case of PARP1 E988Q without inhibitor, which causes lower total PARP2 recruitment, or saruparib treatment, which equally inhibits catalytic activity of PARP1. Interestingly, a previous study found that some PARP inhibitors, such as niraparib and talazoparib, and to a lesser extent, olaparib, enhanced the formation of PARP2 foci, independently of whether or not PARP1 was present (Lin et al., 2022). The same study investigated the exchange rate of PARP2 at the site of damage using FRAP, and found that these inhibitors caused physical stalling of PARP2 at the damage site (Lin et al., 2022). This agrees with *in vitro* findings that the allostery of PARP2 is affected differently by PARP inhibitors than PARP1; PARP1 "pro-release" inhibitors such as rucaparib and niraparib were found to be "pro-retention" in PARP2, increasing its DNA binding affinity (Langelier et al., 2023). The increase in YFP PARP2 at the damage site over time therefore likely reflects true "trapping" of PARP2 at the site of DNA damage by olaparib. Treatment of PARP1 E988Q with saruparib seems to slightly increase the total amount of PARP2 recruited in the first minute after DNA damage induction (Figure 3.19, d).

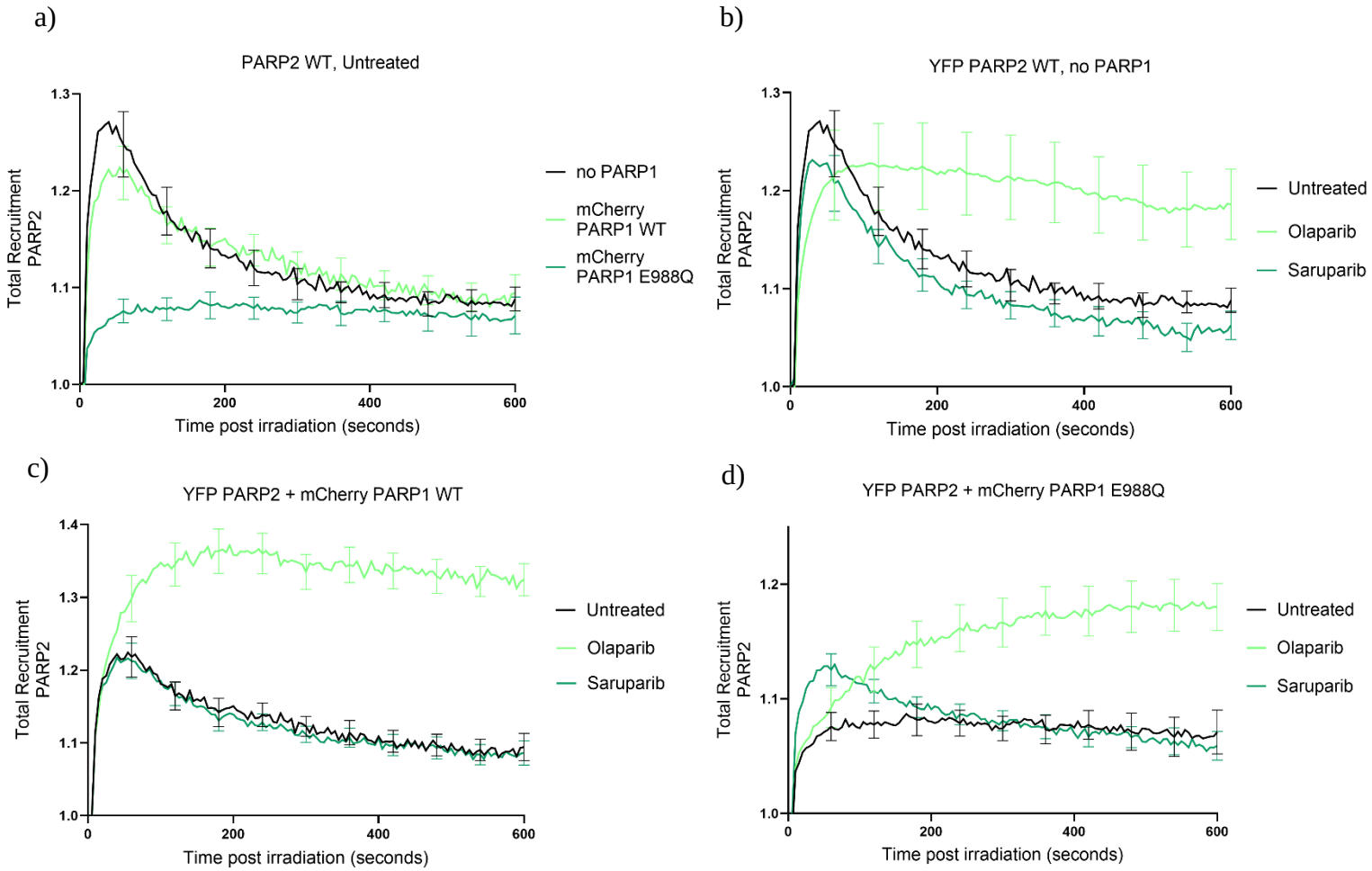

Figure 3.19: Total recruitment of YFP-PARP2 is affected by the presence or absence of PARP1 WT or PARP1 E988Q. Total measured amounts of transiently expressed YFP-PARP2 recruitment over time, with or without mCherry-PARP1 WT or E988Q in U2OS PARP1/PARP2 KO cells are shown. Olaparib was used at 1 µM, and saruparib at 5 nM. Data are shown as mean ± standard error of the mean. Data were collected from 11–15 cells per condition.

To better understand the release and recruitment dynamics of PARP2 at DNA lesions, I also looked at normalised recruitment, which measures the amount of protein relative to the maximum amount over time. This shows that in the absence of PARP1 and any inhibitor, PARP2 is recruited to the damage site quickly, peaking after roughly 30 seconds, compared to 20 seconds for PARP1 WT, and is released thereafter, with roughly 30% remaining at the end of capture (Figure 3.20, a). This is the same for saruparib treatment, confirming that PARP2 is not targeted by this PARP1-selective inhibitor. In response to olaparib treatment, PARP2 recruitment is delayed, peaking only after 2 minutes, and it is trapped at the damage site, with 85% of the original amount remaining after 10 minutes.

When comparing the behaviour of PARP2 in the presence or absence of PARP1 WT or PARP1 E988Q, it becomes apparent that expression of the mono-mutant PARP1 E988Q not only diminishes total recruitment of PARP2 (Figure 3.19, a), but it also prolongs its retention of PARP2 at the damage site (Figure 3.20, b). In the presence of PARP1 E988Q, over 80% of the peak amount remains after 10 minutes. Presence of PARP1 WT does not lead to prolonged trapping of PARP2 at the end of capture, but it does moderately slow its release earlier on, with only 63% of PARP2 remaining at the damage site after two minutes without PARP1, and 81% remaining in the presence of mCherry-PARP1 WT. Both the increased trapping of PARP2 in the presence of PARP1 E988Q, and the slower release in the presence of PARP1 WT, could hint at competition for occupancy at the damage site, and reflect continued attempts at binding and un-binding of the break in the presence of PARP1. It could also reflect PARP2 being recruited by continued PAR signalling by PARP1 (Lin et al., 2022; Chen et al., 2018). However, PARP2 is also trapped in the presence of PARP1 E988Q, despite its own catalytic activity not being impaired, and despite the fact that PARP1 E988Q is unable to generate PAR chains that might continue to recruit PARP2. Interestingly, treatment of mCherry-PARP1 WT with saruparib has no effect on the release dynamics of

PARP2, despite its catalytic inhibition (Figure 3.20, c). PARP1 WT trapping by saruparib is not strong, however, and saruparib has been reported to increase the exchange of PARP1 molecules at sites of DNA damage despite catalytic inhibition (Kanev et al., 2024), which could potentially increase the opportunity for PARP2 to bind and un-bind as well. When looking at the dynamics of PARP2 in the presence of PARP1 E988Q (Figure 3.20, d), it appears that treatment with olaparib does not only increase the total amount recruited over time, (Figure 3.19, d), but that it also greatly delays recruitment, with PARP2 only peaking towards the end of capture. Meanwhile, treatment of PARP1 E988Q with saruparib not only slightly increases total recruitment of PARP2 (Figure 2, d), it also leads to faster release of PARP2; compared to peak occupancy after 50 seconds, only 44% remain after 10 minutes, compared to 80% of PARP2 in the presence of PARP1 E988Q without saruparib (Figure 3.20, d).

Interestingly, when considering the ADP-ribosylation signal around 64 kDa in Figure 3.6, it appears that it is greatly reduced in cells expressing PARP1 catalytic mutants, but not in cells lacking PARP1 altogether. While siRNA-mediated knock-down of PARP2 would be required to unambiguously determine this band as PARP2 automodification, its identity as such is supported by the fact that a similar ADP-ribosylation signal is apparent around 64 kDa in two different PARP1 KO clones, which is lost upon knock-out of PARP2 (Appendix, Figure A.4). As described above, PARP2 recruitment was not impaired by loss of PARP1 (Figure 3.19, a), but by expression of PARP1 E988Q. It could therefore be that loss of PARP2 automodification in these conditions stems from reduced recruitment of PARP2 to sites of DNA damage, and a resulting lack of activation by binding to DNA breaks, partially due to their occupation by catalytically inactive PARP1. This difference in potential PARP2 automodification in cells which lack PARP1 and those which express catalytically impaired PARP1 would further support the notion that PARP2 recruitment to damage sites is more

regulated by competition at the damage site, than by PARP1-mediated ADP-ribosylation. Further repeats of this experiments, as well as siRNA-mediated knock-down of PARP2, would help confirm or dispute this theory.

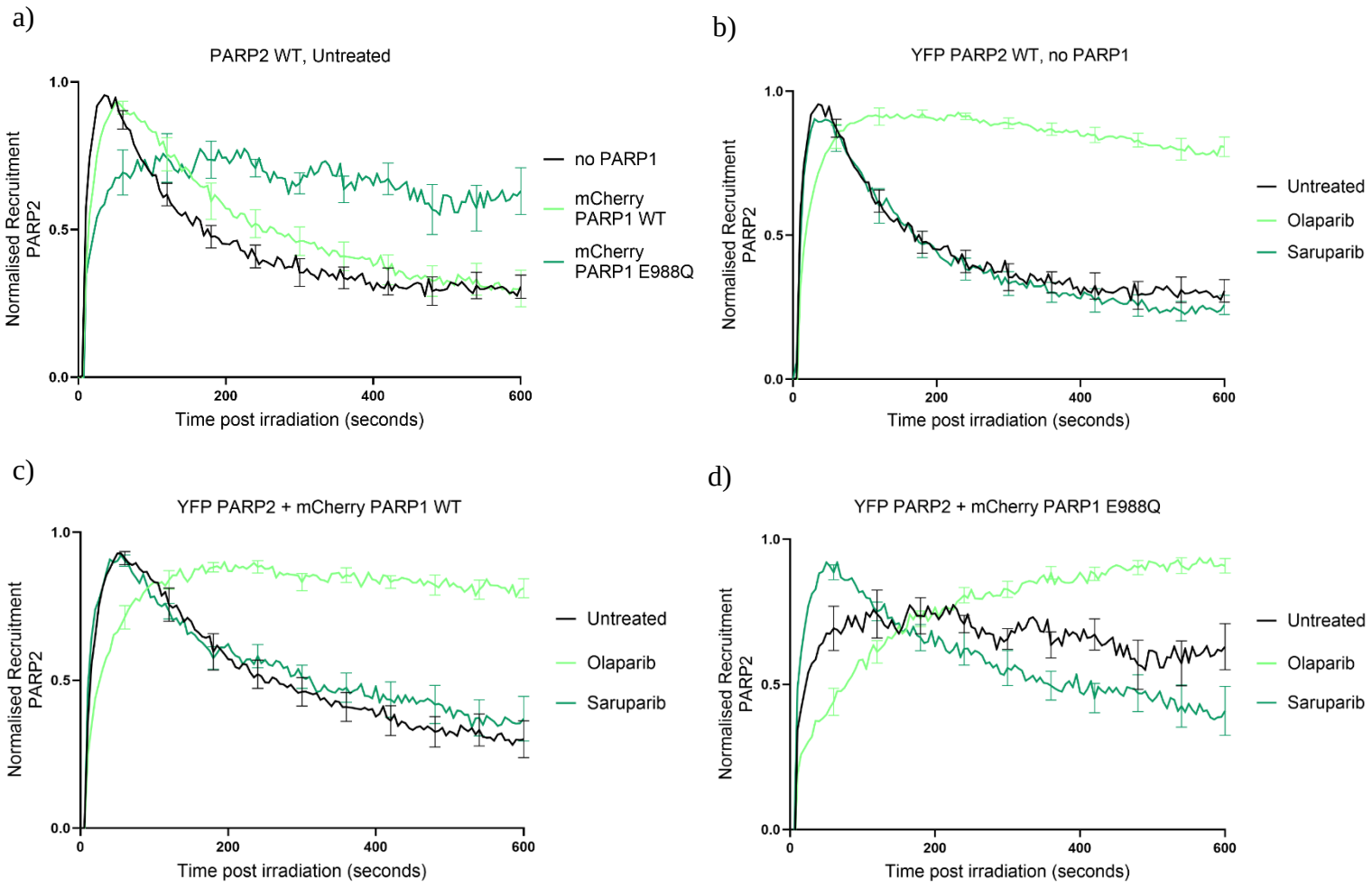

Figure 3.20: Recruitment and release dynamics of PARP2 are affected by the presence or absence of PARP1 WT or E988Q. Recruitment and release dynamic of YFP-PARP2 at the damage site over time are shown, with or without mCherry-PARP1 WT or E988Q in U2OS PARP1/PARP2 KO cells. Olaparib was used at 1 µM, and saruparib at 5 nM. Recruitment was normalised to the maximum fluorescence reached per condition. Data are shown as mean ± standard error of the mean. Data were collected from 11–15 cells per condition.

4. Discussion and Future Plans

The results presented in this work support a novel way of thinking about the type, and amount, of ADP-ribosylation produced and required in the DNA damage response, and for the efficient removal of PARP1 from sites of DNA damage. As part of this, I was able to create a complementation system that allows controlled expression of YFP-tagged PARP1, and YFP-tagged HPF1 mutants, with preserved function and with expression levels comparable to that of endogenous protein using the U2OS Flp-In T-REx cell line. This allowed me to perform structure function analyses of PARP1 mutants in these cells, without constant need for transient transfections, or the potential detrimental effect of stable expression of some mutants. Further, in this work I unexpectedly identified catalytically impaired PARP1 mutants which are released from sites of DNA damage by a novel PARP1-specific inhibitor, rather than being trapped. Finally, the findings in this work could provide an improved understanding of the interplay between PARP1 and PARP2 at the damage site.

I will discuss the implications of these findings, as well as potential future work, in this section.

4.1 The “right” amount of ADP-ribosylation

An effect of ADP-ribose chain length on cellular survival was found relatively soon after the identification of ADP-ribosylation: long-chained PAR (> 60 ADPr units) in response to severe genotoxic stress was linked to cell death, whereas shorter chains (< 16 ADPr units) were found to be well tolerated (Andrabi et al., 2006; Yu et al., 2006). Similarly, different proteins were also reported to interact with specific lengths of PAR chains, hinting at a distinct code recognised, and translated, by a plethora of ADPr readers (Fahrer et al., 2007)

The more recent discovery of HPF1 has drastically changed the understanding of PARP1/2-mediated ADP-ribosylation in the DNA damage response, and has added context to these

early findings, shifting the previous paradigm of PARylation on glutamates and aspartates to shorter chains, and MARylation, mainly on serine residues (Abplanalp et al., 2017; Juan José Bonfiglio et al., 2017; Gibbs-Seymour et al., 2016; Larsen et al., 2018; Leidecker et al., 2016; Palazzo et al., 2018). According to current knowledge, HPF1 is recruited rapidly to sites of DNA damage through the interaction with PARP1/2, where it re-directs catalytic activity of PARP1/2 towards serines by providing the necessary second catalytic glutamate, E284, while simultaneously restricting chain extension, and promoting ADP-ribosylation of histones (Gibbs-Seymour et al., 2016; Sun et al., 2021; Suskiewicz et al., 2020). Meanwhile, a balance between mono- and poly-ADP-ribosylation appears necessary: HPF1 is far less abundant in the nucleus than PARP1, its presence roughly 20-fold less than PARP1 (Juan José Bonfiglio et al., 2017), and it is thought to cycle between PARP1/2 molecules, rapidly binding and unbinding to the DNA damage activated PARPs, enabling frequent initiation on serine residues with MAR, and subsequent extension of chains in its absence (Hendriks et al., 2021; M. F. Langelier et al., 2021). Agreeing with a shift in ratio between PARP1:HPF1 towards more HPF1 at later time points after DNA damage induction (Smith et al., 2023), a recent study found that MARylation persists longer at sites of DNA damage, following an initial, rapid burst of PARylation (Longarini et al., 2023). This separation of ADP-ribosylation in response to DNA damage was therefore suggested to serve as an early emergency signal via a transient PARylation signal, and a slightly later, more sustained MAR signal, which is dependent on HPF1, and the efficient digestion of PAR chains by PARG, which could attract specific DNA repair factors and chromatin remodellers, without the cellular toxicity associated with prolonged PARylation (Fontana et al., 2017a; Longarini et al., 2023; Prokhorova, Agnew, Wondisford, Baets, et al., 2021).

The important role for HPF1 is highlighted by the sensitivity of HPF1 KO cells to treatment with PARP inhibitors (Gibbs-Seymour et al., 2016; Prokhorova, Zobel, et al., 2021), and

HPF1 was previously shown to provide resistance to PARP inhibitors by promoting PARP1 automodification (Prokhorova, Zobel, et al., 2021) and chromatin ADP-ribosylation (Zentout et al., 2024). In this work, I show that HPF1 can overcome the loss of PARP1 automodification and histone ADP-ribosylation in the presence of PARP inhibitor, without causing a spike in PARylation, but rather by promoting MARylation (Figure 3.1). Meanwhile, loss of HPF1, leads to a significant reduction in PARP1 automodification, and complete loss of histone ADP-ribosylation (Figure 3.1). This suggests that it is HPF1-dependent MARylation, and shorter chains, that play an important role in the DNA damage response, rather than PARylation alone.

The potential toxicity of excessive ADPr restriction has not been as extensively studied as excessive PARylation, however. To address this, I used U2OS Flp-In HPF1 KO cells complemented with HPF1 E284A, a catalytic mutant, which binds tightly to PARP1 (Rudolph, Roberts, Muthurajan, et al., 2021), but does not allow ADP-ribosylation of serine residues, or extension of ADP-ribose chains by PARP1/2 (Suskiewicz et al., 2020). This mutant, as expected, caused a loss of histone ADP-ribosylation, and a reduced PARylation PARP1 automodification signal (Figure 3.2, c). Further, cells expressing this mutant were highly sensitive to PARP inhibitor treatment, even more so than cells lacking HPF1 entirely (Figure 3.3). HPF1 E284A, likely as a result of its tight binding to PARP1, was also shown to be recruited to sites of DNA damage at greater levels than wild-type HPF1 (Smith et al., 2023); its prolonged presence at damage sites, where it can continuously associate with PARP1/2, would not only suppress initiation on serine residues, but also PAR elongation, both on PARP1/2 and histones. This could in turn affect PARP1/2 release from damage sites; although further studies of PARP1 behaviour at sites of DNA damage in the presence of this mutant are required to clarify how this mutant affects PARP1 recruitment and release dynamics. The use of HPF1 E284A in combination with PARP1 automodification mutants,

would further inform about the contribution of PARylation on PARP1 itself, and that of histones, to the release of PARP1 from sites of DNA damage.

The question of the ideal amount, and type, of ADP-ribosylation is very complex; I hoped to better understand the roles of mono vs poly-ADP-ribosylation particularly for the release of PARP1 from break sites by using different catalytic PARP1 mutants. This further supported the notion that MARylation, if present at high levels, is sufficient for efficient PARP1 dynamics: PARP1 H862A, a mutant which possesses strong PARylation activity, similar to PARP1 WT, but much lower MARylation activity (Figure 3.4) is more trapped at sites of damage than PARP1 WT (Figure 3.5). PARP1 M890R, which completely lacks any PARylation activity, but has stronger MARylation activity than PARP1 WT (Figure 3.4), strongly resembles the behaviour of PARP1 H862A at the damage site (Figure 3.5). The behaviour of both mutants suggests that MARylation plays an important role in allowing efficient PARP1 release from sites of DNA damage. The PARP1 M890R mutant in particular could in the future serve as an important separation of function mutant – helping to distinguish between the requirement for PARylation not only in the release of PARP1 from damage sites, but also in the recruitment of specific DNA repair factors that require PAR for their recruitment. Expression of another, less active MARylation mutant, PARP1 E988Q, was not tolerated well by cells, however; while not as toxic as complete loss of catalytic activity, it was significantly trapped at sites of DNA damage sites, and induced replication stress and DNA damage (Figure 3.9).

It thus appears that the requirements for ADP-ribosylation in the DDR are tightly regulated; neither too much, nor too little, is tolerated well by cells. Further evidence for this comes from the presence of “excess” PARP1 in the nucleus: while the presence of endogenous PARP1 significantly sped up the release of PARP1 E988Q from damage sites (Figure 3.17, b), agreeing with previous findings (Zentout et al., 2024), it led to slower release of PARP1 WT

(Figure 3.17, a). In section *3.3.9*, I already mentioned that the presence of endogenous, or excess, PARP1 could likely influence the dynamics of over-expressed PARP1 in two ways: one, by increasing the PARP1:HPF1 ratio at breaks this would promote the formation of PAR chains (Smith et al., 2023; Zentout et al., 2024), and two, by providing competition for the occupancy at the break site, and potentially affecting PARP1 exchange at the damage site (Shao et al., 2020). Total recruitment of both YFP PARP1 WT and YFP PARP1 E988Q was reduced in the presence of endogenous PARP1 (Figure 3.17, c). This points towards competition at the damage site with endogenous PARP1. However, despite the similar effects endogenous PARP1 had on the amount of YFP PARP1 WT and E988Q that was recruited, it had opposing effects on their release dynamics; YFP PARP1 E988Q was released faster, and was less trapped at the site of DNA damage at the end of capture; while YFP PARP1 WT was released more slowly, and was slightly more trapped (Figure 3.17, a, b). Importantly, Zentout et al. (2024) previously showed that the improved release of PARP1 E988K in the presence of endogenous PARP1 did not depend on increased auto-modification of PARP1 E988K through trans-ADP-ribosylation, but rather depended on histone modification by endogenous PARP1. After an initial, HPF1-independent burst of PARylation at the site of damage, the ratio of PARP1:HPF1 changes in favour of HPF1, which promotes the generation of a longer-lived MAR shield on histones (Smith et al., 2023). It was this ADPr/MAR shield that was proposed to promote the release of PARP1 E988K in the presence of endogenous PARP1 (Zentout et al., 2024), by preventing the re-association of PARP1 E988K, which otherwise engages in unproductive binding and unbinding cycles with the damaged DNA (Shao et al., 2020). If endogenous PARP1 promotes release of catalytically impaired PARP1 mutants by providing additional ADP-ribosylation of histones, it could be possible that in the presence of YFP PARP1 WT, which is catalytically active itself, there might be even further modification of histones, and with an altered PARP1:HPF1 ratio, promote the formation of PAR, which does not form the same ADPr/MAR shield on histones. Rather than forming an ADPr/MAR shield

that prevents re-association, this in turn could create a chromatin micro-environment that becomes less permissive for dynamic PARP1 movement, and PARP1 WT release from sites of damage. If this were the case; it would support the notion that “excess” ADP-ribosylation can be detrimental (Prokhorova, Agnew, et al., 2021). Further assays to detect levels of histone ADP-ribosylation, for instance by looking at the modification of histones over time in the presence of endogenous PARP1 and over-expressed wild-type or catalytically impaired PARP1 under these conditions, and the effect of this on downstream repair factors and chromatin remodelling factors could be performed in the future to expand on this.

More evidence for the requirement of tightly regulated ADP-ribosylation comes from the recruitment and release dynamics of PARP1 ΔHD. PARP1 ΔHD, a constitutively active PARP1 mutant (Dawicki-McKenna et al., 2015), despite its greater catalytic activity (Figure 3.1, b), is released from sites of DNA damage slightly faster than PARP1 WT, but ultimately resembles PARP1 WT in its retention at the break site after 10 minutes (Figure 3.16).

Taken together, these results suggest a novel paradigm on ADP-ribosylation in the DNA damage response; perhaps more than PARylation, MARylation appears to play a key role. Further, it will be important to test the effect of PARP1 mutants that differ in their catalytic activity and the types of ADP-ribose they produce, such as PARP1 M890R, or PARP1 H862A, on cells. To this end, I have constituted U2OS Flp-In PARP1 KO cells with YFP-tagged PARP1 M890R, M890A, K903A, and H862A. Initial testing of the clones for expression was successful, and they could be used to test their effect on survival, sensitivity to different PARP inhibitors, or their exchange rate at DNA damage sites, through FRAP analysis.

Better understanding of the type of ADP-ribose chains that are beneficial, or detrimental, for cellular survival, particularly in the context of simultaneous PARP inhibitor use, could be valuable for clinical application. This could additionally be useful for targeting of the main

enzymes modifying ADP-ribosylation in the DDR, HPF1, ARH3, and PARG, thereby altering, but not necessarily eliminating PARP1/2-mediated ADP-ribosylation.

4.2 The pro-release effect of saruparib on PARP1 catalytic mutants

Having had the importance of ADP-ribose chain length in PARP1 release as the initial main research objective, the result of one of my experiments led me to investigate the PARP inhibitor response of PARP1 catalytic mutants.

While expression of PARP1 E988Q, a MARylation mutant, was toxic to cells, it was not as toxic as expression of PARP1 E988Q/H862A, a completely catalytically inactive mutant (Figure 3.7). I treated these cells either with olaparib, a PARP1/2 inhibitor, or saruparib, a novel PARP1-specific inhibitor, to potentially distinguish whether PARP1-mediated MARylation is responsible for the greater survival of PARP1 E988Q expressing cells, or whether the catalytic activity of PARP2 contributes to this; either by modifying surrounding chromatin, or by extending PARP1-mediated MAR. Surprisingly, treatment of PARP1 E988Q-expressing cells significantly improved their survival; but not that of PARP1-WT-expressing cells (Figure 3.8). In agreement with saruparib significantly decreasing the expression of replication stress and DNA damage markers that was up-regulated in PARP1 E988Q-expressing cells (Figure 3.9), saruparib promotes its release from sites of DNA damage, revealing this inhibitor to have a pro-release effect on this PARP1 catalytic mutant (Figure 3.10). Of the other PARP1 catalytic mutants I tested, it is notable that the mutants with the lowest catalytic activity, PARP1 E988A, PARP1 E988Q/H862A, and PARP1 K903A, also responded to saruparib with increased release from DNA damage sites; not so, however, more catalytically active PARP1 mutants (Figure 3.12). Independent of the mechanism of how saruparib causes this release, these experiments demonstrate the toxicity of trapped PARP1: the improved survival, and decreased expression of stress signals of PARP1 E988Q-expressing cells treated with saruparib highlights the detrimental effect of

PARP1 trapping on cellular survival; the increased release of PARP1 E988Q from sites of DNA damage alone significantly improves the survival of these cells, without an accompanying increase in catalytic activity, which might further promote chromatin relaxation and recruitment of repair factors.

The literature available on PARP inhibitors and their mechanism of action has grown considerably in the past few years. Their differing PARP1 trapping ability, and thus differing cytotoxicity, has been attributed by different reports to differences in how PARP inhibitors affect PARP1-DNA-binding affinity by inducing allosteric changes in the protein (M. F. Langelier et al., 2023a; Zandarashvili et al., 2020) and in how strongly different PARP inhibitors bind PARP1 (Rudolph, Roberts, & Luger, 2021), as well as the influence of HPF1 on PARP1-inhibitor binding (Stojanovic et al., 2023). These studies were all performed *in vitro*, and their findings do not translate to trapping *in vivo*; inhibitors that were found to be "pro-release", i.e. to decrease the DNA binding affinity of PARP1, such as veliparib, niraparib and rucaparib, importantly, were classified as such in the absence of NAD^+ (Xue et al., 2022; Zandarashvili et al., 2020). In a cellular context, these inhibitors also prolong PARP1 retention at the site of DNA damage, and not in the hierarchy predicted by *in vitro* studies, but rather in the order: talazoparib >> niraparib ≈ olaparib ≈ rucaparib > veliparib (Murai et al., 2012, 2014; Pommier et al., 2016) (Figure 3.11, a). Crucially, the *in vitro* studies performed that found the allosteric effects of different inhibitors on PARP1 were all performed in the absence of HPF1 (Zandarashvili et al., 2020; Xue et al., 2022), which was previously shown to affect binding of PARP inhibitors to PARP1 (Rudolph, Roberts, & Luger, 2021). It is therefore conceivable that in a physiological setting, HPF1 contributes significantly to how effectively different PARP inhibitors inhibit PARP1, and therefore affect trapping at the site of damage. Further off-target effects of PARP inhibitors *in vivo* can also not be ruled out; PARP inhibitors differ in their magnitude of selectivity for PARP1 over

PARP2, as well as in their selectivity for PARP1/2 over other PARPs (Antolin et al., 2020; Langelier et al., 2023; Thorsell et al., 2017). For instance, talazoparib, the most potent PARP inhibitor and trapper *in vivo*, and rucaparib, are less selective for PARP1/2 than other inhibitors (Thorsell et al., 2017), with talazoparib previously shown to inhibit tankyrases 1/2, which have been implicated to play a role in DNA repair (Dregalla et al., 2010), at clinically relevant concentrations (Ryan et al., 2021). The poly-pharmacological profile of different PARP inhibitors also includes various different kinases (Antolin et al., 2020; Antolín & Mestres, 2014). Off-target effects on other proteins of different PARP inhibitors could therefore in turn affect the behaviour of PARP1 at the site of damage. Finally, the chromatin environment provides a very different surrounding for PARP1; *in vitro* studies often use linear or circular DNA constructs that contain gaps, SSBs or simulate a DSB, whereas the dynamic modifications on histones and the surrounding break site in vivo, especially by PARP1 itself and over time, can in turn affect the behaviour of PARP1, which does not operate independently in this context.

Finally, out of the two components that govern PARP inhibitor efficacy, catalytic suppression and allosteric modulation, catalytic suppression appears to be the more dominant in a physiological context, when NAD+ is present. In this context, PARP1 retention at the site of damage can therefore largely be understood as caused by the loss of ADP-ribosylation, and a resulting loss of electrostatic repulsion from DNA (Satoh & Lindahl, 1992). The study of how PARP inhibitors might affect PARP1 allostery, and thereby DNA binding affinity, *in vivo*, is therefore challenging. However, the findings of recent studies that PARP1 “trapping” is not physical stalling at the site of damage, but rather reflects a continuous cycle of association and disassociation with the break site (Juhász et al., 2020; Shao et al., 2020), might have provided a method of doing precisely that. A very recent study measured both overall retention of PARP1 at the site of DNA damage, as well as its recovery/exchange at the site of damage,

representing cycles of association and disassociation, in the presence of different inhibitors (Kanev et al., 2024). Ensuring complete catalytic inhibition at the given concentration of inhibitor, and eliminating differences in catalytic inhibition from the equation, the authors were thus able to see how different inhibitors affected the PARP1 exchange rate at the damage site. This could in turn be correlated with the overall retention of PARP1 at the DNA damage site; thereby identifying how much an inhibitor affects PARP1 turnover – or DNA binding affinity – and how much this contributes to PARP1 trapping (Kanev et al., 2024). This study found that saruparib, despite causing overall PARP1 retention due to catalytic inhibition, increased the turn-over of wild-type PARP1 at break sites.

This study is pivotal for understanding the findings of this work: it shows that suppression of catalytic activity, which is the main determinant of PARP1 removal from DNA damage sites in a cellular context, largely masks the effects inhibitors have on PARP1 allostery. However, in PARP1 mutants which already possess low (E988Q, K903A) or no (E988A, E988Q/H862A) catalytic activity; the inhibitor-driven catalytic suppression would be less significant, and the "pro-release" allosteric component of saruparib would contribute to a greater extent to the overall effect on PARP1 behaviour. The fact that veliparib as the only other inhibitor has no, or a slight pro-release effect on PARP1 E988Q (Figure 3.11, b and Appendix Figure A.2) supports this statement rather than contradict it; in the same study, veliparib was the only inhibitor shown to have no effect on the exchange rate of wild-type PARP1 (Kanev et al., 2024). The response of the other PARP1 mutants tested could further corroborate this; PARP1 M890A, which has similar catalytic activity as PARP1 WT, and behaves similarly at the site of DNA damage, is trapped in response to saruparib, while PARP1 M890R, which is a hyperactive MARylation mutant, that shows slightly prolonged retention at the damage site, shows no response to saruparib (Figure 3.12). This mutant of "intermediate" catalytic activity could therefore represent a response to saruparib governed to

almost similar amounts of catalytic suppression and reduction in DNA binding affinity, thereby cancelling each other out.

Previously, the HD domain of PARP1/2 was found to be critical for the pro-release effect of certain inhibitors via the HD-WGR-Zn allosteric link; “pro-release” inhibitors veliparib, niraparib and rucaparib stabilised the HD in the same region that was de-stabilised upon binding of NAD^+ to PARP1, while the pro-retention reverse-allosteric effect of EB-47 relies on D766/770 in the HD (Zandarashvili et al., 2020); similarly, the opposite allosteric effects some inhibitors have on PARP1 and PARP2 were shown to be due to differences in the amount of space left in the catalytic cleft between the HD and ART domains in these proteins (M. F. Langelier et al., 2023a). Interestingly, when looking at the binding mode analysis of saruparib to PARP1, saruparib establishes a contact with D766 of the αF of the helical domain (Figure 1.7), which could explain the strong allosteric effect of this inhibitor. Loss of the HD, while promoting release of PARP1 E988Q from DNA damage sites, led to a loss of the pro-release effect of saruparib, and to a loss of response to olaparib (Figure 3.16, b); while future experiments are needed to establish the catalytic activity of these mutants in response to inhibitors, this is an indication that the pro-release effect of saruparib is mediated through the HD.

Importantly, the results of this thesis also suggest that PARP1 catalytic mutants could be used in a cellular context as tools to reveal the allosteric properties of PARP inhibitors; devoid of ADP-ribosylation activity that can be suppressed, catalytic mutants could be used to test a variety of PARP inhibitors for their effect on DNA binding. In the future, it would be important to test the effects of saruparib on PARP1 allostery more directly; both by testing the PARP1 exchange rate, by performing FRAP experiments following DNA damage induction *in vivo* (Juhász et al., 2020; Kanev et al., 2024; Shao et al., 2020), as well as the DNA binding

affinity directly *in vitro*, for instance by performing fluorescence polarisation experiments (Zandarashvili et al., 2020).

Previously, the PARP1 R591C mutation was identified in an olaparib-resistant patient (Pettitt et al., 2018). This demonstrates that mutations in PARP1 can be the basis for PARP inhibitor resistance, and improved screening, in combination with better understanding of how different PARP inhibitors contact and affect the protein, might allow better, more individual, fine-tuned choices about which PARP inhibitors to use, or avoid, in a given clinical setting.

4.3 The interplay between PARP1 and PARP2

The roles of PARP1 and PARP2 are simultaneously overlapping and distinct, and while loss of PARP1 is tolerated during embryogenesis, loss of both enzymes is embryonically lethal (Ménissier de Murcia et al., 2003b). They differ in their arrival times at the site of damage, as well as their preference for break sites, and some studies have suggested that PARP1 catalytic activity might stimulate, or even be required, for PARP2 recruitment and activity in turn (Chen et al., 2018b; Lin et al., 2022; Mortusewicz et al., 2007). Given the involvement of PARP2 in erythropoiesis (Farreś et al., 2013; Farrés et al., 2015), it has been suggested that it is the inhibition of PARP2, rather than that of PARP1, underlying the haematological toxicities as common side effects of PARP inhibitors (Hatch et al., 2021; LaFargue et al., 2019). This is supported by a recent study showing that catalytically inactive PARP2 leads to erythropoietic failure during development, causing embryonic lethality (Lin et al., 2024).

This led to the development of saruparib, with over 500-fold greater selectivity for PARP1 over PARP2 (Johannes et al., 2021; Illuzzi et al., 2022), which was shown to have lower incidence of haematological adverse events compared to traditional PARP1/2 inhibitors (Yap et al., 2022). With reports of PARP2 depending on PARP1 for its recruitment and catalytic activity, it is nevertheless important to understand how PARP1 inhibition alone affects the recruitment and release dynamics of PARP2.

Therefore, one potential caveat of my initial test to distinguish between PARP1- and PARP2-mediated ADP-ribosylation using saruparib is that despite not directly targeting the catalytic activity of PARP2, loss of catalytic inhibition of PARP1 could itself impact the function of PARP2.

One, by removing ADP-ribosylation (or specifically, PARP1-E988Q-mediated MARylation) that could be extended by PARP2, or two, by affecting PARP2 recruitment/activity. The use of the MARylation mutant PARP1 E988Q, and the PARP1-specific inhibitor, separately and in combination, therefore served two key purposes; First, to study how recruitment and release dynamics of PARP2 are affected in the presence of MARylation, but the absence of PARP1-directed PARylation, which was previously reported to stimulate PARP2 activity (Chen et al., 2018). Secondly, to inform how PARP1 dynamics, or occupancy, at the site of DNA damage, independent of PARP1 catalytic activity, affect PARP2 recruitment.

The presence of YFP-PARP2 consistently, but to varying degrees, promoted the release of both PARP1 WT and PARP1 E988Q from the damage site in all conditions except for olaparib-treated PARP1 E988Q-expressing cells; this could be a result of PARP2-mediated histone ADP-ribosylation, and support the previous report of chromatin ADP-ribosylation contributing to PARP1 release from DNA damage sites (Zentout et al., 2024) (*section 3.3.9*). The fact that this pro-release effect of PARP2 presence on PARP1 WT release persists despite the presence of olaparib, however, would contradict this, but potentially reflects insufficient catalytic inhibition of both over-expressed enzymes at the concentration used; using a higher concentration of olaparib in a future experiment could resolve this question. Interestingly, the total amount of PARP2 recruited to DNA damage sites was overall lower in the presence of PARP1 E988Q compared to PARP1 WT or no PARP1. Moreover, treatment of PARP1 E988Q with saruparib, also slightly increased the total amount of PARP2 recruited, and promoted its release, despite PARP2 not being targeted by saruparib in the absence of PARP1

(Figure 3.19, b, 3.20, b). This in particular points towards PARP2 recruitment and retention at DNA damage sites being more regulated by occupancy, and its competition with PARP1, than its reliance on PARP1 catalytic activity, since PARP1 E988Q is released from DNA damage sites without a concurrent increase in its catalytic activity (Figure 3.14).

Future experiments will be needed to support these findings; it will be important to compare total and normalised PARP2 recruitment dynamics not only between PARP1 KO cells and PARP1-WT over-expressing cells, but also in the presence of endogenous PARP1. Additionally, the use of PARP2 E545A, a catalytically inactive mutant, would be very informative about whether PARP2 indeed contributes to PARP1 release through its catalytic activity, either by extending PARP1-generated ADP-ribosylation and/or by modifying surrounding chromatin. The latter was previously shown to speed up the release of PARP1, independent of its catalytic activity (Zentout et al., 2024), and further tests, including ADP-ribosylation assays in PARP1/2 KOs, as well as knock-down of PARP2, could inform about the contributory role of PARP2. Further, the use of completely catalytically inactive PARP1 mutants, such as PARP1 E988A or PARP1 E988Q/H862A, would be useful to establish the effect of complete catalytic loss of PARP1 on PARP2 recruitment. In turn, observing these mutants, which are eventually released from the DNA damage site (Figure 3.13, d) in the presence and absence of catalytically active, or inactive, PARP2, could help distinguish the contribution of PARP2 to the release of PARP1 through its modification of histones, or PARP1 itself.

4.4 Conclusion

The findings of this study bring into light the intricacies of ADP-ribosylation in the DNA damage response and the dynamics of PARP1/2 dynamics at the site of damage, and reveal a counter-intuitive effect of a novel PARP inhibitor on catalytic PARP1 mutants. They provide the basis for many potential future experiments investigating the effect of ADP-ribose chain

length on the recruitment of downstream repair and chromatin remodelling factors, PARP inhibitor response, and cellular survival; they also provide further evidence for the mechanistic action of PARP inhibitors, and may help improve the clinical use of these drugs.

Bibliography

Abed, M., Muñoz, D., Seshadri, V., Federowicz, S., Rao, A. A., Bhupathi, D., Liimatta, M., Ousterhout, R., Jaipuri, F., Neilan, C., Lackner, M., White, M., & Mounir, Z. (2023). Abstract 6093: IDE161, a potential first-in-class clinical candidate PARG inhibitor, selectively targets homologous-recombination-deficient and PARP inhibitor resistant breast and ovarian tumors. *Cancer Research*, *83*(7_Supplement), 6093–6093. https://doi.org/10.1158/1538-7445.AM2023-6093

Aberle, L., Krüger, A., Reber, J. M., Lippmann, M., Hufnagel, M., Schmalz, M., Trussina, I. R. E. A., Schlesiger, S., Zubel, T., Schütz, K., Marx, A., Hartwig, A., Ferrando-May, E., Bürkle, A., & Mangerich, A. (2020). PARP1 catalytic variants reveal branching and chain length-specific functions of poly(ADP-ribose) in cellular physiology and stress response. *Nucleic Acids Research*, *48*(18), 10015–10033. https://doi.org/10.1093/nar/gkaa590

Abplanalp, J., Leutert, M., Frugier, E., Nowak, K., Feurer, R., Kato, J., Kistemaker, H. V. A., Filippov, D. V., Moss, J., Caflisch, A., & Hottiger, M. O. (2017). Proteomic analyses identify ARH3 as a serine mono-ADP-ribosylhydrolase. *Nature Communications*, *8*(1). https://doi.org/10.1038/s41467-017-02253-1

Ahel, D., Hořejší, Z., Wiechens, N., Polo, S. E., Garcia-Wilson, E., Ahel, I., Flynn, H., Skehel, M., West, S. C., Jackson, S. P., Owen-Hughes, T., & Boulton, S. J. (2009). Poly(ADP-ribose)-dependent regulation of DNA repair by the chromatin remodeling enzyme ALC1. *Science (New York, N.Y.)*, *325*(5945), 1240–1243. https://doi.org/10.1126/SCIENCE.1177321

Ahel, I., Ahel, D., Matsusaka, T., Clark, A. J., Pines, J., Boulton, S. J., & West, S. C. (2008). Poly(ADP-ribose)-binding zinc finger motifs in DNA repair/checkpoint proteins. *Nature*,

451(7174), 81–85. https://doi.org/10.1038/nature06420

Alemasova, E. E., & Lavrik, O. I. (2019). Poly(ADP-ribosyl)ation by PARP1: reaction mechanism and regulatory proteins. *Nucleic Acids Research*, *47*(8), 3811. https://doi.org/10.1093/NAR/GKZ120

Ali, A. A. E., Timinszky, G., Arribas-Bosacoma, R., Kozlowski, M., Hassa, P. O., Hassler, M., Ladurner, A. G., Pearl, L. H., & Oliver, A. W. (2012). The zinc-finger domains of PARP1 cooperate to recognize DNA strand breaks. *Nature Structural & Molecular Biology*, *19*(7), 685–692. https://doi.org/10.1038/NSMB.2335

Alvarez-Gonzalez, R., & Jacobson, M. K. (1987). Characterization of Polymers of Adenosine Diphosphate Ribose Generated in Vitro and in Vivo1". *Biochemistry*, *26*, 3218–3224. https://pubs.acs.org/sharingguidelines

Amé, J. C., Rolli, V., Schreiber, V., Niedergang, C., Apiou, F., Decker, P., Muller, S., Höger, T., Ménissier-de Murcia, J., & De Murcia, G. (1999). PARP-2, a novel mammalian DNA damage-dependent poly(ADP-ribose) polymerase. *Journal of Biological Chemistry*, *274*(25), 17860–17868. https://doi.org/10.1074/jbc.274.25.17860

Andrabi, S. A., No, S. K., Yu, S. W., Wang, H., Koh, D. W., Sasaki, M., Klaus, J. A., Otsuka, T., Zhang, Z., Koehler, R. C., Hurn, P. D., Poirier, G. G., Dawson, V. L., & Dawson, T. M. (2006). Poly(ADP-ribose) (PAR) polymer is a death signal. *Proceedings of the National Academy of Sciences of the United States of America*, *103*(48), 18308–18313. https://doi.org/10.1073/PNAS.0606526103

Antolin, A. A., Ameratunga, M., Banerji, U., Clarke, P. A., Workman, P., & Al-Lazikani, B. (2020). The kinase polypharmacology landscape of clinical PARP inhibitors. *Scientific Reports 2020 10:1*, *10*(1), 1–14. https://doi.org/10.1038/s41598-020-59074-4

Antolín, A. A., & Mestres, J. (2014). Linking off-target kinase pharmacology to the

differential cellular effects observed among PARP inhibitors. *Oncotarget*, *5*(10), 3023–3028. https://doi.org/10.18632/ONCOTARGET.1814

Ashley, A. K., Shrivastav, M., Nie, J., Amerin, C., Troksa, K., Glanzer, J. G., Liu, S., Opiyo, S. O., Dimitrova, D. D., Le, P., Sishc, B., Bailey, S. M., Oakley, G. G., & Nickoloff, J. A. (2014). DNA-PK Phosphorylation of RPA32 Ser4/Ser8 Regulates Replication Stress Checkpoint Activation, Fork Restart, Homologous Recombination and Mitotic Catastrophe. *DNA Repair*, *21*, 131. https://doi.org/10.1016/J.DNAREP.2014.04.008

Barkauskaite, E., Brassington, A., Tan, E. S., Warwicker, J., Dunstan, M. S., Banos, B., Lafite, P., Ahel, M., Mitchison, T. J., Ahel, I., & Leys, D. (2013). Visualization of poly(ADP-ribose) bound to PARG reveals inherent balance between exo- and endo-glycohydrolase activities. *Nature Communications*, *4*. https://doi.org/10.1038/ncomms3164

Barkauskaite, E., Jankevicius, G., & Ahel, I. (2015). Structures and Mechanisms of Enzymes Employed in the Synthesis and Degradation of PARP-Dependent Protein ADP-Ribosylation. In *Molecular Cell* (Vol. 58, Issue 6, pp. 935–946). Cell Press. https://doi.org/10.1016/j.molcel.2015.05.007

Bartlett, E., Bonfiglio, J. J., Prokhorova, E., Colby, T., Zobel, F., Ahel, I., & Matic, I. (2018). Interplay of Histone Marks with Serine ADP-Ribosylation. *Cell Reports*, *24*(13), 3488-3502.e5. https://doi.org/10.1016/j.celrep.2018.08.092

Beck, C., Boehler, C., Guirouilh Barbat, J., Bonnet, M. E., Illuzzi, G., Ronde, P., Gauthier, L. R., Magroun, N., Rajendran, A., Lopez, B. S., Scully, R., Boussin, F. D., Schreiber, V., & Dantzer, F. (2014). PARP3 affects the relative contribution of homologous recombination and nonhomologous end-joining pathways. *Nucleic Acids Research*, *42*(9), 5616. https://doi.org/10.1093/NAR/GKU174

Beijer, D., Agnew, T., Rack, J. G. M., Prokhorova, E., Deconinck, T., Ceulemans, B., Peric, S., Rasic, V. M., Jonghe, P. De, Ahel, I., & Baets, J. (2021). Biallelic ADPRHL2 mutations in complex neuropathy affect ADP ribosylation and DNA damage response. *Life Science Alliance*, *4*(11). https://doi.org/10.26508/LSA.202101057

Belousova, E. A., Ishchenko, A. A., & Lavrik, O. I. (2018). Dna is a New Target of Parp3. *Scientific Reports 2018 8:1*, *8*(1), 1–12. https://doi.org/10.1038/s41598-018-22673-3

Bilokapic, S., Suskiewicz, M. J., Ahel, I., & Halic, M. (2020). Bridging of DNA breaks activates PARP2–HPF1 to modify chromatin. *Nature*, *585*(7826), 609–613. https://doi.org/10.1038/s41586-020-2725-7

Bonfiglio, Juan J., Colby, T., & Matic, I. (2017). Mass spectrometry for serine ADP-ribosylation? Think o-glycosylation! *Nucleic Acids Research*, *45*(11), 6259–6264. https://doi.org/10.1093/NAR/GKX446

Bonfiglio, Juan José, Fontana, P., Zhang, Q., Colby, T., Gibbs-Seymour, I., Atanassov, I., Bartlett, E., Zaja, R., Ahel, I., & Matic, I. (2017a). Serine ADP-Ribosylation Depends on HPF1. *Molecular Cell*, *65*(5), 932-940.e6. https://doi.org/10.1016/j.molcel.2017.01.003

Bonfiglio, Juan José, Fontana, P., Zhang, Q., Colby, T., Gibbs-Seymour, I., Atanassov, I., Bartlett, E., Zaja, R., Ahel, I., & Matic, I. (2017b). Serine ADP-Ribosylation Depends on HPF1. *Molecular Cell*, *65*(5), 932-940.e6. https://doi.org/10.1016/j.molcel.2017.01.003

Boussios, S., Karihtala, P., Moschetta, M., Abson, C., Karathanasi, A., Zakynthinakis-Kyriakou, N., Ryan, J. E., Sheriff, M., Rassy, E., & Pavlidis, N. (2020). Veliparib in ovarian cancer: a new synthetically lethal therapeutic approach. *Investigational New Drugs*, *38*(1), 181–193. https://doi.org/10.1007/S10637-019-00867-4/TABLES/4

Bouwman, P., Aly, A., Escandell, J. M., Pieterse, M., Bartkova, J., Van Der Gulden, H., Hiddingh, S., Thanasoula, M., Kulkarni, A., Yang, Q., Haffty, B. G., Tommiska, J.,

Blomqvist, C., Drapkin, R., Adams, D. J., Nevanlinna, H., Bartek, J., Tarsounas, M., Ganesan, S., & Jonkers, J. (2010). 53BP1 loss rescues BRCA1 deficiency and is associated with triple-negative and BRCA-mutated breast cancers. *Nature Structural & Molecular Biology*, *17*(6), 688–695. https://doi.org/10.1038/NSMB.1831

Bryant, H. E., Petermann, E., Schultz, N., Jemth, A. S., Loseva, O., Issaeva, N., Johansson, F., Fernandez, S., McGlynn, P., & Helleday, T. (2009). PARP is activated at stalled forks to mediate Mre11-dependent replication restart and recombination. *The EMBO Journal*, *28*(17), 2601. https://doi.org/10.1038/EMBOJ.2009.206

Bryant, H. E., Schultz, N., Thomas, H. D., Parker, K. M., Flower, D., Lopez, E., Kyle, S., Meuth, M., Curtin, N. J., & Helleday, T. (2005a). Specific killing of BRCA2-deficient tumours with inhibitors of poly(ADP-ribose) polymerase.[erratum appears in Nature. 2007 May 17;447(7142):346]. *Nature*, *434*(7035), 913–917.

Bryant, H. E., Schultz, N., Thomas, H. D., Parker, K. M., Flower, D., Lopez, E., Kyle, S., Meuth, M., Curtin, N. J., & Helleday, T. (2005b). Specific killing of BRCA2-deficient tumours with inhibitors of poly(ADP-ribose) polymerase. *Nature*, *434*(7035), 913–917. https://doi.org/10.1038/NATURE03443

Caldecott, K. W. (2019). XRCC1 protein; Form and function. *DNA Repair*, *81*. https://doi.org/10.1016/J.DNAREP.2019.102664

Carter-O'Connell, I., Jin, H., Morgan, R. K., David, L. L., & Cohen, M. S. (2014). Engineering the Substrate Specificity of ADP-Ribosyltransferases for Identifying Direct Protein Targets. *Journal of the American Chemical Society*, *136*(14), 5201. https://doi.org/10.1021/JA412897A

Chambon, P., Weill, J. D., Doly, J., Strosser, M. T., & Mandel, P. (1966). On the formation of a novel adenylic compound by enzymatic extracts of liver nuclei. *Biochemical and*

Biophysical Research Communications, *25*(6), 638–643. https://doi.org/10.1016/0006-291X(66)90502-X

Chambon, P., Weill, J. D., & Mandel, P. (1963). Nicotinamide mononucleotide activation of a new DNA-dependent polyadenylic acid synthesizing nuclear enzyme. *Biochemical and Biophysical Research Communications*, *11*(1), 39–43. https://doi.org/10.1016/0006-291X(63)90024-X

Chaudhuri, A. R., Callen, E., Ding, X., Gogola, E., Duarte, A. A., Lee, J. E., Wong, N., Lafarga, V., Calvo, J. A., Panzarino, N. J., John, S., Day, A., Crespo, A. V., Shen, B., Starnes, L. M., De Ruiter, J. R., Daniel, J. A., Konstantinopoulos, P. A., Cortez, D., … Nussenzweig, A. (2016). Replication fork stability confers chemoresistance in BRCA-deficient cells. *Nature*, *535*(7612), 382–387. https://doi.org/10.1038/NATURE18325

Chen, Q., Kassab, M. A., Dantzer, F., & Yu, X. (2018a). PARP2 mediates branched poly ADP-ribosylation in response to DNA damage. *Nature Communications 2018 9:1*, *9*(1), 1–13. https://doi.org/10.1038/s41467-018-05588-5

Chen, Q., Kassab, M. A., Dantzer, F., & Yu, X. (2018b). PARP2 mediates branched poly ADP-ribosylation in response to DNA damage. *Nature Communications*, *9*(1), 1–13. https://doi.org/10.1038/s41467-018-05588-5

Cleaver, J. E., Lam, E. T., & Revet, I. (2009). Disorders of nucleotide excision repair: the genetic and molecular basis of heterogeneity. *Nature Reviews. Genetics*, *10*(11), 756–768. https://doi.org/10.1038/NRG2663

Cohen, M. S., & Chang, P. (2018). Insights into the biogenesis, function, and regulation of ADP-ribosylation. In *Nature Chemical Biology* (Vol. 14, Issue 3, pp. 236–243). Nature Publishing Group. https://doi.org/10.1038/nchembio.2568

Coleman, R. L., Fleming, G. F., Brady, M. F., Swisher, E. M., Steffensen, K. D., Friedlander,

M., Okamoto, A., Moore, K. N., Efrat Ben-Baruch, N., Werner, T. L., Cloven, N. G., Oaknin, A., DiSilvestro, P. A., Morgan, M. A., Nam, J.-H., Leath, C. A., Nicum, S., Hagemann, A. R., Littell, R. D., … Bookman, M. A. (2019). Veliparib with First-Line Chemotherapy and as Maintenance Therapy in Ovarian Cancer. *New England Journal of Medicine*, *381*(25), 2403–2415. https://doi.org/10.1056/NEJMOA1909707/SUPPL_FILE/NEJMOA1909707_DATA-SHARING.PDF

Cong, K., Peng, M., Kousholt, A. N., Lee, W. T. C., Lee, S., Nayak, S., Krais, J., VanderVere-Carozza, P. S., Pawelczak, K. S., Calvo, J., Panzarino, N. J., Turchi, J. J., Johnson, N., Jonkers, J., Rothenberg, E., & Cantor, S. B. (2021). Replication gaps are a key determinant of PARP inhibitor synthetic lethality with BRCA deficiency. *Molecular Cell*, *81*(15), 3128-3144.e7. https://doi.org/10.1016/J.MOLCEL.2021.06.011

Cortes, U., Tong, W.-M., Coyle, D. L., Meyer-Ficca, M. L., Meyer, R. G., Petrilli, V., Herceg, Z., Jacobson, E. L., Jacobson, M. K., & Wang, Z.-Q. (2004). Depletion of the 110-Kilodalton Isoform of Poly(ADP-Ribose) Glycohydrolase Increases Sensitivity to Genotoxic and Endotoxic Stress in Mice. *Molecular and Cellular Biology*, *24*(16), 7163. https://doi.org/10.1128/MCB.24.16.7163-7178.2004

Crawford, K., Oliver, P. L., Agnew, T., Hunn, B. H. M., & Ahel, I. (2021). Behavioural Characterisation of Macrod1 and Macrod2 Knockout Mice. *Cells*, *10*(2), 368. https://doi.org/10.3390/cells10020368

D'amours, D., Desnoyers, S., Silva, D. ', & Poirier, G. G. (1999). Poly(ADP-ribosyl)ation reactions in the regulation of nuclear functions. In *Biochem. J* (Vol. 342).

Daei Sorkhabi, A., Fazlollahi, A., Sarkesh, A., Aletaha, R., Feizi, H., Mousavi, S. E., Nejadghaderi, S. A., Sullman, M. J. M., Kolahi, A. A., & Safiri, S. (2023). Efficacy and

safety of veliparib plus chemotherapy for the treatment of lung cancer: A systematic review of clinical trials. *PLOS ONE*, *18*(9), e0291044. https://doi.org/10.1371/JOURNAL.PONE.0291044

Danhauser, K., Alhaddad, B., Makowski, C., Piekutowska-Abramczuk, D., Syrbe, S., Gomez-Ospina, N., Manning, M. A., Kostera-Pruszczyk, A., Krahn-Peper, C., Berutti, R., Kovács-Nagy, R., Gusic, M., Graf, E., Laugwitz, L., Röblitz, M., Wroblewski, A., Hartmann, H., Das, A. M., Bültmann, E., … Haack, T. B. (2018). Bi-allelic ADPRHL2 Mutations Cause Neurodegeneration with Developmental Delay, Ataxia, and Axonal Neuropathy. *American Journal of Human Genetics*, *103*(5), 817–825. https://doi.org/10.1016/j.ajhg.2018.10.005

Daniels, C. M., Ong, S. E., & Leung, A. K. L. (2015). The Promise of Proteomics for the Study of ADP-Ribosylation. *Molecular Cell*, *58*(6), 911. https://doi.org/10.1016/J.MOLCEL.2015.06.012

DaRosa, P. A., Wang, Z., Jiang, X., Pruneda, J. N., Cong, F., Klevit, R. E., & Xu, W. (2015). Allosteric activation of the RNF146 ubiquitin ligase by a poly(ADP-ribosyl)ation signal. *Nature*, *517*(7533), 223–226. https://doi.org/10.1038/NATURE13826

Dawicki-McKenna, J. M., Langelier, M. F., DeNizio, J. E., Riccio, A. A., Cao, C. D., Karch, K. R., McCauley, M., Steffen, J. D., Black, B. E., & Pascal, J. M. (2015). PARP-1 Activation Requires Local Unfolding of an Autoinhibitory Domain. *Molecular Cell*, *60*(5), 755–768. https://doi.org/10.1016/j.molcel.2015.10.013

Dias, M. P., Moser, S. C., Ganesan, S., & Jonkers, J. (2021). Understanding and overcoming resistance to PARP inhibitors in cancer therapy. *Nature Reviews Clinical Oncology 2021 18:12*, *18*(12), 773–791. https://doi.org/10.1038/s41571-021-00532-x

Domchek, S. M. (2017). Reversion Mutations with Clinical Use of PARP Inhibitors: Many

Genes, Many Versions. *Cancer Discovery*, *7*(9), 937–939. https://doi.org/10.1158/2159-8290.CD-17-0734

Dregalla, R. C., Zhou, J., Idate, R. R., Battaglia, C. L. R., Liber, H. L., & Bailey, S. M. (2010). Regulatory roles of tankyrase 1 at telomeres and in DNA repair: suppression of T-SCE and stabilization of DNA-PKcs. *Aging*, *2*(10), 691–708. https://doi.org/10.18632/AGING.100210

Dukić, N., Strømland, Ø., Elsborg, J. D., Munnur, D., Zhu, K., Schuller, M., Chatrin, C., Kar, P., Duma, L., Suyari, O., Rack, J. G. M., Baretić, D., Crudgington, D. R. K., Groslambert, J., Fowler, G., Wijngaarden, S., Prokhorova, E., Rehwinkel, J., Schüler, H., … Ahel, I. (2023). PARP14 is a PARP with both ADP-ribosyl transferase and hydrolase activities. *Science Advances*, *9*(37). https://doi.org/10.1126/SCIADV.ADI2687/SUPPL_FILE/SCIADV.ADI2687_DATA_S1_TO_S3.ZIP

Durkacz, B. W., Omidiji, O., Gray, D. A., & Shall, S. (1980). (AD P-ribose) n participates in DNA excision repair. *Nature*, *283*(February), 593–596.

Edwards, S. L., Brough, R., Lord, C. J., Natrajan, R., Vatcheva, R., Levine, D. A., Boyd, J., Reis-Filho, J. S., & Ashworth, A. (2008). Resistance to therapy caused by intragenic deletion in BRCA2. *Nature*, *451*(7182), 1111–1115. https://doi.org/10.1038/NATURE06548

Eliasson, M. J. L., Sampei, K., Mandir, A. S., Hurn, P. D., Traystman, R. J., Bao, J., Pieper, A., Wang, Z. Q., Dawson, T. M., Snyder, S. H., & Dawson, V. L. (1997). Poly(ADP-ribose) polymerase gene disruption renders mice resistant to cerebral ischemia. *Nature Medicine 1997 3:10*, *3*(10), 1089–1095. https://doi.org/10.1038/nm1097-1089

Ettl, J., Hurvitz, S. A., Rugo, H. S., Lee, K.-H., Mina, L. A., Woodward, N. E., Yerushalmi,

R., Diab, S., Martin, M., Tudor, I. C., Czibere, A. G., Gauthier, E. R., Litton, J. K., & Goncalves, A. (2019). Outcomes of talazoparib (TALA) versus physician's choice of chemotherapy (PCT) in patients (pts) with advanced breast cancer (ABC) and a germline BRCA (gBRCA) mutation by line of chemotherapy (CT) in the EMBRACA trial. *Https://Doi.Org/10.1200/JCO.2019.37.15_suppl.1071*, *37*(15_suppl), 1071–1071. https://doi.org/10.1200/JCO.2019.37.15_SUPPL.1071

Eustermann, S., Videler, H., Yang, J. C., Cole, P. T., Gruszka, D., Veprintsev, D., & Neuhaus, D. (2011). The DNA-Binding Domain of Human PARP-1 Interacts with DNA Single-Strand Breaks as a Monomer through Its Second Zinc Finger. *Journal of Molecular Biology*, *407*(1–4), 149. https://doi.org/10.1016/J.JMB.2011.01.034

Eustermann, S., Wu, W.-F., Langelier, M.-F., Yang, J.-C., Easton, L. E., Riccio, A. A., Pascal, J. M., & Neuhaus, D. (2015). Structural Basis of Detection and Signaling of DNA Single-Strand Breaks by Human PARP-1. *Molecular Cell*, *60*(5), 742. https://doi.org/10.1016/J.MOLCEL.2015.10.032

Fahrer, J., Kranaster, R., Altmeyer, M., Marx, A., & Bürkle, A. (2007). Quantitative analysis of the binding affinity of poly(ADP-ribose) to specific binding proteins as a function of chain length. *Nucleic Acids Research*, *35*(21), e143–e143. https://doi.org/10.1093/NAR/GKM944

Farmer, H., McCabe, H., Lord, C. J., Tutt, A. H. J., Johnson, D. A., Richardson, T. B., Santarosa, M., Dillon, K. J., Hickson, I., Knights, C., Martin, N. M. B., Jackson, S. P., Smith, G. C. M., & Ashworth, A. (2005). Targeting the DNA repair defect in BRCA mutant cells as a therapeutic strategy. *Nature*, *434*(7035), 917–921. https://doi.org/10.1038/NATURE03445

Farrés, J., Llacuna, L., Martin-Caballero, J., Martínez, C., Lozano, J. J., Ampurdanés, C.,

López-Contreras, A. J., Florensa, L., Navarro, J., Ottina, E., Dantzer, F., Schreiber, V., Villunger, A., Fernández-Capetillo, O., & Yélamos, J. (2015). PARP-2 sustains erythropoiesis in mice by limiting replicative stress in erythroid progenitors. *Cell Death and Differentiation*, *22*(7), 1144. https://doi.org/10.1038/CDD.2014.202

Farreś, J., Martín-Caballero, J., Martínez, C., Lozano, J. J., Llacuna, L., Ampurdanés, C., Ruiz-Herguido, C., Dantzer, F., Schreiber, V., Villunger, A., Bigas, A., & Yélamos, J. (2013). Parp-2 is required to maintain hematopoiesis following sublethal γ-irradiation in mice. *Blood*, *122*(1), 44. https://doi.org/10.1182/BLOOD-2012-12-472845

Fei, J., Kaczmarek, N., Luch, A., Glas, A., Carell, T., & Naegeli, H. (2011). Regulation of nucleotide excision repair by UV-DDB: prioritization of damage recognition to internucleosomal DNA. *PLoS Biology*, *9*(10). https://doi.org/10.1371/JOURNAL.PBIO.1001183

Feijs, K. L. H., Cooper, C. D. O., & Žaja, R. (2020). The Controversial Roles of ADP-Ribosyl Hydrolases MACROD1, MACROD2 and TARG1 in Carcinogenesis. *Cancers*, *12*(3). https://doi.org/10.3390/CANCERS12030604

Ferraris, D. V. (2010). Evolution of poly(ADP-ribose) polymerase-1 (PARP-1) inhibitors. from concept to clinic. *Journal of Medicinal Chemistry*, *53*(12), 4561–4584. https://doi.org/10.1021/JM100012M/ASSET/JM100012M.FP.PNG_V03

Fontana, P., Bonfiglio, J. J., Palazzo, L., Bartlett, E., Matic, I., & Ahel, I. (2017a). Serine ADP-ribosylation reversal by the hydrolase ARH3. *ELife*, *6*. https://doi.org/10.7554/eLife.28533

Fontana, P., Bonfiglio, J. J., Palazzo, L., Bartlett, E., Matic, I., & Ahel, I. (2017b). Serine ADP-ribosylation reversal by the hydrolase ARH3. *ELife*, *6*. https://doi.org/10.7554/eLife.28533

Fontana, P., Buch-Larsen, S. C., Suyari, O., Smith, R., Suskiewicz, M. J., Schützenhofer, K., Ariza, A., Rack, J. G. M., Nielsen, M. L., & Ahel, I. (2023). Serine ADP-ribosylation in Drosophila provides insights into the evolution of reversible ADP-ribosylation signalling. *Nature Communications*, *14*(1). https://doi.org/10.1038/s41467-023-38793-y

Fouquin, A., Guirouilh-Barbat, J., Lopez, B., Hall, J., Amor-Guéret, M., & Pennaneach, V. (2017). PARP2 controls double-strand break repair pathway choice by limiting 53BP1 accumulation at DNA damage sites and promoting end-resection. *Nucleic Acids Research*, *45*(21), 12325–12339. https://doi.org/10.1093/NAR/GKX881

Galindo-Campos, M. A., Lutfi, N., Bonnin, S., Martínez, C., Velasco-Hernandez, T., García-Hernández, V., Martín-Caballero, J., Ampurdanés, C., Gimeno, R., Colomo, L., Roué, G., Guilbaud, G., Dantzer, F., Navarro, P., Murga, M., Fernández-Capetillo, O., Bigas, A., Menéndez, P., Sale, J. E., & Yélamos, J. (2022). Distinct roles for PARP-1 and PARP-2 in c-Myc-driven B-cell lymphoma in mice. *Blood*, *139*(2), 228–239. https://doi.org/10.1182/BLOOD.2021012805

Gatti, M., Imhof, R., Huang, Q., Baudis, M., & Altmeyer, M. (2020). The Ubiquitin Ligase TRIP12 Limits PARP1 Trapping and Constrains PARP Inhibitor Efficiency. *Cell Reports*, *32*(5). https://doi.org/10.1016/J.CELREP.2020.107985

Ghosh, S. G., Becker, K., Huang, H., Dixon-Salazar, T., Chai, G., Salpietro, V., Al-Gazali, L., Waisfisz, Q., Wang, H., Vaux, K. K., Stanley, V., Manole, A., Akpulat, U., Weiss, M. M., Efthymiou, S., Hanna, M. G., Minetti, C., Striano, P., Pisciotta, L., … Gleeson, J. G. (2018). Biallelic Mutations in ADPRHL2, Encoding ADP-Ribosylhydrolase 3, Lead to a Degenerative Pediatric Stress-Induced Epileptic Ataxia Syndrome. *American Journal of Human Genetics*, *103*(3), 431–439. https://doi.org/10.1016/j.ajhg.2018.07.010

Gibbs-Seymour, I., Fontana, P., Rack, J. G. M., & Ahel, I. (2016). HPF1/C4orf27 Is a PARP-

1-Interacting Protein that Regulates PARP-1 ADP-Ribosylation Activity. *Molecular Cell*, *62*(3), 432–442. https://doi.org/10.1016/j.molcel.2016.03.008

Gibson, B. A., Zhang, Y., Jiang, H., Hussey, K. M., Shrimp, J. H., Lin, H., Schwede, F., Yu, Y., & Kraus, W. L. (2016). Chemical genetic discovery of PARP targets reveals a role for PARP-1 in transcription elongation. *Science*, *353*(6294), 45–50. https://doi.org/10.1126/SCIENCE.AAF7865

Gogola, E., Duarte, A. A., de Ruiter, J. R., Wiegant, W. W., Schmid, J. A., de Bruijn, R., James, D. I., Guerrero Llobet, S., Vis, D. J., Annunziato, S., van den Broek, B., Barazas, M., Kersbergen, A., van de Ven, M., Tarsounas, M., Ogilvie, D. J., van Vugt, M., Wessels, L. F. A., Bartkova, J., … Rottenberg, S. (2018). Selective Loss of PARG Restores PARylation and Counteracts PARP Inhibitor-Mediated Synthetic Lethality. *Cancer Cell*, *33*(6), 1078-1093.e12. https://doi.org/10.1016/j.ccell.2018.05.008

Griffin, R. J., Curtin, N. J., Newell, D. R., Golding, B. T., Durkacz, B. W., & Calvert, A. H. (1995). The role of inhibitors of poly(ADP-ribose) polymerase as resistance-modifying agents in cancer therapy. *Biochimie*, *77*(6), 408–422. https://doi.org/10.1016/0300-9084(96)88154-5

Groslambert, J., Prokhorova, E., & Ahel, I. (2021). ADP-ribosylation of DNA and RNA. *DNA Repair*, *105*, 103144. https://doi.org/10.1016/J.DNAREP.2021.103144

Groslambert, J., Prokhorova, E., Wondisford, A. R., Tromans-Coia, C., Giansanti, C., Jansen, J., Timinszky, G., Dobbelstein, M., Ahel, D., O'Sullivan, R. J., & Ahel, I. (2023). The interplay of TARG1 and PARG protects against genomic instability. *Cell Reports*, *42*(9). https://doi.org/10.1016/J.CELREP.2023.113113

Guzmán, C., Bagga, M., Kaur, A., Westermarck, J., & Abankwa, D. (2014). ColonyArea: An ImageJ Plugin to Automatically Quantify Colony Formation in Clonogenic Assays.

PLOS ONE, *9*(3), e92444. https://doi.org/10.1371/JOURNAL.PONE.0092444

Hailstone, R., Maroofian, R., Woodbine, L., Korneeva, E., Brazina, J., Macaya, A., Severino, M., Tomoum, H., Houlden, H., & Caldecott, K. W. (2023). Biallelic PARP1 Mutations Associated with Childhood-Onset Neurodegeneration. *MedRxiv*, 2023.06.09.23291078. http://medrxiv.org/content/early/2023/06/09/2023.06.09.23291078.abstract

Haince, J. F., McDonald, D., Rodrigue, A., Déry, U., Masson, J. Y., Hendzel, M. J., & Poirier, G. G. (2008). PARP1-dependent kinetics of recruitment of MRE11 and NBS1 proteins to multiple DNA damage sites. *Journal of Biological Chemistry*, *283*(2), 1197–1208. https://doi.org/10.1074/jbc.M706734200

Han, W. D., Zhao, Y. L., Meng, Y. G., Zang, L., Wu, Z. Q., Li, Q., Si, Y. L., Huang, K., Ba, J. M., Morinaga, H., Nomura, M., & Mu, Y. M. (2007). Estrogenically regulated LRP16 interacts with estrogen receptor α and enhances the receptor's transcriptional activity. *Endocrine-Related Cancer*, *14*(3), 741–753. https://doi.org/10.1677/ERC-06-0082

Hanai, S., Kanai, M., Ohashi, S., Okamoto, K., Yamada, M., Takahashi, H., & Miwa, M. (2004). Loss of poly(ADP-ribose) glycohydrolase causes progressive neurodegeneration in Drosophila melanogaster. *Proceedings of the National Academy of Sciences of the United States of America*, *101*(1), 82. https://doi.org/10.1073/PNAS.2237114100

Hanzlikova, H., Kalasova, I., Demin, A. A., Pennicott, L. E., Cihlarova, Z., & Caldecott, K. W. (2018). The Importance of Poly(ADP-Ribose) Polymerase as a Sensor of Unligated Okazaki Fragments during DNA Replication. *Molecular Cell*, *71*(2), 319-331.e3. https://doi.org/10.1016/J.MOLCEL.2018.06.004

Hashimoto, Y., Chaudhuri, A. R., Lopes, M., & Costanzo, V. (2010). Rad51 protects nascent DNA from Mre11-dependent degradation and promotes continuous DNA synthesis. *Nature Structural & Molecular Biology*, *17*(11), 1305–1311.

https://doi.org/10.1038/NSMB.1927

Hatch, R. V., Patel, S. U., Cambareri, C., Uritsky, T., & Martin, L. P. (2021). Evaluation of the management of PARP inhibitor toxicities in ovarian and endometrial cancer within a multi-institution health-system. *Https://Doi.Org/10.1177/10781552211024728*, *28*(5), 1102–1110. https://doi.org/10.1177/10781552211024728

He, F., Tsuda, K., Takahashi, M., Kuwasako, K., Terada, T., Shirouzu, M., Watanabe, S., Kigawa, T., Kobayashi, N., Güntert, P., Yokoyama, S., & Muto, Y. (2012). Structural insight into the interaction of ADP-ribose with the PARP WWE domains. *FEBS Letters*, *586*(21), 3858–3864. https://doi.org/10.1016/J.FEBSLET.2012.09.009

Heacock, M. L., Stefanick, D. F., Horton, J. K., & Wilson, S. H. (2010). Alkylation DNA damage in combination with PARP inhibition results in formation of S-phase-dependent double-strand breaks. *DNA Repair*, *9*(8), 929. https://doi.org/10.1016/J.DNAREP.2010.05.007

Heiss, B. L., Chang, E., Gao, X., Truong, T., Brave, M. H., Bloomquist, E., Shah, A., Hamed, S., Kraft, J., Chiu, H. J., Ricks, T. K., Tilley, A., Pierce, W. F., Tang, L., Abukhdeir, A., Kalavar, S., Philip, R., Tang, S., Pazdur, R., … Suzman, D. L. (2024). US Food and Drug Administration Approval Summary: Talazoparib in Combination with Enzalutamide for Treatment of Patients with Homologous Recombination Repair Gene-Mutated Metastatic Castration-Resistant Prostate Cancer. *Journal of Clinical Oncology*, *42*(15), 1851–1860. https://doi.org/10.1200/JCO.23.02182/SUPPL_FILE/PROTOCOL_JCO.23.02182.PDF

Helleday, T. (2011a). The underlying mechanism for the PARP and BRCA synthetic lethality: clearing up the misunderstandings. *Molecular Oncology*, *5*(4), 387–393. https://doi.org/10.1016/J.MOLONC.2011.07.001

Helleday, T. (2011b). The underlying mechanism for the PARP and BRCA synthetic lethality: Clearing up the misunderstandings. *Molecular Oncology*, *5*(4), 387–393. https://doi.org/10.1016/J.MOLONC.2011.07.001

Hendriks, I. A., Buch-Larsen, S. C., Prokhorova, E., Rebak, A. K. L. F. S., Ahel, I., & Nielsen, M. L. (2021). The regulatory landscape of the human HPF1-and ARH3-dependent ADP-ribosylome. *BioRxiv*.

Hochegger, H., Dejsuphong, D., Fukushima, T., Morrison, C., Sonoda, E., Schreiber, V., Guang, Y. Z., Saberi, A., Masutani, M., Adachi, N., Koyama, H., De Murcia, G., & Takeda, S. (2006). Parp-1 protects homologous recombination from interference by Ku and Ligase IV in vertebrate cells. *The EMBO Journal*, *25*(6), 1305. https://doi.org/10.1038/SJ.EMBOJ.7601015

Honjo, T., Nishizuka, Y., & Hayaishi, O. (1968). Diphtheria toxin-dependent adenosine diphosphate ribosylation of aminoacyl transferase II and inhibition of protein synthesis. *Journal of Biological Chemistry*, *243*(12), 3553–3555. https://doi.org/10.1016/s0021-9258(18)93347-8

Hopkins, T. A., Shi, Y., Rodriguez, L. E., Solomon, L. R., Donawho, C. K., Di Giammarino, E. L., Panchal, S. C., Wilsbacher, J. L., Gao, W., Olson, A. M., Stolarik, D. F., Osterling, D. J., Johnson, E. F., & Maag, D. (2015a). Mechanistic dissection of PARP1 trapping and the impact on in vivo tolerability and efficacy of PARP inhibitors. *Molecular Cancer Research*, *13*(11), 1465–1477. https://doi.org/10.1158/1541-7786.MCR-15-0191-T

Hopkins, T. A., Shi, Y., Rodriguez, L. E., Solomon, L. R., Donawho, C. K., Di Giammarino, E. L., Panchal, S. C., Wilsbacher, J. L., Gao, W., Olson, A. M., Stolarik, D. F., Osterling, D. J., Johnson, E. F., & Maag, D. (2015b). Mechanistic Dissection of PARP1 Trapping and the Impact on In Vivo Tolerability and Efficacy of PARP Inhibitors. *Molecular*

Cancer Research, *13*(11), 1465–1477. https://doi.org/10.1158/1541-7786.MCR-15-0191-T

Horton, J. K., Stefanick, D. F., Naron, J. M., Kedar, P. S., & Wilson, S. H. (2005). Poly(ADP-ribose) polymerase activity prevents signaling pathways for cell cycle arrest after DNA methylating agent exposure. *The Journal of Biological Chemistry*, *280*(16), 15773–15785. https://doi.org/10.1074/JBC.M413841200

Illuzzi, G., Staniszewska, A. D., Gill, S. J., Pike, A., McWilliams, L., Critchlow, S. E., Cronin, A., Fawell, S., Hawthorne, G., Jamal, K., Johannes, J., Leonard, E., Macdonald, R., Maglennon, G., Nikkilä, J., O'Connor, M. J., Smith, A., Southgate, H., Wilson, J., … Leo, E. (2022). Preclinical Characterization of AZD5305, A Next-Generation, Highly Selective PARP1 Inhibitor and Trapper. *Clinical Cancer Research*, *28*(21), 4724. https://doi.org/10.1158/1078-0432.CCR-22-0301

Jankevicius, G., Hassler, M., Golia, B., Rybin, V., Zacharias, M., Timinszky, G., & Ladurner, A. G. (2013). A family of macrodomain proteins reverses cellular mono-ADP-ribosylation. *Nature Structural & Molecular Biology*, *20*(4), 508–514. https://doi.org/10.1038/NSMB.2523

Jarmoskaite, I., Alsadhan, I., Vaidyanathan, P. P., & Herschlag, D. (2020). How to measure and evaluate binding affinities. *ELife*, *9*, 1–34. https://doi.org/10.7554/ELIFE.57264

Johannes, J. W., Balazs, A., Barratt, D., Bista, M., Chuba, M. D., Cosulich, S., Critchlow, S. E., Degorce, S. L., Di Fruscia, P., Edmondson, S. D., Embrey, K., Fawell, S., Ghosh, A., Gill, S. J., Gunnarsson, A., Hande, S. M., Heightman, T. D., Hemsley, P., Illuzzi, G., … Zheng, X. (2021). Discovery of 5-{4-[(7-Ethyl-6-oxo-5,6-dihydro-1,5-naphthyridin-3-yl)methyl]piperazin-1-yl}- N-methylpyridine-2-carboxamide (AZD5305): A PARP1-DNA Trapper with High Selectivity for PARP1 over PARP2 and Other PARPs. *Journal*

of Medicinal Chemistry, *64*(19), 14498–14512. https://doi.org/10.1021/ACS.JMEDCHEM.1C01012/SUPPL_FILE/JM1C01012_SI_003.CSV

Juhász, S., Smith, R., Schauer, T., Spekhardt, D., Mamar, H., Zentout, S., Chapuis, C., Huet, S., & Timinszky, G. (2020). The chromatin remodeler ALC1 underlies resistance to PARP inhibitor treatment. *Science Advances*, *6*(51), 8626–8644. https://doi.org/10.1126/SCIADV.ABB8626/SUPPL_FILE/ABB8626_TABLE_S2.XLSX

Kanev, P. B., Varhoshkova, S., Georgieva, I., Lukarska, M., Kirova, D., Danovski, G., Stoynov, S., & Aleksandrov, R. (2024). A unified mechanism for PARP inhibitor-induced PARP1 chromatin retention at DNA damage sites in living cells. *Cell Reports*, *43*(5). https://doi.org/10.1016/j.celrep.2024.114234

Karras, G. I., Kustatscher, G., Buhecha, H. R., Allen, M. D., Pugieux, C., Sait, F., Bycroft, M., & Ladurner, A. G. (2005). The macro domain is an ADP-ribose binding module. *The EMBO Journal*, *24*(11), 1911. https://doi.org/10.1038/SJ.EMBOJ.7600664

Kedar, P. S., Stefanick, D. F., Horton, J. K., & Wilson, S. H. (2012). Increased PARP-1 association with DNA in alkylation damaged, PARP-inhibited mouse fibroblasts. *Molecular Cancer Research*, *10*(3), 360–368. https://doi.org/10.1158/1541-7786.MCR-11-0477/79623/AM/INCREASED-PARP-1-ASSOCIATION-WITH-DNA-IN

Kim, D., & Nam, H. J. (2022). PARP Inhibitors: Clinical Limitations and Recent Attempts to Overcome Them. *International Journal of Molecular Sciences*, *23*(15). https://doi.org/10.3390/ijms23158412

Koh, D. W., Lawler, A. M., Poitras, M. F., Sasaki, M., Wattler, S., Nehls, M. C., Stöger, T., Poirier, G. G., Dawson, V. L., & Dawson, T. M. (2004). Failure to degrade poly(ADP-

ribose) causes increased sensitivity to cytotoxicity and early embryonic lethality. *Proceedings of the National Academy of Sciences*, *101*(51), 17699–17704. https://doi.org/10.1073/PNAS.0406182101

Kondrashova, O., Nguyen, M., Shield-Artin, K., Tinker, A. V., Teng, N. N. H., Harrell, M. I., Kuiper, M. J., Ho, G. Y., Barker, H., Jasin, M., Prakash, R., Kass, E. M., Sullivan, M. R., Brunette, G. J., Bernstein, K. A., Coleman, R. L., Floquet, A., Friedlander, M., Kichenadasse, G., … Scott, C. L. (2017). Secondary Somatic Mutations Restoring RAD51C and RAD51D Associated with Acquired Resistance to the PARP Inhibitor Rucaparib in High-Grade Ovarian Carcinoma. *Cancer Discovery*, *7*(9), 984–998. https://doi.org/10.1158/2159-8290.CD-17-0419

Krietsch, J., Rouleau, M., Pic, É., Ethier, C., Dawson, T. M., Dawson, V. L., Masson, J. Y., Poirier, G. G., & Gagné, J. P. (2013). Reprogramming cellular events by poly(ADP-ribose)-binding proteins. *Molecular Aspects of Medicine*, *34*(6), 1066. https://doi.org/10.1016/J.MAM.2012.12.005

Kusakabe, M., Onishi, Y., Tada, H., Kurihara, F., Kusao, K., Furukawa, M., Iwai, S., Yokoi, M., Sakai, W., & Sugasawa, K. (2019). Mechanism and regulation of DNA damage recognition in nucleotide excision repair. *Genes and Environment*, *41*(1), 1–6. https://doi.org/10.1186/S41021-019-0119-6/FIGURES/3

Kutuzov, M. M., Khodyreva, S. N., Amé, J. C., Ilina, E. S., Sukhanova, M. V., Schreiber, V., & Lavrik, O. I. (2013). Interaction of PARP-2 with DNA structures mimicking DNA repair intermediates and consequences on activity of base excision repair proteins. *Biochimie*, *95*(6), 1208–1215. https://doi.org/10.1016/J.BIOCHI.2013.01.007

LaFargue, C. J., Dal Molin, G. Z., Sood, A. K., & Coleman, R. L. (2019). Exploring and comparing adverse events between PARP inhibitors. *The Lancet. Oncology*, *20*(1), e15.

https://doi.org/10.1016/S1470-2045(18)30786-1

Langelier, M.-F., Billur, R., Sverzhinsky, A., Black, B. E., & Pascal, J. M. (2021a). HPF1 dynamically controls the PARP1/2 balance between initiating and elongating ADP-ribose modifications. *Nature Communications 2021 12:1*, *12*(1), 1–14. https://doi.org/10.1038/s41467-021-27043-8

Langelier, M.-F., Billur, R., Sverzhinsky, A., Black, B. E., & Pascal, J. M. (2021b). HPF1 dynamically controls the PARP1/2 balance between initiating and elongating ADP-ribose modifications. *Nature Communications 2021 12:1*, *12*(1), 1–14. https://doi.org/10.1038/s41467-021-27043-8

Langelier, M.-F., Planck, J. L., Roy, S., & Pascal, J. M. (2012). Structural basis for DNA-dependent poly(ADP-ribosyl)ation by human PARP-1. *Science (New York, N.Y.)*, *336*(6082), 728. https://doi.org/10.1126/SCIENCE.1216338

Langelier, M. F., Billur, R., Sverzhinsky, A., Black, B. E., & Pascal, J. M. (2021). HPF1 dynamically controls the PARP1/2 balance between initiating and elongating ADP-ribose modifications. *Nature Communications 2021 12:1*, *12*(1), 1–14. https://doi.org/10.1038/s41467-021-27043-8

Langelier, M. F., Lin, X., Zha, S., & Pascal, J. M. (2023a). Clinical PARP inhibitors allosterically induce PARP2 retention on DNA. *Science Advances*, *9*(12). https://doi.org/10.1126/sciadv.adf7175

Langelier, M. F., Lin, X., Zha, S., & Pascal, J. M. (2023b). Clinical PARP inhibitors allosterically induce PARP2 retention on DNA. *Science Advances*, *9*(12). https://doi.org/10.1126/SCIADV.ADF7175/SUPPL_FILE/SCIADV.ADF7175_SM.PDF

Langelier, M. F., Planck, J. L., Roy, S., & Pascal, J. M. (2011). Crystal Structures of Poly(ADP-ribose) Polymerase-1 (PARP-1) Zinc Fingers Bound to DNA:

STRUCTURAL AND FUNCTIONAL INSIGHTS INTO DNA-DEPENDENT PARP-1 ACTIVITY*. *The Journal of Biological Chemistry*, *286*(12), 10690. https://doi.org/10.1074/JBC.M110.202507

Langelier, M. F., Riccio, A. A., & Pascal, J. M. (2014). PARP-2 and PARP-3 are selectively activated by 5′ phosphorylated DNAbreaks through an allosteric regulatory mechanism shared with PARP-1. *Nucleic Acids Research*, *42*(12), 7762. https://doi.org/10.1093/NAR/GKU474

Langelier, M. F., Zandarashvili, L., Aguiar, P. M., Black, B. E., & Pascal, J. M. (2018). NAD+ analog reveals PARP-1 substrate-blocking mechanism and allosteric communication from catalytic center to DNA-binding domains. *Nature Communications*, *9*(1). https://doi.org/10.1038/S41467-018-03234-8

Larsen, S. C., Hendriks, I. A., Lyon, D., Jensen, L. J., & Nielsen, M. L. (2018a). Systems-wide Analysis of Serine ADP-Ribosylation Reveals Widespread Occurrence and Site-Specific Overlap with Phosphorylation. *Cell Reports*, *24*(9), 2493-2505.e4. https://doi.org/10.1016/J.CELREP.2018.07.083

Larsen, S. C., Hendriks, I. A., Lyon, D., Jensen, L. J., & Nielsen, M. L. (2018b). Systems-wide Analysis of Serine ADP-Ribosylation Reveals Widespread Occurrence and Site-Specific Overlap with Phosphorylation. *Cell Reports*, *24*(9), 2493-2505.e4. https://doi.org/10.1016/j.celrep.2018.07.083

Leidecker, O., Bonfiglio, J. J., Colby, T., Zhang, Q., Atanassov, I., Zaja, R., Palazzo, L., Stockum, A., Ahel, I., & Matic, I. (2016). Serine is a new target residue for endogenous ADP-ribosylation on histones. *Nature Chemical Biology*, *12*(12), 998. https://doi.org/10.1038/NCHEMBIO.2180

Lemaçon, D., Jackson, J., Quinet, A., Brickner, J. R., Li, S., Yazinski, S., You, Z., Ira, G.,

Zou, L., Mosammaparast, N., & Vindigni, A. (2017). MRE11 and EXO1 nucleases degrade reversed forks and elicit MUS81-dependent fork rescue in BRCA2-deficient cells. *Nature Communications*, *8*(1). https://doi.org/10.1038/S41467-017-01180-5

Li, M., & Yu, X. (2013a). Function of BRCA1 in the DNA damage response is mediated by ADP-ribosylation. *Cancer Cell*, *23*(5), 693. https://doi.org/10.1016/J.CCR.2013.03.025

Li, M., & Yu, X. (2013b). Function of BRCA1 in the DNA damage response is mediated by ADP-ribosylation. *Cancer Cell*, *23*(5), 693–704. https://doi.org/10.1016/J.CCR.2013.03.025

Li, P., Lei, Y., Qi, J., Liu, W., & Yao, K. (2022). Functional roles of ADP-ribosylation writers, readers and erasers. *Frontiers in Cell and Developmental Biology*, *10*, 941356. https://doi.org/10.3389/FCELL.2022.941356/BIBTEX

Li, X., & Zou, L. (2024). BRCAness, DNA gaps, and gain and loss of PARP inhibitor–induced synthetic lethality. *The Journal of Clinical Investigation*, *134*(14), e181062. https://doi.org/10.1172/JCI181062

Liao, H., Ji, F., Helleday, T., & Ying, S. (2018). Mechanisms for stalled replication fork stabilization: new targets for synthetic lethality strategies in cancer treatments. *EMBO Reports*, *19*(9). https://doi.org/10.15252/EMBR.201846263

Lin, X., Gupta, D., Vaitsiankova, A., Bhandari, S. K., Leung, K. S. K., Menolfi, D., Lee, B. J., Russell, H. R., Gershik, S., Gu, W., McKinnon, P. J., Dantzer, F., Rothenberg, E., Tomkinson, A. E., & Zha, S. (2024). Inactive Parp2 causes Tp53-dependent lethal anemia by blocking replication-associated nick ligation in erythroblasts. *BioRxiv*, 2024.03.12.584665. https://doi.org/10.1101/2024.03.12.584665

Lin, X., Jiang, W., Rudolph, J., Lee, B. J., Luger, K., & Zha, S. (2022). PARP inhibitors trap PARP2 and alter the mode of recruitment of PARP2 at DNA damage sites. *Nucleic Acids*

Research, *50*(7), 3958. https://doi.org/10.1093/NAR/GKAC188

Liu, C., Wu, J., Paudyal, S. C., You, Z., & Yu, X. (2013). CHFR is important for the first wave of ubiquitination at DNA damage sites. *Nucleic Acids Research*, *41*(3), 1698. https://doi.org/10.1093/NAR/GKS1278

Liu, S., Opiyo, S. O., Manthey, K., Glanzer, J. G., Ashley, A. K., Amerin, C., Troksa, K., Shrivastav, M., Nickoloff, J. A., & Oakley, G. G. (2012). Distinct roles for DNA-PK, ATM and ATR in RPA phosphorylation and checkpoint activation in response to replication stress. *Nucleic Acids Research*, *40*(21), 10780–10794. https://doi.org/10.1093/nar/gks849

Longarini, E. J., Dauben, H., Locatelli, C., Wondisford, A. R., Smith, R., Muench, C., Kolvenbach, A., Lynskey, M. L., Pope, A., Bonfiglio, J. J., Jurado, E. P., Fajka-Boja, R., Colby, T., Schuller, M., Ahel, I., Timinszky, G., O'Sullivan, R. J., Huet, S., & Matic, I. (2023). Modular antibodies reveal DNA damage-induced mono-ADP-ribosylation as a second wave of PARP1 signaling. *Molecular Cell*, *83*(10), 1743. https://doi.org/10.1016/J.MOLCEL.2023.03.027

Lord, C. J., & Ashworth, A. (2012). The DNA damage response and cancer therapy. *Nature*, *481*(7381), 287–294. https://doi.org/10.1038/NATURE10760

Love, S., Barber, R., & Wilcock, G. K. (1999). Neuronal accumulation of poly(ADP-ribose) after brain ischaemia. *Neuropathology and Applied Neurobiology*, *25*(2), 98–103. https://doi.org/10.1046/J.1365-2990.1999.00179.X

Luijsterburg, M. S., de Krijger, I., Wiegant, W. W., Shah, R. G., Smeenk, G., de Groot, A. J. L., Pines, A., Vertegaal, A. C. O., Jacobs, J. J. L., Shah, G. M., & van Attikum, H. (2016). PARP1 Links CHD2-Mediated Chromatin Expansion and H3.3 Deposition to DNA Repair by Non-homologous End-Joining. *Molecular Cell*, *61*(4), 547.

https://doi.org/10.1016/J.MOLCEL.2016.01.019

Lüscher, B., Ahel, I., Altmeyer, M., Ashworth, A., Bai, P., Chang, P., Cohen, M., Corda, D., Dantzer, F., Daugherty, M. D., Dawson, T. M., Dawson, V. L., Deindl, S., Fehr, A. R., Feijs, K. L. H., Filippov, D. V., Gagné, J.-P., Grimaldi, G., Guettler, S., … Ziegler, M. (2021). ADP-ribosyltransferases, an update on function and nomenclature. *The FEBS Journal*. https://doi.org/10.1111/FEBS.16142

Ma, N. F., Hu, L., Fung, J. M., Xie, D., Zheng, B. J., Chen, L., Tang, D. J., Fu, L., Wu, Z., Chen, M., Fang, Y., & Guan, X. Y. (2008). Isolation and characterization of a novel oncogene, amplified in liver cancer 1, within a commonly amplified region at 1q21 in hepatocellular carcinoma. *Hepatology (Baltimore, Md.)*, *47*(2), 503–510. https://doi.org/10.1002/HEP.22072

Makvandi, M., Pantel, A., Schwartz, L., Schubert, E., Xu, K., Hsieh, C. J., Hou, C., Kim, H., Weng, C. C., Winters, H., Doot, R., Farwell, M. D., Pryma, D. A., Greenberg, R. A., Mankoff, D. A., Simpkins, F., Mach, R. H., & Lin, L. L. (2018). A PET imaging agent for evaluating PARP-1 expression in ovarian cancer. *The Journal of Clinical Investigation*, *128*(5), 2116–2126. https://doi.org/10.1172/JCI97992

Mansour, W. Y., Rhein, T., & Dahm-Daphi, J. (2010). The alternative end-joining pathway for repair of DNA double-strand breaks requires PARP1 but is not dependent upon microhomologies. *Nucleic Acids Research*, *38*(18), 6065. https://doi.org/10.1093/NAR/GKQ387

Markham, A. (2021). Pamiparib: First Approval. *Drugs*, *81*(11), 1343–1348. https://doi.org/10.1007/S40265-021-01552-8/METRICS

Marsischky, G. T., Wilson, B. A., & Collier, R. J. (1995). Role of Glutamic Acid 988 of Human Poly-ADP-ribose Polymerase in Polymer Formation: EVIDENCE FOR ACTIVE

SITE SIMILARITIES TO THE ADP-RIBOSYLATING TOXINS (∗). *Journal of Biological Chemistry*, *270*(7), 3247–3254. https://doi.org/10.1074/JBC.270.7.3247

Mashimo, M., Kato, J., & Moss, J. (2013). ADP-ribosyl-acceptor hydrolase 3 regulates poly (ADP-ribose) degradation and cell death during oxidative stress. *Proceedings of the National Academy of Sciences of the United States of America*, *110*(47), 18964–18969. https://doi.org/10.1073/pnas.1312783110

Masson, G. R., Burke, J. E., Ahn, N. G., Anand, G. S., Borchers, C., Brier, S., Bou-Assaf, G. M., Engen, J. R., Englander, S. W., Faber, J., Garlish, R., Griffin, P. R., Gross, M. L., Guttman, M., Hamuro, Y., Heck, A. J. R., Houde, D., Iacob, R. E., Jørgensen, T. J. D., … Rand, K. D. (2019). Recommendations for performing, interpreting and reporting hydrogen deuterium exchange mass spectrometry (HDX-MS) experiments. *Nature Methods 2019 16:7*, *16*(7), 595–602. https://doi.org/10.1038/s41592-019-0459-y

Mateo, J., Lord, C. J., Serra, V., Tutt, A., Balmaña, J., Castroviejo-Bermejo, M., Cruz, C., Oaknin, A., Kaye, S. B., & De Bono, J. S. (2019). A decade of clinical development of PARP inhibitors in perspective. *Annals of Oncology*, *30*(9), 1437. https://doi.org/10.1093/ANNONC/MDZ192

Mazouzi, A., Velimezi, G., & Loizou, J. I. (2014). DNA replication stress: Causes, resolution and disease. *Experimental Cell Research*, *329*(1), 85–93. https://doi.org/10.1016/J.YEXCR.2014.09.030

McQuin, C., Goodman, A., Chernyshev, V., Kamentsky, L., Cimini, B. A., Karhohs, K. W., Doan, M., Ding, L., Rafelski, S. M., Thirstrup, D., Wiegraebe, W., Singh, S., Becker, T., Caicedo, J. C., & Carpenter, A. E. (2018). CellProfiler 3.0: Next-generation image processing for biology. *PLoS Biology*, *16*(7). https://doi.org/10.1371/JOURNAL.PBIO.2005970

Ménissier de Murcia, J., Ricoul, M., Tartier, L., Niedergang, C., Huber, A., Dantzer, F., Schreiber, V., Amé, J. C., Dierich, A., LeMeur, M., Sabatier, L., Chambon, P., & De Murcia, G. (2003a). Functional interaction between PARP-1 and PARP-2 in chromosome stability and embryonic development in mouse. *The EMBO Journal*, *22*(9), 2255. https://doi.org/10.1093/EMBOJ/CDG206

Ménissier de Murcia, J., Ricoul, M., Tartier, L., Niedergang, C., Huber, A., Dantzer, F., Schreiber, V., Amé, J. C., Dierich, A., LeMeur, M., Sabatier, L., Chambon, P., & De Murcia, G. (2003b). Functional interaction between PARP-1 and PARP-2 in chromosome stability and embryonic development in mouse. *The EMBO Journal*, *22*(9), 2255. https://doi.org/10.1093/EMBOJ/CDG206

Messner, S., & Hottiger, M. O. (2011). Histone ADP-ribosylation in DNA repair, replication and transcription. In *Trends in Cell Biology* (Vol. 21, Issue 9, pp. 534–542). Elsevier Current Trends. https://doi.org/10.1016/j.tcb.2011.06.001

Mikolčević, P., Hloušek-Kasun, A., Ahel, I., & Mikoč, A. (2021). ADP-ribosylation systems in bacteria and viruses. In *Computational and Structural Biotechnology Journal* (Vol. 19, pp. 2366–2383). Elsevier B.V. https://doi.org/10.1016/j.csbj.2021.04.023

Min, W., Bruhn, C., Grigaravicius, P., Zhou, Z. W., Li, F., Krüger, A., Siddeek, B., Greulich, K. O., Popp, O., Meisezahl, C., Calkhoven, C. F., Bürkle, A., Xu, X., & Wang, Z. Q. (2013). Poly(ADP-ribose) binding to Chk1 at stalled replication forks is required for S-phase checkpoint activation. *Nature Communications 2013 4:1*, *4*(1), 1–14. https://doi.org/10.1038/ncomms3993

Mirza, M. R., Monk, B. J., Herrstedt, J., Oza, A. M., Mahner, S., Redondo, A., Fabbro, M., Ledermann, J. A., Lorusso, D., Vergote, I., Ben-Baruch, N. E., Marth, C., Mądry, R., Christensen, R. D., Berek, J. S., Dørum, A., Tinker, A. V., du Bois, A., González-Martín,

A., … Matulonis, U. A. (2016). Niraparib Maintenance Therapy in Platinum-Sensitive, Recurrent Ovarian Cancer. *New England Journal of Medicine*, *375*(22), 2154–2164. https://doi.org/10.1056/NEJMOA1611310/SUPPL_FILE/NEJMOA1611310_DISCLOSURES.PDF

Mohyuddin, G. R., Aziz, M., Britt, A., Wade, L., Sun, W., Baranda, J., Al-Rajabi, R., Saeed, A., & Kasi, A. (2020). Similar response rates and survival with PARP inhibitors for patients with solid tumors harboring somatic versus Germline BRCA mutations: a Meta-analysis and systematic review. *BMC Cancer*, *20*(1). https://doi.org/10.1186/S12885-020-06948-5

Mortusewicz, O., Amé, J.-C., Schreiber, V., & Leonhardt, H. (2007). Feedback-regulated poly(ADP-ribosyl)ation by PARP-1 is required for rapid response to DNA damage in living cells. *Nucleic Acids Research*, *35*(22), 7665. https://doi.org/10.1093/NAR/GKM933

Mortusewicz, O., Fouquerel, E., Amé, J. C., Leonhardt, H., & Schreiber, V. (2011). PARG is recruited to DNA damage sites through poly(ADP-ribose)- and PCNA-dependent mechanisms. *Nucleic Acids Research*, *39*(12), 5045. https://doi.org/10.1093/NAR/GKR099

Munnur, D., Bartlett, E., Mikolčević, P., Kirby, I. T., Rack, J. G. M., Mikoč, A., Cohen, M. S., & Ahel, I. (2019). Reversible ADP-ribosylation of RNA. *Nucleic Acids Research*, *47*(11), 5658–5669. https://doi.org/10.1093/nar/gkz305

Muoio, D., Laspata, N., Dannenberg, R. L., Curry, C., Darkoa-Larbi, S., Hedglin, M., Uttam, S., & Fouquerel, E. (2024). PARP2 promotes Break Induced Replication-mediated telomere fragility in response to replication stress. *Nature Communications 2024 15:1*, *15*(1), 1–18. https://doi.org/10.1038/s41467-024-47222-7

Murai, J., Huang, S. Y. N., Das, B. B., Renaud, A., Zhang, Y., Doroshow, J. H., Ji, J., Takeda, S., & Pommier, Y. (2012). Differential trapping of PARP1 and PARP2 by clinical PARP inhibitors. *Cancer Research*, *72*(21), 5588. https://doi.org/10.1158/0008-5472.CAN-12-2753

Murai, J., Huang, S. Y. N., Renaud, A., Zhang, Y., Ji, J., Takeda, S., Morris, J., Teicher, B., Doroshow, J. H., & Pommier, Y. (2014). Stereospecific PARP trapping by BMN 673 and comparison with olaparib and rucaparib. *Molecular Cancer Therapeutics*, *13*(2), 433. https://doi.org/10.1158/1535-7163.MCT-13-0803

Naumenkoa, N. V., Petrusevaa, I. O., & Lavrik, O. I. (2022). Bulky Adducts in Clustered DNA Lesions: Causes of Resistance to the NER System. *Acta Naturae*, *14*(4), 38. https://doi.org/10.32607/ACTANATURAE.11741

Obaji, E., Haikarainen, T., & Lehtiö, L. (2016). Characterization of the DNA dependent activation of human ARTD2/PARP2. *Scientific Reports*, *6*. https://doi.org/10.1038/SREP34487

Oka, S., Kato, J., & Moss, J. (2006). Identification and characterization of a mammalian 39-kDa poly(ADP-ribose) glycohydrolase. *Journal of Biological Chemistry*, *281*(2), 705–713. https://doi.org/10.1074/jbc.M510290200

Palazzo, L., Leidecker, O., Prokhorova, E., Dauben, H., Matic, I., & Ahel, I. (2018). Serine is the major residue for ADP-ribosylation upon DNA damage. *ELife*, *7*. https://doi.org/10.7554/eLife.34334

Palazzo, L., Mikolčević, P., Mikoč, A., & Ahel, I. (2019). ADP-ribosylation signalling and human disease. *Open Biology*, *9*(4). https://doi.org/10.1098/RSOB.190041

Panzarino, N. J., Krais, J. J., Cong, K., Peng, M., Mosqueda, M., Nayak, S. U., Bond, S. M., Calvo, J. A., Doshi, M. B., Bere, M., Ou, J., Deng, B., Zhu, L. J., Johnson, N., & Cantor,

S. B. (2021). Replication Gaps Underlie BRCA Deficiency and Therapy Response. *Cancer Research*, *81*(5), 1388–1397. https://doi.org/10.1158/0008-5472.CAN-20-1602

Perina, D., Mikoč, A., Ahel, J., Ćetković, H., Žaja, R., & Ahel, I. (2014). Distribution of protein poly(ADP-ribosyl)ation systems across all domains of life. *DNA Repair*, *23*, 4–16. https://doi.org/10.1016/j.dnarep.2014.05.003

Pettitt, S. J., Frankum, J. R., Punta, M., Lise, S., Alexander, J., Chen, Y., Yap, T. A., Haider, S., Tutt, A. N. J., & Lord, C. J. (2020). Clinical BRCA1/2 Reversion Analysis Identifies Hotspot Mutations and Predicted Neoantigens Associated with Therapy Resistance. *Cancer Discovery*, *10*(10), 1475–1488. https://doi.org/10.1158/2159-8290.CD-19-1485

Pettitt, S. J., Krastev, D. B., Brandsma, I., Dréan, A., Song, F., Aleksandrov, R., Harrell, M. I., Menon, M., Brough, R., Campbell, J., Frankum, J., Ranes, M., Pemberton, H. N., Rafiq, R., Fenwick, K., Swain, A., Guettler, S., Lee, J. M., Swisher, E. M., … Lord, C. J. (2018). Genome-wide and high-density CRISPR-Cas9 screens identify point mutations in PARP1 causing PARP inhibitor resistance. *Nature Communications 2018 9:1*, *9*(1), 1–14. https://doi.org/10.1038/s41467-018-03917-2

Pleschke, J. M., Kleczkowska, H. E., Strohm, M., & Althaus, F. R. (2000). Poly(ADP-ribose) binds to specific domains in DNA damage checkpoint proteins. *The Journal of Biological Chemistry*, *275*(52), 40974–40980. https://doi.org/10.1074/JBC.M006520200

Polo, L. M., Xu, Y., Hornyak, P., Garces, F., Zeng, Z., Hailstone, R., Matthews, S. J., Caldecott, K. W., Oliver, A. W., & Pearl, L. H. (2019). Efficient Single-Strand Break Repair Requires Binding to Both Poly(ADP-Ribose) and DNA by the Central BRCT Domain of XRCC1. *Cell Reports*, *26*(3), 573. https://doi.org/10.1016/J.CELREP.2018.12.082

Pommier, Y., Nussenzweig, A., Takeda, S., & Austin, C. (2022). Human topoisomerases and

their roles in genome stability and organization. *Nature Reviews Molecular Cell Biology 2022 23:6*, *23*(6), 407–427. https://doi.org/10.1038/s41580-022-00452-3

Pommier, Y., O'Connor, M. J., & De Bono, J. (2016). Laying a trap to kill cancer cells: PARP inhibitors and their mechanisms of action. *Science Translational Medicine*, *8*(362). https://doi.org/10.1126/SCITRANSLMED.AAF9246

Prakash, R., Zhang, Y., Feng, W., & Jasin, M. (2015). Homologous Recombination and Human Health: The Roles of BRCA1, BRCA2, and Associated Proteins. *Cold Spring Harbor Perspectives in Biology*, *7*(4). https://doi.org/10.1101/CSHPERSPECT.A016600

Prokhorova, E., Agnew, T., Wondisford, A. R., Baets, J., O'sullivan, R. J., Correspondence, I. A., Tellier, M., Kaminski, N., Beijer, D., Holder, J., Groslambert, J., Suskiewicz, M. J., Zhu, K., Reber, J. M., Krassnig, S. C., Palazzo, L., Murphy, S., Nielsen, M. L., Mangerich, A., … Ahel, I. (2021). Unrestrained poly-ADP-ribosylation provides insights into chromatin regulation and human disease. *Molecular Cell*, *81*, 2640-2655.e8. https://doi.org/10.1016/j.molcel.2021.04.028

Prokhorova, E., Agnew, T., Wondisford, A. R., Tellier, M., Kaminski, N., Beijer, D., Holder, J., Groslambert, J., Suskiewicz, M. J., Zhu, K., Reber, J. M., Krassnig, S. C., Palazzo, L., Murphy, S., Nielsen, M. L., Mangerich, A., Ahel, D., Baets, J., O'Sullivan, R. J., & Ahel, I. (2021). Unrestrained poly-ADP-ribosylation provides insights into chromatin regulation and human disease. *Molecular Cell*, *81*(12), 2640. https://doi.org/10.1016/J.MOLCEL.2021.04.028

Prokhorova, E., Zobel, F., Smith, R., Zentout, S., Gibbs-Seymour, I., Schützenhofer, K., Peters, A., Groslambert, J., Zorzini, V., Agnew, T., Brognard, J., Nielsen, M. L., Ahel, D., Huet, S., Suskiewicz, M. J., & Ahel, I. (2021). Serine-linked PARP1 auto-modification controls PARP inhibitor response. *Nature Communications*, *12*(1), 4055.

https://doi.org/10.1038/s41467-021-24361-9

Purnell, M. R., & Whish, W. J. D. (1980). Novel Inhibitors of Poly (ADP-Ribose) Synthetase. *Biochem. J*, *185*(3), 775–777.

Q, C., MA, K., F, D., & X, Y. (2018). PARP2 mediates branched poly ADP-ribosylation in response to DNA damage. *Nature Communications*, *9*(1). https://doi.org/10.1038/S41467-018-05588-5

Rack, J. G. M., Liu, Q., Zorzini, V., Voorneveld, J., Ariza, A., Honarmand Ebrahimi, K., Reber, J. M., Krassnig, S. C., Ahel, D., van der Marel, G. A., Mangerich, A., McCullagh, J. S. O., Filippov, D. V., & Ahel, I. (2021). Mechanistic insights into the three steps of poly(ADP-ribosylation) reversal. *Nature Communications 2021 12:1*, *12*(1), 1–14. https://doi.org/10.1038/s41467-021-24723-3

Rack, J. G. M., Perina, D., & Ahel, I. (2016). Macrodomains: Structure, Function, Evolution, and Catalytic Activities. *Http://Dx.Doi.Org/10.1146/Annurev-Biochem-060815-014935*, *85*, 431–454. https://doi.org/10.1146/ANNUREV-BIOCHEM-060815-014935

Ray Chaudhuri, A., & Nussenzweig, A. (2017). The multifaceted roles of PARP1 in DNA repair and chromatin remodelling. *Nature Reviews. Molecular Cell Biology*, *18*(10), 610. https://doi.org/10.1038/NRM.2017.53

Reber, J. M., Božić-Petković, J., Lippmann, M., Mazzardo, M., Dilger, A., Warmers, R., Bürkle, A., & Mangerich, A. (2023). PARP1 and XRCC1 exhibit a reciprocal relationship in genotoxic stress response. *Cell Biology and Toxicology*, *39*(1), 345. https://doi.org/10.1007/S10565-022-09739-9

Ren, J., Quan, X., Liu, Y., Li, J., Zhang, X., Li, Z., & Zhang, X. (2022). Synthesis and in vitro biological evaluation of 3-ethyl-1,5-naphthyridin-2(1H)-one derivatives as potent PARP-1 selective inhibitors and PARP-1 DNA trappers. *Bioorganic & Medicinal Chemistry*

Letters, *78*, 129046. https://doi.org/10.1016/J.BMCL.2022.129046

Riccio, A. A., Cingolani, G., & Pascal, J. M. (2016a). PARP-2 domain requirements for DNA damage-dependent activation and localization to sites of DNA damage. *Nucleic Acids Research*, *44*(4), 1691. https://doi.org/10.1093/NAR/GKV1376

Riccio, A. A., Cingolani, G., & Pascal, J. M. (2016b). PARP-2 domain requirements for DNA damage-dependent activation and localization to sites of DNA damage. *Nucleic Acids Research*, *44*(4), 1691. https://doi.org/10.1093/NAR/GKV1376

Robu, M., Shah, R. G., Petitclerc, N., Brind'amour, J., Kandan-Kulangara, F., & Shah, G. M. (2013). Role of poly(ADP-ribose) polymerase-1 in the removal of UV-induced DNA lesions by nucleotide excision repair. *Proceedings of the National Academy of Sciences of the United States of America*, *110*(5), 1658–1663. https://doi.org/10.1073/PNAS.1209507110/SUPPL_FILE/PNAS.201209507SI.PDF

Robu, M., Shah, R. G., Purohit, N. K., Zhou, P., Naegeli, H., & Shah, G. M. (2017). Poly(ADP-ribose) polymerase 1 escorts XPC to UV-induced DNA lesions during nucleotide excision repair. *Proceedings of the National Academy of Sciences of the United States of America*, *114*(33), E6847–E6856. https://doi.org/10.1073/PNAS.1706981114/-/DCSUPPLEMENTAL

Rodriguez-Vargas, J. M., Nguekeu-Zebaze, L., & Dantzer, F. (2019). PARP3 comes to light as a prime target in cancer therapy. *Cell Cycle*, *18*(12), 1295. https://doi.org/10.1080/15384101.2019.1617454

Rolli, V., O'Farrell, M., Ménissier-de Murcia, J., & De Murcia, G. (1997). Random Mutagenesis of the Poly(ADP-ribose) Polymerase Catalytic Domain Reveals Amino Acids Involved in Polymer Branching†. *Biochemistry*, *36*(40), 12147–12154. https://doi.org/10.1021/BI971055P

Rose, M., Burgess, J. T., O'Byrne, K., Richard, D. J., & Bolderson, E. (2020). PARP Inhibitors: Clinical Relevance, Mechanisms of Action and Tumor Resistance. In *Frontiers in Cell and Developmental Biology* (Vol. 8). Frontiers Media S.A. https://doi.org/10.3389/fcell.2020.564601

Rosenthal, F., Feijs, K. L. H., Frugier, E., Bonalli, M., Forst, A. H., Imhof, R., Winkler, H. C., Fischer, D., Caflisch, A., Hassa, P. O., Lüscher, B., & Hottiger, M. O. (2013). Macrodomain-containing proteins are new mono-ADP-ribosylhydrolases. *Nature Structural & Molecular Biology 2013 20:4*, *20*(4), 502–507. https://doi.org/10.1038/nsmb.2521

Roy, R., Chun, J., & Powell, S. N. (2011). BRCA1 and BRCA2: different roles in a common pathway of genome protection. *Nature Reviews. Cancer*, *12*(1), 68–78. https://doi.org/10.1038/NRC3181

Rudolph, J., Jung, K., & Luger, K. (2022). Inhibitors of PARP: Number crunching and structure gazing. *Proceedings of the National Academy of Sciences of the United States of America*, *119*(11), e2121979119. https://doi.org/10.1073/PNAS.2121979119/SUPPL_FILE/PNAS.2121979119.SAPP.PDF

Rudolph, J., Muthurajan, U. M., Palacio, M., Mahadevan, J., Roberts, G., Erbse, A. H., Dyer, P. N., & Luger, K. (2021). The BRCT domain of PARP1 binds intact DNA and mediates intrastrand transfer. *Molecular Cell*, *81*(24), 4994-5006.e5. https://doi.org/10.1016/j.molcel.2021.11.014

Rudolph, J., Roberts, G., & Luger, K. (2021a). Histone Parylation factor 1 contributes to the inhibition of PARP1 by cancer drugs. *Nature Communications*, *12*(1), 1–11. https://doi.org/10.1038/s41467-021-20998-8

Rudolph, J., Roberts, G., & Luger, K. (2021b). Histone Parylation factor 1 contributes to the inhibition of PARP1 by cancer drugs. *Nature Communications*, *12*(1). https://doi.org/10.1038/S41467-021-20998-8

Rudolph, J., Roberts, G., Muthurajan, U. M., & Luger, K. (2021). Hpf1 and nucleosomes mediate a dramatic switch in activity of parp1 from polymerase to hydrolase. *ELife*, *10*. https://doi.org/10.7554/ELIFE.65773

Ruf, A., Rolli, V., De Murcia, G., & Schulz, G. E. (1998). The mechanism of the elongation and branching reaction of poly(ADP-ribose) polymerase as derived from crystal structures and mutagenesis. *Journal of Molecular Biology*, *278*(1), 57–65. https://doi.org/10.1006/JMBI.1998.1673

Ryan, K., Bolaños, B., Smith, M., Palde, P. B., Cuenca, P. D., VanArsdale, T. L., Niessen, S., Zhang, L., Behenna, D., Ornelas, M. A., Tran, K. T., Kaiser, S., Lum, L., Stewart, A., & Gajiwala, K. S. (2021). Dissecting the molecular determinants of clinical PARP1 inhibitor selectivity for tankyrase1. *The Journal of Biological Chemistry*, *296*, 100251. https://doi.org/10.1074/JBC.RA120.016573

Satoh, M. S., & Lindahl, T. (1992). Role of poly(ADP-ribose) formation in DNA repair. *Nature*, *356*(6367), 356–358. https://doi.org/10.1038/356356A0

Schlacher, K., Christ, N., Siaud, N., Egashira, A., Wu, H., & Jasin, M. (2011). Double-strand break repair-independent role for BRCA2 in blocking stalled replication fork degradation by MRE11. *Cell*, *145*(4), 529–542. https://doi.org/10.1016/J.CELL.2011.03.041

Schlacher, K., Wu, H., & Jasin, M. (2012). A distinct replication fork protection pathway connects Fanconi anemia tumor suppressors to RAD51-BRCA1/2. *Cancer Cell*, *22*(1), 106–116. https://doi.org/10.1016/J.CCR.2012.05.015

Schützenhofer, K., Rack, J. G. M., & Ahel, I. (2021). The Making and Breaking of Serine-

ADP-Ribosylation in the DNA Damage Response. *Frontiers in Cell and Developmental Biology*, *0*, 3119. https://doi.org/10.3389/FCELL.2021.745922

Sellou, H., Lebeaupin, T., Chapuis, C., Smith, R., Hegele, A., Singh, H. R., Kozlowski, M., Bultmann, S., Ladurner, A. G., Timinszky, G., & Huet, S. (2016). The poly(ADP-ribose)-dependent chromatin remodeler Alc1 induces local chromatin relaxation upon DNA damage. *Molecular Biology of the Cell*, *27*(24), 3791–3799. https://doi.org/10.1091/MBC.E16-05-0269

Shall, S. (1975). Experimental manipulation of the specific activity of poly(ADP-ribose) polymerase. *Biochem. J (Tokyo)*, *77*(2).

Shao, Z., Lee, B. J., Rouleau-Turcotte, É., Langelier, M. F., Lin, X., Estes, V. M., Pascal, J. M., & Zha, S. (2020a). Clinical PARP inhibitors do not abrogate PARP1 exchange at DNA damage sites in vivo. *Nucleic Acids Research*, *48*(17), 9694. https://doi.org/10.1093/NAR/GKAA718

Shao, Z., Lee, B. J., Rouleau-Turcotte, É., Langelier, M. F., Lin, X., Estes, V. M., Pascal, J. M., & Zha, S. (2020b). Clinical PARP inhibitors do not abrogate PARP1 exchange at DNA damage sites in vivo. *Nucleic Acids Research*, *48*(17), 9694–9709. https://doi.org/10.1093/nar/gkaa718

Shao, Z., Lee, B. J., Rouleau-Turcotte, É., Langelier, M. F., Lin, X., Estes, V. M., Pascal, J. M., & Zha, S. (2020c). Clinical PARP inhibitors do not abrogate PARP1 exchange at DNA damage sites in vivo. *Nucleic Acids Research*, *48*(17), 9694–9709. https://doi.org/10.1093/NAR/GKAA718

Shao, Z., Lee, B. J., Zhang, H., Lin, X., Li, C., Jiang, W., Chirathivat, N., Gershik, S., Shen, M. M., Baer, R., & Zha, S. (2023). Inactive PARP1 causes embryonic lethality and genome instability in a dominant-negative manner. *Proceedings of the National Academy*

of Sciences of the United States of America, *120*(31), e2301972120. https://doi.org/10.1073/PNAS.2301972120/SUPPL_FILE/PNAS.2301972120.SAPP.PDF

Sharifi, R., Morra, R., Denise Appel, C., Tallis, M., Chioza, B., Jankevicius, G., Simpson, M. A., Matic, I., Ozkan, E., Golia, B., Schellenberg, M. J., Weston, R., Williams, J. G., Rossi, M. N., Galehdari, H., Krahn, J., Wan, A., Trembath, R. C., Crosby, A. H., … Ahel, I. (2013a). Deficiency of terminal ADP-ribose protein glycohydrolase TARG1/C6orf130 in neurodegenerative disease. *The EMBO Journal*, *32*(9), 1225. https://doi.org/10.1038/EMBOJ.2013.51

Sharifi, R., Morra, R., Denise Appel, C., Tallis, M., Chioza, B., Jankevicius, G., Simpson, M. A., Matic, I., Ozkan, E., Golia, B., Schellenberg, M. J., Weston, R., Williams, J. G., Rossi, M. N., Galehdari, H., Krahn, J., Wan, A., Trembath, R. C., Crosby, A. H., … Ahel, I. (2013b). Deficiency of terminal ADP-ribose protein glycohydrolase TARG1/C6orf130 in neurodegenerative disease. *The EMBO Journal*, *32*(9), 1225. https://doi.org/10.1038/EMBOJ.2013.51

Shen, Y., Rehman, F. L., Feng, Y., Boshuizen, J., Bajrami, I., Elliott, R., Wang, B., Lord, C. J., Post, L. E., & Ashworth, A. (2013). BMN 673, a novel and highly potent PARP1/2 inhibitor for the treatment of human cancers with DNA repair deficiency. *Clinical Cancer Research : An Official Journal of the American Association for Cancer Research*, *19*(18), 5003. https://doi.org/10.1158/1078-0432.CCR-13-1391

Shirai, H., Poetsch, A. R., Gunji, A., Maeda, D., Fujimori, H., Fujihara, H., Yoshida, T., Ogino, H., & Masutani, M. (2013). PARG dysfunction enhances DNA double strand break formation in S-phase after alkylation DNA damage and augments different cell death pathways. *Cell Death & Disease 2013 4:6*, *4*(6), e656–e656.

https://doi.org/10.1038/cddis.2013.133

Singh, H. R., Nardozza, A. P., Möller, I. R., Knobloch, G., Kistemaker, H. A. V., Hassler, M., Harrer, N., Blessing, C., Eustermann, S., Kotthoff, C., Huet, S., Mueller-Planitz, F., Filippov, D. V., Timinszky, G., Rand, K. D., & Ladurner, A. G. (2017). A Poly-ADP-Ribose Trigger Releases the Auto-Inhibition of a Chromatin Remodeling Oncogene. *Molecular Cell*, *68*(5), 860-871.e7. https://doi.org/10.1016/j.molcel.2017.11.019

Smith, R., Lebeaupin, T., Juhász, S., Chapuis, C., D'Augustin, O., Dutertre, S., Burkovics, P., Biertümpfel, C., Timinszky, G., & Huet, S. (2019). Poly(ADP-ribose)-dependent chromatin unfolding facilitates the association of DNA-binding proteins with DNA at sites of damage. *Nucleic Acids Research*, *47*(21), 11250. https://doi.org/10.1093/NAR/GKZ820

Smith, R., Zentout, S., Rother, M., Bigot, N., Chapuis, C., Mihuț, A., Zobel, F. F., Ahel, I., van Attikum, H., Timinszky, G., & Huet, S. (2023). HPF1-dependent histone ADP-ribosylation triggers chromatin relaxation to promote the recruitment of repair factors at sites of DNA damage. *Nature Structural & Molecular Biology*, *30*(5), 678–691. https://doi.org/10.1038/S41594-023-00977-X

Spiegel, J. O., Van Houten, B., & Durrant, J. D. (2021). PARP1: Structural Insights and Pharmacological Targets for Inhibition. *DNA Repair*, *103*, 103125. https://doi.org/10.1016/J.DNAREP.2021.103125

Staniszewska, A. D., Pilger, D., Gill, S. J., Jamal, K., Bohin, N., Guzzetti, S., Gordon, J., Hamm, G., Mundin, G., Illuzzi, G., Pike, A., McWilliams, L., Maglennon, G., Rose, J., Hawthorne, G., Gonzalez, M. C., Halldin, C., Johnstrom, P., Schou, M., … Hamerlik, P. (2024). Preclinical Characterization of AZD9574, a Blood–Brain Barrier Penetrant Inhibitor of PARP1. *Clinical Cancer Research*, *30*(7), 1338–1351.

https://doi.org/10.1158/1078-0432.CCR-23-2094/730126/AM/PRECLINICAL-CHARACTERIZATION-OF-AZD9574-A-BLOOD

Stinson, B. M., & Loparo, J. J. (2021). Repair of DNA Double-Strand Breaks by the Non-homologous End Joining Pathway. *Annual Review of Biochemistry*, *90*, 137. https://doi.org/10.1146/ANNUREV-BIOCHEM-080320-110356

Stojanovic, P., Luger, K., & Rudolph, J. (2023). Slow Dissociation from the PARP1-HPF1 Complex Drives Inhibitor Potency. *Biochemistry*, *62*(16), 2382–2390. https://doi.org/10.1021/ACS.BIOCHEM.3C00243/ASSET/IMAGES/LARGE/BI3C00243_0006.JPEG

Strickfaden, H., McDonald, D., Kruhlak, M. J., Haince, J. F., Th'Ng, J. P. H., Rouleau, M., Ishibashi, T., Corry, G. N., Ausio, J., Underhill, D. A., Poirier, G. G., & Hendzel, M. J. (2016). Poly(ADP-ribosyl)ation-dependent transient chromatin decondensation and histone displacement following laser microirradiation. *Journal of Biological Chemistry*, *291*(4), 1789–1802. https://doi.org/10.1074/jbc.M115.694992

Ström, C. E., Johansson, F., Uhlén, M., Szigyarto, C. A. K., Erixon, K., & Helleday, T. (2011). Poly (ADP-ribose) polymerase (PARP) is not involved in base excision repair but PARP inhibition traps a single-strand intermediate. *Nucleic Acids Research*, *39*(8), 3166. https://doi.org/10.1093/NAR/GKQ1241

Sugasawa, K., Okuda, Y., Saijo, M., Nishi, R., Matsuda, N., Chu, G., Mori, T., Iwai, S., Tanaka, K., Tanaka, K., & Hanaoka, F. (2005). UV-induced ubiquitylation of XPC protein mediated by UV-DDB-ubiquitin ligase complex. *Cell*, *121*(3), 387–400. https://doi.org/10.1016/J.CELL.2005.02.035

Sukhanova, M. V., Hamon, L., Kutuzov, M. M., Joshi, V., Abrakhi, S., Dobra, I., Curmi, P. A., Pastre, D., & Lavrik, O. I. (2019). A Single-Molecule Atomic Force Microscopy

Study of PARP1 and PARP2 Recognition of Base Excision Repair DNA Intermediates. *Journal of Molecular Biology*, *431*(15), 2655–2673. https://doi.org/10.1016/J.JMB.2019.05.028

Sun, F. H., Zhao, P., Zhang, N., Kong, L. L., Wong, C. C. L., & Yun, C. H. (2021). HPF1 remodels the active site of PARP1 to enable the serine ADP-ribosylation of histones. *Nature Communications*, *12*(1), 1–10. https://doi.org/10.1038/s41467-021-21302-4

Suskiewicz, M. J., Prokhorova, E., Rack, J. G. M., & Ahel, I. (2023). ADP-ribosylation from molecular mechanisms to therapeutic implications. *Cell*, *186*(21), 4475–4495. https://doi.org/10.1016/J.CELL.2023.08.030

Suskiewicz, M. J., Zobel, F., Ogden, T. E. H., Fontana, P., Ariza, A., Yang, J. C., Zhu, K., Bracken, L., Hawthorne, W. J., Ahel, D., Neuhaus, D., & Ahel, I. (2020). HPF1 completes the PARP active site for DNA damage-induced ADP-ribosylation. *Nature*. https://doi.org/10.1038/s41586-020-2013-6

Swisher, E. M., Aghajanian, C., O'Malley, D. M., Fleming, G. F., Kaufmann, S. H., Levine, D. A., Birrer, M. J., Moore, K. N., Spirtos, N. M., Shahin, M. S., Reid, T. J., Friedlander, M., Steffensen, K. D., Okamoto, A., Sehgal, V., Ansell, P. J., Dinh, M. H., Bookman, M. A., & Coleman, R. L. (2022). Impact of homologous recombination status and responses with veliparib combined with first-line chemotherapy in ovarian cancer in the Phase 3 VELIA/GOG-3005 study. *Gynecologic Oncology*, *164*(2), 245–253. https://doi.org/10.1016/j.ygyno.2021.12.003

Szántó, M., Yélamos, J., & Bai, P. (2024). Specific and shared biological functions of PARP2 – is PARP2 really a lil' brother of PARP1? *Expert Reviews in Molecular Medicine*, *26*, e13. https://doi.org/10.1017/ERM.2024.14

Teloni, F., & Altmeyer, M. (2016). Readers of poly(ADP-ribose): designed to be fit for

purpose. *Nucleic Acids Research*, *44*(3), 993. https://doi.org/10.1093/NAR/GKV1383

Thomas, A., Murai, J., & Pommier, Y. (2018). The evolving landscape of predictive biomarkers of response to PARP inhibitors. *The Journal of Clinical Investigation*, *128*(5), 1727. https://doi.org/10.1172/JCI120388

Thomas, C., Ji, Y., Wu, C., Datz, H., Boyle, C., MacLeod, B., Patel, S., Ampofo, M., Currie, M., Harbin, J., Pechenkina, K., Lodhi, N., Johnson, S. J., & Tulin, A. V. (2019). Hit and run versus long-term activation of PARP-1 by its different domains fine-tunes nuclear processes. *Proceedings of the National Academy of Sciences of the United States of America*, *116*(20), 9941–9946. https://doi.org/10.1073/PNAS.1901183116/-/DCSUPPLEMENTAL

Thorsell, A. G., Ekblad, T., Karlberg, T., Löw, M., Pinto, A. F., Trésaugues, L., Moche, M., Cohen, M. S., & Schüler, H. (2017). Structural Basis for Potency and Promiscuity in Poly(ADP-ribose) Polymerase (PARP) and Tankyrase Inhibitors. *Journal of Medicinal Chemistry*, *60*(4), 1262. https://doi.org/10.1021/ACS.JMEDCHEM.6B00990

Timinszky, G., Till, S., Hassa, P. O., Hothorn, M., Kustatscher, G., Nijmeijer, B., Colombelli, J., Altmeyer, M., Stelzer, E. H. K., Scheffzek, K., Hottiger, M. O., & Ladurner, A. G. (2009). A macrodomain-containing histone rearranges chromatin upon sensing PARP1 activation. *Nature Structural & Molecular Biology 2009 16:9*, *16*(9), 923–929. https://doi.org/10.1038/nsmb.1664

Valdiglesias, V., Giunta, S., Fenech, M., Neri, M., & Bonassi, S. (2013). γH2AX as a marker of DNA double strand breaks and genomic instability in human population studies. *Mutation Research*, *753*(1), 24–40. https://doi.org/10.1016/J.MRREV.2013.02.001

Vodenicharov, M. D., Ghodgaonkar, M. M., Halappanavar, S. S., Shah, R. G., & Shah, G. M. (2005). Mechanism of early biphasic activation of poly(ADP-ribose) polymerase-1 in

response to ultraviolet B radiation. *Journal of Cell Science*, *118*(Pt 3), 589–599. https://doi.org/10.1242/JCS.01636

Vyas, S., Matic, I., Uchima, L., Rood, J., Zaja, R., Hay, R. T., Ahel, I., & Chang, P. (2014). Family-wide analysis of poly(ADP-ribose) polymerase activity. *Nature Communications*, *5*. https://doi.org/10.1038/NCOMMS5426

Wang, M., Wu, W., Wu, W., Rosidi, B., Zhang, L., Wang, H., & Iliakis, G. (2006). PARP-1 and Ku compete for repair of DNA double strand breaks by distinct NHEJ pathways. *Nucleic Acids Research*, *34*(21), 6170–6182. https://doi.org/10.1093/NAR/GKL840

Wei, H., & Yu, X. (2016). Functions of PARylation in DNA Damage Repair Pathways. In *Genomics, Proteomics and Bioinformatics* (Vol. 14, Issue 3, pp. 131–139). Beijing Genomics Institute. https://doi.org/10.1016/j.gpb.2016.05.001

Wei, Y., He, L., Liu, T., Guo, T., Xie, C., Jia, J., Lin, Y., Liu, J., & Fan, J. (2024). Efficacy and safety of PARP inhibitors combined with antiangiogenic agents in the maintenance treatment of ovarian cancer: a systematic review and meta-analysis with trial sequential analysis of randomized controlled trials. *Frontiers in Pharmacology*, *15*, 1372077. https://doi.org/10.3389/FPHAR.2024.1372077/BIBTEX

Wu, Q., Jubb, H., & Blundell, T. L. (2015). Phosphopeptide interactions with BRCA1 BRCT domains: More than just a motif. *Progress in Biophysics and Molecular Biology*, *117*(2–3), 143. https://doi.org/10.1016/J.PBIOMOLBIO.2015.02.003

Xue, H., Bhardwaj, A., Yin, Y., Fijen, C., Ephstein, A., Zhang, L., Ding, X., Pascal, J. M., VanArsdale, T. L., & Rothenberg, E. (2022). A two-step mechanism governing PARP1-DNA retention by PARP inhibitors. *Science Advances*, *8*(36), 414. https://doi.org/10.1126/SCIADV.ABQ0414

Yang, J., Zhao, Y. L., Wu, Z. Q., Si, Y. L., Meng, Y. G., Fu, X. B., Mu, Y. M., & Han, W. D.

(2009). The single-macro domain protein LRP16 is an essential cofactor of androgen receptor. *Endocrine-Related Cancer*, *16*(1), 139–153. https://doi.org/10.1677/ERC-08-0150

Yang, Y. G., Cortes, U., Patnaik, S., Jasin, M., & Wang, Z. Q. (2004). Ablation of PARP-1 does not interfere with the repair of DNA double-strand breaks, but compromises the reactivation of stalled replication forks. *Oncogene*, *23*(21), 3872–3882. https://doi.org/10.1038/SJ.ONC.1207491

Yap, T. A., Im, S.-A., Schram, A. M., Sharp, A., Balmana, J., Baird, R. D., Brown, J. S., Schwaederle, M., Pilling, E. A., Moorthy, G., Linardopoulos, S., Dowson, A., Pound, C., Lukacs, E., Cosulich, S., & Luen, S. J. (2022). Abstract CT007: PETRA: First in class, first in human trial of the next generation PARP1-selective inhibitor AZD5305 in patients (pts) with BRCA1/2, PALB2 or RAD51C/D mutations. *Cancer Research*, *82*(12_Supplement), CT007–CT007. https://doi.org/10.1158/1538-7445.AM2022-CT007

Yu, S. W., Andrabi, S. A., Wang, H., No, S. K., Poirier, G. G., Dawson, T. M., & Dawson, V. L. (2006). Apoptosis-inducing factor mediates poly(ADP-ribose) (PAR) polymer-induced cell death. *Proceedings of the National Academy of Sciences of the United States of America*, *103*(48), 18314. https://doi.org/10.1073/PNAS.0606528103

Zandarashvili, L., Langelier, M. F., Velagapudi, U. K., Hancock, M. A., Steffen, J. D., Billur, R., Hannan, Z. M., Wicks, A. J., Krastev, D. B., Pettitt, S. J., Lord, C. J., Talele, T. T., Pascal, J. M., & Black, B. E. (2020). Structural basis for allosteric PARP-1 retention on DNA breaks. *Science (New York, N.Y.)*, *368*(6486). https://doi.org/10.1126/SCIENCE.AAX6367

Zentout, S., Imburchia, V., Chapuis, C., Duma, L., Schützenhofer, K., Prokhorova, E., Ahel, I., Smith, R., & Huet, S. (2024). Histone ADP-ribosylation promotes resistance to PARP

inhibitors by facilitating PARP1 release from DNA lesions. *Proceedings of the National Academy of Sciences of the United States of America*, *121*(25), e2322689121. https://doi.org/10.1073/PNAS.2322689121/SUPPL_FILE/PNAS.2322689121.SAPP.PDF

Zhong, Q., Xiao, X., Qiu, Y., Xu, Z., Chen, C., Chong, B., Zhao, X., Hai, S., Li, S., An, Z., & Dai, L. (2023). Protein posttranslational modifications in health and diseases: Functions, regulatory mechanisms, and therapeutic implications. *MedComm*, *4*(3). https://doi.org/10.1002/MCO2.261

Appendix

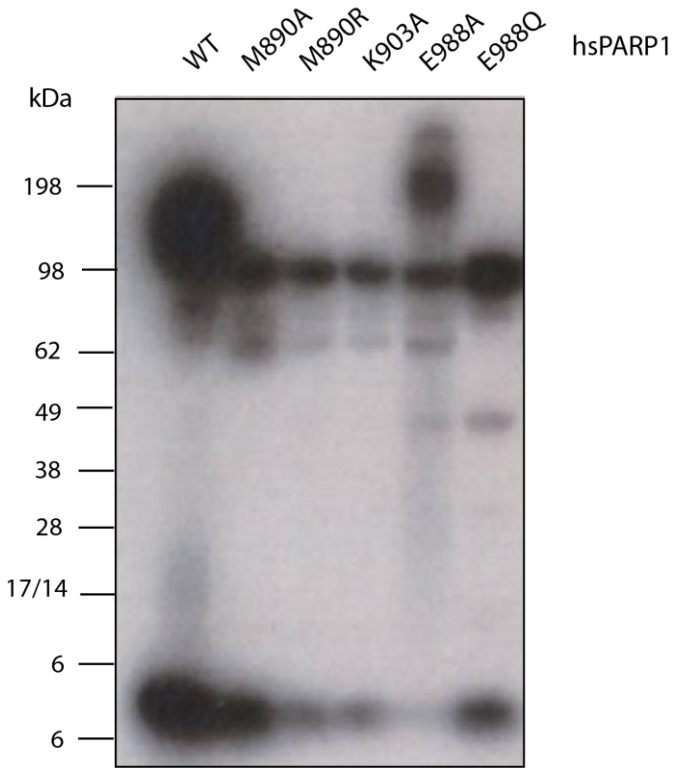

Figure A.1: Radioactive ADPr experiment showing the catalytic activity of PARP1 WT and other mutants. The experiment consisted of purified hsPARP1 (0.8µM), hsHPF1 (1.6 µM), histone H3 peptide (0.05 mg/ml), nicked DNA (0.5 µM) and 32P-labelled NAD^+ (50 µM). The experiment was performed by Marcin Suskiewicz.

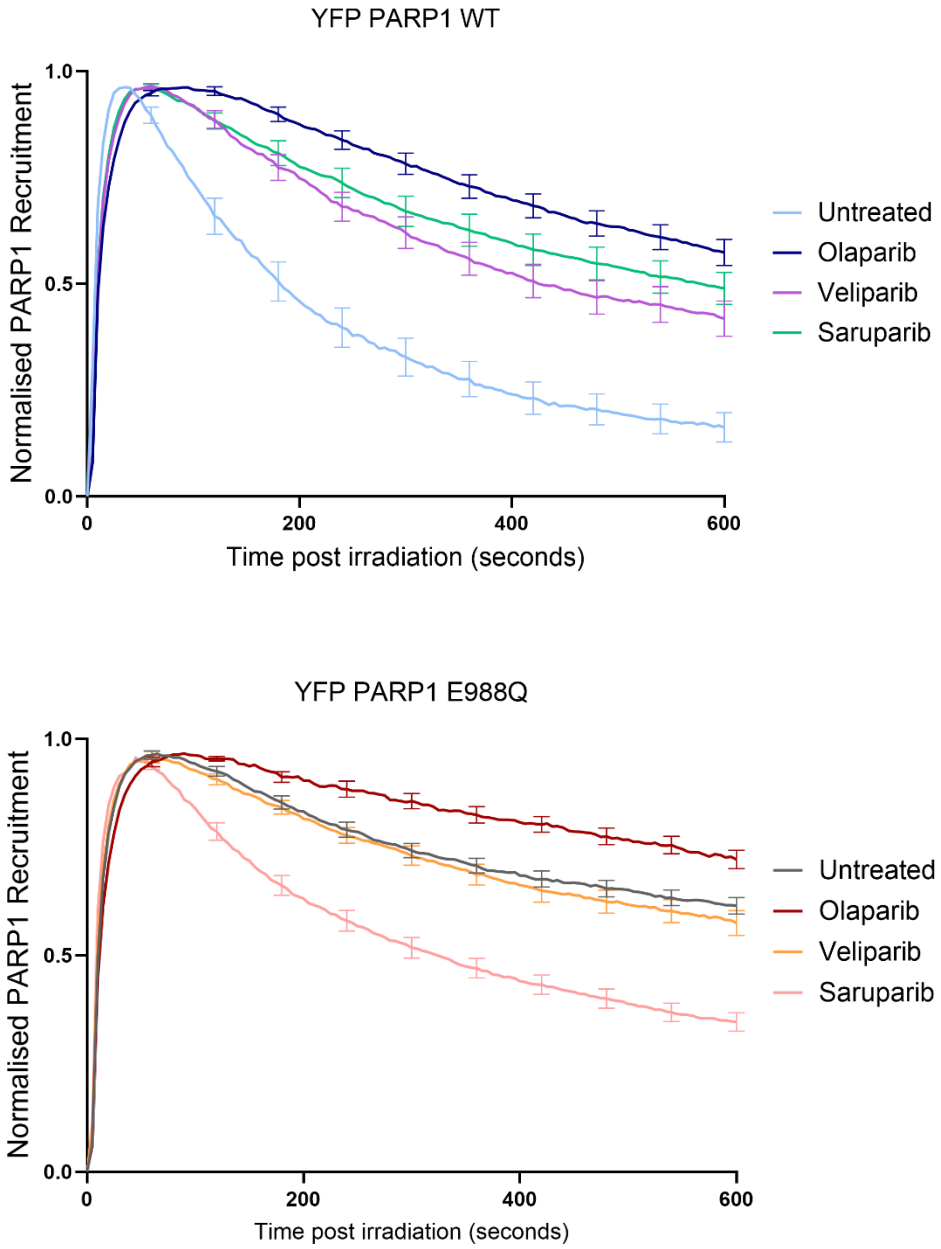

Figure A.2: Recruitment and release dynamics of YFP PARP1 WT and YFP PARP1 E988Q in response to olaparib, veliparib and saruparib. U2OS Flp-In PARP1 KO cells were treated with 0.1 µg/mL Doxycycline 24 hours before imaging to induce expression of YFP PARP1. Cells were either left un-treated, or treated with 1 µM olaparib, 1 µM veliparib or 5 nM saruparib. Recruitment was normalised to the maximum amount of fluorescence reached in each condition. Data are shown as mean ± standard error of the mean. Data were collected from 20–24 cells per condition.

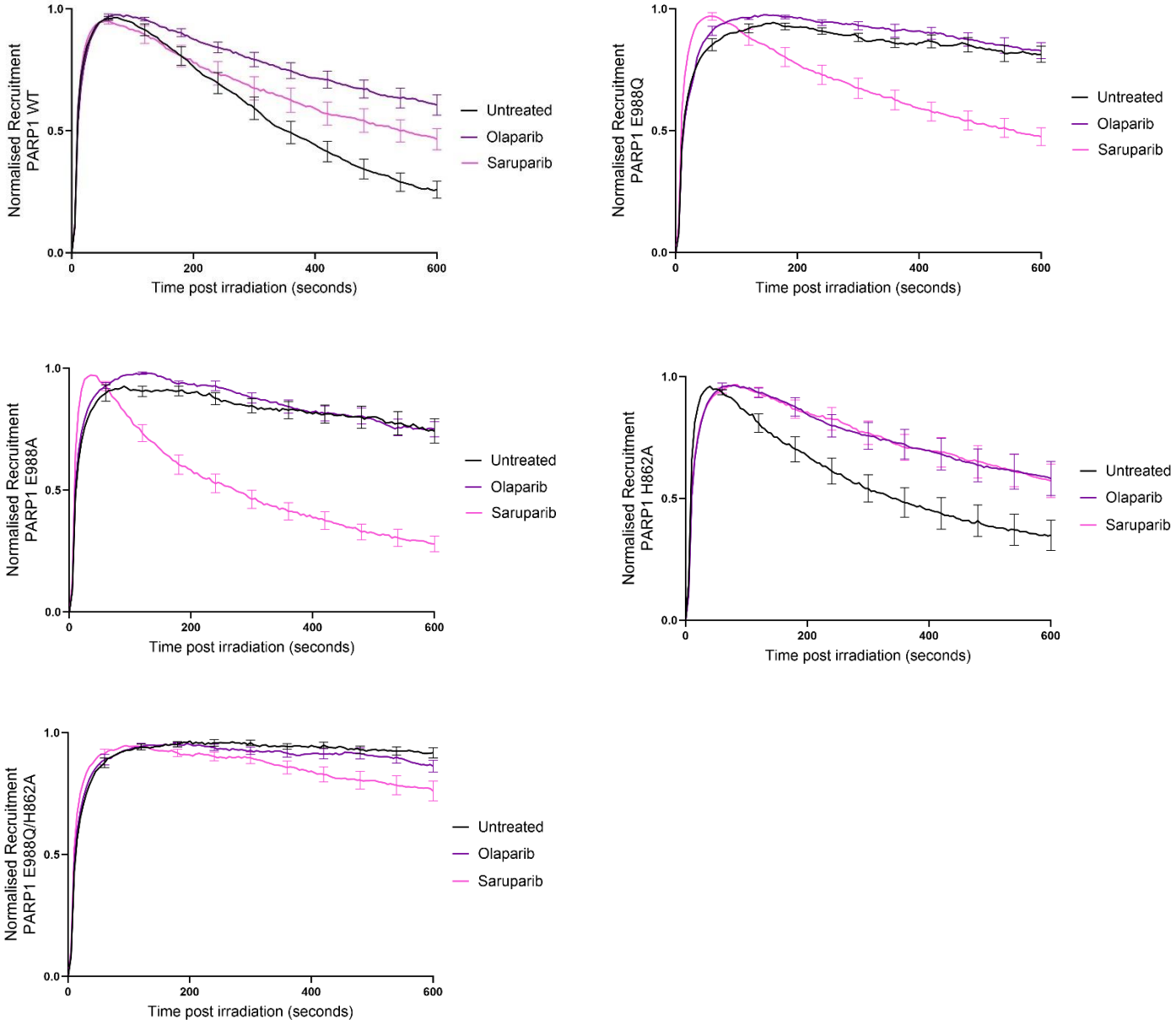

Figure A.3: Recruitment and release dynamics of different PARP1 catalytic mutants in response to olaparib or saruparib. U2OS PARP1 KO cells were transfected with the indicated YFP-tagged wild-type or mutant PARP1, and cells were either left un-treated, or treated with 1 μM olaparib or 5 nM saruparib. Recruitment was normalised to the maximum amount of fluorescence reached in each condition. Data are shown as mean ± standard error of the mean. Data were collected from 8–14 cells per condition.

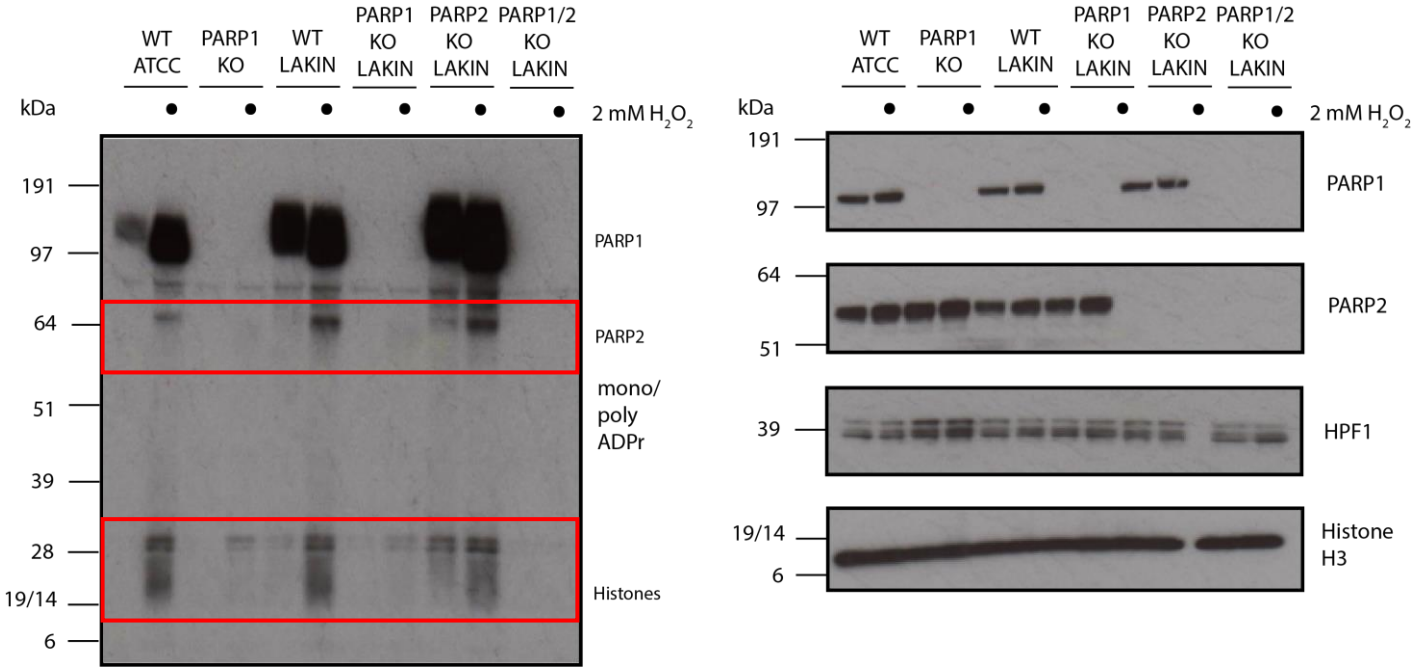

Figure A.4: Comparison of the ADP-ribosylation activity in cells lacking PARP1, PARP2, or both. Western blot showing that upon loss of PARP1, some ADP-ribosylation is left both on histones, and around the 64 kDa mark. In U2OS PARP1/PARP2 KO cells, as seen in lanes 11 and 12, this signal is completely lost. The relevant signals on the gel are highlighted in red. Blots were examined with the indicted antibodies. Histone H3 was used as a loading control.

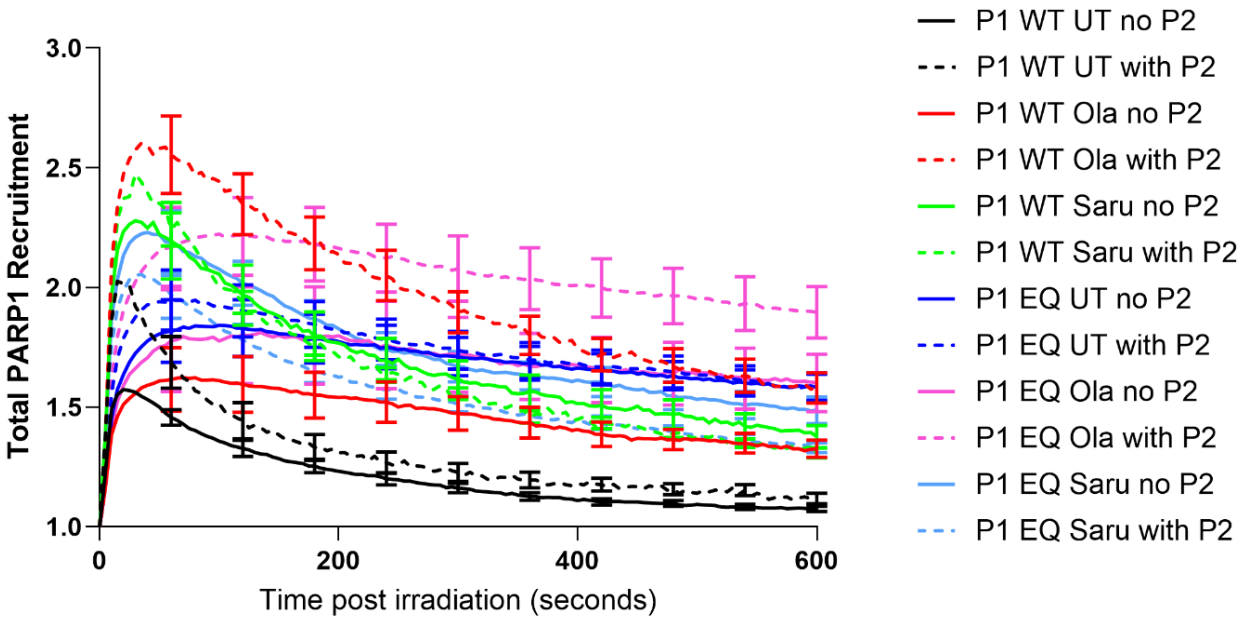

Figure A.5: Total amount of mCherry-PARP1 WT and E988Q recruited to DNA damage sites in the presence or absence of YFP-PARP2. Total quantified recruitment of transiently transfected mCherry-PARP1 (P1) WT or mCherry-PARP1 E988Q to sites of laser micro-irradiation in the presence or absence of YFP PARP2 (P2) in U2OS PARP1/PARP2 KO cells. Cells were left un-treated, or treated with 1 μM olaparib (Ola) or 5 nM saruparib (Saru). Data are shown as mean ± standard error of the mean. Data were collected from 8–15 cells per condition.